The Role of D6 in Neutrophil Migration, Melanoma Growth and Metastasis

Claire Louise Burt
Bsc Honours Immunology

Thesis submitted to the University of Glasgow for the Degree of Doctor of Philosophy

Division of Immunology, Infection and Inflammation
Faculty of Medicine
University of Glasgow

May 2011

Acknowledgements

First of all I would like to thank my supervisor Gerry Graham, for giving me the chance to stay on in his lab, as well as all the support, encouragement and for his positive outlook, which balanced out my negative one! Everyone in the CRG group (pre- and post-divorce) has been a great help over the years. In particular Clare McCulloch, who despite helping me as an undergrad, welcomed me back into the lab and has helped me in many ways throughout my PhD, and has been a great bench buddy. Numerous people have helped me with various techniques throughout my PhD. In particular, I would like to thank Clive McKimmie for all his help with primer design and molecular biology techniques, Emma Blair (AKA PC Blair) and Jim Reilly, for help with tissue processing and section cutting, Alasdair Fraser, Chris Hansell and Catherine Hurson for help with FACS, Catherine Wilson for help with platelet isolation, Ashley Gilmour for help with Luminex assays, all the staff at the Central Research Facility, in particular Craig Begley and Colin Chapman, and the staff in the histology department at the Vet School. I would also like to thank Lesley Shield at the LRF for providing me with Hut 78 and H9 cells, as well as Dr Mike Edwards for the B16 cell lines. I would like to thank the Medical Research Council for funding me throughout my PhD.

I would like to thank my family, for all their encouragement and moral support, even though I moved out in my first year, their support was greatly appreciated. Mum & Dad, I couldn't have done it without you. Kris, I hope that all my stories about the lab haven't made you think we just fool around all day, believe it or not actual science does get done! Laura, I suppose I better dedicate this to you ☺! Mum, now you can call me Doctor! (well almost!)

My time in the lab would not have been the same if it wasn't for the banter! In particular, Wilson and Irish who, with the addition of a few bottles of vino, have made my time in the lab fantastic. Cat, you brightened up our bay, and I hope you don't lose too many things now I'm gone! Make sure you torment Kenny twice as much now I'm gone and remember we'll always have daddycatchers realm! Catherine…..potatoes, that is all! I was really glad when you decided to join our lab…..actually Rob still owes me money for that! I can always rely on you for a trip to the pub, and I hope I still will in the future. Ross and Kenjamin, I've lost track of how many band names you two have come up with. I hope to

get backstage passes when Bitter Salty Grapes play their first gig. I can always rely on you two for some ‘casual’ opinions and fact biscuits. I have to mention sporcle.com, you have greatly expanded my knowledge of world geography, and almost made me fail my PhD. Derek for all his encouraging words, don’t worry I won’t be back! Thanks to all the japesters, you know who you are. Long may your japes continue even though you’re a man down.

Lastly I would like to thank Paul, for all your love and support, and putting up with me during the past few months (and past 3 years!). I know it hasn’t been easy, and I just want to let you know how much I appreciate you being there for me. This is really dedicated to you (hopefully Laura won’t read down this far, she’s got a short attention span!), oh and Hans Gruber!

No smiling Jim, only a cactus!

List of Tables

List of Figures

Author’s Declaration

I declare that I am the sole author of this thesis and that all the work described within was performed by me unless otherwise stated.

Abbreviations

APC	Allophycocyanin
BCA	B cell attracting chemokine
BCG	Bacille Calmette Guerin
BLC	B lymphocyte chemokine
BLP	Bacterial lipoprotein
BRAK	Breast and kidney expressed chemokine
BRET	Bioluminescence resonance energy transfer
BSA	Bovine serum albumin
CCX-CKR	Chemocentryx chemokine receptor
CD	Clusters of differentiation
CFA	Complete Freund's adjuvant
CFSE	Carboxyfluorescein succinimidyl ester
CFU	Colony forming unit
CLA	Cutaneous lymphocyte-associated antigen
CMTMR	(5-(and6-)-(((4-chloromethyl)benzoyl)amino)tetramethylrhodamine)
CMV	Cytomegalovirus
COPD	Chronic obstructive pulmonary disease
CSF	Colony stimulating factor
CTACK	Cutaneous T cell attracting chemokine
C-terminus	Carboxyl -terminus
CTL	Cytotoxic T lymphocyte

DAB	3, 3'-diaminobenzidine
DAG	1,2-Diacylglycerol
DAPI	4’, 6-diamidino-2-phenylindole
DARC	Duffy antigen receptor for chemokines
DC	Dendritic cell
DC-CK1	Dendritic cell chemokine –1
DMBA	7,12-Dimethylbenz(α)anthracene
DMEM	Dulbecco’s modified Eagle's medium
DNA	Deoxyribonucleic acid
DPX	Di-n-butyl Phthalate in xylene
EAE	Experimental autoimmune encephalitis
ECM	Extracellular matrix
EDTA	Ethylenediaminetetraacetic acid
ELC	Epstein-Barr virus induced molecule-1 ligand chemokine
ENA-78	Epithelial neutrophil-activating protein-78
EST	Expressed sequence tag
FACS	Fluorescence-activated cell sorter
FCS	Foetal calf serum
FITC	Fluorescein isothiocyanate
FRET	Fluorescence resonance energy transfer
GAG	Glycosaminoglycan
GCP	Granulocyte chemotactic protein
GDP	Guanosine diphosphate

GFP	Green fluorescent protein
GPCR	G-protein coupled receptor
GRK	G-protein coupled receptor kinases
GRO	Growth related oncogene
GTP	Guanosine triphosphate
HA	Haemagglutinin
HCC	Hemofiltrate CC chemokine
HHV8	Human herpesvirus 8
HIF-1	Hypoxia inducible factor-1
HRP	Horseradish peroxidase
IBD	Inflammatory bowel disease
ICAM-1	Inter-cellular adhesion molecule-1
IDO	Indoleamine 2,3-dioxygenase
IFN	Interferon
Ig	Immunoglobulin
IL	Interleukin
IP	Interferon inducible protein
I-TAC	Interferon inducible T cell α chemoattractant
i.v.	Intravenous
KC	Keratinocyte derived chemokine
kDa	Kilodalton
KO	Knock out
LARC	Liver and activation regulated chemokine

LFA-1	Lymphocyte function associated antigen-1
LPS	Lipopolysaccharide
LYVE-1	Lymphatic Vessel Endothelial Receptor-1
mAb	Monoclonal antibody
MACS	Magnetically activated cell sorting
MART-1	Melanoma antigen recognised by T cells
MCAF	Monocyte chemotactic and activating factor
MCP	Monocyte chemoattractant protein
MDSC	Myeloid derived suppressor cells
MGSA	Melanoma growth stimulatory activity
MHC	Major histocompatibility complex
MICA/B	MHC class I related chain A/B
Mig	Monokine induced by interferon
MIP-1α	Macrophage inflammatory protein
MMP	Matrix metalloproteinase
MPIF	Myeloid progenitor inhibitory factor
mRNA	Messenger ribonucleic acid
MRP-1	Macrophage inflammatory related protein - 1
MS	Multiple sclerosis
MSC	Mesenchymal stem cells
MTb	Mycobacterium tuberculosis
NAP	Neutrophil activating peptide
NBF	Neutral buffered formalin

NK	Natural killer
NKT	Natural killer T cell
NSAID	Non-steroidal anti-inflammatory drugs
N-terminus	Amino-terminus
PAF	Platelet activating factor
PAMPs	Pathogen associated molecular patterns
PBS	Phosphate buffered saline
PCR	Polymerase chain reaction
PE	Phycoerythrin
PF	Platelet factor
PGC	Primordial germ cell
PLC	Phospholipase C
PKC	Protein kinase C
PSGL-1	P-selectin glycoprotein ligand-1
PTx	Pertussis toxin
QPCR	Quantitative real time polymerase chain reaction
RANTES	Regulation on activation normal T cell expressed and secreted
RNA	Ribonucleic acid
RNAi	Ribonucleic acid interference
RPMI	Roswell park memorial institute-1640 medium
RT	Reverse transcriptase
RT-PCR	Reverse transcriptase polymerase chain reaction
SDF	Stromal derived factor

s.c.	Subcutaneous
SCID	Severe combined immunodeficiency
SLC	Secondary lymphoid tissue chemokine
TAM	Tumour associated macrophages
TAMRA	Tetramethyl-6-Carboxyrhodamine
TARC	Thymus and activation regulated chemokine
TBT	Tris buffered tween
TCR	T cell receptor
TECK	Thymus expressed chemokine
TGF	Transforming growth factor
Th	T helper
TLR	Toll like receptor
TNF	Tumour necrosis factor
TPA	12-tetradecanoyl 13-phorbol acetate
Treg	Regulatory T cell
TUNEL	Terminal deoxynucleotidyl transferase dUTP nick end labelling
UVR	Ultra violet radiation
VCAM-1	Vascular cell adhesion molecule-1
VEGF	Vascular endothelial growth factor
VLA-4	Very late antigen – 4
vWF	von Willebrand factor
WT	Wild type
g	grams

mg	milligrams
µg	micrograms
ng	nanograms
M	molar
mM	millimolar
µM	micromolar
µl	microlitre
ml	millilitre

Summary

Chemokines are members of a family of small structurally related proteins, which can be classified according to the positioning of four conserved cysteine residues, into four families – CC, CXC, CX3C and XC. They have a wide range of functions, from being involved in embryonic development, disease processes and cell migration. Broadly speaking, chemokines can be divided into homeostatic, those that are involved in development, and inflammatory chemokines, which are produced at high levels during infection.

In order to exert their function, chemokines bind to seven transmembrane G protein coupled receptors; this causes the activation of numerous different signalling pathways which can lead to cell activation, migration, survival or apoptosis. The chemokine system is further complicated by the existence of a family of atypical receptors. Four of these receptors have been identified to date; CXCR7, CCX-CKR, DARC and D6, and they all share the apparent inability to signal after ligand binding.

D6 has been identified as a member of this atypical receptor family with the ability to bind and internalise 12 inflammatory CC chemokines. D6 expression has been demonstrated in barrier tissues, such as the skin, gut and lung, as well as being expressed by numerous leukocyte subsets. Studies looking at the function of D6 have demonstrated its involvement in the resolution phase of inflammation, and D6 may be involved in cell migration and inflammation driven tumourigenesis. Here the analysis of the role of D6 in neutrophil migration has been carried out, in the well-characterised TPA model of skin inflammation. This work also shows that D6 plays a crucial role in melanoma metastasis.

In the TPA model of skin inflammation, 129/Bl6 D6KO mice display an exaggerated inflammatory response, which causes the development of a psoriasis-like pathology. This pathology is dependent on T cells and mast cells, and is associated with an alteration in neutrophil positioning. In the inflamed skin of D6KO mice, neutrophils are found at the dermal/epidermal junction, whilst in WT mice, neutrophils are restricted to the dermis. In this model, D6 is required to prevent neutrophils migrating to the dermal/epidermal junction. D6 expression has been demonstrated both in the skin and on neutrophils, so there are two hypotheses to describe how D6 is influencing neutrophil movement in this model. First, D6 on neutrophils is required to limit their migration within the skin, keeping

them away from the dermal/epidermal junction, alternatively D6 in the skin may be responsible for chemokine clearance during inflammation, and the localisation of neutrophils is influenced by these chemokines. This work aimed to investigate the role that D6 played on neutrophil localisation in inflamed skin, carried out using a model of neutrophil adoptive transfer. These results demonstrate that expression of D6 by neutrophils does not alter their positioning in inflamed skin, suggesting that the role for D6 in this model is in regulating chemokines within the skin, a hypothesis which requires further investigation.

The second part of this work aimed to investigate the role of D6 in melanoma growth and metastasis. D6 has been shown to be involved in murine models of inflammation driven skin tumourigenesis and colon cancer. These data presented here show that D6 does not influence the primary melanoma growth, but has a profound effect on the development of metastases in the lungs, in the murine B16 model. D6 is required for the development of lung metastases, but the precise mechanism is yet unknown. These data suggest that D6 can alter macrophage numbers within the lungs, which permits the development of metastases, as well as pointing towards a role for D6 in lymphangiogenesis within the lungs, which affects metastasis development, perhaps by altering the development of the pre-metastatic niche. Overall, these studies contribute to the investigation of the role of D6 in skin inflammation, and show, for the first time, that D6 is involved in the pulmonary metastasis of melanoma, suggesting D6 may be a potential therapeutic target in pulmonary metastasis.

1 Introduction

1.1 Chemokines

Chemokines are members of a family of small proteins (8-12 kDa) that are best known for their role in cell movement. The name chemokine is in fact derived from their main purpose; CHEMOtactic cytoKINE. Chemokines have essential roles in a wide range of processes, such as cell movement, development, proliferation, cell transformation, metastasis and the development of immune responses (1, 2). PF-4 (Platelet factor 4) was originally discovered in 1961 (3). At this time, the biological role of chemokines was unknown, but they were known to be associated with inflammatory conditions (4). Since then 46 chemokines and around 20 receptors have been identified. The chemokine family of genes is thought to have derived from a primordial chemokine gene, which after duplication and divergence became the chemokine system we know today (1).

Most chemokines are secreted, with the exception of fractalkine and CXCL16, which can be produced as membrane bound forms (1). Almost all cell types have the ability to produce chemokines. They can be rapidly synthesised and produced in response to various stimuli, and they can be stored in a wide variety of cell types, e.g. endothelial cells store chemokines in Weibel Palade bodies. Neutrophils, eosinophils and mast cells can store chemokines and release these when required and platelets can store CXCL1, 4, 5, 7, 8, CCL1, 5 and 7 (2).

1.1.1 Chemokine Structure

The members of the chemokine family share a common structure. Chemokines have a flexible N-terminus (amino terminus) that is joined to the rest of the structure by disulphide bonds. This leads into an extended loop with three anti-parallel β pleated sheets. These create a flat base from which the C-terminus (carboxy terminus) extends (5). The N-terminus of chemokines is important for their activity as shown by deletion and substitution analysis (5-7).

1.1.1.1 Classification of Families

The development of EST (expressed sequence tag) databases allowed rapid identification of sequences similar to chemokines, using molecular cloning techniques. As a result, this led to many chemokines being identified simultaneously by different groups. One drawback from the rapid rate of chemokine discovery was that many chemokines were reported under different names, e.g. MIP3β, ELC and exodus-3 were names reported for what is now known as CCL19. In 1999 it was decided to adopt a systematic nomenclature for chemokines and their receptors (1). The nomenclature is described in table 1.1 along with their previous names (1, 5)

The nomenclature system was developed according to the positioning of highly conserved cysteine residues found in the N-terminus of chemokines. The four families of chemokines identified to date are the CXC, CC, XC and CX3C families. These can also be referred to as α, β, γ and δ chemokine families. The two biggest groups are the CXC and CC, with 16 and 28 members respectively. The XC and CX3C families are much smaller, with only two members of the XC family (XCL1 and XCL2) and the sole member of CX3C family is fractalkine (CX3CL1)(1). Within the CXC family further subdivision can occur, based on the presence of three amino acids – ELR (glutamic acid, leucine and arginine). CXC chemokines can either be ELR+ or ELR-; ELR positive chemokines can recruit neutrophils to the site of inflammation. The addition of an ELR motif to PF4 (which lacks one) causes it to become a potent neutrophil chemoattractant (5).

Systemic Nomenclature	Human Ligand	Mouse Ligand	Receptor
CXCL1	GROα/MGSAα	KC	CXCR2
CXCL2	GROβ/MGSAβ/MIP-2	MIP-2	CXCR2
CXCL3	GROγ/MGSA γ/MIP-2β	DCIP1	CXCR2
CXCL4	PF4	PF4	CXCR3
CXCL5	ENA-78	LIX?	CXCR2
CXCL6	GCP-2	LIX?	CXCR1, CXCR2
CXCL7	NAP-2	unknown	CXCR1, CXCR2
CXCL8	IL-8	unknown	CXCR1, CXCR2
CXCL9	Mig	Mig	CXCR3
CXCL10	IP-10	IP-10	CXCR3
CXCL11	I-TAC	I-TAC	CXCR3
CXCL12	SDF-1α/β	SDF-1	CXCR4
CXCL13	BLC/BCA-1	BLC/BCA-1	CXCR5
CXCL14	BRAK/bolekine	BRAK	unknown
CXCL15	unknown	Lungkine	unknown
CXCL16	CXCL16	CXCL16	CXCR6
CCL1	I-309	TCA-3, P500	CCR8
CCL2	MCP-1/MCAF	JE	CCR2
CCL3	MIP-1αS	MIP-1α	CCR1, CCR5
CCL3L1	MIP-1αP	MIP-1α	CCR5
CCL4	MIP-1β	MIP-1β	CCR5
CCL4L1	MIP-1β	MIP-1β	CCR5
CCL5	RANTES	RANTES	CCR1, CCR3, CCR5
CCL6	unknown	C10, MRP-1	unknown
CCL7	MCP-3	MARC/MCP-3	CCR1, CCR2, CCR3
CCL8	MCP-2	MCP-2?	CCR2, CCR5
CCL9	unknown	MRP-2, CCF18, MIP-1γ	CCR1
CCL10	unknown	MRP-2, CCF18, MIP-1γ	CCR1
CCL11	eotaxin	eotaxin	CCR3
CCL12	unknown	MCP-5	CCR2
CCL13	MCP-4	unknown	CCR1, CCR5
CCL14	HCC-1	unknown	CCR1
CCL15	HCC-2/Lkn-1/MIP-1δ	unknown	CCR1, CCR3
CCL16	HCC-4/LEC	LCC-1	CCR1, CCR3
CCL17	TARC	TARC	CCR4
CCL18	DC-CK1/PARC AMAC-1	unknown	unknown
CCL19	MIP-3β/ELC/exodus-3	MIP-3β/ELC/exodus-3	CCR7
CCL20	MIP-3α/LARC/exodus-1	MIP-3α/LARC/exodus-1	CCR6
CCL21	6Ckine/SLC/exodus-2	6Ckine/SLC/exodus-2/TCA-4	CCR7
CCL22	MDC/STCP-1	MDC	CCR4
CCL23	MPIF-1	unknown	CCR1
CCL24	MPIF-2/eotaxin-2	eotaxin-2/MPIF-2	CCR3
CCL25	TECK	TECK	CCR9
CCL26	Eotaxin-3	unknown	CCR3
CCL27	CTACK/ILC/PESKY	ALP/CTACK/ILC Eskine/PESKY	CCR10
CCL28	CCL28/MEC	CCL28/MEC	CCR10
CX3CL1	Fractalkine	Neurotactin	CX3CR1
XCL1	lymphotactin/SCM-1α/ATAC	lymphotactin	XCR1
XCL2	SCM-1γ	unknown	XCR1

Table 1-1: Chemokine and receptor nomenclature (adapted from (1, 8)).

The nomenclature assigns a number according to when the genes were cloned, and is based on the human chemokine system. The human and murine chemokine systems are

very similar, but there are some human chemokines with no mouse homologue and vice versa, e.g. there is no mouse CXCL8 and no human CXCL15 (1, 5). The number of chemokines described above can be expanded by the existence of splice variants and various different chemokine isoforms. Chemokines can also be processed by different enzymes, which can create products which have very different effects (further details found in section 1.1.2.3) (2).

As well as classification on a structural basis, chemokines within families can be subdivided according to their function, into inflammatory (inducible) or homeostatic (constitutive) chemokines. The inflammatory chemokines were amongst the first to be identified, e.g. CCL2 and CCL5, as cells in vitro can be induced to produce a large amount of inflammatory chemokines. Inflammatory chemokines have been identified in a wide variety of inflammatory processes, with both pathogenic and protective roles. Homeostatic chemokines were discovered later, as they are expressed normally at low levels. These chemokines play vital roles during development, as exhibited by studies using gene null mice, e.g. CCL19 and CCL21.

Animal models have been extensively used to elucidate the role of chemokines and their receptors in vivo. These studies initially used blocking antibodies and were rapidly followed by gene targeting to create null mice. Mice with a single chemokine gene removal often have no overt phenotype, this includes null mice that lack CCL2 or CCL3 or CCL11, as well as CCR1 or CCR2, or CCR3 or CCR4 or CCR5, or CXCR3. This is a characteristic of many null mice involving the chemokine system, due to the redundancy involved. Inflammatory chemokine receptors are much more promiscuous than homeostatic chemokine receptors. For example CCR5 can bind to CCL3, CCL4, CCL5 and CCL8. This can make it difficult to clearly interpret the results from gene null animal studies (9).

1.1.2 Chemokine regulation

In vivo, the majority of chemokines are secreted; they bind to receptors and induce downstream effects. After secretion, the function of chemokines can be altered by the formation of multimers, they can be post-translationally modified and degraded by proteases. Chemokines can be regulated at the level of gene transcription and protein translation. During inflammation, chemokines are not expressed until tissue damage or

infection occurs, which leads to mRNA stabilisation. Post-translationally, chemokines can be secreted from granular stores, activated or inactivated by proteases, or proteases can generate receptor antagonists (10).

1.1.2.1 Aggregation

Chemokines are able to form multimers – usually dimers but oligomers are possible, e.g. CXCL4 can form tetramers and CCL3, 4, and 5 can form higher order oligomers (5, 6). Dimer formation allowed the crystal structure of chemokines to be resolved and was responsible for identifying chemokine dimers. The shape of dimers differs between CC and CXC chemokines, with CXC chemokines such as CXCL8 forming globular dimers, whilst CC chemokines, such as CCL4, form a dimer which is more elongated and has a cylindrical shape (11). Variants of chemokines can be created which are unable to form dimers. For example PM2 is a mutant of CCL3, which has two acidic amino acids in the C-terminus neutralised. This makes it non-aggregating but it still retains its function in vitro (12). Chemokine binding to GAGs (glycosaminoglycans) is thought to involve dimer formation, which may be involved in chemotaxis in vivo (13). Heterodimerisation can take place, as chemokines share 20-70% structural homology (14, 15). Although dimers can form, it is commonly thought that chemokines interact with their receptors in a monomeric form. Data argue against direct interactions between heterodimers and chemokine receptors – they may be involved in negatively regulating chemokine receptor activation or regulating chemokine function in vivo (7).

1.1.2.2 Glycosaminoglycans

When chemokines are secreted, they are thought to move away from the site of production and form chemokine gradients, although there is limited evidence for gradients in vivo. Chemokines have been shown to bind to GAGs in vivo and in vitro. GAGs are carbohydrate structures found on almost all cells, e.g. heparan sulphate, chondroitin sulphate, dermatan sulphate and keratan sulphate. They are linked to the plasma membrane via a transmembrane helix or a lipid anchor. Heparin and hyaluronan can be secreted; heparin may protect chemokines against proteolytic cleavage (16). GAGs are extremely heterogeneous with different chemokines having varying affinities for different GAGs . In the extracellular matrix and the vasculature, chemokine binding to GAGs is

thought to prevent chemokines from flowing away, which allows chemokines to be presented to the appropriate cells (17).

CCL2, 3 and 5 mutants with no GAG binding domain can induce chemotaxis in vitro but not in vivo (18). GAGs may be important under shear flow, preventing chemokines from flowing away in the blood (potentially allowing the formation of 'gradients'), so they act as a mechanism for chemokine localisation and can be involved in chemokine receptor signalling (19). CCL2 and CCL8 dimers bind to GAGs better (hetero>homo) than each chemokine alone (7). GAGs can provide a substrate for chemokine presentation to chemokine receptors, as well as being able to protect chemokines from proteolytic cleavage (20-22).

1.1.2.3 N-terminal Cleavage

As briefly mentioned earlier, the N terminal of chemokines can be processed by proteases, for example CD26 (dipeptidyl peptidase) and MMPs (matrix metalloproteases). Processing of chemokines can alter the affinity for the receptor, as well as affecting receptor specificity and downstream signalling (23, 24). Proteolysis can lead to chemokine inactivation or create receptor antagonists (25, 26). CD26 cleaves chemokines at the last two N terminal amino acids, if they have a proline, hydroxyproline or alanine at the second position, meaning it cannot cleave all chemokines (23).

During inflammation, stromal cells and leukocytes produce MMPs. These are involved in ECM (extracellular matrix) remodelling; they can mediate inflammation, angiogenesis and metastasis. As with CD26, not all chemokines are cleavable by MMPs. CCL2, 7, 8, 11 and 13 can be cleaved by MMPs in vitro but they still retain their chemokine receptor binding ability (27). Cleavage of chemokines by MMPs can create antagonists of inflammation (7). MMPs can also cleave GAGs, and in doing so can release bound chemokines (27).

1.2 Chemokine receptors

Chemokines mediate their effects through binding to seven transmembrane G protein coupled receptors (GPCRs) that bear similarities to the rhodopsin family of receptors (28). As with chemokines, chemokine receptors are classed according to the positioning of conserved cysteine residues of their cognate ligands and fall into the same structural families (CXC, CC, XC and CX3C). Chemokine receptors can also be classified as inflammatory or homeostatic, according to the chemokines that they bind. Chemokine receptors and the ligands they bind are described in table 1.1.

Many chemokine receptors have the ability to bind to numerous different chemokines, but these tend to be within the same family (with the exception of DARC – see section 1.8.2). Inflammatory chemokines and receptors tend to be more 'promiscuous' than homeostatic chemokines and receptors. Homeostatic chemokines tend to form monogamous relationships with their receptors, for example the B cell associated chemokine CXCL13 only binds to CXCR5 (2, 29).

1.2.1 Chemokine Receptor Structure

Chemokine receptors share a common structure; all are ~350 amino acids in length (~40kDa). A diagram is shown in figure 1.1. The extracellular domain of chemokine receptors has an acidic N-terminus with three extracellular loops which are involved in chemokine binding (3, 6). This N-terminus is critical for chemokine binding; N-terminal truncation of chemokine receptors abrogates ligand binding and fragments containing the N-terminal of chemokine receptors can bind chemokines (9, 30, 31).

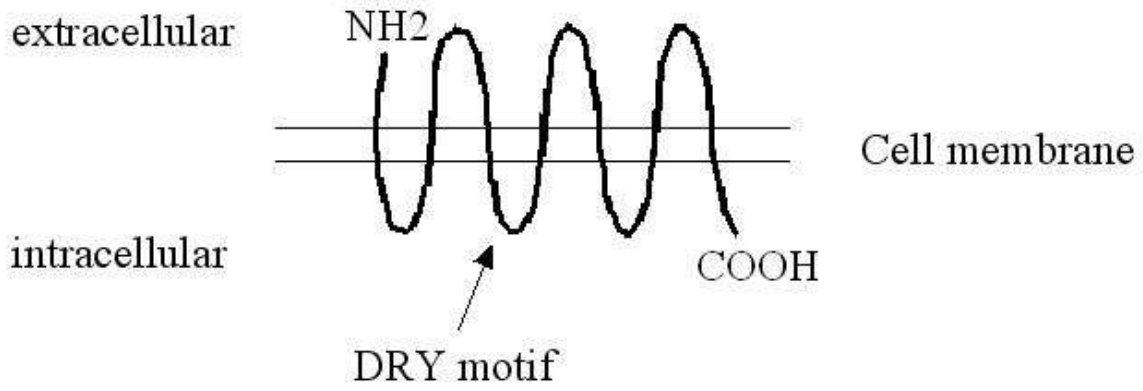

Figure 1-1: Basic chemokine receptor structure.

Chemokine receptors have a seven-transmembrane spanning structure. The extracellular acidic amino-terminus interacts with the three extracellular loops to bind to chemokines. The carboxy-terminus and the intracellular loops are involved in downstream signalling, in particular the DRY motif is essential for interactions with G proteins, required to induce signalling events.

The C-terminus and three intracellular loops are found within the cell. A common feature of chemokine receptors is the DRYLAIV motif, found in the second intracellular loop, which is essential for signalling. Chemokine receptors can be glycosylated and/or sulphated on tyrosine residues present at the N-terminal. Tyrosinase sulphation can increase the affinity of the receptor for the ligand (7).

1.2.2 Chemokine Receptor Dimerisation

Chemokine receptors have been shown to interact with one another and form dimers, this has been shown by BRET (bioluminescence resonance energy transfer) and FRET (fluorescence resonance energy transfer) analysis; homodimerisation has been shown for CCR5, CXCR2 and CXCR4 (32-35). Dimerisation can occur shortly after synthesis and is ligand independent, although ligand dependent dimerisation has been described (for CCR2 (3)). Dimerisation of chemokine receptors has been shown to alter signalling, e.g. in CCR2 co-expression with CCR5, binding of chemokine to CCR5 can block CCR2 signalling and vice versa (7, 36). This could mean that dimerisation may represent a mechanism for alternative chemokine receptor signalling in certain contexts.

1.2.3 Viral Chemokine Receptors

Viruses have evolved the ability to exploit the chemokine system to assist in their propagation throughout the body. They can do this by producing soluble chemokine binding proteins, e.g. HHV8 (herpes virus 8) encoded M3 protein binds chemokines from

all four families. CMV (cytomegalovirus) produces US28, which is a chemokine receptor thought to use constitutive trafficking to clear chemokines from the site of production, MT-7 (expressed by myxoma) is a chemokine binding protein which does not resemble chemokine receptors, but binds chemokines with high affinity (10, 37). Virally encoded chemokine binding proteins can help viruses subvert and evade the immune response, allowing their survival within the body and demonstrate the essential roles chemokines play in viral infections.

1.3 Chemokine Receptor Signalling

1.3.1 Ligand Binding

Chemokine binding modifies the tertiary structure of the chemokine receptor, which causes changes within the cell. The intracellular C-terminus of chemokine receptors is coupled to G proteins, which are essential for chemokine receptor signalling. This has been shown by treatment of cells with pertussis toxin (PTx), which blocks interactions between G proteins and GPCRs. PTx treatment does not fully block chemokine induced signalling, it only blocks association with Gi, which means that chemokine receptors can couple to other G proteins, e.g. Gq (3). The G protein complex that associates with chemokine receptors is the Gαβγ complex (common signalling pathways are shown in figure 1.2).

Upon chemokine binding, G proteins exchange GDP for GTP which causes Gαi and Gβγ to dissociate. Gαi binds to the receptor and causes conformational changes that lead to JAK (Janus kinase) association and receptor phosphorylation. Gαi and the phosphorylated receptor promotes recruitment of GRK family proteins which cause recruitment of β-arrestins and further receptor phosphorylation, which prevents further G-protein coupling (3). Gβγ induces PLC (phosholipase C) activation, which results in the release of 1,4,5-Inositol triphosphate (IP3), which causes intracellular calcium mobilization and activation of Ras and Rho pathways (4). PLC activation also causes DAG (1,2-Diacylglycerol) release that acts with free calcium to activate PKC (Protein kinase C) isoforms. PKC activates signal transduction which results in chemotaxis, adhesion, and downstream gene expression (3, 7, 38).

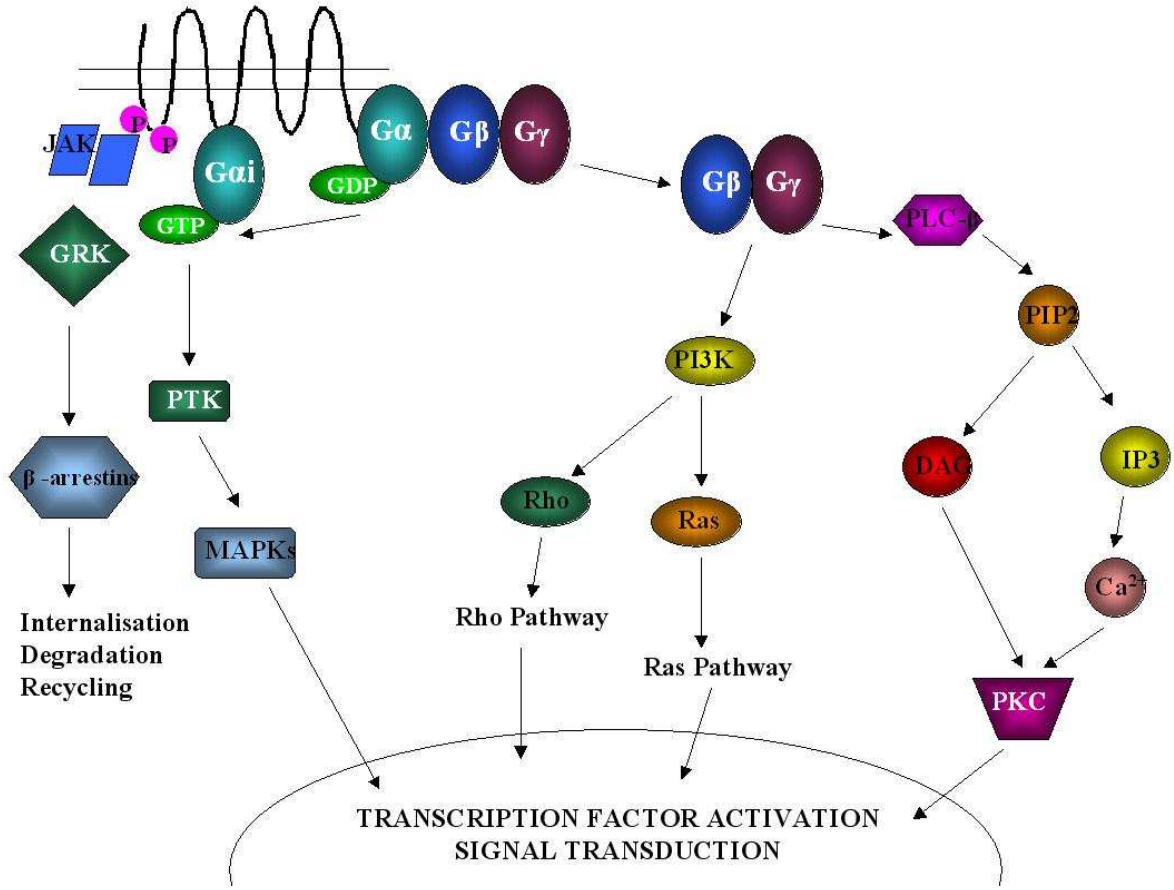

Figure 1-2: Signalling pathways activated after chemokine receptor activation.

Upon chemokine receptor binding, the G protein complex associated with the receptor exchanges GDP for GTP, which causes dissociation of Gβγ from Gαi. Gαi associates with the receptor resulting in phosphorylation and subsequent JAK/STAT association. Gαi activity also causes activation of protein tyrosine kinases and GRK which cause further receptor phosphorylation and recruitment of β-arrestins, which causes receptor desensitisation. MAPK pathways become activated, which can result in activation of transcription factors. Gβγ induce downstream signaling by activating PLC, which causes mobilization of intracellular calcium stores, and together with DAG, activates various PKC isoforms, which cause activation of transcription factors and signal transduction.

Downstream signalling can have different effects, e.g. CXCL12 induced signalling can be pro or anti-apoptotic depending on the signalling pathway induced. The downstream signalling pathways induced depend in the cell type, for example CXCL12 signalling in human CD4+ T cells induces both pro and anti-apoptotic pathways, but this has an overall anti-apoptotic effect. But in neurons, CXCL12 signalling results in apoptosis, so the downstream effects are cell dependent (39, 40). Multiple chemokine signals may result in synergy or dominance of one over the other (41, 42).

1.3.2 Receptor desensitisation

After ligand binding, the chemokine receptor can be down regulated, in a ligand dependent manner. For example, CXCL8 binding can cause down-regulation of more than

90% of chemokine receptor (CXCR1 or CXCR2) expression from the surface within 10 minutes of binding (43). The down-regulation of chemokine receptors involves interactions between GRK (G-protein coupled receptor kinase), arrestins, clathrin and dynamin.

Desensitisation of chemokine receptors can occur via steric hindrance, caused by receptor phosphorylation by GRK family proteins (3), which act on serine and threonine residues in the C-terminal tail of the receptor. Phosphorylation of the C-terminus increases the affinity for arrestins which bind and prevent G protein recruitment, this causes endocytosis, via clathrin coated pits and/or lipid rafts/caveolae. This method of desensitisation was first described for CCR2 (44). The two methods of internalisation, caveolae and clathrin coated pits, are regulated independently(2).

1.4 Chemotaxis

The movement of cells can be described in a variety of different ways, for example cell motility would be used to describe a cell that is able to move independently, sperm cells or bacterial cells for example. With respect to leukocytes, numerous different terms are used – cell migration, trafficking, chemotaxis. Cell migration tends to describe the orchestrated movement of cells to defined locations, but cells can do this in a number of different ways. Directed cell migration towards a chemical stimulus is known as chemotaxis, whilst cell movement along adhesion molecules is known as haptotaxis, both are types of cell migration (45, 46).

Not all leukocytes have the capacity to move, they require expression of the relevant chemokine receptors, for example, and they need to be in the appropriate stage of the cell cycle. If a leukocyte has this intrinsic locomotor capability, then it has the potential to undergo random or directed locomotion (45, 46). Random locomotion can be used to describe 'random walking', which has been used to describe the movement of T cells in the lymph node, observed using two photon microscopy (47). Directional locomotion describes a cell moving with either a preference or avoidance of a direction. Chemotaxis describes the directed movement towards a chemical stimulus, but this stimulus may not cause directed movement, instead it may increase the speed of a cells movement, a process known as chemokinesis (45, 46).

In relation to chemokines, the best definition of cell movement is chemotaxis, which will be described here, as it is the most common effect of a chemokine binding to its relevant receptor. Chemotaxis involves detection of a chemokine (or chemical stimulus), which causes establishment of polarity, and results in directed cell movement. Establishment of cell polarity involves changes in cell shape, integrin affinity changes and recycling at the leading edge (3). During chemotaxis, cells can interact with selectins, integrins, GAGs and chemokine receptors (7). Leukocyte migration, i.e. chemotaxis, is essential for the development of immune responses. Defective leukocyte migration (leukocyte adhesion deficiency) causes recurrent bacterial and fungal infections (48).

Chemokine binding to chemokine receptors induces a cascade of signalling events which leads to reorganisation of the cytoskeleton, to create a 'leading edge' or pseudopod, and a uropod at the other end of the cell (3). The pseudopod has a high concentration of

integrins and chemokine receptors which makes it specialised for chemokine detection (49). The uropod is similar to the pseudopod but at the opposite end of the cell and is important for motility and adhesion. Adhesion molecules such as, ICAM-1 (Inter-cellular adhesion molecule-1), L-selectin, Mac-1 and CD43 are concentrated here (2). This promotes binding of other cells which enhances recruitment and allows transendothelial migration (3). The induction of polarised morphology is not a response to a chemotactic 'gradient' as it can be seen in cells during random walking. Chemotaxis is characterised by an enhanced rate of locomotion and a unidirectional response (2).

1.4.1 Signalling - Chemotaxis

After chemokines bind to chemokine receptors the resulting signalling cascade is involved in chemotaxis. As mentioned above, chemokine receptor signalling causes the production of PI3K and PIP3 (phosphatidylinositol (3,4,5) triphosphate), which translocate to the pseudopod and co localise with Rac. PIP3 then activates Rac via guanine nucleotide exchange factors (GEFs). PIP3 can become a docking site for PKB (protein kinase B), which also translocates to the pseudopod and causes actin polymerisation. PI3K causes activation of PKC, Akt and Ras pathways that are involved in altering integrin adhesiveness, cell migration and polarisation (2).

Rho and Rac are confined to the uropod and pseudopod respectively, as they are mutually inhibitory (50). Rho activation causes focal adhesion of myosin II, which forms and contracts actin:myosin complexes. This is involved in uropod contraction. Rho prevents lamelliopodia formation, which is essential for the formation of the pseudopod. Rho family proteins have a role in regulating the actin cytoskeleton. (2).

1.4.2 Leukocyte Adhesion Cascade

In order to leave the blood, leukocytes must be able to detect chemokines. This process involves a cascade of events often referred to as the leukocyte adhesion cascade. This occurs sequentially, each step being conditional for the next.

The first step is known as rolling, which involves leukocytes in the bloodstream, binding to the vasculature via selectins. These interactions are not very strong and can easily be broken due to the shear force in the blood. This causes cells to roll along the vessel wall.

In order to stop rolling, cells require integrin activation (e.g. VLA-4, α4β7, LFA-1). Specific combinations of chemokine binding to chemokine receptors causes integrin activation, which leads to stable interactions and the cell comes to a stop (48). Once the cell has come to a stop, the cell must migrate between or through endothelial cells lining the vasculature and migrate through the basement membrane (51).

1.4.2.1 Selectins

The family of selectins consists of three members of the highly conserved C-type lectin family. L-selectin is found on most circulating leukocytes. It initiates the binding of cells to the vessel walls at sites of inflammation or injury and in HEVs. P-selectin can be expressed rapidly by endothelial cells (it is found in preformed granules) which is quickly followed by E-selectin expression, in response to inflammatory stimuli (52). These selectins are important for T cell, B cell, neutrophil, monocyte, NK cell and eosinophil recruitment (48). Rolling is mediated by L-selectin expressed by leukocytes, which can bind to P-selectin and E-selectin, on the inflamed epithelium. Selectins bind to sialyl Lewis-x like carbohydrate ligands presented by sialomucin like surface molecules, e.g. PSGL-1 (P-selectin glycoprotein ligand-1). PSGL-1 binding to L-selectin causes interactions between leukocytes and the endothelium to facilitate tethering. This selectin binding allows leukocytes to adhere to inflamed endothelium. The shear stress caused by the blood flow is required for L- and P-selectin to support their adhesion. This type of bonding is known as a catch bond, which strengthens when shear stress is applied. Selectin mediated rolling of leukocytes allows activating signals to be transmitted via the binding of chemokines to their receptors (51, 53).

1.4.2.2 Integrins

The next stage of the leukocyte adhesion cascade involves integrins, which stabilise cell rolling interactions on the inflamed endothelium. Different families of integrins exist, e.g. β1 and β2 integrins. The β2 integrin family is the main class expressed on leukocytes, e.g. LFA-1, Mac-1. LFA-1 can change its conformation to increase the ligand binding affinity under shear stress (48, 51). Chemokine induced signalling causes conformational change of integrins from intermediate to high affinity causing cell arrest, e.g. PLC (phospholipase C) activation causes activation of small GTPases which leads to integrin conformational changes (51).

1.4.2.3 Chemokine receptors

Selectin mediated rolling is stabilised by integrin interactions, but chemokine receptor signalling is required for cell arrest. Chemokine receptor signalling causes tight binding of integrins, expressed on leukocytes, to Ig (Immunoglobulin) superfamily members on endothelial cells, e.g. ICAM-1 and VCAM-1. During inflammation endothelial cells can become activated which causes expression of adhesion molecules, production of chemokines and lipid chemoattractants. These can be presented on the luminal surface of the blood vessel (51).Platelets can also deposit CCL5, CXCL4 and 5 on inflamed endothelium which can trigger the arrest of rolling monocytes. Chemokines can also be presented on GAGs which may be required for efficient leukocyte recruitment (51).

1.4.2.4 Diapedesis

Once the cell has come to a stop in the blood vessel, it must exit the vessel in the final stage of the leukocyte adhesion cascade. Diapedesis is the movement of leukocytes from the blood stream through post-capillary venules. Rap1 and RhoA are required to coordinate the process of allowing leukocytes to cross the inflamed endothelium. During inflammation, the ECM undergoes constant remodelling, and leukocytes can induce local proteolysis to aid their migration. This proteolysis may modulate chemokine binding specificity and release chemokines stored in the matrix (48). Diapedesis through endothelial vessels can occur via transendothelial, paracellular and transcellular routes. These methods require the presence of apical and junctional endothelium ICAM-1 and VCAM-1 (51).

After passing through the endothelial cell barrier, leukocytes need to get through the basement membrane and pericytes (mesenchymal cells associated with blood vessels). Within the basement membrane there are areas with low expression of matrix proteins, which makes these areas permissive for migrating neutrophils and T cells (54, 55) . These areas are found to co-localise with gaps between pericytes. In extravascular tissue, these areas may be more permissive to chemoattractants, and so create areas with high chemoattractant expression (51).

1.4.3 Therapies Targeting Chemotaxis

Altering cell migration is an attractive target for combating inflammatory conditions. There are numerous points where intervention may be possible to inhibit leukocyte extravasation, e.g. selectins, integrins or chemoattractant receptors. Targeting chemotaxis can be thought of as a 'double-edged sword'. It is difficult to develop drugs to target integrins or selectins, as the small number of targets means that drugs may be too effective, and have serious side effects. Targeting chemokine receptors is also difficult, due to the vast number of targets and the high level of redundancy in the system (53).

Despite these problems, treatments exist which target various steps in the leukocyte adhesion cascade. Natalizumab is a monoclonal antibody (mAb) against the integrin α4 chain. This blocks binding of α4β1 (VLA-4) to VCAM-1 and α4β7 binding to MadCAM-1. This has been used in MS (multiple sclerosis) and Crohns disease but it has side effects, e.g. the activation of latent viral infections which can cause encephalitis (56, 57). Efalizumab is a mAb against LFA-1 which is used in chronic moderate to severe psoriasis (51). Inhibitors of selectins can help in ischaemia-reperfusion injury and atherosclerosis (53). Although therapies do exist which target cell movement, they carry serious side effects and may not be the ideal target for these diseases, as they could have effects on normal cell trafficking.

1.5 Chemokines and Development

1.5.1 Development

Homeostatic chemokines are involved in tissue specific migration and lymphoid tissue development. CXCL12 and CXCR4 are essential for normal development, they are known as the primordial chemokine and receptor. Gene null mouse studies have been very useful in defining the roles that CXCL12 and CXCR4 play throughout development. CXCL12 null mice die perinatally and have B cell lymphopoiesis defects, as well as problems with the bone marrow microenvironment. These effects can also be seen in CXCR4 null mice. These studies revealed the essential role that CXCR4 has in embryogenesis, myelopoeisis, B cell lymphopoiesis and organ development. CXCL12 and CXCR4 are also involved in the localisation and retention of progenitors in the bone marrow (58-62).

1.5.1.1 Thymus

Throughout T cell development in the thymus, thymocytes change their chemokine receptor expression in order to move into different areas of the thymus. Thymic dendritic cells produce CCL25 and the expression of CCL25 is important for the early stages of thymocyte development, where they express CCR9. This CCR9 expression is lost as thymocytes undergo maturation and CCR7 expression is upregulated. This switching of chemokine receptors allows mature thymocytes to leave the thymus, and is essential for T cell development. As a result of this chemokine receptor expression, the important chemokines in thymic development are CCL19, CCL21 and CCL25 (63, 64).

The use of CCR7 KO mice has clarified the essential role that CCR7 plays in the development of T cells and how T cells rely on the thymic microenvironment. CCR7 is important for thymic compartmentalisation, if mice lack CCR7 (CCR7 KO mice or plt/plt mice – see section 1.5.1.2 for more details) then the architecture of the thymus is altered, which results in impaired T cell development and a reduction in the numbers of thymocytes (65-68). CCR7KO mice also have problems with the process of negative selection, which is responsible for eliminating autoreactive T cells – this process does not occur in CCR7 KO mice. This impaired negative selection may be due to a reduced responsiveness of these cells to TCR stimulation (69), or due to impaired migration from the cortex to the medulla (70). This may contribute to the spontaneous autoimmunity

exhibited in these mice; alternatively it could be caused by incomplete peripheral tolerance or defects in Tregs (71). As well as having problems with the development of T cells within the thymus, CCR7KO mice have a reduction in foetal haematopoietic progenitors in the thymus. These cells are the precursors for T cells and require CCR7 to get into the thymus.

1.5.1.2 Lymphoid Tissue

As with embryonic and thymic development, the development of lymphoid tissue (e.g. lymph nodes and Peyers patches) is dependent on chemokines. Chemokines are important during development and during the initiation of immune responses in lymphoid tissue; chemokines are involved in naïve T cell homing, B cell localisation in follicles, and cell recruitment via HEVs (37). The most important chemokine receptors with respect to lymphoid tissue development and function are CCR7 and CXCR5.

The development or organogenesis of lymphoid tissue has been shown to rely on the chemokines CXCL13, CCL19 and CCL21. The initial development of lymphoid tissue starts with clustering of two groups of cells – lymphoid tissue inducer cells (LTICs), which are IL17R+CD3-CD4+CD45+ and stromal cells (VCAM1+ and ICAM1+). After this initial clustering, LTICs express LTα1β2 which can bind to LTβR on the stromal cells, and cell adhesion occurs via interactions with VCAM1. LTβR signalling causes the production of CXCL13, CXCL4, CCL19 and CCL21, which recruit more haematopoietic and stromal cells, creating a positive feedback loop. Once a large enough cell cluster has developed, blood vessels differentiate to become HEVs, and a lymphoid organ is formed (72-74).

CCR7 is essential for cell entry into the lymph node; it is used to guide T cells, B cells and DCs into the T cell areas of lymph nodes, facilitating antigen presentation and the initiation of an adaptive immune response. CCR7 is able to guide cells here due to the production of its ligands, CCL19 and CCL21, which are constitutively produced by stromal cells, CCL21 can also be produced by the endothelial layer of HEVs (75, 76). Mice lacking CCR7 have impaired cell migration into Peyers patches and peripheral LNs, they have increased numbers of T cells in the peripheral blood, which correlates with reduced T cell numbers in the LN (77). These mice have migration problems with their T cells, which fail to home to the LN, and DCs which are unable to leave dermal tissue to get to the draining

LN. Further problems with these mice, include the development of spontaneous autoimmunity and disorganised lymphoid architecture (71).

The plt/plt (paucity of lymph node T cells) is a naturally occurring strain of mutant mouse, which has lost the genes encoding CCL19 and CCL21-ser isoform, but the genes for CCL21-leu still remain. This means that these mice lack expression of CCL21 in lymphoid organs, but still express CCL21 in lymphatic vessels of non-lymphoid organs. These mice suffer from various defects, including defective thymic architecture, which means T cell development is impaired. Plt/plt mice have impaired migration of CCR7 positive T cells and DCs into lymphoid organs, resulting in reduced numbers. The mobilisation of DCs can still occur in the periphery, due to the expression of CCL21-leu (67, 68, 78, 79). Studies using these mice have shown the essential role that CCR7 and its ligands, CCL19 and CCL21, play in the recruitment of cells into the lymph node and the development of immune responses.

Whilst CCR7 and its ligands are mainly responsible for T cell and DC migration and placement in lymphoid organs, CXCR5 and its ligand CXCL13 are responsible for the segregation of lymphoid organs into distinct T and B cell areas and the movement of B cells within lymphoid tissue. Stromal cells in the B cell follicles of secondary lymphoid organs constitutively express CXCL13 and CXCR5 is expressed on mature circulating B cells. In mice lacking CXCR5, there is a defect in the segregation of T and B cells in the spleen and PP, which is similar to that seen in CXCL13 KO mice. Study of these mice led to a startling discovery that CXCL13 and CXCR5 are involved in lymphoid organ development, these mice lack (or are present at low frequency), peripheral LNs and PP (76, 80, 81).

As well as being involved in homeostasis and development, homeostatic chemokines can be upregulated during chronic inflammation. Here they can contribute to the formation of ectopic lymphoid follicles, e.g. in rheumatoid arthritis (82, 83).

1.6 Chemokines and the Immune Response

1.6.1 Innate Cells

Pathogens first encounter the immune system via the innate immune system. This developed to respond rapidly to invading pathogens, and to allow an adaptive immune response to be generated. Pathogens cause activation of TLRs (Toll-like receptors) via conserved PAMPs (pathogen associated molecular patterns). These trigger production of a wide range of inflammatory cytokines and chemokines, which creates a pro-inflammatory environment. Chemokines can also be produced under the influence of fibrinogen, elastins, defensins, and cytokines such as, IL1, TNFα, IFNγ, IL4, IL5, IL6, IL13 and IL17, all of which can be produced during infection (84-86). Chemokines then cause cellular recruitment to the site of inflammation, which include neutrophils, macrophages, NK cells and DCs (dendritic cells). Dendritic cells, both resident and those recruited via inflammatory chemokines, are specialised to phagocytose foreign antigens. They act as the 'bridge' between the innate and the adaptive immune system by presenting antigens to T cells in the lymph nodes (87).

The main job of neutrophils and monocytes is to arrive at the site of infection to phagocytose pathogens, as well as to produce nitric oxide and reactive oxygen species. Neutrophils are the first cells to arrive at the site of infection and can both protect and cause tissue injury. IL1 and TNFα cause the production of chemokines which attract and activate neutrophils at the site of infection and inflammation, as well as chemokines that bind to CXCR1 and CXCR2, the main chemokine receptors expressed by human neutrophils. Blocking both of these receptors can inhibit neutrophil migration in vivo (38). Monocytes are the next cells to arrive at the site of inflammation, their recruitment involves CCL2, 7, 8 and 13 (CCR2 and CCL2 have a non-redundant role in monocyte recruitment (88)).

1.6.2 Dendritic Cells

In order to communicate between the innate and adaptive immune systems dendritic cells (DCs) are essential. Immature DCs arise in the bone marrow and they are able to migrate to the periphery and secondary lymphoid organs. DCs can also arise from circulating monocytes. Within a lymph node there can be up to 6 different DC subsets

(89). The main job of DCs is to process antigen and present it to T cells in the context of MHC, thus helping to mount an adaptive immune response. In order to do this, DCs must mature and migrate to the lymph node from the site of inflammation, where they can interact with antigen specific T cells. This involves down-regulation of chemokine receptors (which are required to get to the site of inflammation) and upregulation of CCR7. This can occur under the influence of bacterial products such as BLP (bacterial lipoprotein) (90). CCR7 allows DCs to migrate into the lymph node and reach the T cell area (2). Immature DCs express CCR6 (which binds CCL20), as well as inflammatory CC chemokine receptors, such as CCR1-3. As DCs become mature they express CCR7 (binds CCL19 and 21). LPS causes a reduction of CCR1-3 expression, and causes an increase in CCR7 on DCs (91). This receptor switching is essential for DCs to leave the site of inflammation and reach the lymph node (38).

1.6.3 T Cells

T cells are responsible for mounting an adaptive immune response to antigens. Once dendritic cells become activated at the site of infection, they migrate to the lymph nodes, where they present antigen (in the context of MHC) to antigen specific T cells. These T cells become activated and can provide help to B cells to produce antibody, or have directly cytotoxic effects on infected host cells, depending on the type of T cell activated (CD4+ and CD8+ respectively).

Naïve T cells circulate and express L-selectin, LFA-1, α4β7 integrin, CXCR4 and CCR7. CCR7 is the chemokine receptor responsible for T cell entry into the lymph node. CCR7 ligands can be produced by HEVs (CCL21), or produced in the lymph node and transcytosed to the luminal surface of the HEVs (CCL19) (2). Within the lymph node, T cells move into the T cell area due to production of CCL19 and CCL21, which are produced by mature DCs and stromal cells (79, 92). For T cells to move into the B cell follicles and provide help for antibody production, CXCR5 must be up regulated. Cell exit from the lymph node involves the alteration of chemokine receptor expression, but more importantly, it depends on the expression of a different type of seven transmembrane receptor, S1P. S1P is a receptor that is involved in T and B cell exit from lymphoid tissues. The discovery of the role this receptor plays in lymphocyte egress occurred through studies using FTY720. FTY720 is a compound that was found to induce a rapid loss of lymphocytes from the blood, in actual fact, it inhibits lymphocyte egress from LNs, by binding to 4 out of the 5 S1P receptors. In

the LN, when T and B cells have recognised antigen on DCs, S1P1 is down regulated. This allows them to remain in the LN (through signals from chemokines) to activate and proliferate. After activation and proliferation, S1P1 is upregulated, which allows cells to leave the LN. Studies in vitro have shown that high concentrations of S1P (an S1P1 ligand) causes cells to have reduced responsiveness to chemokines, which may explain the mechanism by which S1P allows egress from the LN (76).

CCR7 expression is essential to allow T cell exit from the site of inflammation and entry to the lymph (93). The location of chemokines within the lymph node, allows co-localisation of T cells with DCs, which allows the initiation of immune responses (94, 95). Evidence suggests that chemokines signalling through chemokine receptors are able to modulate T cell responses via the TCR, which may allow T cell movement to the lymph nodes or keep T cells at the site of inflammation, depending on the chemokine stimulus (96). Mice with defects in CCR7 expression, or its ligands, have numerous problems relating to T cell localisation and lymphoid tissue organisation, which have been discussed in detail above.

T cells can fall into various different subsets, depending on the production of cytokines and expression of chemokine receptors. Th1 cells develop under the influence of IFNγ. They produce IFNγ and IL-2, which can be involved in acute and chronic inflammatory diseases. CCR5 and CXCR3 are expressed by Th1 cells and their ligands are expressed in Th1 associated diseases, e.g. rheumatoid arthritis, atherosclerosis and MS (95).Th2 cells develop under the influence of IL4, they are CCR3 positive and its ligands are expressed in allergic inflammation. Th2 cells can also transiently express CCR4 and CCR8 (37, 95).

Th17 cells are a recently discovered T cell subset that has distinct functions from Th1 and Th2 cells. Th17 cells are involved in the clearance of pathogens that are not cleared by Th1 or Th2 cells. Naïve T cells develop into Th17 cells under the influence of TGFβ plus IL6 and IL21, and they produce IL17, IL22 and IL23. Th17 cells have close ties to another T cell subset, regulatory T cells (Tregs). In the presence of TGFβ, a naïve T cell will become a FOXP3+ Treg, but if TGFβ is present with IL6 plus/or IL21 then that cell will become a Th17 cell. IL6 is crucial in determining the balance between Tregs and Th17 cell, CCR6KO mice have increased numbers of Treg and defective Th17 cell generation. Th17 cells are found mainly at barrier sites, mucosal surfaces in particular, and are thought to protect the host against microorganisms which invade at these sites (97-99). Th17 cells have been

implicated in autoimmune diseases and inflammation, for example EAE, CIA and some colitis models (100).

T cells are not only activators of the immune system; populations exist which have suppressive capabilities. FOXP3+ Tregs are required for immune homeostasis – they are able to suppress immune responses and inflammation. The initial discovery of Tregs was after the observation that mice that underwent a neonatal thymectomy had chronic inflammation in numerous tissues (101). Tregs are CD4+ CD25+ FOXP3+, but in contrast to CD4+CD25- T cells, they do not proliferate after TCR engagement. Instead Tregs suppress the proliferation of other effector T cells, and this occurs in a contact dependent manner. FOXP3 expression is essential for Treg differentiation, high expression is a characteristic feature of Tregs. They are produced in the thymus, but can also develop in the periphery, particularly in the gut where retinoic acid and TGFβ act together to induce high numbers of Tregs, at the cost of effector T cells (102-104).

Tregs are able to suppress the activation, proliferation and effector functions of a wide range of cells, meaning they are able to prevent autoimmunity, allergy, and can suppress responses against tumours. CD4+CD25+ FOXP3+ are known as natural Tregs, but other subsets of regulatory T cells exist, subsets that are inducible T regs. These include Tr1 cells, which can be induced if naïve T cells are primed with antigen in the presence of IL10. Tr1 cells produce large amounts of IL10, IL5 and TGFβ, but low levels of IFNγ and IL2 (105). CD4+CD25- T cells can be induced to express CD25 and FOXP3 in the periphery, under the influence of TGFβ, a cell population referred to as inducible periphery Tregs (106). Whilst TGFβ can induce the development of inducible Tregs in the periphery, by upregulating the expression of FOXP3, if IL4 (a classical Th2 associated cytokine) is present at the point of priming, the expression of FOXP3 is suppressed (107). These cells can produce IL9 and IL10, but don't appear to have any regulatory function; after adoptive transfer they promote tissue inflammation (108). This recently discovered subset has been named 'Th9' cells. Th9 cells have also been shown to develop from Th2 cells, TGFβ can reprogram Th2 cells to lose expression of IL4, IL5 and IL13 and upregulate IL9 (109). The role for Th9 cells is not yet clear, but it has been suggested that they are involved in both tissue inflammation and responses against helminths (107-109).

Another subset of T cells are known as follicular helper cells (Tfh), they have the unique ability to home to B cell follicles. Tfh are CXCR5+, can secrete IL10 and have a role in B cell

differentiation. Tfh precursors migrate to the border of the T and B cell area, and they can continue into the follicle where they can continue their differentiation, under the influence of B cell interactions and cytokines. There is evidence that Tfh can produce IFNγ and IL17, and they may have a role in autoimmunity (110-112).

Following activation, naïve T cells can become memory T cells. These cells are specialised to mount rapid responses if re-challenge occurs with the same antigen, which is a unique feature of the adaptive immune response. There are two main types of memory T cells, central memory and effector memory. Central memory T cells can migrate into lymph nodes and enter sites of inflammation. Central memory T cells have a high proliferative capability as well as being able to stimulate DCs and provide B cell help (113). Effector memory T cells do not express CCR7, so they cannot traffic to the lymph node and are subsequently found in the tissues. This means they are suitably positioned to mediate direct cytotoxic effects upon re-challenge and can rapidly create an inflammatory environment through the production of cytokines (2, 113).

1.6.4 B Cells

The main purpose of B cells is to produce specific antibodies, essential for the mounting of an adaptive immune response. As with other cells of the immune system, B cell responses can be controlled by chemokine receptors. All mature circulating B cells express CXCR5, which is involved in their developmental positioning. CXCR5 binds to CXCL13, which is produced in the B cell areas of lymphoid tissue and is found on HEVs in the follicles. It is essential for follicle formation in the spleen and lymph node. CXCR5 can be found on a small subset of T cells (114, 115). CXCL13 can increase integrin affinity and allow B cells to traverse the T cell areas of the lymph node to enter the follicles (116). IgG producing plasma B cells are found in the bone marrow due to interactions between CXCR4 and CXCL12. IgA secreting B cells are CCR9 or CCR10 positive, and are found in the gut or the skin respectively (2).

1.7 Tissue Specificity

1.7.1 Skin Homing

Chemokines and chemokine receptors can be used as a type of 'address' system, to confer tissue specificity to cells. This tissue specificity is imprinted in the draining lymph node and is dependent on APCs (antigen presenting cells). Populations of DCs exist which are skin specific. These are known as Langerhans cells. In the skin, antigens are phagocytosed and presented by Langerhans cells in the draining lymph node. The combination of a skin-specific DC (which may be a Langerhans cell or another type of skin specific DC), presentation in the skin draining lymph node and the presence of vitamin D, confers skin-specificity to T cells (117-119). To generate T cells that are capable of migrating into the skin, specific chemokine receptors must be upregulated; CCR4 and CCR10 are required for cell homing to the skin. Skin homing T cells express CCR4, which binds CCL17 and CCL22 in blood vessels in the skin, and CCR10, which binds CCL27 and CCL28. As well as the expression of skin specific chemokine receptors T cells have to express CLA (cutaneous lymphocyte-associated antigen). CLA positive cells can enter the skin via E-selectin expression in the blood vessels in the skin (95, 120, 121).

1.7.2 Small Intestine Homing

Similar to the skin, the gut has its own chemokine 'address' system, which is imprinted onto T cells at the point of antigen presentation. In the gut and its associated lymphoid tissue (Peyers patches and mesenteric lymph nodes), DCs present antigen to T cells in the presence of the vitamin A metabolite, retinoic acid. The presence of retinoic acid 'imprints' T cells in the gut, causing upregulation of α4β7 integrin and CCR9 (122). CCR9 is needed for homing to the small intestine, where it binds CCL25. Gut homing T cells express CCR9 which binds CCL25, and α4β7 which binds MadCAM1 on intestinal blood vessels (123). Myeloid DC localisation in the subepithelial dome of the Peyers patch is CCR6 dependent. When DCs in the gut become mature, the levels of CCR6 expression is reduced, which allows the cells to leave the dome and enter the T cell area in the Peyers patches. The crucial role of CCR6 in intestinal immunity is shown using CCR6 null mice, which have defects in humoral immunity in the intestinal mucosa. (124). Closely regulated

expression of these chemokine receptors ensures that gut-specific cells are able to home to the gut.

1.8 Atypical Receptors

The chemokine system is further complicated by the existence of a family of 'atypical' receptors. All members of this chemokine 'receptor' family share the apparent inability to signal in response to ligand binding, which is a result of an alteration in amino acid sequences within the second intracellular loop, known as the DRY motif. This motif is responsible for coupling the receptor to G proteins and resulting downstream signalling (125, 126). This appears to be the only unifying characteristic of these receptors. The apparent lack of signalling means that these receptors should be referred to as chemokine binding proteins, as they do not fit into the classical definition of a receptor (127). Members of this family include D6, DARC, CCX-CKR and CXCR7 (128). The ligands they bind are described in Table 1-2.

Receptor	Ligands
D6	CCL2, CCL3, hCCL3L1, CCL4, hCCL4L1, CCL5, CCL7, CCL8, CCL11, CCL13, CCL17, CCL22
DARC	CCL2, CCL5, CCL7, CCL11, CCL13, CCL14, CCL17, CXCL5, CXCL6, CXCL8, CXCL11
CCX-CKR	CCL19, CCL21, CCL25
CXCR7	CXCL11, CXCL12

Table 1-2: Ligands of atypical chemokine receptors in both humans and mice (adapted from (129, 130)).

1.8.1 D6

1.8.1.1 Discovery of D6

D6 was first discovered in 1997 during a search for novel CCL3 receptors (130, 131). D6 was identified as a novel human β chemokine receptor that had high structural and functional homology to murine D6 (also discovered around the same time). In order to be given a name according to the systematic nomenclature, evidence of signalling had to be demonstrated, but since there was no evidence of signalling, the receptor was designated D6 (otherwise it would have been CCR9) (130). Murine D6 was originally cloned from brain cDNA (131) and its sequence contained the predicted seven transmembrane spanning regions and four conserved cysteines characteristic of a chemokine receptor (131).

1.8.1.2 D6 Ligands

D6 has the ability to bind to 12 different CC chemokines, as shown in table 1.2. All of the ligands that D6 can bind to are inflammatory CC chemokines and there appears to be a certain degree of specificity in ligand binding, requiring a proline residue in position 2 of the mature chemokine. As a result, the binding of chemokines to D6 can be regulated by CD26 processing, since CD26 can cleave chemokines which have a proline or serine at position 2 (132). For example, human CCL3L1 has a proline at position 2 and binds D6 with high affinity, whilst CCL3 with a serine at position 2 has reduced binding capability for D6 (133) and another D6 ligand, CCL22 loses the ability to bind to D6 with high affinity after processing by CD26 (128).

1.8.1.3 Structural Characteristics

The amino acid arrangement of D6 was inferred from its amino acid sequence, and was predicted to have seven transmembrane spanning domains, similar to all other chemokine receptors. Features common to chemokine receptors that were identified include the presence of four conserved cysteines, as well as a putative N-linked glycosylation site at the amino terminus. The carboxy terminus of D6 was found to contain potential phosphorylation sites, as it was rich in serine and threonine residues. Subsequent studies showed that D6 undergoes glycosylation and sulphation in a ligand independent manner, as well as being constitutively phosphorylated (134). Human and murine D6 were found to be similar (with 71% identity and 86% similarity), and compared to other CC chemokine receptors, D6 has on average, 40% identity and 50% similarity. The signalling motif which is found in the second intracellular loop of other chemokine receptors, DRYLAIVHA, was found to be altered in D6, to DKYLEIVHA (130). This alteration in the key signalling motif is thought to be responsible for the absence of calcium fluxes and chemotaxis upon ligand binding. D6 is capable of binding chemokines, internalising them, and subsequently targets them for degradation (135).

In vitro more than 95% of D6 is found in early and recycling endosomes meaning only ~5% of D6 is found on the surface at any one time (136), this is because D6 is constitutively recycling, even in the absence of ligand. In the absence of ligand D6 internalisation is dependent on Rab4 and Rab11 (137) whilst after ligand binding, D6 internalisation requires Rab5, and may or may not require β arrestins (138, 139). Internalisation of D6

occurs via recycling endosomes, which results in the ligand bound to D6 being deposited in acidic lysosomes and being degraded. Ligands that are bound and internalised by D6 are more readily retained within the cell, compared to ligand internalisation by CCR5, as the movement through acidic endosomes causes rapid dissociation of ligands from D6 but not CCR5 (136). D6 contains a serine cluster in its carboxy terminus, which prevents it from entering Rab 7 positive late endosomes, and ensures receptor recycling, rather than degradation of D6 (138). The internalisation of D6 is associated with, but apparently not dependent on, ligand-independent phosphorylation of the C-terminus. Evidence for this has been shown by the removal of the most C-terminal 44 amino acids, or mutating 6 serine residues in the C-terminus, which blocks phosphorylation but has little effect on ligand internalisation (138).

Evidence exists to suggest that D6 is able to interact with other signalling chemokine receptors. Despite its low cell surface expression, D6 has been found to form homodimers, and heterodimers with CCR1, and within the cell D6 can form heterodimers with CCR5 (140). In transfected L1-2 cells, D6 does not induce calcium fluxes after ligand binding, and it appears to be able to blunt chemotactic responses to CCL22, which can bind both D6 and CCR4. When co-expressed with CXCR4, D6 has no effect on chemotaxis towards CXCL12. These results suggest that D6 may in some way, perhaps through an as yet undefined signalling mechanism, interfere with CCR4 signalling and disrupt chemotactic responses, but this work uses an artificial system of transfected cells, and may not reflect the true function of D6 in vivo (141).

These characteristics of D6 have been led to the suggestion that it is a chemokine decoy receptor and functions by clearing inflammatory chemokines from the site of inflammation.

1.8.1.4 D6 Expression

D6 has been shown to be expressed in the lung, skin, liver, spleen, heart, brain, thymus, ovary and muscle in mouse (142). In humans, expression of D6 has been demonstrated on trophoblast cells of the placenta, skin, lymphatic endothelial cells, lung and leukocytes (143, 144).

1.8.1.4.1 Leukocyte Expression

Interest in leukocyte expression of D6 was based on analysis of its promoter and the discovery that it has many putative transcription factor binding sites associated with haematopoietic cells, e.g. GATA1, Ikaros (144). In human cell lines, D6 is expressed on K562, HMC-1, Meg-01, THP-1, Jurkat and Molt-4 cells (listed from highest expressing to lowest expressing) (144, 145), but expression levels of D6 may not correlate with its function. For example, HMC-1 cells have higher D6 expression than THP-1 cells, but they have a lower level of CCL2 uptake (which can be out-competed with CCL3 – this shows D6 specific uptake). The expression of D6 can be altered by causing cell differentiation, for example in Meg01 cells, an increase in D6 expression is seen upon differentiation with TPA (12-tetradecanoyl 13-phorbol acetate)(144). D6 expression has also been demonstrated on breast cancer cell lines, high expression on lowly invasive cells, low expression on highly invasive cells (146).

As well as expression by human cell lines, expression has been shown on primary human cells, with B cells showing the highest expression of D6. In particular, marginal zone B cells express more D6 compared to follicular B cells in the spleen (147). Plasmacytoid dendritic cells, myeloid dendritic cells and B cells from human peripheral blood, as well as human monocytes have been shown express D6, and the expression of D6 on monocytes has been shown to increase 100 fold upon maturation to macrophages (144). The analysis of D6 expression on human cells was carried out using an antibody against D6, unfortunately no antibody is available that is specific for murine D6, so analysis in murine cells has been carried out by QPCR (144). Primary murine cells express D6 at the highest levels on B cells, mast cells and dendritic cells, whilst murine CD4+ T cells, macrophages and neutrophils express D6 at low levels. On B cells, D6 is expressed at a higher level than on T cells. (144).

If D6 does indeed function as a scavenging decoy receptor on leukocytes it may be involved in regulating chemokine levels in situ. Its expression may be constitutive or inducible, depending on the cell type involved. In vitro work suggests that D6 may affect responses of CCR4, so it is possible that in vivo, D6 co-expression with signalling chemokine receptors may alter that cells movement, but this work was carried out in transfected cells, that may express higher levels of D6 than those found in vivo. More work is required to determine the precise role that D6 plays in leukocytes. D6 expression on leukocytes may be involved in regulating chemokine levels in situ, for example

leukocytes that express D6 may be able to degrade chemokines presented on the luminal face of the vasculature. If D6 expressing cells express other inflammatory chemokine receptors, they may be involved in reducing the chemokine levels at the site of inflammation, through the activity of D6. D6 expression may be constitutive or inducible, and previous work suggests that D6 may blunt chemotactic responses to other signalling CC chemokine receptors (141). This may represent a mechanism by which D6 can limit cell movement, e.g. stopping cells once they get to the site of inflammation. If D6 on leukocytes blocks responses to inflammatory CC chemokines, it may allow cells to exit via CCR7, e.g. dendritic cells and T cells (148).

1.8.1.4.2 Regulation of Expression

As mentioned above, leukocyte expression of D6 can be regulated by maturation of both primary cells and cell lines. The expression of D6 in DCs has been shown to be dependent on GATA1, as mice with a conditional deletion of GATA1 lack D6 expression on DCs. The expression of D6 has also been shown to be affected by both pro and anti inflammatory stimuli, in monocytes LPS reduces D6 expression, whilst TGFβ increases D6 expression (90). These results suggest that during ongoing inflammation, D6 levels may be at a low level, and when inflammation is being resolved, D6 expression may be upregulated, which could aid in the resolution of inflammation. In the breast cancer cell line MDA MB 231, D6 expression can be up-regulated by IL-1β and TNF (128, 146). These data show that the expression of D6 is dynamic and can be regulated by both pro and anti-inflammatory cytokines, which may effect the expression of D6 by leukocytes, and this may vary depending on the cell type.

1.8.1.4.3 Lymphatic Endothelial Cells

In humans, D6 has been shown to be expressed by lymphatic endothelial cells, in the gut, the skin and secondary lymphoid tissues. D6 expression is lost after in vitro culture of these cells, and not all lymphatic epithelial cells express D6 (143). D6 expression on lymphatic endothelial vessels may ensure that inflammatory CC chemokines are not present on the surface of the vessels. This environment may allow GAGs to present constitutive chemokines, such as CCL21 that can bind to CCR7 on circulating dendritic cells and only allow mature DCs to enter the lymph node. If inflammatory chemokines are presented on the lymphatic endothelium, this may allow entry of immature dendritic cells to the lymph node. The role for D6 in preventing inflammatory chemokine entry to the lymph node has been supported by observations that in D6KO mice, more inflammatory

chemokines are present in the lymph node, but the source has not been determined (149). During inflammation large levels of inflammatory chemokines are produced, and these may overwhelm the scavenging capabilities of D6, which may explain the presence of these chemokines in the draining lymph nodes (148). However D6 expression has not been shown in murine lymphatic endothelial cells, so these observations may be caused by a lack of chemokine scavenging by cells that would normally express D6. Further work needs to be carried out to conclusively define the role that D6 plays on chemokine entry into the lymph nodes.

1.8.1.4.4 Placenta

Within the placenta, D6 has been found on invading trophoblast cells, on the apical side of syncytiotrophoblasts and decidual macrophages (150). JAR, JEG3 and Bewo cells (syncytiotrophoblast cell lines) are all D6 positive and D6 has been shown to function as a scavenger in trophoblast cell lines (151). The expression of D6 within the placenta has been investigated using in vivo models, which will be discussed in section 1.8.1.5.7

1.8.1.5 D6 in Pathology

Using a variety of murine models, the role of D6 has been investigated in numerous disease states, from inflammation to cancer. These will be discussed in detail below.

1.8.1.5.1 TPA Induced Skin Inflammation

The model of TPA induced skin inflammation involves treating mice with TPA (painted on shaved dorsal skin) on three consecutive days. This treatment causes inflammation typified by an increase in chemokine levels, and the development of a psoriasis like pathology. The pathology is characterised by skin thickening and keratinocyte hyper-proliferation. Cytokines are rapidly produced after TPA application and TNFα levels are increased after 60 minutes. Chemokines such as CCL1, CCL2, CCL3, CCL4, CCL5, CCL11, CXCL2 and CXCL10 are produced within 4-8 hours after TPA administration. Comparing the inflammatory response in WT mice and those lacking D6, show that both genotypes have increased levels of CC chemokines during inflammation, with chemokine levels peaking at 8-12 hours in WT mice, clearing by 24 hours. In contrast, D6KO skin takes longer to clear inflammatory CC chemokines, resulting in an exaggerated inflammation that does not resolve until 6-10 days post treatment, compared to 4 days for the resolution of inflammation in WT mice (152).

The cells that have been identified as being involved in the exaggerated inflammatory pathology exhibited in D6KO mice include dermal macrophages, mast cells, epidermal T cells and neutrophils. Neutralising antibodies, used to block CD4+ and CD8+ cell recruitment prevents the pathology caused by TPA. Further antibody neutralisation studies show that the inflammatory pathology is dependent on TNFα, which is produced by cells within the skin, and this increase in TNFα levels causes further cell recruitment via chemokine production, e.g. mast cells. Therefore it can be said that the pathology induced by TPA in D6KO mice is dependent on TNFα and T cells, as well as being characterised by an influx of mast cells (152).

To summarise these findings, after TPA treatment of the skin WT mice produce inflammatory chemokines, which causes a transient leukocyte recruitment to the skin and resolution of inflammation 4 days after TPA treatment. In contrast, D6KO mice show an exaggerated response to TPA treatment of the skin, with epidermal hyper-proliferation, differentiation, angiogenesis, accumulation of epidermal T cells and mast cells, which all contribute to an exaggerated pathology, which remains 10 days after TPA treatment. These data illustrate the role that D6 plays in the resolution of cutaneous inflammation (128).

Recent work using the TPA model of skin inflammation has focused in on dissecting the role that D6 plays on neutrophil migration. In D6KO skin after treatment with a single dose of TPA, neutrophils are found at the dermal/epidermal junction, whilst in WT skin, neutrophils are found lower down in the dermal compartment. In this model there could be two explanations; a lack of D6 prevents clearance of inflammatory chemokines at the dermal/epidermal junction, allowing neutrophils to localise here, or a lack of D6 on neutrophils means that their migration into the skin is altered. The addition of a CCR1 antagonist reverses this aberrant neutrophil accumulation seen in D6KO skin, suggesting that CCR1 is involved in this phenomenon. Experiments injecting compound 48/80 (a mast cell degranulation agent) into the skin shows that D6KO mice have more severe tissue damage than WT, with increased numbers of neutrophils at the site. Intraperitoneal injection of CCL3 shows an increased neutrophil infiltrate in D6KO mice compared to WT. These data point to a role for D6 in influencing neutrophil migration, potentially by modulating chemokine levels at the site of inflammation, or influencing their responses to inflammatory chemokines (140).

1.8.1.5.2 EAE

EAE is used as a mouse model of MS; it involves immunising mice against a component of the myelin sheath, known as the MOG peptide that is administered subcutaneously in CFA (Complete Freunds adjuvant). Administration of the MOG peptide causes the production of antigen specific T cells that contribute to the destruction of the myelin sheath, causing disease symptoms. The contribution of T cells to disease development can be shown by adoptively transferring T cells from mice showing EAE symptoms, to untreated mice, which will develop disease (153). D6KO mice appear relatively resistant to EAE, with a reduced disease severity, reduced cell infiltration and demyelination. The reduced disease severity in D6KO mice appears to be caused by an impaired priming of T cells. Adoptively transferring T cells from D6KO mice shows that these cells have a reduced ability to cause EAE, but this is not due to a defect in proliferation – these cells can still proliferate with mitogen, but with antigen they cannot proliferate to the same extent as WT cells. T cells isolated from D6KO mice produce less IFNγ, so it has been suggested that a lack of D6 results in altered antigen presentation and as a result T cells are not activated effectively. Looking at the site of immunisation, D6KO mice show an altered and enhanced inflammatory response, revealed by the presence of inflammatory foci, leukocyte infiltrate (including aggregates of CD11c+ DCs) and angiogenesis. The presence of accumulations of DCs in the skin of D6KO mice may indicate that these cells cannot leave the skin, which may cause a reduction in antigen specific T cell activation, and may explain the reduced disease severity exhibited (153, 154).

1.8.1.5.3 Allergic Asthma

In the classic model of allergic lung inflammation, OVA was used to induce lung inflammation in both D6KO and WT mice, using two different challenge protocols – short and long term. During short-term challenge protocols, CCL17 levels were increased in D6KO mice compared to WT mice, but this was not seen in prolonged challenge models. D6KO mice consistently had more eosinophils, CD4+ T cells, B cells and DCs in the lungs, in both challenge protocols, which indicates a higher level of inflammation. Despite this higher inflammation, D6KO mice showed reduced airway responsiveness. These results suggest that D6 may be able to alter the local chemokine concentration of the lungs, when low levels are produced (i.e. in the short term challenge protocol), but when higher levels are present (long term challenge) D6 has no effect on chemokine levels, as the concentration may overwhelm the scavenging ability of D6. In light of these results, it has

been proposed that inhibition of D6 may represent a potential treatment for patients with allergic asthma (155).

1.8.1.5.4 Inflammation Induced Skin Tumours

The development of cancer is a multi-step process, which can be driven by inflammation and chronic inflammation is well known to predispose people to cancer (156). A murine model of inflammation driven skin carcinogenesis involves painting the skin with a mutagen, in this case DMBA (7,12-Dimethylbenz (α) anthracene), followed by the induction of cutaneous inflammation by painting the skin with TPA. Tumours begin as benign papillomas, which can develop to become invasive squamous cell tumours, which is dependent on TNFα and T cells. Different strains of mice have different tumour susceptibilities in this model, B6/129 mice are resistant to tumour formation, whilst FvB/N mice are susceptible to tumour development. When D6 expression is 'knocked out' in B6/129 mice this renders them susceptible to tumour development, and D6KO mice on a FvB/N background show an increase in tumour development, compared to WT mice. D6KO tumours contained more mast cells and CD3+ cells which suggests that the tumour micro-environment is producing chemokines which are recruiting these cells which have been shown to contribute to tumour growth. Over-expression of D6 in the basal keratinocyte layer was able to resolve inflammation in the skin much more rapidly than WT mice, and the increased levels of D6 expression in the skin delayed the development of tumours. To summarise the results found here, tumours which develop in D6KO mice have higher numbers of mast cells and CD3+ T cells and increased keratinocyte proliferation which contribute to an increase in tumour formation. When D6 is transgenically expressed in the epidermis, the tumour burden is reduced, but this protective effect can be overcome by increasing the inflammatory episodes, suggesting that D6 has a limited capability to clear inflammatory chemokines, and high chemokine levels can overcome this. These data illustrate that D6 may have therapeutic potential as an inflammation specific tumour suppressor, and highlight the importance of inflammatory chemokines in this model of tumour development. Further evidence supporting a role for D6 in human cancer, comes from the presence of D6+ lymphatic endothelial cells in squamous cell carcinomas, endometrial carcinoma and Kaposis sarcoma samples. (142).

1.8.1.5.5 Mycobacterium Tuberculosis

Infection with Mycobacterium tuberculosis (Mtb) leads to an inflammatory response in the lungs, which causes to the formation of granulomas and subsequent clearance of the bacteria. When D6KO mice are infected with Mtb they have an increased mortality despite having no difference in bacterial load, compared to WT mice. Infection in D6KO mice causes an exaggerated leukocyte infiltrate, diffuse liver necrosis, lung inflammation, renal and liver failure. Intranasal administration of Mtb means that the lungs are the first site of infection, D6KO lungs have increased levels of CD4+, CD8+ T cells and macrophages, compared to WT mice. This increase in cell number was also found in the draining lymph node of D6KO mice. Levels of inflammatory cytokines and chemokines were measured in the broncho-alveolar lavage fluid, CCL2, CCL3, CCL4, CCL5, IFNγ, TNFα and IL1β levels were all increased in D6KO mice, demonstrating that a lack of D6 causes an increased inflammatory response in the lungs after Mtb infection. These results suggest that these mice have an increased innate inflammatory response towards Mtb, which causes upregulation of chemokines that would normally be controlled by D6. Blocking antibodies against CCL2-5 led to a prolonged survival in D6KO mice by controlling the inflammation, but this resulted in an increase in infection, shown by increased CFU (colony forming units) in the lungs. These data show that an inflammatory response is required to clear Mtb infection but this must be limited, which is where D6 may play a role in Mtb infection (157).

1.8.1.5.6 Colitis and Colon Cancer

As mentioned above, D6 is expressed in the skin, the lungs and the gut. In the gut, D6 expression has been shown in lymphatic endothelial cells and some leukocytes. In the mouse, D6 expression has also been shown in stromal cells in the colon (using bone marrow chimeras), and D6 expression levels are up-regulated during colitis induction (158, 159). There is conflicting evidence as to the role that D6 may play in colitis. One report describes D6KO mice developing more severe colitis, than WT counterparts, which makes them more susceptible to colon cancer. This susceptibility is attributed to higher levels of inflammatory chemokines and increased leukocyte infiltrate(158). Another report, published around the same time, describes D6KO mice as having reduced colitis severity, which is attributed to alterations in the positioning of IL17 producing γδ T cells (159). The conflicting evidence here may be due to subtle genetic differences in mice strain used, or due to conditions in the respective animal facilities, which may alter gut flora and affect colitis development, so the role of D6 in colitis has not yet been clarified.

Whatever the role that D6 may play in the development of colitis, both reports suggest that it is D6 on non-haematopoeitic cells that is affecting the outcome. D6 expression in the gut occurs mostly on CD45- cells, and a subset of colonic B cells (159). Bone marrow chimera experiments show that restoration of D6 expression to the non-haematopoietic compartment protects mice from the development of colitis (who were previously susceptible in this model) (158). As the only non-haematopoietic cells that have been shown to express D6 are lymphatics, these reports suggest a role for lymphatic endothelium expressed D6 in affecting colitis outcome, and subsequently colon cancer.

A role for D6 in the development of colon cancer has been suggested, D6KO mice have increased tumour incidence and tumour size, correlated with an increased leukocyte infiltrate. This murine work is supported by identification of D6 in the lymphatic vascular bed of IBD samples, with increased expression on those cases that lead onto colon cancer (158). Together with the work mentioned in section 1.8.1.5.4, these studies point to a role for D6 in inflammation induced tumour development.

1.8.1.5.7 Inflammation Induced Foetal Loss

The expression of D6 on the placenta has led to studies into the role that D6 may play in pregnancy. The presence of D6 transfected into trophoblast cells causes increased degradation of chemokines, compared to un-transfected cells. Murine models of foetal loss, induced by LPS or anti-phospholipid antibodies illustrate that D6 is protective against inflammation driven foetal loss. D6 expressed on the placenta is thought to reduce placental inflammation and subsequently reduce the levels of infiltrating cells, e.g. lymphocytes and macrophages, which are increased in pregnant D6KO mice. In humans, D6 expression has been shown on the invading human trophoblast cells and the apical side of syncytiotrophoblast cells, so D6 may potentially have a similar role in humans, in keeping the levels of inflammation in the placenta at a level to permit foetal development (151).

1.8.1.5.8 Inflammation

D6 has been implicated in other models of inflammation, for example the administration of CFA subcutaneously causes a granuloma like lesion, which develops earlier in D6KO mice, compared with WT mice. This granuloma development is coupled with an increased inflammatory response, increased leukocyte infiltrate and necrosis, confirming the role suggested for D6 in limiting inflammatory responses(149). Promoter analysis of D6 has

recently identified small nucleotide polymorphisms which may be associated with the grade of liver inflammation in humans, and there is evidence that D6 may be involved in murine models of liver inflammation (160, 161).

1.8.1.6 Summary

In vivo studies have been valuable in defining the role of D6, clarifying its involvement in the resolution of inflammation, as well as highlighting the potential for D6 to be used as a therapeutic in inflammation induced skin cancer (142, 152). The expression of D6 in the placenta appears to play a vital role in the survival of the foetus under inflamed conditions (151). As well as limiting inflammatory responses, D6 may play a role in the initiation of adaptive immune responses, shown by the accumulation of DCs at the site of injection, in D6 null mice, using the EAE model, which results in impaired T cell responses (153). Future work analysing the promoter of D6 will shed more light on how D6 is regulated and how D6 may potentially be involved in a wide range of inflammatory conditions and diseases.

1.8.2 DARC

DARC (Duffy antigen receptor for chemokines) was originally identified as the cellular entry point for Plasmodium vivax, and has subsequently been characterised as the only mammalian receptor which is capable of binding chemokines from more than one family (162). DARC can bind to 11 different inflammatory CXC and CC chemokines, shown in table 1.2 (163). DARC shares very little sequence similarity to other chemokine receptors, or even with other members of the atypical receptor family. The expression of DARC is restricted to red blood cells and vascular endothelial cells, as well as Purkinje cells, kidney epithelial cells and type II pneumocytes. A significant proportion of the human population have suppressed red blood cell expression of DARC, which is caused by polymorphisms in GATA1 sites in the promoter, but endothelial cell expression of DARC is unaffected (164).

DARC expressed by erythrocytes is though to act as a chemokine ‘sink’ which prevents the activation of leukocytes in the blood, which has been shown using studies in DARC KO mice (165, 166). DARC has also been shown to maintain chemokine levels in the blood, acting as a chemokine reservoir (167, 168). Erythrocyte expression of DARC has also been proposed to be anti-angiogenic in a model of prostate cancer, clearing angiogenic

chemokines from the tumour circulation (169). The difficulty with using DARC KO mice to try to define its role, is separating the relative roles of DARC expressed by red blood cells and endothelial cells (170). On endothelial cells, DARC has been shown to transport chemokines from the apical to the basolateral side of endothelial cell monolayers, and retain chemokine on the surface of cells (168, 171). This function of DARC has been suggested to be involved in leukocyte recruitment, using transgenic mice which only express DARC on endothelial cells (168, 172).

1.8.3 CCX-CKR

CCX-CKR (Chemocentryx chemokine receptor) was originally identified by a group at Chemocentryx, hence the name (173). CCX-CKR (which has also been referred to as CCR11) can bind to CCL19, CCL21 and CCL25, internalise these chemokines and target them for degradation (174). It falls into the atypical receptor group as it fails to demonstrate signalling after ligand binding. The expression of CCX-CKR is highest in the heart and lung, and was found to be expressed by stromal cells in the thymus (175). CCX-CKR has been shown to internalise, retain and degrade CCL19 much more efficiently than CCR7, which is due to the fact that CCR7 undergoes ligand-induced desensitisation. The marked capacity of CCX-CKR to degrade ligand is not dependent on constitutive trafficking, shown by a lack of requirement for β-arrestins and clathrin. The internalisation of CCX-CKR has been shown to use caveolae, which could suggest potential roles in transcytosis, similar to DARC (176). DCs have been shown to have reduced lymph node migration in CCX-CKR null mice, as well as reduced migration if embryonic thymic precursors. CCX-CKR expression on stromal cells has been proposed to alter levels of chemokines in the extracellular space, which is required for DC and thymic precursor migration (175).

1.8.4 CXCR7

CXCR7 is the most recently discovered member of the atypical receptor family, and has been studied extensively with the use of zebrafish. CXCL12 was thought to bind a single chemokine receptor, CXCR4, until the discovery of CXCR7. CXCR7 (also known as RDC1) can bind to CXCL11 and CXCL12, without evidence of calcium flux or chemotaxis (177). Although no signalling has been demonstrated, expression of CXCR7 in transfected cells provides increased survival and adhesion, so it is possible that some form of signalling

may occur (177, 178). The expression of CXCR7 appears to be confined to development, although it has been shown to be expressed on a wide range of tumours. These include gliomas, colon, lung, breast and prostate cancer (177, 179-182). CXCR7 has also been shown to be increased on tumour associated vasculature and may be involved in the survival of tumour cells (183). The role of CXCR7 in development has been studied using zebrafish. These studies have shown that CXCR7 is involved in the migration of primordial gem cells in the lateral line primordium of the zebrafish. Primordial germ cells respond to CXCL12 produced during zebrafish development by expressing CXCR4. CXCR7 is expressed on the surrounding somatic cells, which can alter levels of CXCL12 and subsequently affect the migration of germ cells (184). As well as influencing germ cell migration in zebrafish, CXCR7 is expressed on emerging blood vessels and plays a role in cardiac development. Studies with CXCR7 null mice show that CXCR7 is essential for development, as these mice die at birth. Conditional CXCR7 KO mice, with a deletion of CXCR7 in endothelial cells, shows that CXCR7 is involved in heart valve formation, as well as having roles in endothelial cell growth and survival (185).

1.8.5 'Functional' Decoys

The group of decoy receptors mentioned above differ from signalling chemokine receptors due to alterations in the key signalling motif, but typical chemokine receptors have the ability to act in an atypical manner. At the site of inflammation, LPS triggers the down-regulation of inflammatory chemokine receptors on DCs and causes up-regulation of CCR7. This chemokine receptor switching can be modulated by the presence of IL10. IL10 inhibits the down regulation of CCR1, CCR2 and CCR5 on dendritic cells and monocytes, following exposure to LPS. These receptors still remain on the cell surface, but have become 'frozen', i.e. they are uncoupled to signal pathways. This means that DCs no longer have the ability to migrate using these receptors, but these receptors are still able to bind chemokines. In this way, these 'frozen' receptors can help to clear inflammatory chemokines from the microenvironment, and they become what are known as 'functional decoys'. These receptors may block excessive cellular recruitment and activation, as well as helping to resolve inflammation (186). Further evidence to suggest a regulatory role for signalling chemokine receptors comes from work showing that chemokine receptor null mice have increased levels of circulating chemokines. This

suggests that chemokine receptors are required to clear chemokines from the circulation and tissues (187).

1.9 Chemokines in Disease

The chemokine system has vital roles during inflammation and as a result, chemokines can be associated with inflammatory diseases. The chemokine system is involved in many diseases and chemokines are essential in viral, parasitic and bacterial infections. Chemokines can have detrimental effects in diseases such as asthma, rheumatoid arthritis and MS (188). As well as being important in responses to pathogens, chemokines are also involved in responses against self, for example in autoimmunity. IFNγ activated CD4+ and CD8+ T cells and activated macrophages can create a Th1 environment which has been shown to contribute to diabetes, atherosclerosis and Crohns disease (188).

1.9.1 HIV

HIV infection involves interactions between viral surface proteins, CD4 and the chemokine receptors CXCR4 and CCR5. Initial infection occurs via CD4, with CCR5 as a co-receptor, by M-tropic viruses, so called because they usually infect macrophages. As the disease progresses, the virus mutates and uses CXCR4 as a co-receptor (T-tropic), allowing infection of a wider range of cell (189, 190). CCR5 mutations can confer HIV resistance; about 1% of the Caucasian population have a mutation in CCR5 that is essentially a natural knock out for the receptor. This mutation is known as CCR5Δ32, and appears to have no adverse effects for the carriers. (191). CCR5 has become an attractive target for the development of HIV therapies, but targeting CCR5 may leave people susceptible for West Nile virus (WNV), as a lack of CCR5 has been shown to increase symptomatic WNV infection (192).

1.9.2 Multiple Sclerosis

Multiple sclerosis is an autoimmune disease that targets the central nervous system (CNS), causing demyelination of nerves, leading to a chronic debilitating condition. The pathology of MS is caused by the infiltration of the CNS by inflammatory leukocytes, which cause specific destruction of the myelin sheath. The murine model of MS is EAE, which is induced by immunisation of mice with a peptide specific for a component of the myelin sheath. This model causes symptoms similar to human disease, with progressive paralysis and cell infiltration of the CNS (154). The cell populations involved in EAE include CD4+ and CD8+ T cells, as well as macrophages. Chemokines implicated in cellular

recruitment in EAE pathogenesis include CCL1, CCL2, CCL3 and CXCL10 (193, 194). CCR6 and its ligand CCL20 have also been implicated in EAE pathogenesis, with CCR6 KO mice having alterations in DC and CD4+ T cell migration (195, 196). CCR2 KO mice are completely protected from the development of EAE, illustrating that CCR2 is required for the development of disease (197).

1.9.3 Rheumatoid Arthritis

Rheumatoid arthritis (RA) is a chronic inflammatory condition which is characterised by an inflammatory cell infiltrate into the joints, which causes bone and cartilage destruction. Many different leukocytes have been found in the synovial tissue of rheumatoid patients, and the chemokine receptors have been analysed on these infiltrating leukocytes. Common receptors expressed include CCR2, CCR3, CCR5, CXCR2 and CXCR3 (198). A wide range of chemokines are also implicated in the pathogenesis of RA, these include CCL2, CCL3 and CCL5 (199-201), as well as members of the CXC chemokine family (198). Chemokines are though to play a role in the degradation of cartilage, through the induction of MMP expression, and by recruiting cells into the inflamed joint to cause further joint destruction (202).

1.9.4 Cancer & Metastasis

The role that chemokines and their receptors play in cancer and metastasis will be dealt with in more detail in section 1.10.3. In cancer, chemokine receptors can be upregulated and are involved in growth, and cell survival (38). Chemokine receptors are also thought to play a role in organ specific metastasis.

1.9.5 Therapies Targeting the Chemokine System

Targeting chemokines and chemokine receptors may be a successful therapeutic strategy, useful in a wide range of diseases. Chemokines and receptors are involved in a wide variety of inflammatory disorders, for example, CCR1 is associated with MS, asthma and rheumatoid arthritis, whilst CXCR4 has roles in HIV infection and cancer (9). The antagonism of the chemokine system may have beneficial effects for a wide range of diseases, which could be achieved using neutralising antibodies, modified chemokines (antagonists) or using small molecule receptor antagonists. Studies have shown the

potential benefit of chemokine therapies. In mouse models, treatment with an anti-CXCR3 antibody has the same effect in vivo as generating a CXCR3 null mouse, demonstrating that this antibody is very specific and potentially useful in transplantation (203). Use of a CCR1 inhibitor (BX741) in the rodent model of EAE shows a reduction in disease severity of 50%, illustrating that CCR1 blocking may be a potential therapeutic for MS (204). The use of an antagonist to human CCL2 is able to prevent disease development in a murine model of spontaneous arthritis (205). The results from these studies show that different methods of chemokine antagonism can be effective in various different diseases.

Met-RANTES is a form of RANTES that has an extra methionine at the amino-terminal. It still has the capability to bind CCR1 and CCR5, but the presence of this methionine residue abolishes CCR3 binding (206). This single amino addition alters the function of RANTES, making it anti inflammatory in a model of Th2 inflammation (OVA induced lung inflammation). Modified forms of chemokines therefore may have some therapeutic potential. In addition small molecules that could inhibit chemokine receptors may be useful therapeutic agents. For example TAK779 blocks CCR5 binding to its ligands (CCL3, 4, 5) in an allosteric manner by binding at a cavity near the surface, which is not where the ligand binds (207). There is a great deal of interest in creating therapies that target CCR5, which could potentially have roles in HIV treatment; the most successful therapy in recent years has been Maraviroc. Maraviroc is a CCR5 antagonist that can be tolerated in both healthy individuals and HIV infected patients, it was approved for use in 2007 (208). CXCR4 targeting has also had a great deal of interest, with respect to HIV, but the first CXCR4 antagonist to be approved was AMD3100, as a stem cell mobilisation drug, for stem cell transplantation in 2008 (209). Although research into therapies for HIV have been extensive, other chemokine targeting treatments have had varying success in clinical trials. For example CXCL8 targeting in COPD patients was not very successful, and trials have since been discontinued (210, 211), similar to trials with a monoclonal against CCR2, which had no beneficial effects in rheumatoid arthritis patients (212).

There are many problems with designing anti-chemokine therapies – redundancy being the main one. The mouse may not be an ideal model organism as there are differences in the way that the chemokine genes are organised, but other alternatives are limited. Despite this, chemokine receptors still represent one of the most attractive targets on the

market for drug targeting and murine models are required for testing before human trials can be considered (38).

1.10 Tumour Growth

Tumours arise from normal cells, which have undergone numerous mutations to allow them to grow uncontrollably and remain undetected by the immune system. Mutations occur over time and create a tumour that has unlimited proliferative potential, and can allow cells to survive with cell division defects (213). Cells are undergoing mutations on a regular basis, but usually the immune system can recognise these cells and eliminate them before they form tumours, or the mutations may cause the cells to die.

Chronic inflammation can contribute to the development of many different forms of tumours, and appropriately NSAIDS (non-steroidal anti-inflammatory drugs) are associated with protection against various tumours (156). At the moment, there is limited evidence for their benefit with respect to melanoma treatment. Only two human studies have been conducted, these show that NSAIDs are associated with a reduction in melanoma incidence (in females) and in melanoma patients, they are associated with a lower incidence of new melanoma, recurrence and metastasis (214, 215). In most tumours, an inflammatory component is present, e.g. leukocytes, inflammatory cytokines and chemokines. There are two ways in which inflammation can be linked to cancer development. The intrinsic pathway, is when the developing tumour cells actually cause inflammation, creating an inflammatory microenvironment, or the extrinsic pathway, which is when inflammatory conditions facilitate cancer development, e.g. Helicobacter infection and gastric cancer (156). Inflammation in the tumour microenvironment can promote the recruitment of bone marrow derived cells to the tumour, which in turn can help promote its growth (216). An inflammatory microenvironment has been shown to contribute to all aspects of tumour growth; the proliferation and survival of tumour cells (e.g. NFkB signalling (156)), angiogenesis (TNFα, IL1 and myeloid cells, amongst others, have been shown to contribute to angiogenesis (217-219)), and metastasis.

Once cells have mutated and become cancerous, they may lie dormant for years, undergoing a steady balance of proliferation and apoptosis, without being detected by the immune system. The survival of these cells involves interactions between the tumour cells and the surrounding stroma, which evolve as the tumour develops. The microenvironment is essential for contributing to cell survival, e.g. the protective microenvironment of a mouse blastocyst can suppress the tumourigenicity of

teratocarcinoma cells, but this protective microenvironment can be overridden by chronic inflammation (216). Stromal cells that can be involved in tumour development include endothelial cells (both blood and lymphatic), pericytes, fibroblasts, macrophages, neutrophils, mast cells, myeloid derived suppressor cells (MDSCs) and mesenchymal stem cells (MSCs). More details can be found below (216). An overview of cells involved in tumour growth is shown in figure 1.3.

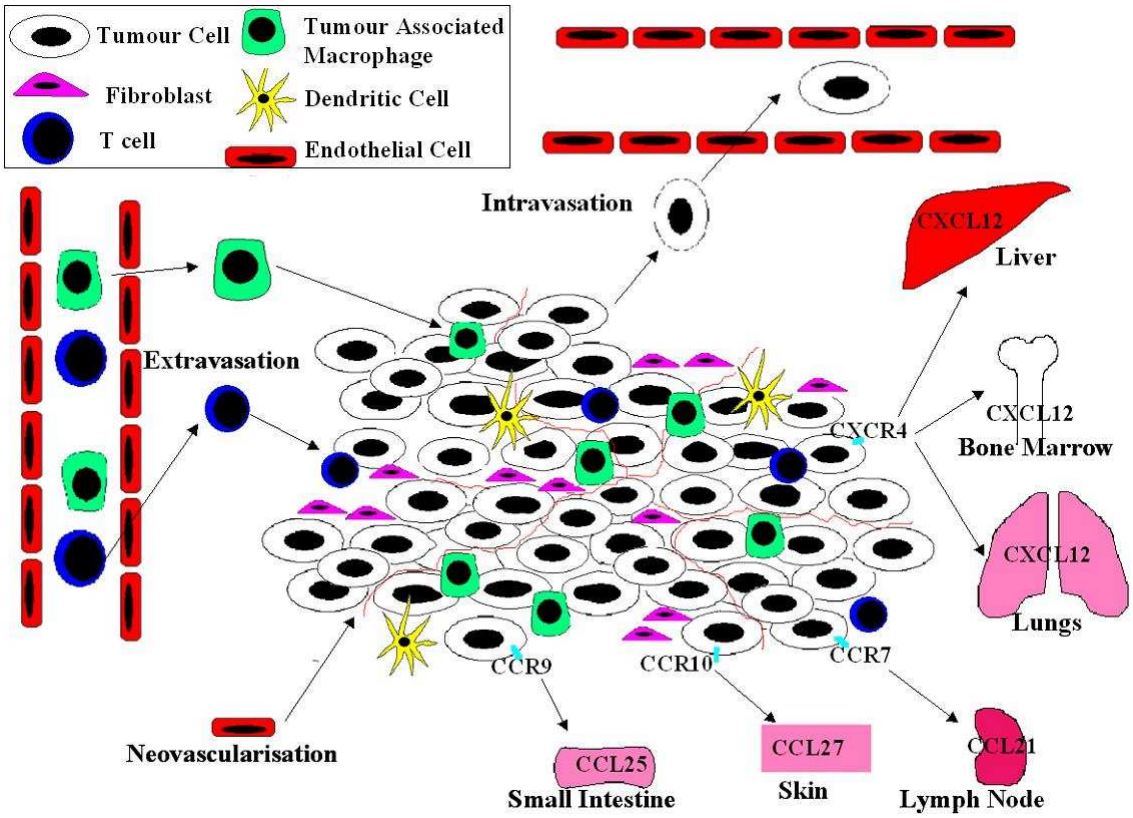

Figure 1-3: Chemokines and chemokine receptors involved in tumour growth

As the tumour grows, it develops blood vessels through the process of neovascularisation. Chemokines play a vital role in the development of blood vessels and the recruitment of leukocytes such as T cells and macrophages. In the tumour microenvironment, leukocytes can have anti-tumour or pro-tumour effects. Blood vessels, and lymphatic vessels within the tumour provide 'escape routes' which tumour cells can use to metastasise to different sites. Chemokines and chemokine receptors are thought to play roles in determining the sites of metastasis, as shown above (described in detail in section 1.11). Tumour cells develop new blood vessels via the process of neovascularisation. Blood vessels allow T cells and macrophages to enter the tumour environment where they can help tumour growth. Tumour cells can leave via blood vessels and metastasise to various organs depending on chemokine receptor expression.

1.10.1 Immunosurveillance & Immunoediting

The evasion of the immune system is a crucial step for tumour growth, as tumour cells have undergone mutations and may be recognised as non-self. Evasion is made difficult by the presence of cells of the immune system with tumour killing capabilities, which are constantly surveying the body. In order to successfully grow, tumours have to escape

from this immunosurveillance (220). The process of immunosurveillance was originally suggested by Burnet in 1970 (221). He described the sentinel thymus dependent cells of the body (T cells) constantly surveying host tissues for transformed cells; this theory has been expanded as knowledge of the immune system increased. Immunosurveillance can detect tumour cells and eliminate them, but this killing may be inefficient, which may allow tumour cells to continue to grow and mutate, making them unrecognisable by the immune system. This process is known as immunoediting and can be characterised by a period of immune mediated latency, when the remaining tumour cells can still proliferate and may eventually escape this latency and tumour re-growth may occur (222, 223)

1.10.1.1 Immunosurveillance and Destruction

The cells of the immune system which are responsible for immunosurveillance include cells of both the innate and adaptive systems, in particular γδT cells, αβT cells, NKT and NK cells, all of which can eliminate tumour cells completely (224-226). NK and NKT cells are involved in innate control of the tumour, they can produce IFNγ which has numerous anti-tumour effects including activating NK cell cytotoxicity, the enhancement of CD8+ cell killing, Th1 cell differentiation, reducing the rate of cell proliferation and up-regulating MHC molecules. Tumour cells can down-regulate their expression of MHC molecules, in order to evade the immune system, but NK cells are able to recognise tumour cells that do not express MHC molecules. They can recognise tumour cells using non-classical MHC molecules such as NKG2D (227, 228). Other cells involved in anti-tumour responses include γδT and αβT cells, which can also produce IFNγ, mediate direct cell killing, as well as being able to recognise tumour cells via both NKG2D (γδ T cells) and classical MHC (αβT cells)(223).

During the process of tumour development, mutations can be acquired which can cause the up-regulation of tumour specific antigens; these are usually self-proteins, which have undergone alterations during the tumour growth phase. These antigens may be expressed by cells which would not normally express them, for example testes associated antigens can be expressed by tumour cells. These tumour antigens can be classified as differentiation antigens (melan-A), mutational antigens (abnormal p53), over-expressed or amplified antigens (Her-2/Neu), cancer-testis antigens (MAGE), or viral antigens (EBV or HPV) (229, 230). As well as being able to express tumour specific antigens, tumour cells can over-express other molecules, e.g. MICA/B (which bind NKG2D), which are highly

polymorphic non-classical MHC molecules, also known as stress molecules. These can be induced by heat shock, CMV infection or E.coli, and can also be expressed during the process of cell transformation (231). Despite expression of tumour-associated antigens and the expression of non-classical MHC molecules, tumours still may not be recognised, which may be due to the tumour microenvironment. The tumour microenvironment may not produce a classical 'danger signal' (e.g. LPS activating TLR4), but work has shown that substances such as uric acid, heat shock proteins and ECM derivatives can all act as danger signals, as well as the presence of a pro-inflammatory microenvironment (224).

1.10.1.2 Equilibrium

As mentioned above, after immune mediated destruction, tumour cells may survive which can undergo low levels of proliferation and apoptosis, and this permits the development of new mutations. This acquisition of new mutations may allow tumour cells to grow undetected, or an immunosuppressive microenvironment may allow these cells to proliferate (223). This low level of cell proliferation is described as immune mediated latency. Examples supporting tumour latency include a case of metastatic melanoma occurring 1-2 years after two patients received a kidney from the same donor. It was discovered that the donor had melanoma 16 years previously, but melanoma cells still existed in the kidney. When placed in to an immunocompromised host, the tumour cells were able to grow (232). Despite evidence that latency occurs, it is probable that tumours can be successfully eliminated on a regular basis.

Examples of mutations that can occur in tumour cells to facilitate the escape of immune detection, include altering antigen processing or presentation. Evidence has shown that when patients with metastatic melanoma were given MART-1 specific T cells, this treatment led to the loss of MART-1 expression on tumour cells (233). As well as being able to alter antigen presentation, tumour cells may create an immunosuppressive environment by producing IL10, TGFβ, soluble NKG2D ligands, galectin 3, and IDO. This microenvironment may permit the tumour to grow and remain undetected by the immune system (231, 234, 235).

1.10.2 Leukocyte Infiltration

Tumour cells, stromal cells and leukocytes populate the tumour microenvironment, as shown in figure 1.3. A wide variety of immune cells have been found to infiltrate tumours, these include cytotoxic T cells (CTLs), NK cells, neutrophils, mast cells, immature myeloid cells, macrophages and granulocytes. Leukocytes can contribute to the tumour microenvironment by producing cytokines and chemokines, which can cause remodelling of the ECM and create a pro or anti inflammatory microenvironment (216, 236, 237). As well as being able to influence the local microenvironment, leukocytes can also be affected by the microenvironment, e.g. a hypoxic environment can alter chemokine receptor expression (29). Infiltrating leukocytes have the potential to be both pro and anti-tumourigenic, depending on the extent of cell infiltration and the types of cytokines and chemokines they produce. In this way, leukocyte infiltration has the ability to influence angiogenesis, tumour cell invasion, metastasis and tumour survival (29, 216, 236, 238).

1.10.2.1 Tumour Associated Macrophages

One major leukocyte population known to have wide ranging effects on tumour development are macrophages. In animal models they have been shown to promote angiogenesis, invasion, intravasation and metastasis (239). The presence of macrophages in tumours can have either tumour promoting or suppressing actions, but this is cancer subtype dependent (29). The infiltration of macrophages appears to be essential for tumour growth, as shown with studies in CSF (colony stimulating factor) KO mice. These mice lack normal macrophage numbers, and as a result tumours in these mice have reduced growth and reduced angiogenesis (240). Tumour associated macrophages (TAMs) can produce CCL2, which can influence tumour progression depending on the concentration; in melanoma, high CCL2 levels are associated with increased TAM infiltration (good prognosis), low CCL2 is associated with a reduced TAM infiltrate (bad prognosis) (29, 238).

The numbers of macrophages and their phenotype can influence the tumour; M1 macrophages typically have anti-tumour effects (produce IL12, IFNγ, pro-inflammatory cytokines and increase MHC expression) whilst M2 macrophages have pro-tumour effects (angiogenesis, matrix remodelling and immunosuppressive actions). The majority of TAMs

commonly have a M2 like phenotype (238, 241, 242). As well as producing cytokines and chemokines which can recruit cells and influence tumour growth, TAMs can produce VEGFs (vascular endothelial growth factors) and proteases, which have been shown to influence angiogenesis in breast cancer (236). It may be possible to alter the phenotype of macrophages within the tumour microenvironment, to promote tumour regression. NFkB has been shown to maintain the immunosuppressive phenotype of M2 macrophages, when NFkB is inhibited, TAMs change phenotype from M2 to M1, allowing tumour regression (243).

1.10.3 Chemokines and Receptors

The expression of chemokines in tumours has been extensively studied and chemokine expression has been shown to contribute to tumour growth, angiogenesis, cell survival and metastasis. The production of chemokines can be induced by cytokines secreted by tumour cells and infiltrating leukocytes, e.g. VEGFA, TGFβ and TNFα (222). With respect to chemokine receptor expression, one of the most common chemokine receptors expressed in tumours is CXCR4, which has been detected in 23 different human cancers, and its ligand, CXCL12 has also be found in the tumour microenvironment (29). Stromal cells, tumour cells and infiltrating leukocytes, may produce CXCL12. The centre of tumours tends to have a hypoxic environment and this can influence CXCR4 expression, via the upregulation of HIF-1 (hypoxia inducible factor), which can up-regulate CXCR4 on normal and tumour cells (244). The expression of CXCL12 produced in the tumour microenvironment can also promote survival of CXCR4+ cells (29). Numerous other chemokines have been detected in tumours, these include CCL2, CCL5, CCL17, CCL22, CXCL1, CXCL8 and CXCL13 (238).

1.10.4 Angiogenesis

The growth of tumour cells can reach ~1-2mm diameter before a blood vasculature must develop, in order for the tumour to survive (245). The development of vasculature involves interactions between tumour cells, stromal cells and infiltrating leukocytes. Angiogenesis is essential to provide growth factors for the tumour and can allow haematogenous metastasis. The process of angiogenesis can be regulated by chemokines in particular the CXC family of chemokines are important in the development of blood vessels within tumours. The CXC chemokine family can be broadly divided into two

groups, those that are angiogenic ('ELR' positive) and those that are angiostatic ('ELR' negative). Angiogenic chemokines include CXCL1, CXCL2, CXCL3, CXCL5, CXCL6, CXCL7 and CXCL8, and these bind to CXCR1 and CXCR2 (only CXCR2 in mice). Angiostatic chemokines include CXCL4, CXCL9, CXCL10, CXCL11 and CXCL14, which exert their effects by binding CXCR3 (246). Chemokines which promote angiogenesis have been detected in almost all human tumours, CXCL1, 2, and 3 were discovered in cultures of melanoma cells (247). Initially, it appeared that all angiostatic chemokines bound to CXCR3, but CXCR3 has been shown to undergo alternative splicing, which creates three new isoforms, CXCR3A, CXCR3B and CXCR3-alt. Each isoform of CXCR3 differs in its ligand specificity; CXCL9, 10 and 11 can bind to CXCR3A and CXCR3B, whilst CXCL4 can only bind to CXCL3B. CXCR3-alt has a reduced binding affinity for CXCL9 and CXCL10 but retains high affinity for CXCR11 (248, 249).

1.10.5 Lymphangiogenesis

As well as the development of blood vessels, tumours can often develop lymphatic vessels. The development of lymphatics within a tumour can allow metastasis to the local draining lymph node, which can lead to more disseminated spread. The extent of lymphangiogenesis in primary cutaneous melanoma may be a prognostic factor to predict the presence of sentinel lymph node metastases. Lymphatics can be induced by the expression of VEGFC expression, which is correlated with lymphatic vessel density in primary melanomas; it can influence tumour and lymphatic endothelial cell interactions. Lymphangiogenesis can also be induced in lymph nodes, if VEGFA produced by the tumour drains into the lymph node (250).

1.11 Metastasis

When a tumour has developed a blood and lymphatic supply it is possible for tumour cells to enter the blood stream and lymphatics. Once tumour cells have entered the vasculature, they can reach and colonise distant organs, in a process known as metastasis. Not all tumours have the ability to metastasise, but often when they do it is a poor prognostic factor. In order to metastasise, genetic changes in tumour cells have to occur to allow the cells to survive in the circulatory or lymphatic system. As soon as a tumour develops vasculature, tumour cells can be found in the blood, but not all of these cells have the ability to form metastases. The same can be said about organs, whilst metastatic cells may be present in many organs, they will usually only form metastases in some of these organs. This is illustrated by the presence of disseminated tumour cells (DTCs) which can be detected in the blood of cancer patients, but not all of these develop to become metastases (245).

1.11.1 Stages of Metastasis

Similar to tumour development, metastasis is a multi-step process. Cells from the primary tumour must invade the vasculature or lymphatics, be able to survive in the circulation, extravasate in distant organs and have the ability to colonise the new organ. Genetic changes can occur in metastatic cells, which permit these stages to occur, certain genes are associated with different stages of metastasis. Initiation genes are involved in cell motility, immune system evasion and ECM degradation. Metastasis progression genes allow entry and survival in the new organs. These genes may have the same role in the primary tumour as they do in the metastatic cells, or they may have different roles (213). During tumour growth, the exact stage at which metastases occur is unknown; there are differing theories that have been described. A linear progression model has been described, which defines a stepwise accumulation of mutations in the primary tumour that leads to cells acquiring a metastatic phenotype. This means that metastatic cells have much of the same characteristics of the primary tumour, and the extent of metastasis can be linked to the primary tumour size (245). The parallel progression model (originally described in 1956 (251)) describes tumour cells leaving the primary tumour whilst it is small, so before any symptoms are evident. This allows cells to grow in distant organs, which leads to the acquisition of distinct phenotypes different from the primary tumour.

This theory indicates that metastasis must occur before the primary tumour is clinically detectable (245).

1.11.1.1 Survival and Growth

In order to metastasise, tumour cells must be able to survive the haemodynamic forces in the bloodstream and remain undetected by the immune system. Detection by the immune system may be prevented by tumour cells interacting with platelets in the blood, which can act as a shield. This platelet aggregation may have two roles; it can shield tumour cells from the immune system and platelet aggregation can increase the size of metastatic colonies (252, 253). An increased platelet count has been correlated with a decrease in cancer survival (216).

Metastasis can occur via the blood and lymphatics, but lymphatic metastasis can occur without spread in the blood. Once metastasis occurs in the sentinel lymph node (the first lymph node which metastasis occurs), further lymph node metastasis can occur in a sequential manner due to the lymphatic drainage (250, 254, 255). The likelihood of lymphatic metastasis can be predicted by certain markers expressed in the primary tumour, e.g. VEFC or VEGFD expressed in primary breast, colon and lung tumours is associated with lymphatic metastasis (256).

There are two theories as to how organs are 'chosen' as sites for metastasis. In 1889 Paget described the seed and soil theory, which likens tumours cells as 'seeds' that require the correct 'soil' (i.e. organ environment) to grow. This theory was used to describe the pattern of metastasis in breast cancer (257). A differing theory was proposed in 1928 by Ewing, which suggested that circulatory patterns were responsible for the patterns of metastasis and the organs colonised were determined by the site of the primary tumour (258). Elements of both theories are though to explain the location of metastases, and can be supported by expression of chemokine receptors in metastasis that are associated with colonisation of specific organs. For example, in human breast cancer and malignant melanoma, the same pattern of metastasis occurs as cells have been shown to express CCR7, CXCR4 and CCR10 (256). This could fit with the seed and soil theory, but whilst the sites of metastasis may be chosen due to chemokine receptor expression, certain organs are thought to be common metastatic sites as they have small

capillary beds, e.g. liver and lungs (236, 259), which would fit with the theory suggested by Ewing.

1.11.1.2 Pre-Metastatic Niche

However tumour cells decide which organs to colonise during metastasis, evidence exists that the primary tumour can pre-condition organs to become receptive to metastasis creating, what is known as the pre-metastatic niche. Factors secreted by the primary tumour, such as VEGFA, TGFβ and TNFα, can help create this niche in distant organs, by increasing fibronectin expression (260, 261). As well as increasing fibronectin expression, these cytokines cause the recruitment of VEGFR1+ VLA4+ haematopoietic cells to areas with increased fibronectin expression. The newly recruited cells interact with the surrounding stromal cells to produce chemokines and growth factors, such as the chemokines S100A8 and S100A9, which have been found to be up regulated specifically in the lungs, in response to VEGFA and TNFα from primary tumours in mice. This up-regulation only occurs in the lungs, the organ where the tumour cells specifically metastasise, using the B16 F10 model of metastasis. Neutralising S100A8 and S100A9 was able to reduce the number of metastatic lung colonies, indicating that this niche was required for their development (261, 262). As well as causing chemokine expression, VEGFA from the primary tumour can cause the expression of MMP9 at the pre-metastatic niche (261). This causes remodelling of the lung parenchyma which allows metastatic cells to colonise (236, 263). The ability of the primary tumour to induce these pre-metastatic niches may be essential for metastasis to occur, but this may be dependent on the type of cancer.

1.12 Melanoma

Skin cancer can fall into two classes, non-melanoma and malignant melanoma. Malignant melanoma is the most fatal type of skin cancer that is on the increase, with cases in the past 30 years increasing more than five fold (Statistical Information Team, Cancer Research UK, 2006). One of the major risk factors for developing melanoma is intense exposure to UVR (ultra violet radiation), but there is a significant genetic component to the disease (264). UVR can initiate a stress response in the cells of the skin, which induces numerous signalling pathways and genes that can cause cellular proliferation, apoptosis, DNA repair and survival (264). If caught at the early stages, melanoma can be treated with surgery, but late stage melanoma (which has often metastasised) has a 6 month survival, irrespective of treatment (264). Current treatments include adjuvant therapy with high dose IFNα, which has some benefit in advanced disease, but currently there are no effective treatments for melanoma (265).

As previously described, with respect to tumour development, melanoma develops in a stepwise manner, beginning as a benign nevus, which is a clonal population of melanocytes in the epidermis. These cells can then mutate to become a hyperplastic lesion, which does not progress due to senescence. If this senescence is overcome, it leads to dysplasia and superficial spreading of the cells. This spreading leads into the dermis, which can then cause metastasis. Murine melanoma differs from human melanoma due to the distribution of melanocytes; in humans they are throughout the basal layer of the epidermis, in mice they can be found in hair follicles in the dermis (264).

1.12.1.1 Leukocyte Infiltration

As described in section 1.10.2, the infiltration of leukocytes can influence tumour progression. Leukocytes have been detected in melanoma, both in primary tumours and metastases, including T cells, B cells, neutrophils, DCs and macrophages (266). In humans, specific melanoma cytotoxic T cells can be found in the blood, and within primary tumours there are areas with high numbers of localised T cell clones, which provides evidence that T cells can enter and proliferate within the tumour (266). The presence of neutrophils may enhance melanoma cell adhesion to endothelium, which may aid extravasation of melanoma cells via integrin expression (267).

Melanomas typically have a macrophage content of between 0-30%, melanoma metastases have less than 10% macrophages. Murine models have supported this observation. There seems to be an inverse correlation between the macrophage content of melanoma and the capacity to metastasise (268). The level of macrophage infiltration can correlate with tumour stage and angiogenesis (269). As mentioned previously, macrophages can be growth promoting in melanoma, they are able to produce MMP9 under the influence of CCL2, CCL4 and CCL5, which can promote ECM breakdown and promote tumour invasion (270). On the other hand, macrophages can have anti-tumour effects if activated by IL2, IL12 and IFNγ (222). Other cells identified in melanoma include NK cells; the expansion of peripheral NK cells has been tested as a therapeutic agent, with limited success (222). Dendritic cells have also been identified in human primary melanomas, plasmacytoid DCs in particular. Often there are more immature DCs than mature within a tumour. Similar to TAMs, it is thought that DCs can have both pro- and anti-tumour effects. Anti-tumour plasmacytoid DCs can be suppressed by the tumour microenvironment (255, 271), and indeed the presence of leukocytes may alter the tumour microenvironment. Melanoma cells have been shown to evade the immune system by retaining MICA inside the cell which prevents NK cell recognition (272). A pro-inflammatory environment can be detrimental to melanoma growth, as melanoma proliferation has been shown to be inhibited by IL2, IL12, IFNγ, TNFα and IL6 (267).

1.12.1.2 Chemokines & Chemokine Receptors

In melanoma, chemokines can recruit leukocytes, which can increase growth and survival factors as well as inducing angiogenesis (as described in section 1.10.3). The expression of a wide range of chemokines and their receptors have been found to be expressed by melanoma cells, including CXCR1, CXCR2, CXCR3, CXCR4, CXCR6, CXCR7, CCR1, CCR2, CCR5, CCR7, CCR9 and CCR10 (241, 273, 274). Chemokines expressed by melanoma cells include CXCL1, CXCL2, CXCL3, CXCL5, CXCL6, CXCL7, CXCL8, CXCL10, CCL2, and CCL5 (274, 275). This wide range of chemokines may have roles in promoting melanoma growth, angiogenesis, recruiting leukocytes to the tumour and promoting metastasis. For example, CXCL1 is an essential autocrine growth factor for melanoma cell lines (originally called MGSA – melanoma growth stimulatory activity), which is constitutively expressed. Blocking of CXCL1 or its receptor CXCR2 prevents melanoma cell growth in vitro (274). The expression of CXCR1, CXCR2 and CXCL8 correlates with vessel density and aggressiveness in human melanoma, and in murine models, over expression of CXCR1 or

CXCR2 increases tumour cell survival (276, 277). Other chemokine receptors expressed in melanoma include CXCR3, which is correlated with an absence of tumour infiltrating lymphocytes and a poorer prognosis (278). CCR5 and CCR7 can be expressed by primary melanoma and metastases; CXCR4 and CCR1 are expressed in melanocytes, melanoma cell lines, primary tumours and metastases (279).

In human studies, melanomas have been found to be CCR10 positive, which may promote their survival, as CCL27 binding of CCR10 on melanoma cells has been shown to increase cell survival in a model of murine melanoma (273). UVB irradiation of human skin can cause inflammation which results in the production of CXCL8, which has been shown to promote tumour growth and cell migration in human melanoma cells (280). Other chemokines involved in melanoma include CCL2, which promotes the infiltration of the tumour by macrophages (the level of CCL2 can determine the level of macrophage infiltration); the degree of macrophage infiltration can correlate with tumour stage and angiogenesis in human melanoma. (281)

1.12.2 Melanoma Metastasis

Melanoma metastasis is the main cause of death in cases of melanoma. The location of the primary tumour often predicts where metastasis is likely to occur, but this is not always the case. For example in melanoma, the most common site of metastasis is the lungs, but metastases can also be found in lymph nodes, brain, skin, liver, bone marrow and small intestine (213, 267). The expression of chemokine receptors by melanoma cells are thought to play a role in determining the organs in which metastasis can occur, e.g. in human melanoma CCR9 expression is associated with metastasis to the small intestine (282). As mentioned above melanoma cells are CXCR4, CCR7 and CCR10 positive, and this chemokine receptor expression can correlate with the site of metastasis, to the lungs, lymph nodes and skin respectively (274). Much of the work relating to melanoma growth and metastasis has been performed using the B16 model of murine melanoma, which will be discussed below.

1.13 B16 Murine Model of Melanoma

The B16 murine model of melanoma growth and metastasis has been extensively characterised and is the 'gold standard' for melanoma metastasis models (283). B16 cells are derived from a tumour that spontaneously developed in a C57Bl/6 mouse in 1954. This model is still used widely today as a model for studying human malignant melanoma (284). B16 cells can be grown in vitro and can induce tumours when injected subcutaneously into syngeneic mice. The size of the tumours increase in size as the cell number administered increases, and they can cause death with no obvious metastasis (284). Other models of tumour growth involve injecting human cancer cells into SCID (severe combined immunodeficient) mice, but syngeneic tumour models are better, as the role of the immune system in tumour development can be more accurately defined and metastatic cells from humans will not always grow in mice (283). Different variants of B16 cells exist, the original cell line isolated is known as B16 F0. B16 F0 cells from the original tumour were cultured in vitro, injected intravenously into C57Bl/6 mice and then lung colonies were selected and grown in culture. This process was carried out ten times to create a B16 variant which is highly specific for the lungs, known as B16 F10 (more details can be found in section 1.13.2) (285).

1.13.1 B16 F0 Tumour Growth

Subcutaneous administration of B16 F0 cells causes tumour growth in the skin, which is easy to identify as B16 cells produce melanin (286). B16 cells are histocompatible with the host, and they express tumour-associated antigens, which has been shown by immunising mice with irradiated B16 cells; this leads to partial immunity against rechallenge (284, 287). The immunisation must be performed before tumour challenge, as immunisation strategies fail if the animal has a pre-established tumour (287). B16 cells are lacking, or have very low levels of MHC I and II, which means despite tumour antigen expression, they have low immunogenicity. IFNγ can up-regulate MHC I on B16 F0 cells, which can cause lysis of tumour cells by CTLs and NK cells, as well as increasing CD95 and CD95L expression, which can lead to apoptosis (288).

1.13.1.1 Chemokines & Cytokines

The B16 tumour model has been used to analyse the role of chemokines and their receptors in tumour growth, often using transfected cells. CCL2 is associated with macrophage recruitment and its role in melanoma growth has been studied by transfecting B16 cells with CCL2. This increases macrophage infiltration, which reduces tumour growth. This effect is dependent on the level of CCL2 produced, low levels of CCL2 recruit low macrophage numbers which has pro-tumour growth effects (289). Blocking of CCL2 production causes a reduction in tumour volume, reducing angiogenesis as well as reducing TAM infiltration (290). Other chemokines associated with metastasis and cell infiltration include CXCL12, which when over-expressed causes a reduction in the level of T cell infiltration in B16 tumours, which can be restored following CXCR4 blocking. The effect of CXCL12 is concentration dependent, similar to that of CCL2, low levels of CXCL12 can attract tumour specific T cells to the tumour and reduce growth, but high levels of CXCL12 may cause chemo-repulsion of T cells, and permit tumour growth (291). When tumour cells express CXCR4 this causes an increase in metastasis to the lungs, with no effect on tumour size (292).

Chemokines have also been shown to be involved in angiogenesis, tumour growth and metastasis. B16 F0 cells produce the membrane bound form of fractalkine; RNAi inhibition of fractalkine causes a reduction in tumour size, with a reduction in tumour vessels. This suggests fractalkine has a role in tumour angiogenesis (293). Transfection of CCL20 inhibits the growth of B16 tumours by increasing CD8+ CTL responses, as does transfection with CCL21 which acts to inhibit tumour growth (294, 295). The over-expression of CCR10 in B16 cells slightly increases the size of tumours developing in the footpad, and CCL27 treatment of these cells caused protection against IFNγ stimulated Fas mediated death (273). Transfection with CCR7 increases metastasis to the draining lymph node, which can be blocked by CCL21 inhibition, and causes increased tumour growth (296).

Chemokine receptors can influence tumour growth and metastasis, for example CXCR2 KO mice have a reduced tumour growth, as well as reduced lung metastasis. These tumours have increased apoptotic cells, reduced micro vessels and reduced neutrophils (297). Whilst mice which over express CXCR2 have larger tumours showing increased levels of angiogenesis (298).

Cytokines, as well as chemokines, can affect different aspects of tumour growth. IFNα treatment of B16 cells in vitro inhibits cell proliferation in a dose and time dependent manner. In vivo, IFNα can reduce the size of subcutaneous tumours, by reducing cell proliferation and increasing the inflammatory infiltrate (299). Transfection of cells with IRF3 (transcription factor which regulates type I IFNs, CCL5 and IFN stimulated genes), inhibits tumour development by causing an increase in inflammatory cell recruitment (300). Other cytokines which can influence tumour growth include IL12 produced by T cells, NK cells and macrophages, which can have anti-tumour and anti-angiogenic (via IFNγ mediated CXCL9 and CXCL10 production) activity (301). ECM degrading enzymes have a crucial role in tumour growth, these have been transfected into B16 cells. MMP 13 is produced by B16 tumours and has a role in tumour growth, angiogenesis and metastasis, as shown by tumour development in MMP13 KO mice (302).

1.13.2 B16 F10 Metastasis

As mentioned above, the B16 cell line has variants that can be used in tumour growth models and variants that can be used in experimental metastasis models. The B16 F10 cell line was derived from the B16 F0 cell line, but has underwent in vitro and in vivo selection to create a cell line which is highly specific for lung metastasis (286). Intravenous administration of B16 F10 cells causes metastatic colony formation in the lungs. This type of model is known as a model of experimental metastasis, which differs from spontaneous metastasis models in that there is no requirement for primary tumour formation. Models of experimental metastasis, such as the B16 F10 model, have fewer variables, and can be carried out over a shorter time compared to spontaneous metastasis models, and these models allow manipulation of the cells, by transfection for example (283).

The B16 F10 cell line is very stable in vitro; the potential to form metastatic colonies is still present after 60 passages (both in vivo and in vitro) (303). Whilst all B16 cell lines have the ability to grow on lung tissue extracts in vitro, this does not correlate with colonisation in vivo, only B16 F10 cells have this ability (304). Compared to B16 F1 cells, B16 F10 cells have increased glycoslyltransferase activity, which makes them more likely to form aggregates with lung cells. Few other differences have been identified between B16 F0 cells and B16 F10 cells which can explain their lung specificity (286, 305-307).

When B16 F10 cells are injected intravenously, more than 80% of F10 cells survive in the circulation and make it to the lungs. These cells develop into metastases in the lungs, in particular at the surface and near major structures in the lungs. The initial distribution of cells is random, but preferential growth of B16 F10 cells occurs adjacent to blood vessels and the pleural surface (308). Parabiosis experiments has confirmed the lung specificity of B16 F10 cells (309).

As with the B16 tumour growth model, the B16 F10 metastasis model has been extensively characterised and is commonly used as a murine model of melanoma metastasis. Treatment of metastasis in humans often includes surgery, but (with respect to pulmonary metastasis) re-growth is common. Mice that underwent surgical resection of lungs had 2-3 times more B16 F10 metastatic colonies after surgery, which was associated with rapid lung growth. This suggests that surgery may not be the ideal method of treatment for melanoma metastasis, as wound repair environments appear to be beneficial for metastatic growth (310).

The B16 F10 model requires an immune response to form metastasis, shown by performing experiments in immunosuppressed mice, which causes a reduction in pulmonary metastasis (311). Evidence also exists to show that inflammation can affect metastasis in this model. B16 F10 cells express TLR2 and TLR4; the expression of both can be increased by LPS treatment. Modulation of TLR expression has been shown to modulate pulmonary metastasis; TLR2 knock down reduces metastasis, whilst TLR4 knock down increases metastasis. After B16 F10 cells are injected intravenously, levels of IFNγ decrease, which causes TGFβ and IL10 production in the lungs. The knock down of TLR2 reduces TGFβ and IL10 levels, which are required for lung colonisation. TLR4 knock down enhances Stat3 activation which can increase T regs and facilitate metastasis (312). IFNγ has also been shown to increase MHC expression on B16 F10 cells. When injected intravenously, IFNγ can reduce lung metastasis, which is thought to be due to activation of NK cells and CTLs, which inhibit B16 F10 cell proliferation and cause apoptosis (313, 314). Other evidence supporting inflammation in metastasis development come from the use of the OVA model of allergic lung inflammation, along with the B16 F10 metastasis model. The combination of the two models causes an increase in the level of metastasis by B16 F10 cells. This can be reduced by depleting CD4+ cells and treating with corticosteroids to reduce inflammation (315). Other pro-inflammatory cytokines, such as TNFα can increase metastatic colonies by increasing VCAM-1 expression on lung

endothelium, which can binds to VLA4 on B16 F10 tumour cells (256). The role of inflammation in metastasis seems to be complicated, it will depend on the cytokines produced and their potential downstream effects on the lungs, and it may depend on the type of inflammation, e.g. Th1 or Th2.

1.13.2.1 B16 F10 & Cell Interactions

Cell interactions can play a role in metastasis, as mentioned in section 1.12.1.1. B16 F10 cells can form emboli with each other and with host cells such as lymphocytes and platelets. When B16 F10 cells cluster with lymphocytes, this causes an increase in the level of metastatic colonies on the lungs (286, 306). Interactions with other cell types can influence metastasis; these include B1 cells. The pleura and the peritoneal cavity are environments rich in B1 cells. These are described as innate B cells, which express IgM+ and CD5+, have a limited antibody repertoire and are capable of self renewal (316, 317). When B1 cells are co-cultured with low metastatic B16 cells, their metastatic potential increases. This effect is cell contact dependent, and induces increased levels of CXCR4 and MMP9 on the B16 cells (318). When B1 cells are depleted the development of metastatic colonies is inhibited. The role of B1 cells in human metastatic melanoma has been investigated and B1 cells have been identified in sections from human melanoma samples. Their presence correlates with MUC18 expression, which is though to be responsible for the interactions between melanoma cells and B1 cells (319).

As mentioned above, platelet interactions with cancer cells can protect them from rapid clearance in the blood stream. The production of thrombin, tissue factor, fibrinogen, vWF and PAF (platelet activating factor) by tumour cells can activate platelets and cause platelet binding to tumour cells (267). PAF is responsible for platelet aggregation and has been shown to mediate angiogenesis as well as having roles in tumour growth and metastasis (320). When PAF is inhibited, tumour growth is reduced in the B16 model (321). The production of PAF by B16 F10 cells can be caused by IFNγ which can also inhibit B16 F10 growth in vitro (322). In the B16 F10 model of metastasis, a single injection of PAF increases the number of metastatic colonies, by increasing expression of MMP9 in the lungs (323). In vitro, B16 F10 cells form aggregates with platelets, and platelets have a role in metastasis – thrombocytopoenia reduces metastasis (324). Platelets can coat circulating cancer cells, facilitating adhesion to endothelium (325). Mice lacking Gp 1b-1x (the primary adhesion receptor for platelets) have a reduction in B16 F10 metastasis

(326). B16 F10 cells produce low levels of PGD2 (prostaglandin D2) which can cause platelet aggregation and is though to increase metastasis (327).

1.13.2.2 Chemokines & Chemokine Receptors in B16 Metastasis

Chemokines and chemokine receptors have long been associated with metastasis. As mentioned previously (section 1.13.1.1), transfection of a single chemokine receptor gene can increase organ specific metastasis in the B16 tumour model. Chemokines and their receptors can also affect the development of colonies in the B16 F10 experimental metastasis model.

CCR5 expression by non-haematopoietic cells is important in metastatic colony development, shown using bone marrow chimera studies in CCR5KO mice, which have reduced metastatic colonies (328). These data suggests that B16 F10 cells may be creating a pre-metastatic niche, by recruiting pulmonary fibrocytes, via CCR5, which is essential to the development of metastatic colonies as they produce MMP9 (329). When CXCR4 is over-expressed in B16 F10 cells, the number of metastatic colonies increases, and CXCR4 can also promote cell survival in vitro (292, 330). The enhanced metastasis to the lungs caused by CXCR4 can be blocked using T22, an inhibitor of CXCR4 (330). These results show that chemokine receptors may play a role in the development of the pre-metastatic niche, and determining where metastasis occurs.

1.14 Cancer Immunotherapy

The main difficulty with treating cancer cell is that cancer cells are essentially 'self' cells that have mutated. This makes it difficult to design specific therapies that will not cause autoimmunity. Current treatments such as radiotherapy and chemotherapy, target actively dividing cells, rather than tumour cells specifically, which means they have many undesirable side effects. Problems identifying the stage of growth the tumour is in can make it difficult to determine whether or not metastasis has occurred (259). Breaking self-tolerance is an attractive therapy for treating cancer, but again this runs the risk of inducing autoimmunity. Mechanisms to break self tolerance include triggering inflammation, e.g. injecting live BCG (Bacille Calmette Guerin) into the tumour, but this can cause pneumonia, hepatitis and BCG infection (331).

Cytokines which are currently used in melanoma treatment, include high doses of IFNα and IL2, which unfortunately have high levels of cytotoxicity (267, 332, 333). Chemokines also have the potential to be used as cancer therapeutics; in particular there has been interest in using angiostatic chemokines (CXCL9-11) to inhibit tumour growth. In vitro studies have shown that CXCL10 can inhibit human melanoma cell growth in vitro. In vivo studies have shown that IL12 therapy, along with IFNγ can induce the production of CXCL9-11, which can have anti-tumour effects, possibly by inhibiting tumour growth (241, 334). Monoclonal antibody therapies have been shown to be effective against breast cancer and melanoma, but these are often toxic to host (332). There are currently trials using anti-CTLA4 and anti-α4β7 monoclonal antibodies as treatments for melanoma, but these have had limited success (267).

Other types of cancer immunotherapies include vaccines against tumour antigens. In melanoma, potential antigens include gp100, MART-1, TRP1 and TRP2. Unfortunately tumour vaccines do not come without problems; they have limited efficacy and can cause autoimmunity. Regrettably, the presence of autoimmunity seems to be associated with treatment success (333). Cellular therapies have been successful in haematogenous malignancies, e.g. stem cell transplants. Infusion of tumour specific lymphocytes has had good results in 50% of melanoma cases, but this is limited to a defined set of patients (333). It may be impossible to eliminate the side effects attributed to cancer therapies, unless more specific targets can be defined and treatments become more refined.

1.15 Aims & Objectives

D6 has been shown to be involved in the resolution of inflammation and studies have suggested that D6 may play roles in chemotaxis and tumour development. This thesis aims to define the role of D6 in cell movement and to clarify the role of D6 in tumour development. The experiments within this thesis set out to do the following:

1. Determine the role that D6 plays in chemotaxis, in response to inflammatory and constitutive chemokines

2. Determine the role of D6 in melanoma growth and metastasis

These aims will be investigated using a variety of experimental approaches:

1. Analysis of D6 in chemotaxis will be performed using in vitro chemotaxis assays with cells that either over-express (transfected cell lines) or with cells lacking D6 (primary murine cells)

2. Analysis of D6 in neutrophil chemotaxis will be analysed in vivo using a well characterised skin inflammation model with a neutrophil adoptive transfer protocol

3. The role of D6 in melanoma growth will be analysed using a murine model of melanoma, the B16 F0 model, comparing tumour growth in WT mice and D6KO mice

4. The B16 F10 murine model of experimental melanoma metastasis will be used to determine the role that D6 plays in melanoma metastasis

2 Materials & Methods

2.1 Cell culture and transfection

2.1.1 Cell Lines

The B16 murine melanoma cell lines (B16 F0 and B16 F10) were acquired from Dr Mike Edward (Dermatology, Glasgow University) and maintained in DMEM (Dulbecco's modified Eagle's medium), plus 10% FCS, 10 units pen/strep and 2mM glutamine (complete DMEM). All tissue culture reagents were purchased from Invitrogen, Paisley, UK.

2.1.2 Primary Cells

2.1.2.1 Neutrophils

Neutrophils were isolated by first dissecting the femur and the surrounding muscle from 129/Bl6 D6KO and WT mice. In a laminar flow hood, the surrounding muscle was removed from the femur, and the bone placed in sterile PBS (Phosphate Buffered Saline). The ends of the bone were trimmed off using dissecting scissors, and the bone marrow was flushed with ~2ml sterile PBS using a 25G needle. The resulting cell suspension was disaggregated by passing through an 18G needle at least ten times, followed by passing through a 70µm, then a 40µm cell filter (BD Falcon, UK). Cells were counted using a haemocytometer (Sigma Aldrich, UK) before neutrophils were isolated by positive selection using the Ly6G Isolation kit (Miltenyi Biotec, UK). Neutrophils were isolated to ~96% purity using this kit (see figure 3.12). The average yield of neutrophils isolated from murine bone marrow is discussed further in section 3.2.

An alternative method of isolating the bone marrow from the femurs was used, which involved crushing the bones in a sterile mortar and pestle. The muscle was stripped from the bones which were then placed in the mortar, with ~10ml sterile PBS. Bones were crushed with the pestle until the bones appeared clear (this meant all the bone marrow had been removed from the bones). The cell suspension was then passed through filters and underwent magnetic selection for neutrophils, as described above.

2.1.3 Transfection

2.1.3.1 Fugene HD

B16 F0 and B16 F10 cells were transfected using Fugene HD lipofection reagent (Roche Diagnostics GmbH, Mannheim Germany) according to the manufacturers' protocol. The optimal DNA:Fugene reagent ration was calculated by performing an optimisation experiment with B16F0 cells and a GFP expressing plasmid. The optimal ratio was determined to be 4µl Fugene HD to 2µg DNA. The day before transfection, B16F0 cells were harvested by trypsinisation and added to a 6 well culture plate at a concentration of 5×10^5 cells per well. The plasmids to be used in the transfection reaction (murine D6 in pcDNA 3 (Rob Nibbs) and pmax GFP) were diluted to a concentration of 2µg in 100µl sterile water. 4µl Fugene HD reagent was added to the DNA and incubated at room temp for 15 mins. The DNA:Fugene complex was added to the appropriate wells in a 'drop wise' manner. The cells were incubated at 37ºC for 24 hours before GFP expression was analysed to determine transfection efficiency. Transfected cells were then transferred into the appropriate concentration of G418, described below.

2.1.4 Kill Curve

For all cell lines used, a kill curve was created using G418 (Promega, UK) as the selective antibiotic. G418 was chosen as all plasmids used for transfection contained a gentamycin resistance gene. For all cell types, a known cell concentration was plated into a six well tissue culture plate with the appropriate media, plus G418 in a range of concentrations from 0mg/ml up to 2 mg/ml. Fresh media and antibiotics were added halfway through the incubation period. Once the incubation period was over, the cells were harvested, stained with Trypan blue (Sigma Aldrich, UK) and dead cells were counted. The percentage cell death was calculated after 7-14 days for each cell type. The G418 concentration that killed 90-100% of un-transfected cells for each cell type was used when trying to create stable transfectants. The selection of stable transfectants of both B16 F0 and B16 F10 cells was carried out using 2mg/ml G418.

2.1.5 FACS analysis of D6 Expression

2.1.5.1 D6 Function Analysis

B16 F0 and B16 F10 cells were analysed for stable D6 expression using a FACS based chemokine competition assay developed by Chris Hansell. At the time, there was no available antibody against murine D6, so the only way to show expression was at the mRNA level, which gives no indication of protein levels. This assay uses a fluorescently labelled version of CCL2, with an Alexa-fluor labelled lysine residue at the C-terminus (Almac, UK) that can bind to CCR2 and D6. Cells of interest are incubated with PM2 (a mutant of CCL3 which does not form aggregates at high concentrations(12)) that can bind to CCR1, CCR5 and D6. Due to the nature of D6, if a vast excess of PM2 is added to the cells before the addition of labelled CCL2, all the D6 will bind PM2 and will be unable to bind to the fluorescent CCL2. The uptake of CCL2 in the absence of PM2 is compared to the uptake in the presence of PM2, and if addition of PM2 abrogates CCL2 binding, then this shows that CCL2 uptake must be through D6, as there is no other chemokine receptor that binds to both of these chemokines. The cells of interest were harvested and resuspended in binding buffer (20mM HEPES in RPMI) to a concentration of 1×10^6 cells per 100µl. 2.5 µl of PM2 (0.1mg/ml) was added to the cells and the whole volume was mixed. 0.5µl of CCL2-Alexa 647 (Almac, UK) was added to the cells and mixed. Cells were incubated for 40 minutes at 37ºC, with periodic re-suspending. Following incubation with chemokines, cells were washed twice with FACS buffer before fixing with 2% paraformaldehyde. Cells were analysed using the FACS Calibur.

2.2 Neutrophil Adoptive Transfer

2.2.1 Maintenance of mice

Mice were housed within the animal facility at the Central Research Facility at Glasgow University. All procedures performed on mice were in accordance with United Kingdom Home Office guidelines and were in accordance with the appropriate project and personal licenses.

2.2.2 Neutrophil Isolation and Labelling

Differential labelling of 129/Bl6 D6KO and WT neutrophils was performed using CFSE (Carboxyfluorescein succinimidyl ester) and CMTMR (5-(and6-)-(((4-chloromethyl)benzoyl)amino)tetramethylrhodamine) or TAMRA (Tetramethyl-6-Carboxyrhodamine) (Molecular Probes, Invitrogen, UK). Neutrophils were isolated from 129/Bl6 mice, as described in section 2.1.2.1. For CFSE labelling, neutrophils were resuspended at a concentration of 1 x 10^6 per ml in PBS 0.1%/BSA. 2µl of 5mM CFSE stock was added per ml of cells to give a final concentration of 10µM, and the cells were incubated at 37ºC for 10 minutes. The staining was quenched by adding 5 volumes of ice cold PBS, and incubating for 5 minutes on ice. Cells were centrifuged at 1200rpm for 5 minutes and washed 3 times in fresh media (RPMI). TAMRA staining was performed as described for CFSE staining, but 0.5µl of 10mM TAMRA was added per ml of cells to give a final concentration of 5µM, and cells were incubated for 20 minutes at 37ºC. Quenching and washing was performed as per CFSE staining. CMTMR was used to stain neutrophils at a concentration of 5µM in RPMI. Cells were incubated in the staining solution for 30 minutes at 37ºC. Stained neutrophils were washed in PBS before counting on a haemocytometer then re-suspending at the appropriate cell concentration (cell numbers are described in tables 3.1 and 3.2)

2.2.3 Neutrophil Adoptive Transfer

129/Bl6 mice were shaved and dorsal skin was painted with TPA (12-tetradecanoyl 13-phorbol acetate, 150µl of 50µM TPA in acetone). WT and D6KO labelled neutrophils were mixed together in equal concentrations (numbers described in tables 3.1 and 3.2) in a maximum volume of 200µl sterile PBS. At indicated time points after TPA treatment,

fluorescently labelled neutrophils were administered into the tail vein of the treated mice. For all neutrophil adoptive transfer experiments, mice were on a 129/Bl6 mixed background, were aged between 6-8 weeks, and age matched.

2.2.4 Frozen Sections

After sacrifice, 5mm punch biopsies of the inflamed dorsal skin from mice that received labelled neutrophils, were collected and snap frozen in liquid nitrogen. Skin biopsies were embedded in OCT (Optimal Cutting Temperature, Thermo Shandon, Cheshire, UK). 4µm frozen sections were either cut at the Vet School (University of Glasgow, UK), or cut in-house using the cryostat (Bright, UK). Frozen sections were stored at -80ºC prior to use. Frozen sections were left to thaw and air dry before mounting in Vectashield plus DAPI (4'-6-Diamidino-2-phenylindole, Vector Laboratories, UK), before adding a coverslip and sealing with nail varnish, or permanent mount (Sub X Mounting Media, SurgiPath, UK).

2.2.5 Confocal Analysis

Frozen sections, mounted using Vectashield with DAPI as described above, were analysed on the LSM 510 Meta (Zeiss, Germany) confocal microscope. The 200x objective was used to take pictures of the entire skin section. This allowed an ‘overlay’ picture to be generated; using which the whole skin section could be viewed in one picture (see figure 3.31). Positive cells were identified and the distance from their position to the epidermis was measured using Axiovision software.

2.3 Melanoma Model

2.3.1 Tumour Model

B16 F0 murine melanoma cells were cultured in DMEM before harvesting during log phase, by adding trypsin (Trypsin EDTA 0.25%, Sigma Aldrich, UK) to the cells in culture flasks (2ml for T25 flask, 4ml for T75 flask). After five minutes incubation, cells were collected by addition of 2-8ml complete DMEM. Cells were counted using a haemocytometer, centrifuged and resuspended in PBS at the desired concentration. C57Bl/6 mice housed in the Central Research Facility (Glasgow University) were used for tumour models. Mice were between 6-8 weeks old at the time of experiment, and were age and sex matched. Mice were shaved and received 5 x 10^5 B16 F0 cells in 200µl PBS subcutaneously in the dorsal skin. The injection site was monitored daily until signs of tumour formation became visible. When the tumour became palpable, it was measured using callipers on a daily basis. Two tumour lengths were measured and the mean diameter was calculated as the average of the two lengths. Mice were sacrificed when the mean tumour diameter reached greater than 1.2 cm (according to Project licence). Tumours were excised and fixed in 10% NBF (neutral buffered formalin) (Surgipath, UK) for a minimum of 24 hours before processing for histology, as described in section 2.4.6.

2.3.2 Metastasis Model

The B16 F10 melanoma cell line was cultured as described above for B16 F0 cells. C57Bl/6 mice were between 6-8 weeks old at the time of experiment (mice were sex and age-matched). B16 F10 cells were harvested in trypsin, as described above, counted and resuspended in PBS to get a final concentration of 5 x 10^5 cells in 200µl. Mice were placed into a heat box to dilate the tail vein, before 200µl of the B16 F10 cell suspension in PBS was injected into the tail vein. The mice were left for up to two weeks (with daily monitoring) at which point they were sacrificed by CO_2 overdose. The ribcage was exposed and removed to expose the lungs. A 25G needle was introduced into the trachea and the lungs were slowly filled with PBS or NBF until they were fully inflated. The trachea was tied with suture thread to prevent the fluid escaping and the lungs were removed ‘en bloc’. The lungs were placed into 10% NBF for later histological analysis, or in cold RPMI

for FACS analysis. Melanoma colonies on the lungs surface were counted using a dissecting microscope.

2.3.2.1 Pleural Washes

C57Bl/6 mice that had received melanoma cells intravenously, or untreated mice (both WT and D6KO mice) were sacrificed by CO_2. The ribcage was exposed and ~5 ml of sterile PBS was injected into the pleural cavity, between two ribs, being careful not to puncture the lungs. The fluid was removed, placed on ice, and the protein concentration measured by NanoDrop (Thermo Scientific, UK). Pleural wash samples had to be concentrated into a smaller volume using an Amicon Ultra-15 Centrifugal filter device (Millipore, UK), which retained all protein samples above 3,000 kDa. This concentrated the samples, to give a range of protein concentrations from 0.06mg/ml-1.57mg/ml, compared to 0.01mg/ml-0.36mg/ml prior to concentration.

2.3.2.2 Luminex

Pleural wash samples were analysed for the presence of 11 different chemokine and cytokines (see table 5.1), using a custom designed mouse cytokine/chemokine Milliplex kit (Millipore, UK). The assay was carried out according to the manufacturers protocol. This involved preparing the Luminex plate by adding 200µl wash buffer to each well, this was left to incubate for 10 minutes at room temperature on a plate shaker. The wash buffer was removed by vacuum and excess buffer was blotted from the bottom of the plate. Standards and controls (both provided with the kit) were added onto the plate (25µl), following the plan described below in table 2.1. 25µl of assay buffer was then added to each sample well, followed by 25µl of PBS (which was the appropriate matrix solution), which was added to all wells. Finally 25µl of sample was added to the appropriate wells. This was followed by the addition of the mixed beads (one per cytokine/chemokine to be analysed), to each well (25µl). The plate was sealed and incubated at 4ºC with agitation overnight.

	1	2	3	4	5
A	0 pg/ml standard	400 pg/ml standard	QC-2 control	KO1 untreated	WT3 F10
B	0 pg/ml standard	400 pg/ml standard	QC-2 control	KO1 untreated	WT3 F10
C	3.2 pg/ml standard	2000 pg/ml standard	WT 1 untreated	KO2 untreated	KO1 F10
D	3.2 pg/ml standard	2000 pg/ml standard	WT 1 untreated	KO2 untreated	KO1 F10
E	16 pg/ml standard	10,000 pg/ml standard	WT2 untreated	WT1 F10	KO2 F10
F	16 pg/ml standard	10,000 pg/ml standard	WT2 untreated	WT1 F10	KO2 F10
G	80 pg/ml standard	QC-1 control	WT3 untreated	WT2 F10	KO3 F10
H	80 pg/ml standard	QC-1 control	WT3 untreated	WT2 F10	KO3 F10

Table 2-1: Layout of Milliplex plate for analysis of pleural washes

The chemokine and cytokine content of pleural washes was analysed using a custom-designed Luminex kit from Millipore. The table above shows the plate outline, with the standards provided by the company in the first two rows, followed by two quality control samples. (QC= quality control). The remainder of the plate was used by another member of the lab. This was used for the analysis of pleural wash samples.

The following day, the fluid was removed from the plate by vacuum and washed twice with 200µl of wash buffer. Excess wash buffer was blotted from the plate and then 25µl of detection antibodies were added into each well. The plate was then sealed and incubated for an hour with agitation at room temperature. 25µl of streptavidin-PE was then added to each well containing detection antibodies; the plate was sealed and incubated with agitation for 30 minutes at room temperature. All the contents of the plate were removed by vacuum, and the plate was washed twice with 200µl wash buffer per well. Finally, 150µl sheath fluid was added to all the wells and the beads were resuspended on a plate shaker for 5 minutes. The plate was run using the Bioplex System (Biorad, UK), with the help of Ashley Gilmour.

2.3.2.3 AMD 3100

After receiving intravenous injections of B16F10 cells, as described above, C57Bl/6 mice were treated with the specific CXCR4 antagonist AMD3100. AMD3100 is a bicyclam molecule that was initially developed as a potential treatment for HIV. It specifically interacts with CXCR4, and as a result, has effects on HIV replication, stem cell mobilisation from the bone marrow and cancer metastasis (335). Mice that had received B16 F10 cells

intravenously were given twice daily doses of AMD3100, or PBS control, for the duration of the metastasis experiment (14 days). AMD3100 was administered subcutaneously, at 60µg per dose in 50µl PBS. Mice were sacrificed and organs were taken for histological analysis after 14 days.

2.3.3 Tissue Processing

Tumours and lungs were processed for histology using the Shandon Citadel 1000 (Thermo Shandon, Cheshire, UK). The processing cycle is described in table 2.2. After processing, tissues were embedded using the Shandon Histocentre 3. For histological analysis all tissue sections were cut at 4µm thick using a Shandon Finesse 325 microtome. Sections were floated in a water bath at 40ºC before placing onto polysine-coated slides (VWR, UK). Sections were left overnight at 65ºC on a hot plate before staining.

Solution	**Time**
Neutral Buffered Formalin	30 minutes
70% Alcohol	1 hour
90% Alcohol	1 hour
95% Alcohol	1 hour
100% Alcohol	1 hour
100% Alcohol	2 hours
100% Alcohol	2.5 hours
Xylene	1 hour
Xylene	1 hour
Xylene	1.5 hours
Wax	4 hours
Wax	5 hours

Table 2-2: Tissue processing protocol.

The above processing protocol was used to process tissues from both the B16 F0 tumour model and the B16 F10 metastasis model. The program was created and stored on the Shandon Citadel 1000. After tissue processing using the above program, samples were embedded in paraffin wax using the Shandon Histocentre 3, in order to allow cutting of paraffin embedded sections.

2.3.4 Histological Analysis

Haematoxylin and eosin (H&E) staining was carried out as follows. Sections were de-waxed and rehydrated by incubating in xylene for 3 minutes, followed by 10 dips in 100% alcohol, another 10 dips in fresh 100% alcohol, 10 dips in 70% alcohol followed by washing in running water. Slides were placed in haematoxylin (CellPath, UK) for 7

minutes, followed by rinsing in running water until clear. Slides were then dipped in 1% acid alcohol for 12 dips, washed in running water, placed in Scotts tap water substitute (CellPath, UK) for 2 minutes, washed in running water then placed in Putts Eosin (CellPath, UK) for 4 minutes. Slides were washed in running water for 2 minutes, followed by 10 dips in 70% alcohol, 10 dips in 100% alcohol, another 10 dips in fresh 100% alcohol followed by 3 washes in xylene for 1 minute each. Sections were then permanently mounted using DPX (Di-n-butyl Phthalate in xylene, VWR, UK).

2.3.5 Immunohistochemistry

2.3.5.1 Von Willebrand Factor

Von Willebrand factor (vWF) antibody staining was performed on tumour and lung sections using a rabbit anti-human antibody from Dako (UK). Sections were de-paraffinised and rehydrated using the following protocol:

5 minutes in Xylene (times 2)

3 minutes in 100% alcohol (times 2)

3 minutes in 90% alcohol (times 2)

3 minutes in 70% alcohol (times 2)

This was followed by washing sections in tris-buffered tween (TBT 10mM pH 7.5) for 3 minutes. Slides were incubated in 0.5% hydrogen peroxide in methanol for 3 minutes to block endogenous peroxidase activity. This was followed by two 5-minute washes in TBT. Antigen retrieval was performed by boiling Tris EDTA buffer in a microwave, placing slides in the solution and boiling them in the microwave for 30 minutes, followed by 20 minutes cooling time. Slides were then washed in distilled water for 5 minutes, followed by a 5-minute wash in TBT. A wax ring was drawn around the section using an ImmEdge pen (Vector Laboratories, UK). To prevent non-specific binding of the antibody, sections were incubated in a solution of 20% normal goat serum (Vector Laboratories, UK) in PBS for 30 minutes. Slides were washed briefly in TBT before adding the primary antibody diluted in antibody diluent (Dako, UK). The antibody was used at a 1 in 300 dilution and incubated at 4ºC overnight. Sections were brought to room temperature then washed twice in TBT

for 5 minutes each wash. The secondary antibody was added to the sections (Envision kit, Dako, UK) and incubated at 37ºC overnight. Secondary antibody was drained from the sections that were then washed in TBT for two 5-minute washes. The peroxidase substrate Nova Red (Vector Laboratories, UK) was added to the sections and incubated for 5 minutes. Washing sections in distilled water terminated the peroxidase reaction. Sections were then counterstained by placing in haematoxylin for 20 seconds, followed by washing in running water until the water ran clear. Sections were then dehydrated by placing in 70% alcohol for 30 seconds, 90% alcohol for 1 minute, 100% alcohol for 3 minutes, then 3 x 3 minute incubations in Xylene. The sections were then mounted using DPX.

2.3.5.2 LYVE-1

LYVE-1 (Lymphatic Vessel Endothelial Receptor 1) antibody staining was performed using a biotinylated anti-mouse LYVE-1 antibody (R& D Systems, UK). Sections were de-paraffinised and rehydrated as for the vWF antibody staining. Peroxidase blocking and antigen retrieval was performed as described above. The blocking step involved incubating the sections in 20% normal horse serum (Vector Laboratories, UK) in PBS for 30 minutes. After briefly washing in TBT, the primary antibody was added at a final concentration of 10µg/ml and incubated overnight at 4ºC. The primary antibody was washed off with TBT and streptavidin HRP (Horseradish Peroxidase, Dako, UK) was added at a concentration of 1 in 500; this was incubated overnight at 37ºC. Sections were washed in TBT for two 5 minute washes before adding DAB (3, 3'-diaminobenzidine,Vector Laboratories, UK) for 5 minutes. The sections were counterstained, dehydrated and mounted as described above.

An alternative protocol was used for LYVE-1 staining. Sections were de-paraffinised, dehydrated, and underwent peroxidase blocking and antigen retrieval as described above. After antigen retrieval, sections were fixed in ice-cold acetone for 5 minutes before air-drying. This was followed by three 5-minute washes in PBS. A further blocking step was performed by incubating the sections in 2% fish gelatine (Sigma Aldrich, UK) in PBS, with the addition of 10µg/ml rat IgG (VectorLabs, UK), for 20 minutes at room temperature. Avidin and biotin blocking was performed using a kit available from VectorLabs (UK). This involved adding 4 drops of avidin blocking solution per ml of blocking solution (2% fish gelatine in PBS) and incubating for 5 minutes followed by a brief

rinse in PBS. Biotin blocking was performed in the same manner, adding 4 drops of biotin blocking solution per ml of blocking buffer and incubating for 5 minutes. Sections were then incubated overnight at 4ºC with 10µg/ml LYVE-1 antibody prepared in 1% fish gelatine/PBS. Following primary antibody incubation, sections were washed 3 times (5 minutes each) with PBS/Tween (0.05%). Streptavidin conjugated to Cy-5 (Invitrogen, UK) was added to the sections at a concentration of 1:30 in 1% fish gelatine/PBS. This was incubated for 30 minutes at room temperature. Sections were then washed with PBS/Tween for 3 times 5 minutes, followed by three 5-minute washes in PBS. Sections were then mounted using Vectashield plus DAPI (VectorLabs, UK); a coverslip was placed over the section and sealed with nail varnish.

2.3.5.3 Mac-2

The protocol for macrophage staining was adapted from a protocol by Robert Macdonald (Cardiovascular Research Centre, Glasgow University). Sections cut at 4µm were left on the heat block overnight before placing in xylene for two times 5 minute washes, then rehydrated by placing in 100% ethanol for 5 minutes, 70% ethanol for 5 minutes, then running water for 5 minutes. Wax rings were drawn around the section, followed by addition of 3% hydrogen peroxide in distilled water for 5 minutes to block endogenous peroxidase activity. Sections were washed in PBS for 2 minutes, twice. Blocking was performed with 20% normal goat serum in PBS for 30 minutes. The primary antibody was rat anti-mouse Mac-2 (Cedarlane, USA), which was diluted 1 in 6000 in PBS/1% BSA, added to sections and left overnight at 4ºC. Sections were washed in PBS for 3 times 5 minute washes. The secondary antibody was goat anti-rat IgG (Vector Laboratories, UK), which was diluted 1 in 200 in PBS/1% BSA. The secondary antibody was added to the sections and was incubated for 30 minutes. Sections were washed in PBS 3 x five minutes before adding Extravidin Peroxidase LSAB reagent (Sigma Aldrich, UK) diluted 1 in 200 in PBS/1%BSA and incubated for 30 minutes. Sections were washed in PBS 3 x five minutes before adding DAB reagent (3, 3'-diaminobenzidine,Vector Laboratories, UK) and incubating for 5 minutes. The reaction was quenched with distilled water (5 minutes) and counterstained in haematoxylin for five dips. Sections were rehydrated by placing in 70% ethanol for two times 1 minute, 100% ethanol for one minute, xylene for two times 2 minutes, then permanently mounting with DPX.

2.3.5.4 TUNEL

TUNEL (Terminal deoxynucleotidyl transferase dUTP nick end labelling) staining was performed using the Dead End colorimetric TUNEL system from Promega (UK), according to manufacturers instructions. Tissue sections were cut at 4µm as described previously. Slides were de-paraffinised by placing in xylene for two 5-minute washes. This was followed by five minutes in 100% ethanol, then 3 minutes in fresh 100% ethanol. Slides were then placed into 90% ethanol for 3 minutes, followed by 70% ethanol for 3 minutes. Slides were then washed in 0.85% NaCl for 5 minutes at room temperature. This was followed by a 5-minute wash in PBS. Sections were then fixed by placing in 10% NBF for 15 minutes at room temperature. Two 5-minute washes in PBS followed this step. Whilst sections were washing, a 20µg/ml proteinase K solution was prepared using stock solution provided with the kit. 100µl of proteinase K was added to each slide and incubated for 10 minutes at room temp. Slides were washed in PBS for 5 minutes, before re-fixing in 10% NBF for 5 minutes at room temp. Another two five minute PBS washes followed, and then excess fluid was removed from the sections. Samples were then covered with 100µl equilibration buffer and incubated for 5-10 minutes. Whilst the sections were equilibrating, the biotinylated nucleotide mix was thawed on ice, and the rTdT (recombinant Terminal Deoxynucleotidyl Transferase) reaction mix was prepared for all sections and kept on ice (98µl equilibration buffer, 1µl biotinylated nucleotide mix and 1µl rTdT enzyme per section). Areas around the sections were blotted with a tissue to remove equilibration buffer, and 100µl of rTdT mix was added to each section. These were covered with a plastic coverslip and incubated at 37ºC for 1 hour in a humidified chamber. The reaction was terminated by immersing the slides in SSC (saline sodium citrate) buffer for 15 minutes at room temperature. Slides were then washed three times in PBS for 5 minutes each. Endogenous peroxidase activity was then blocked by immersing slides in 0.3% H_2O_2 in PBS for 5 minutes at room temperature. This was followed by another three 5 minute washes in PBS. 100µl of streptavidin HRP solution was added to each sample and incubated for 30 minutes at room temperature, followed by another three 5 minute washes in PBS. DAB components (provided with the kit) were prepared prior to use and kept in the dark until needed. 100µl of DAB solution was added to each sample and the reaction was left to develop for 10 minutes. Rinsing several times in deionised water terminated the reaction. Slides were mounted using aqueous mounting media (Vectamount AQ aqueous mounting media, VectorLabs, UK).

2.3.5.5 CD3

CD3 staining was used to identify T cells in tissue sections. Sections were deparaffinised and rehydrated with a series of xylene and alcohol washes:

Xylene for 5 minutes

100% ethanol for 1 minute

100% ethanol for 1 minute

70% ethanol for 1 minute

Tap water for 5 minutes

Endogenous peroxidase activity was blocked by incubating sections in 0.5% H_2O_2 in methanol for 30 minutes at room temperature. Sections were then washed in TBT for 5 minutes. Antigen retrieval was performed by boiling Tris EDTA buffer in a microwave, placing slides in the solution and boiling them in the microwave for 30 minutes, followed by 20 minutes cooling time. Slides were then washed in distilled water for 5 minutes followed by a 5-minute wash in TBT. Non-specific binding was blocked by incubating sections in ready to use 2.5% horse blocking serum (ImmPRESS anti-rabbit peroxidase kit, VectorLabs, UK) for 45 minutes at room temperature. The blocking serum was 'tapped' off the slides and the primary antibody; a polyclonal rabbit anti human CD3 (Dako, UK) was added to the sections, at a concentration of 1/1000 in Dako antibody diluent solution containing 2.5% horse serum (VectorLabs, UK) and 2.5% mouse serum. The primary antibody was incubated on the sections overnight at 4ºC. The primary antibody was removed and sections were washed in TBT for 5 minutes, twice. Sections were then incubated with the rabbit ImmPRESS reagent for 30 minutes. Slides were then washed for 5 minutes with TBT. Sections were then incubated with Novared for 5 minutes, this reaction was terminated by the addition of distilled water. Sections were then washed with TBT for 5 minutes, followed by a 5-minute wash in distilled water. Sections were then counterstained by dipping twice into haematoxylin, rinsing in tap water and dehydrating by placing in 70% ethanol for 30 seconds, 100% ethanol for 1 minute and 100% ethanol for 3 minutes. Sections were placed in 2 washes of xylene for 5 minutes and mounted permanently using DPX.

2.3.6 Flow cytometry

Lungs from C57Bl/6 mice, with and without intravenous administration of B16 F10 cells, were perfused with PBS and placed into 5ml RPMI on ice. The lung tissue was cut into small pieces (mm^2) with dissecting scissors. The resulting tissue suspension was incubated in 1mg/ml collagenase D in PBS (Roche Diagnostics GmbH, Mannheim, Germany), for 1 hour at 37ºC with constant shaking. The remaining lung pieces were placed into a 70µm cell strainer, and any remaining tissue fragments were pushed through with the end of a syringe into a 50ml tube. The resulting cell suspension was passed through a 40µm cell strainer and centrifuged at 300g for five minutes at 4ºC. The cell pellet was resuspended in red blood cell lysis buffer and incubated for 1 minute. The reaction was stopped by adding 20ml RPMI and centrifuged for 5 minutes. Cells were washed twice with PBS and counted using a haemocytometer. Lung cells were resuspended at a final concentration of 1×10^6 cells per 150µl PBS, before proceeding to antibody labelling. Fc block (Miltenyi Biotec, UK) was added to the cells at a dilution of 1:10 and incubated for 10 mins to block non-specific antibody binding. A panel of lineage markers were used to stain lung cell populations. 10µl each of CD3-FITC, CD19-Cy5, CD11b-APC, CD11c-Cy7, Ly5.2-PE (All antibodies from eBioscience, UK, except CD11b-APC which was from Abcam, UK) were added to the cells and incubated for 20 minutes on ice. The stock concentration for all antibodies was 0.2mg/ml. Cells were washed in PBS before adding to FACS tubes and analysed using the MACSQuant (Miltenyi Biotec, UK) with the help of Alasdair Fraser. Results were analysed using CAP software (Miltenyi Biotec, UK)

2.4 Molecular Biology

2.4.1 PCR

PCR reactions were performed using ReddyMix PCR Master Mix (Abgene, Surrey, UK). Each reaction contained 0.2 mM of each dNTP and 1.5 mM $MgCl_2$. Primers were added to the master mix at varying concentrations (from 0.4µM to 0.5µM final primer concentration). Primers used were from VHBio (subsequently became IDT DNA, UK); sequences are shown in table 2.3.

Gene	Forward Primer	Reverse Primer	Annealing Temp
Murine CCR1	GCCCTCATTTCCCCTACAA	CGGCTTTGACCTTCTTCTCA	50.81ºC 52.07ºC
Murine CCR2	AGAGAGCTGCAGCAAAAAGG	GGAAAGAGGCAGTTGCAAAG	55.8ºC 54.5ºC
Murine CCR3	TTTCCTGCAGTCCTCGCTAT	ATAAGACGGATGGCCTTGTG	56ºC 54.8ºC
Murine CCR4	ATTTGCTGTTCGTCCTGTCC	CGTGTGGTTGTGCTCTGTGT	55.5ºC 58.1ºC
Murine CCR5	TTTGTTCCTGCCTTCAGACC	TTGGTGCTCTTTCCTCATCTC	54.9ºC 54.6ºC
Murine CCR7	GTGTGCTTCTGCCAAGATGA	CCACGAAGCAGATGACAGAA	55.5ºC 54.9ºC
Murine D6	TTCTCCCACTGCTGCTTCAC	TGCCATCTCAACATCACAGA	57.5ºC 54.9ºC
Murine GAPDH	TGTCTCCTGCGACTTCAA	TGCAGCGAACTTTATTGATG	53.5ºC 51.2ºC

Table 2-3: Nucleotide sequences used for PCR.

Primer sequences used for all PCR reactions. Primers were designed using Primer 3 software. The melting temperatures for each primer pair is shown, which was used to calculate the ideal annealing temperature for the PCR programs.

Two different PCR programs were used throughout, with different annealing temperatures depending on the primers used (described for each PCR reaction). PCR program 1: (referred to as CLIVE program) 95ºC for 3 minutes, 95ºC for 15 seconds, 59.5ºC for 20 seconds, 72ºC for 30 seconds (step 2 through 4 repeated 35 times), followed by a final 72ºC for 7 minutes. PCR program 2: (CBPCR1 program) reactions using this PCR program were started with a 'hot start'. This meant the samples were heated to 95ºC before adding the final component (this could be primers or template DNA). This

PCR program started with 95ºC for 3 minutes, 95ºC for 15 seconds, 60ºC for 20 seconds, and 72ºC for 40 seconds (step 2 through 4 repeated 35 times), followed by 72ºC for 7 minutes. PCR program 3: (CBPCR2 program) 95ºC for 2 minutes, 95ºC for 1 minute, 55ºC for 30 seconds, 72ºC for 2 minutes (step 2 to 4 repeated 30 times), followed by 72ºC for 7 minutes.

PCR products were analysed on agarose (Invitrogen, UK) gels, varying from 1-2% (in TAE (tris acetate EDTA) buffer). Ethidium bromide (Invitrogen, UK) was added to the molten agarose to a final concentration of 0.5µg/ml. Once the gel was set, 5-8µl of each PCR product was added to each well of the gel, along with a DNA ladder (Hyperladder IV, Bioline) in at least one of the wells. The gel was allowed to run for 30-40 minutes at 100-110 volts. The gel was imaged using the AlphaImager (AlphaInnotech, UK).

2.4.2 RNA Extraction

For RNA extraction from cell lines, cells were harvested, counted and pelleted. The pellet was kept frozen at -80ºC until the RNA was extracted. RNase free filter tips and plastics were used throughout all RNA work. Before RNA was isolated, surfaces were wiped down with 70% ethanol and RNase ZAP (Ambion, UK) to remove endonucleases. The RNA was extracted using the RNeasy mini kit (Qiagen, UK) following the manufacturers protocol for animal cells. On column DNase digestion (Qiagen, UK) was performed for all samples following the manufacturers instructions. RNA was eluted in RNase-free water and stored at -80ºC. RNA was isolated from mouse tissues by placing the tissue of interest in RNA Later (Qiagen, UK), or snap freezing the tissue in liquid nitrogen. The tissue was crushed to a fine powder using liquid nitrogen and a mortar and pestle. RNA was then extracted using the RNeasy mini kit, following the manufacturers protocol for animal tissues. RT-PCR

cDNA was generated from RNA using the Superscript II (or III) kit (Invitrogen, UK). 5µg of RNA was mixed with 1 µl (0.5 µg) oligo-dT primer, 1 µl dNTPs (10 mM with respect to each / 40 mM total). The reaction mix was denatured at 65^{o}C for 5 minutes then placed on ice for 5 minutes. A master mix was made up containing the following; 4 µl 5X buffer, 2 µl 0.1 M DTT, 0.5 µl RNasin (RNase inhibitor). 6.5 µl of master mix was added to each denatured RNA sample and incubated for 2 minutes at 42^{o}C. 50 units (1 µl) of Superscript

II (or III) was added and incubated for 60 minutes at 42^{o}C, followed by a 15-minute inactivation step at 70^{o}C.

Some cDNA samples were generated using the Affinityscript kit (Stratagene, UK). It was decided to start using this kit as it was more cost effective and worked just as well as Superscript kit. cDNA was generated using Affinityscript according to the following protocol. 1ng-5µg of RNA was added to an RNase free micro centrifuge tube along with 1µl oligo dT primers (0.5µg/µl) and RNase free water to a final volume of 15.7µl. The reaction was incubated at 65ºC for 5 minutes, then left to cool for 10 minutes at room temp to allow the primers to anneal to the RNA. The following components were added to the reaction: 2µl 10x Affinityscript buffer, 0.8µl dNTP mix (25mM each dNTP), 0.5µl RNase block ribonuclease inhibitor (40U/µl) and 1µl AffinityScript Multiple Temperature RT. The reaction was incubated at 42ºC for 5 minutes followed by 55ºC for 55 minutes. Incubating at 70ºC for 15 minutes terminated the reaction. The resulting cDNA was diluted 1 in 5 in DEPC treated water (Ambion, UK) and stored at -20ºC to be used for future experiments

2.4.3 Ethanol Precipitation

Plasmid DNA was purified by Miniprep (Qiagen), and ethanol precipitation was performed before using the plasmid DNA for transfection. 1/10 volume of 3M NaAc was added to the DNA solution that was to be precipitated. This was followed by adding 2 volumes ice cold 100% ethanol. The DNA solution was placed into the -80ºC freezer for 30 minutes, followed by centrifugation at high speed (10,000rpm) for 10 minutes. The supernatant was discarded and the pellet resuspended in 70% ethanol and spun for another 3 minutes. The supernatant was discarded under sterile conditions and the pellet was left to air dry, before re-suspending in the buffer of choice for use in transfection experiments.

2.5 Statistical Analysis

Statistical analysis was performed using Graphpad Prison software version 4.0. Results shown throughout are mean +/- standard error of the mean (SEM) unless stated in the figure legend. Statistical tests used were unpaired students t test, two way ANOVA with Bonferroni's post test and the Logrank test. Values of p less than or equal to 0.05 were considered to be statistically significant.

3 In vivo migration of neutrophils

3.1 D6 and chemotaxis

As mentioned in the introduction, chemotaxis is essential in a wide variety of cellular processes. During development, chemotaxis allows stem cells and progenitors to migrate to the correct position in the embryo, and it is required for the development of organs and the immune system (336). Chemokines and their receptors play an essential role in development, as revealed by studies using KO mice. CXCL12 and CXCR4 are believed to be the primordial chemokine ligand and receptor – KO for both are perinatally lethal with defects in B cell lymphopoiesis, haematopoietic stem cell development, primordial germ cell development, cardiogenesis and neural development (61, 337).

In addition, the immune system relies on cell movement for the initiation and maintenance of immune responses. In the innate response, neutrophils, monocytes and DCs must be able to enter the site of inflammation and infection in order to try to clear the pathogen and resolve the inflammation (48). Defects in cell movement cause diseases such as leukocyte adhesion deficiency, which results from a deficiency in the β2 integrin subunit. This results in the development of persistent infections (338). In the case of DCs, they must be able to migrate in response to inflammatory stimuli, and once at the site of inflammation, their chemokine receptors have to switch from inflammatory chemokine receptors such as CCR 1 and CCR2 to CCR7 (94). This is required to allow them to migrate to the draining lymph node, where they interact with T cells and help to mount an adaptive immune response, which involves numerous other cells.

As well as expression of conventional signalling chemokines receptors, leukocytes have been shown to express D6, an atypical chemokine receptor. In particular, DCs and B cells have high levels of D6 expression (144, 145). Work using D6KO mice has suggested that D6 may play a role in cell movement. In the EAE model, DCs are unable to leave the site of inoculation in D6KO mice, which appears to result in reduced T cell activation, and a reduced disease severity (153). In the TPA model of skin inflammation, D6KO mice display an aberrant localisation of neutrophils compared to WT mice. In D6KO skin, neutrophils are found at the dermal/epidermal junction, whilst in WT mice neutrophils are found in the dermis (140, 152). As neutrophils have been shown to express D6, it has been

suggested that D6 may somehow influence their migration into inflamed skin. In vitro work, using transfected cell lines, shows that cells which co-express CCR4 and D6 have reduced chemotactic abilities to CCL22. When D6 is co-expressed with CXCR4, migration to CXCL12 is unaffected. These data suggest that D6 may compete for ligand with signalling CC chemokine receptors, or may interfere with the signalling mechanism for CCR4 (141). These results were obtained using transfected cell lines, which are likely to express the transfected receptors at levels higher than those found in vivo, so this data needs to be analysed with that caveat in mind.

Taken together, these data suggest that D6 may act on a cell autonomous basis to influence cell movement. Looking more in detail at the aberrant location of neutrophils in inflamed skin from D6KO mice, there are two possible explanations of the role of D6 in cell movement. D6KO neutrophils may be found at the dermal epidermal junction due to increased levels of chemokines in this area (i.e. as a secondary effect of the inflammatory response and not due to a defect in neutrophil movement), allowing neutrophils to migrate here (A in figure 3.1). Alternatively, a lack of D6 on neutrophils may mean that they are able to enter the skin normally under the influence of signalling chemokine receptors, but once there, these neutrophils are unable to halt their movement and continue moving to the dermal/epidermal junction (B in figure 3.1). These two hypotheses are illustrated in figure 3.1.

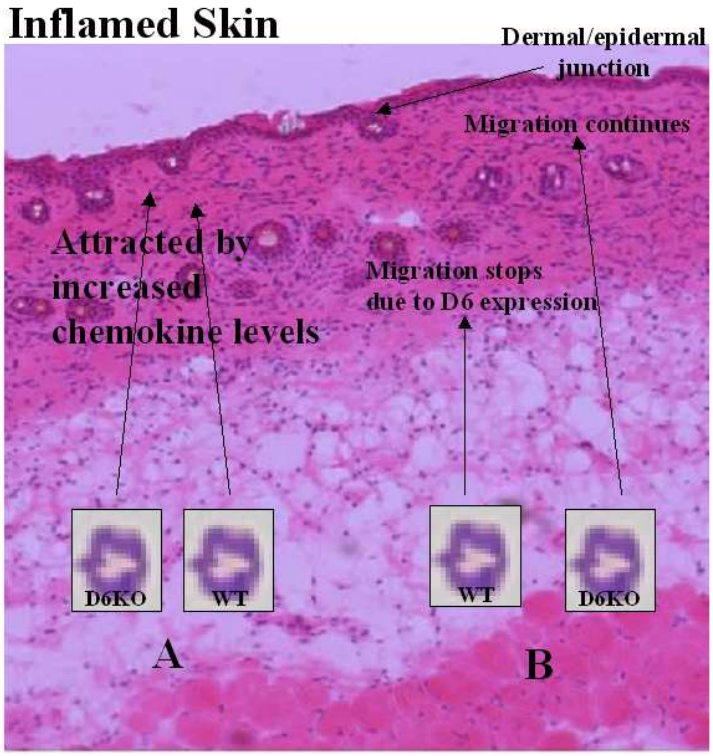

Figure 3-1: Potential mechanisms of D6 influencing neutrophil migration into the skin

Hypothesis A: A lack of D6 in the skin means that increased levels of chemokines at the dermal/epidermal junction allows both WT and D6KO neutrophils to localise here. Hypothesis B: A lack of D6 on neutrophils means they are unable to halt their migration in response to chemokines, meaning they continue moving towards the dermal/epidermal junction.

These data led us to investigate if this phenomenon was receptor or cell type specific, i.e. could D6 affect migration in response to other D6 ligands when co-expressed with the appropriate signalling receptor. This hypothesis was tested using in vitro chemotaxis assays, with cells that stably over-express D6, primary murine cells and eventually using in vivo models of cell movement. Initially attempts were made at creating cell lines that stably expressed D6 to analyse the effects, if any, that D6 would have on in vitro chemotaxis towards both inflammatory and constitutive chemokines. Unfortunately these experiments failed repeatedly, due to a failure to generate stably transfected cell lines, and problems with the initial optimisation of chemotaxis assays.

An alternative approach was taken, which involved isolating different cell populations from WT and D6KO mice, and analysing their chemotaxis in vitro, using two types of chemotaxis assays, the Transwell assay and the Neuroprobe chamber (a modified Boyden chamber). Again, these experiments were unsuccessful as, despite some early results using these assays, the results were extremely variable and as a result, no clear conclusions could be drawn. These results have been omitted from the thesis.

3.2 Neutrophil Adoptive Transfer

3.2.1 Neutrophil movement in inflammation

Using the well-characterised TPA skin inflammation model (339, 340), D6KO mice have shown an exaggerated inflammatory response, typified by the development of a psoriasis like pathology in the dorsal skin. This model, and the features unique to D6KO mice, have been discussed in further detail elsewhere, and in the introduction (152). The main pathology caused by the lack of D6 is due to a failure to clear CC chemokines from the site of inflammation, in this case the skin. The presence of these chemokines in the skin of D6KO mice is thought to promote an exaggerated influx of T cells and dermal mast cells, which are thought to contribute to the development of the psoriasis-like pathology. Although there were no observed differences in neutrophil numbers, when comparing D6KO skin to WT, there was a difference in the location of neutrophils in D6KO mice. In WT mice, neutrophils were situated primarily in the dermal layer of the skin (picture A figure 3.2), whilst in D6KO mice, neutrophils were present at the dermal/epidermal junction, as shown in picture B of figure 3.2.

Two alternative hypotheses have been proposed to explain the differences in neutrophil localisation in D6KO skin. A lack of D6 in the skin has been shown to increase levels of chemokines, and these chemokines may localise to the dermal/epidermal junction, allowing both WT and D6KO neutrophils to localise to this area. Alternatively, a lack of D6 in neutrophils may prevent neutrophils from being able to halt their migration, meaning they are found at the dermal/epidermal junction (illustrated in figure 3.1).

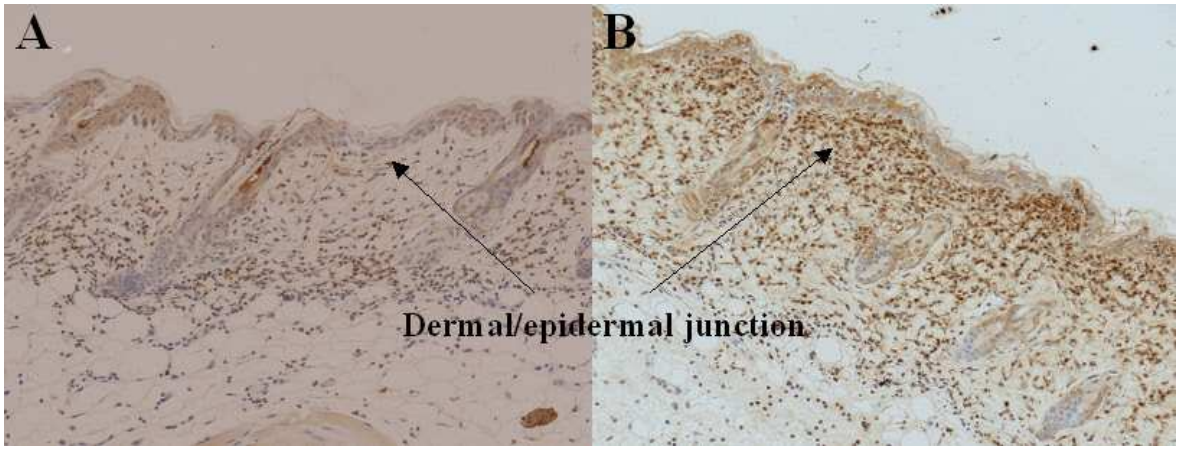

Figure 3-2: Differential positioning of neutrophils in the skin of TPA treated D6KO mice

The skin of WT and D6KO 129/Bl6 mice was inflamed with one treatment of TPA, which was then processed for histological analysis. Staining for neutrophils was performed using an antibody against myeloperoxidase. A: WT skin, B: D6KO skin. More neutrophils are present at the dermal/epidermal junction in D6KO mice (manuscript submitted, 137).

To try to address these possibilities, the TPA skin inflammation model was used, along with adoptive transfer of labelled neutrophils. This would allow identification of the genotype of the neutrophils, as D6KO and WT neutrophils are labelled with different fluorescent dyes, and would allow analysis of the position of neutrophils in the inflamed skin. These experiments would illustrate if a lack of D6 on neutrophils is responsible for their positioning at the dermal/epidermal junction – if this is the case, more D6KO neutrophils would be expected at the dermal/epidermal junction in the inflamed skin of D6KO mice, whilst WT neutrophils would remain lower down in the dermal compartment of the skin.

D6KO and WT neutrophils were isolated from 129/Bl6 mice (materials and methods section 2.2.2), fluorescently labelled and injected into the tail vein of 129/Bl6 D6KO mice that had received a single TPA treatment to the dorsal skin. The treated skin was sampled at various time points after neutrophil transfer, 'snap frozen' in liquid nitrogen, and skin sections were analysed for the presence and location of labelled neutrophils.

3.2.1.1 Fluorescent Labelling - Optimisation

Initial optimisation experiments were performed using THP-1 cells, rather than neutrophils, to determine the ideal concentration for each fluorescent dye to be used. These cells were used as they were easy to grow in culture and meant that mice would not need to be sacrificed for the optimisation of the fluorescent dyes. Initially CFSE and CMTMR were the fluorescent dyes used. CFSE fluoresces green and CMTMR fluoresces

orange/red. These dye combinations were used, as they allow easy identification of labelled neutrophils, without interfering with the DAPI staining of nuclei.

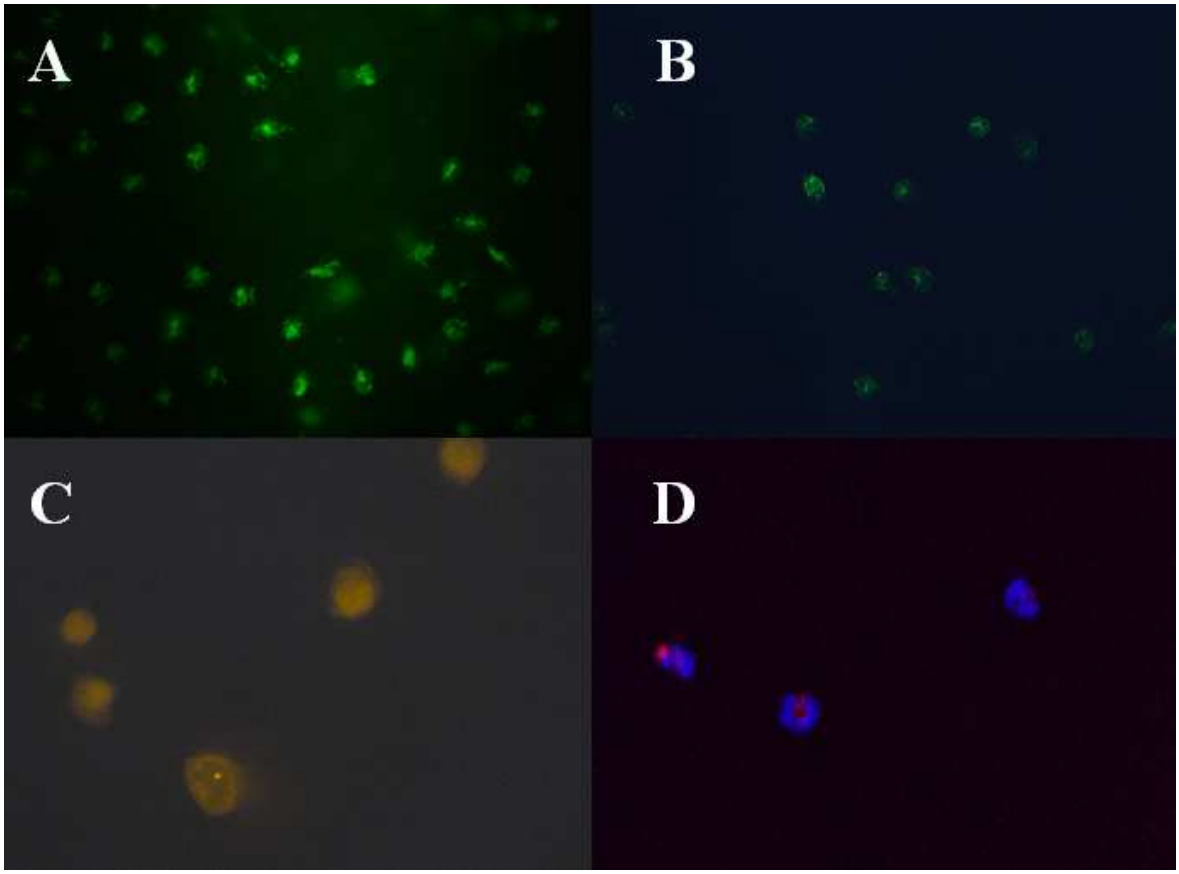

Figure 3-3: Optimisation of neutrophil staining.

Following optimisation of staining using THP1 cells, neutrophils were stained using the same protocol. CFSE staining could be detected on both WT and D6KO neutrophils (picture A and B respectively). Images were taken at 200x magnification using the Axiostar plus microscope. CMTMR stained neutrophils are shown in picture C, taken at 400x magnification. TAMRA stained neutrophils are shown in picture D, with DAPI counterstain, this image was taken at 200x using the LSM 510 Meta Zeiss confocal microscope.

A dose response curve was obtained to determine the optimal concentration of CFSE and CMTMR; labelled THP-1 cells were analysed using both flow cytometry and fluorescent microscopy. The concentration of fluorescent dye which gave a strong signal using the fluorescent microscope, in the appropriate channel, without too much 'bleed-through' into other channels (e.g. the lowest bleed through in the rhodamine channel for the CFSE and the lowest bleed through in the FITC channel for CMTMR.) was the concentration used (CFSE 10µM, CMTMR 5µM) (data not shown). After the optimal concentration was determined using THP1 cells, this concentration was then tested on neutrophils and used for adoptive transfer experiments, see figure 3.3.

3.2.1.2 Neutrophil Adoptive Transfer - Optimisation

Neutrophils are one of the first cell types recruited to a site of inflammation and can appear as early as 2 hours after the induction of inflammation (341). The initial neutrophil adoptive transfer experiment was carried out in order to try to determine the optimal time after cell injection when neutrophils could be detected in the inflamed skin. Experiments were named according to the date they were carried out; the initial experiment was carried out on the 15/01/07. A summary of all neutrophil adoptive transfer experiments can be found in tables 3.1 and 3.2. All mice used in these experiments were on a 129/Bl6 background, both WT and D6KO.

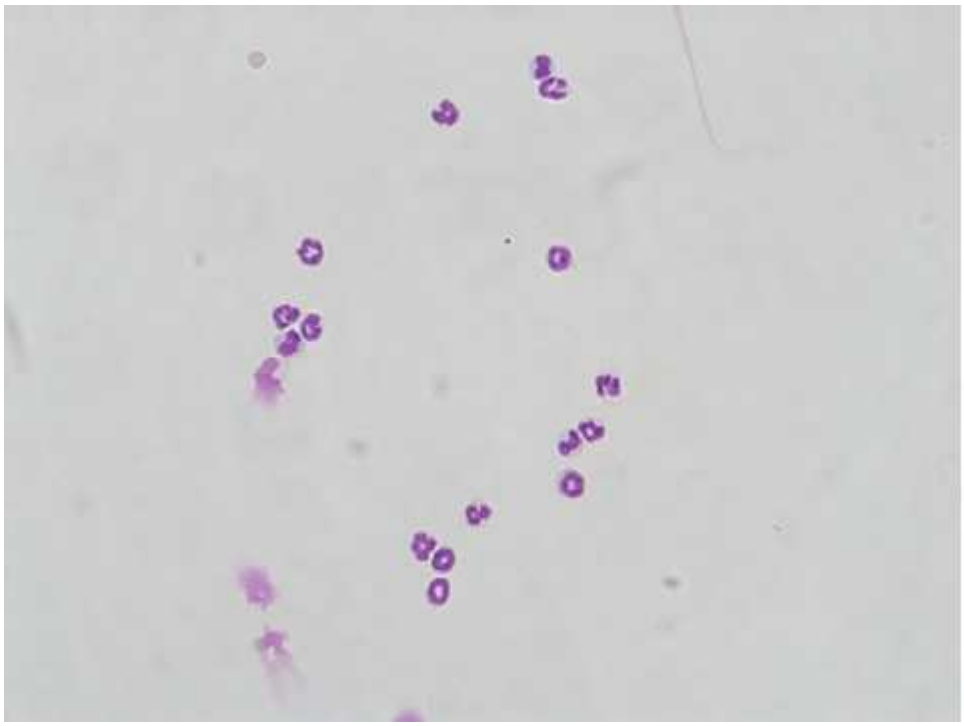

Figure 3-4: Giemsa stained murine neutrophils

Murine neutrophils were isolated from murine bone marrow using the Ly6G kit from Miltenyi (materials and methods section 2.1.2.1), put onto a slide by cytospin and stained with Giemsa. This allowed assessment of the purity of neutrophil preps by light microscopy. Neutrophil preps were consistently ~96% using this kit. 200x magnification, Axiostar plus microscope

Date of Experiment	Time of TPA painting	Time of neutrophil injection	Time of sampling	Type of cell staining	No. of cells injected
15/01/2007	8am	3pm	8am (24hours after TPA)	CFSE and CMTMR (reciprocal)	1×10^6 of each genotype (2×10^6 total)
29/01/2007	8am	3pm	7pm (11 hrs after TPA) 9pm (13 hrs after TPA)	CFSE and CMTMR	1.25×10^6 of each genotype (2.5×10^6 total)
05/03/2007	8am	3pm	9pm (13 hrs after TPA)	CFSE	4×10^6 of any one genotype (either D6KO or WT)
27/03/2007	5pm	12pm (following day)	3pm (22hrs after TPA) 5pm (24 hrs after TPA)	CFSE	1×10^7 of D6KO neutrophils
03/05/2007	8am	1pm	7pm (11hrs after TPA) 8am (24hrs after TPA)	CFSE and TAMRA	1×10^7 of each genotype (2×10^7 total neutrophils)
26/07/2007	8am	1pm	7pm (11hrs after TPA) 8am (24hrs after TPA)	CFSE and TAMRA	1×10^7 of each genotype (2×10^7 total neutrophils)

Table 3-1: Summary of neutrophil adoptive transfer experiments

This table shows the details for each neutrophil adoptive transfer experiment which was performed during the optimisation stages. The time course of TPA treatment, neutrophil administration and sampling are shown for each experiment. The fluorescent dyes used, the total number of neutrophils injected, and their genotype, are also described here.

For the initial experiment, 129/Bl6 D6KO mice were treated with TPA once (which has been shown to induce an inflammatory response in the skin (152)), then 7 hours later, a total of 2×10^6 labelled neutrophils were injected into the tail vein of these TPA treated mice. Each mouse received a 50:50 mixture of labelled WT and D6KO neutrophils. All neutrophils were isolated from 129/Bl6 mice, either WT or D6KO, and all mice receiving neutrophils were 129/Bl6 background. Two mice received WT neutrophils labelled with CFSE and D6KO neutrophils labelled with CMTMR, whilst the remaining two mice received the same number of cells, with the opposite staining combination (WT labelled with CMTMR and D6KO labelled with CFSE). Neutrophils were isolated using the Ly6G isolation kit from Miltenyi (materials and methods section 2.1.2.1). Initial optimisation experiments were performed to determine the percentage purity of neutrophil preparations. These were determined by performing cytospins of neutrophil preps, staining with Giemsa, and

calculating the percentage of neutrophils by light microscopy, see figure 3.4. Consistently neutrophil preps were 96% neutrophils, with few mononuclear cells contaminating the preparations.

Experiment Date	No. mice sacrificed	No. mice receiving cells	Method of bone marrow cell extraction	Yield (neutrophils per mouse)
15/01/2007	7 WT 7 D6KO	4 D6KO	Flushing	WT: 1.23×10^6 D6KO: 9.5×10^5
29/01/2007	9 WT 9 D6KO	8 D6KO (4 D6KO CFSE WT CMTMR, 4 WT CFSE D6KO CMTMR)	Crushing	WT: 1.11×10^6 D6KO: 1.44×10^6
05/03/2007	12 WT 12 D6KO	8 D6KO (4 WT CFSE, 4 D6KO CFSE)	Crushing	WT: 2.9×10^6 D6KO: 2.225×10^6
27/03/2007	12 D6KO	4 D6KO	Crushing	D6KO: 3.94×10^6
03/05/2007	12 WT 12 D6KO	4 D6KO (2 WT CFSE D6KO TAMRA, 2 WT TAMRA D6KO CFSE)	Crushing	WT: 3.33×10^6 D6KO: 3.33×10^6
26/07/2007	12 WT 12 D6KO	4 D6KO (2 WT CFSE D6KO TAMRA, 2 WT TAMRA, D6KO CFSE)	Crushing	WT: 4.05×10^6 D6KO: 3.56×10^6

Table 3-2: Summary of neutrophil adoptive transfer experiments – neutrophil isolation details.

The number of mice that were treated with TPA, and the cell labelling combinations used are detailed here. The method of isolating bone marrow from murine femurs was either flushing of crushing (further details can be found in materials and methods section 2.1.2.1). The average yield of neutrophils per mouse is shown for each adoptive transfer experiment.

Mice were sacrificed 24 hours after TPA painting and 5mm punch biopsies of the inflamed dorsal skin were snap frozen in liquid nitrogen. Skin sections were cut to 6µm thickness and mounted on polysine-coated slides, before mounting using Vectashield plus DAPI (to label the nuclei of the skin cells). Slides were analysed initially using the Axiostar plus microscope with fluorescent filters. Neutrophils were checked for successful fluorescent labelling by performing cytospins (data not shown)

Upon analysing the skin sections using the fluorescent microscope, it was discovered that under the UV light, hair follicles auto-fluoresce. This made it very difficult to identify any

labelled cells in the skin (see figure 3.5-A and B). The skin sections from the first neutrophil adoptive transfer experiment were re-analysed using the LSM 510 Meta confocal microscope, as this could be used to help reduce the auto fluorescence. The main difference between these two types of microscopy is that in fluorescence microscopy the whole image is illuminated which can create a haze, and can result in high background. With confocal microscopy a laser is used to focus the illumination, which gives a higher intensity and, as the illumination is focused onto a smaller area, it reduces background fluorescence. Another advantage of using the confocal microscope was that all three colours, orange for CMTMR, green for CFSE and blue for DAPI, could be shown on the same picture, which could not be done using the fluorescent microscope. The more precise wavelength of the confocal allowed identification of labelled cells.

The confocal images shown in figure 3.5 (C and D) show that labelled neutrophils can be detected in the skin of treated mice following neutrophil adoptive transfer. These labelled cells could not be detected with the fluorescent microscope, due to the hair follicle auto-fluorescence. Very few labelled neutrophils, either WT or D6KO could be detected using the confocal microscope, so it was decided to alter the adoptive transfer protocol.

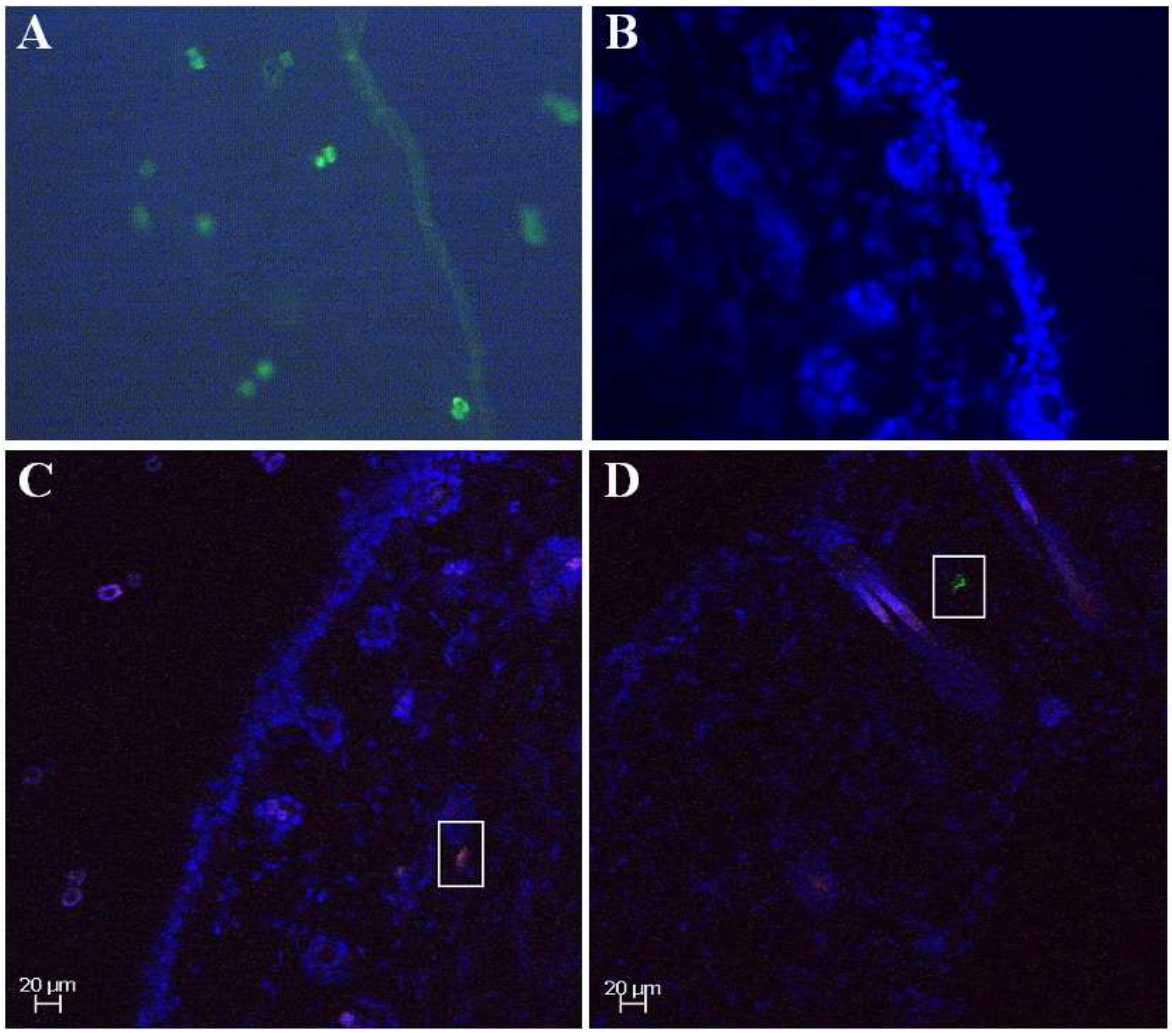

Figure 3-5: Inflamed skin from a mouse (15/01/07) that had received CFSE and CMTMR labelled WT and D6KO neutrophils.

Pictures from D6KO 129/Bl6 mouse that received one dose of TPA followed by tail vein injection of $1x10^6$ CFSE and CMTMR labelled neutrophils (D6KO and WT neutrophils at 1:1 ratio) 7 hours later. Skin samples were taken 24 hours after TPA painting, frozen sections were cut and analysed for the presence of labelled neutrophils. A – image taken at 200x magnification with Axiostar plus microscope, with the CFSE filter, showing autofluorescent hair follicles. B – same skin section taken with the DAPI filter on the Axiostar plus microscope, showing skin cells and hair follicles. C& D – skin sections analysed using the LSM 510 Meta confocal microscope, showing CMTMR labelled neutrophils (C) and CFSE labelled neutrophils (D). These images were taken at 200x magnification. N = 4 (2 received CFSE D6KO neutrophils with CMTMR WT neutrophils, 2 received the reciprocal staining combination).

The second neutrophil adoptive transfer protocol was altered to add more neutrophils at the injection stage and sampling the skin less than 24 hours after TPA painting, as very few neutrophils could be detected at 24 hours after TPA painting. The details of this experiment (29/01/07) can be found in tables 3.1 and 3.2. For this experiment, femurs from WT and D6KO mice were crushed using a mortar and pestle, rather than flushing the bone marrow, to try to increase the neutrophil yields. This method increased neutrophil numbers; these are detailed in table 3.2. Confocal analysis of frozen skin sections showed that cells stained with both fluorescent dyes could be detected in the skin, and that both cell genotypes could be detected (figure 3.6). The results from this experiment showed

that neutrophils could be detected in the skin, but indicated that more may be needed at the time of transfer, as only a few cells could be detected per picture. As neutrophils tend to have a short half-life in vivo (342), it is possible that a large number of neutrophils are dying before they reach the skin. Using a large number of neutrophils in the adoptive transfer protocols we hoped to overcome the problem of the neutrophils dying. The protocols were optimised to try to minimise the length of time that neutrophils were ex vivo, unfortunately analysis of the proportion of live to dead neutrophils was not carried out before injection. It is likely that a large number of cells die during the process of labelling, but by injecting a large enough number of neutrophils, we hoped to overcome this effect.

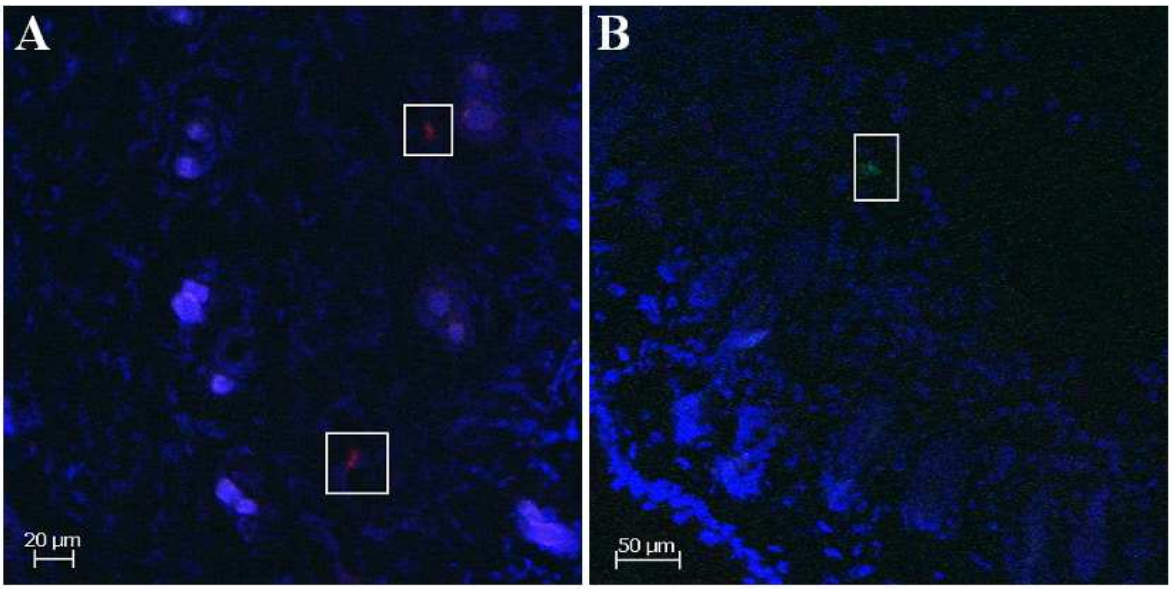

Figure 3-6: Skin sections from mouse treated with neutrophil adoptive transfer protocol 29/01/07

Skin sections from 129/Bl6 D6KO mice that received a 1:1 mixture of WT and D6KO neutrophils, labelled with CFSE and CMTMR. Each mouse (n = 8) received 2.5 x 10^6 labelled neutrophils, at a 1:1 mix WT to D6KO, with reciprocal staining combinations. Frozen sections were mounted with Vectashield plus DAPI to visualise skin cells, images were taken at 200x magnification on the LSM 510 Meta confocal. A – CMTMR labelled neutrophils are identified, B – CFSE labelled neutrophils are identified. These skin sections are from the 9pm sampling point (see tables 3.1 and 3.2 for further details). Control skin sections consistently showed no fluorescently labelled cells (not shown).

These results show that neutrophils can be detected in inflamed skin 13 hours after the induction of inflammation, but very few neutrophils (relative to the number of cells injected) were detectable. For the next adoptive transfer experiment (05/03/07), the same general timeline as the previous experiment was used, with only the later 9pm time point (see table 3.2) used for sampling, as this was when fluorescent cells could be detected in the skin. To further increase the number of neutrophils that could be injected into treated mice, more mice were sacrificed (12 of each genotype) and crushing of the

femurs was used to isolate the bone marrow. Crushing the femurs increased the neutrophil yield, which allowed 4 x 10^6 neutrophils to be injected per mouse. For this experiment, mice received either CFSE labelled D6KO neutrophils or CFSE labelled WT neutrophils alone.

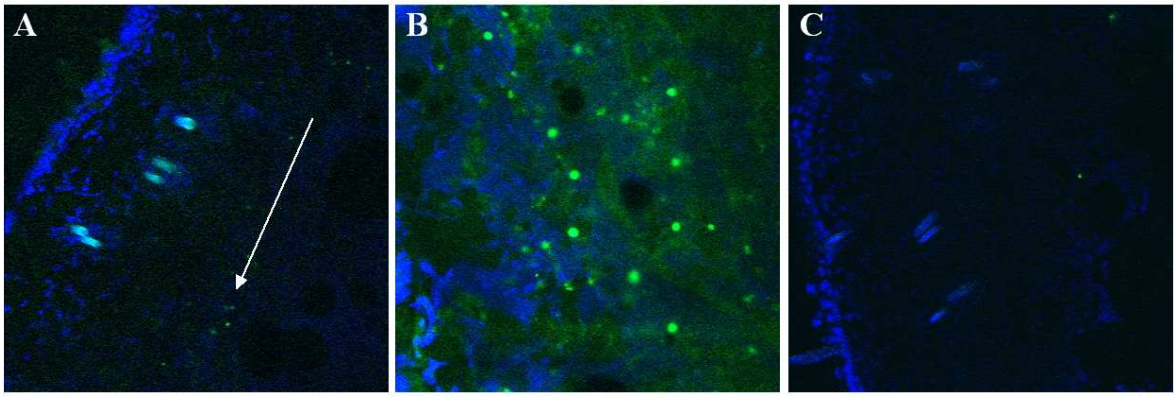

Figure 3-7: Fluorescent images of inflamed skin from D6KO mice receiving CFSE labelled neutrophils according to protocol 05/03/07

Representative images of inflamed skin from 129/Bl6 D6KO mice that received 4 x 10^6 CFSE labelled neutrophils, either WT or D6KO. Skin sections are mounted with Vectashield plus DAPI to stain nuclei. A – confocal image showing CFSE labelled neutrophils in the subdermal region of the skin, 200x magnification. B – same skin section as A at 400x magnification. C – CFSE labelled WT neutrophils in the subdermal region of D6KO inflamed skin, 200x magnification. N = 4 per group receiving either CFSE WT neutrophils or CFSE D6KO neutrophils.

CFSE labelled neutrophils could be detected for both cell genotypes injected, but with the D6KO neutrophils the majority of cells were present below the dermis (in the fatty layer) of the inflamed skin (see figure 3.7). Fewer cells were obvious in the sections from mice that had received WT neutrophils. The cell number for this experiment (05/03/07) seemed to be better for detecting labelled neutrophils in the inflamed skin, but there may be a problem with the time point of sampling. D6KO neutrophils may require longer getting from the sub dermal area to the site of inflammation (13 hour time point).

As a result, the next adoptive transfer experiment (27/03/07) was re-designed, so that mice received TPA treatment at 5pm on the day before neutrophil administration. Neutrophils were isolated, labelled and injected at 12pm the following day. Mice were sacrificed at both 22 hours and 24 hours after TPA treatment in the hope that letting the inflammation develop for longer would attract more neutrophils into the skin. For this experiment, only D6KO neutrophils were labelled with CFSE and transferred into TPA treated D6KO mice. More than double the number of neutrophils (see tables 3.1 and 3.2) were injected intravenously.

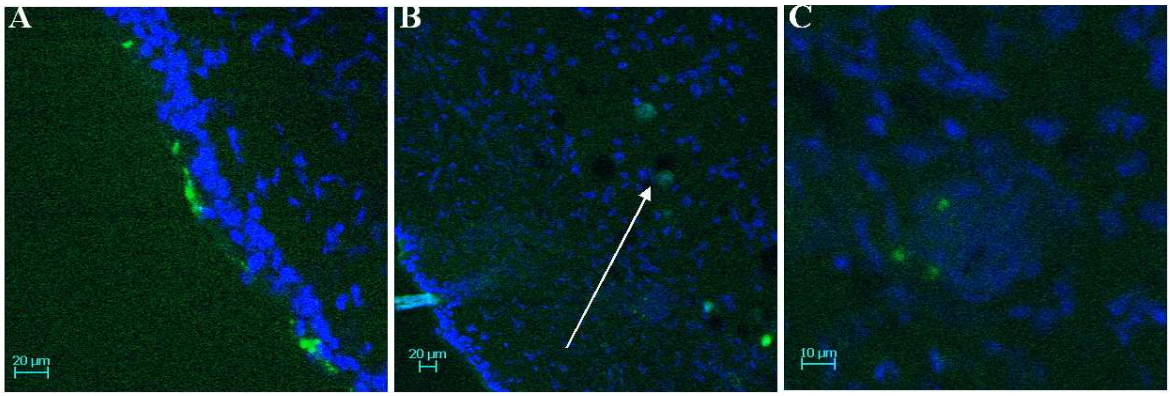

Figure 3-8: Fluorescent skin sections from neutrophil adoptive transfer protocol 27/03/07

129/Bl6 D6KO mice received 1 x 10^7 CFSE labelled D6KO neutrophils following TPA painting, 22-24 hours after injection, mice were sacrificed and dorsal skin samples were taken. A – CFSE labelled D6KO neutrophils at the edge of the skins surface, 200x magnification. B – CFSE labelled D6KO neutrophils detected beside a hair follicle, 200x magnification. C – picture B at 400x magnification. Images are representative of 4 mice.

The skin sections from the adoptive transfer experiment performed on the 27/03/07 (see figure 3.8) show that CFSE labelled D6KO neutrophils could be detected in the skin 22 and 24 hours after TPA treatment. Even though a higher number of neutrophils were administered intravenously, this does not seem to correspond with higher numbers of labelled neutrophils present in the inflamed skin. It appears (see picture A of figure 3.8) that some of the labelled cells may be reaching the outer edge of the skin, but this was not seen in every mouse. These results suggest that this time point may be too late to fully analyse the location of D6KO neutrophils in inflamed skin.

The results of the neutrophil adoptive transfer experiments performed on the 05/03/07 and 27/03/07, suggested that the ideal time point for analysing neutrophil location in this model was between 11 and 24 hours. The experiment was repeated; following the protocols detailed in tables 3.1 and 3.2 (03/05/07), and transferring a 50:50 mixture of CFSE and TAMRA labelled D6KO and WT neutrophils. It was decided to start using TAMRA, rather than CMTMR because very few CMTMR positive cells had been detected in previous experiments, and it was thought that an alternative dye, which fluoresces in a similar wavelength, might be more suitable. Other groups had used this cell dye combination in adoptive transfer experiments successfully (343). Skin samples were taken at 11 hours and 24 hours after TPA painting, in the hope that these time points would be suitable to identify labelled neutrophils entering the inflamed skin.

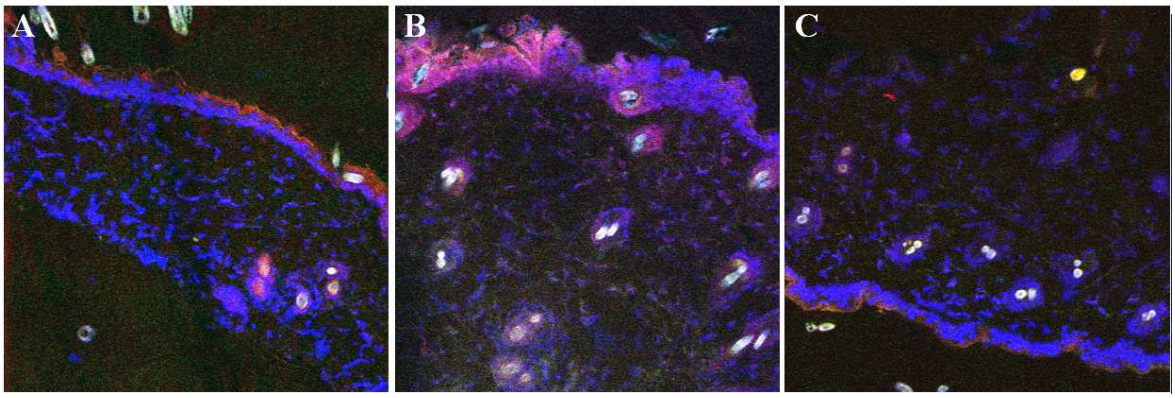

Figure 3-9: Fluorescent skin sections from D6KO mice that received neutrophils according to protocol 04/05/07

129/Bl6 D6KO mice received tail vein injections of a total of 2 x 10^7 labelled neutrophils, a combination of CFSE and TAMRA labelling, at a 1:1 ratio. N = 2 mice received CFSE WT neutrophils, TAMRA D6KO neutrophils, n= 2 mice received CFSE D6KO neutrophils and TAMRA WT neutrophils. Mice were sacrificed and skin samples taken at 11 and 24 hours post TPA treatment. Skin sections were mounted with Vectashield plus DAPI, as described previously. A – control skin section, B – skin from a D6KO mouse that received TAMRA labelled D6KO neutrophils and CFSE WT neutrophils, C – Skin section from D6KO mouse that received TAMRA WT neutrophils and CFSE WT neutrophils. All sections were taken at 200x magnification and show a high red background, making identification of TAMRA positive cells difficult.

Skin sections were cut on the cryostat and mounted on polysine slides. Vectashield plus DAPI was added to the sections and they were analysed on the confocal microscope as described previously. The majority of the sections analysed from this experiment had a very high red background, which could not be reduced using the confocal microscope (see figure 3.9). This made it very difficult to identify TAMRA positive cells. The whole area of the skin section was searched for positive cells, but very few (of either TAMRA or CFSE labelled cell populations) could be identified.

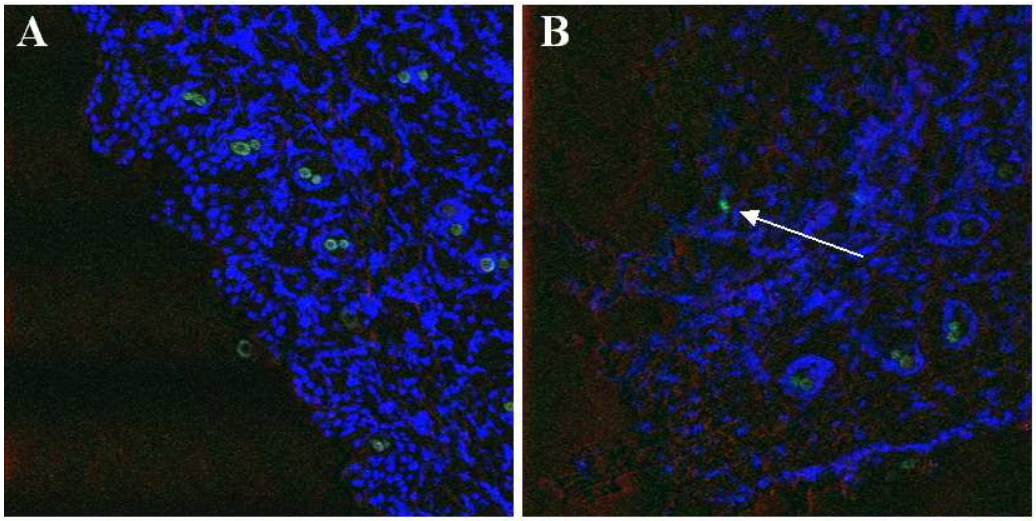

Figure 3-10: Fluorescent skin sections from neutrophils adoptive transfer protocol 26/07/07.

The 03/05/07 protocol was repeated on 26/07/07 (4 129/Bl6 D6KO mice received TPA painting followed by 2 mice receiving $2x10^7$ labelled neutrophils, 1:1 mixture of TAMRA WT and CFSE D6KO neutrophils, and 2 mice receiving the reciprocal staining combination). Skin sections were mounted using Vectashield plus DAPI; skin sections from this repeated experiment lacked the high red background shown previously (figure 3.10). A – Skin section from D6KO mouse that received TAMRA D6KO neutrophils and CFSE WT neutrophils. B – Skin section from D6KO mouse that received TAMRA labelled WT neutrophils and CFSE D6KO neutrophils. Images taken at 200x magnification, LSM 510 Meta confocal microscope.

This experiment was repeated (26/07/07) with the same combination of dyes and time course. Skin sections from the adoptive transfer performed on 26/07/07 were mounted using Vectashield and analysed as before. Upon analysing the skin sections from this experiment, it was discovered that all of the sections again had a substantial red background, which made it difficult to see any TAMRA labelled cells. CFSE cells could still be detected, as shown in figure 3.10. More sections were cut from this experiment to determine if the high red background was present throughout the skin samples. The second batch of sections had a reduced red background that allowed identification of CFSE and TAMRA labelled neutrophils (representative images are shown in figure 3.11)

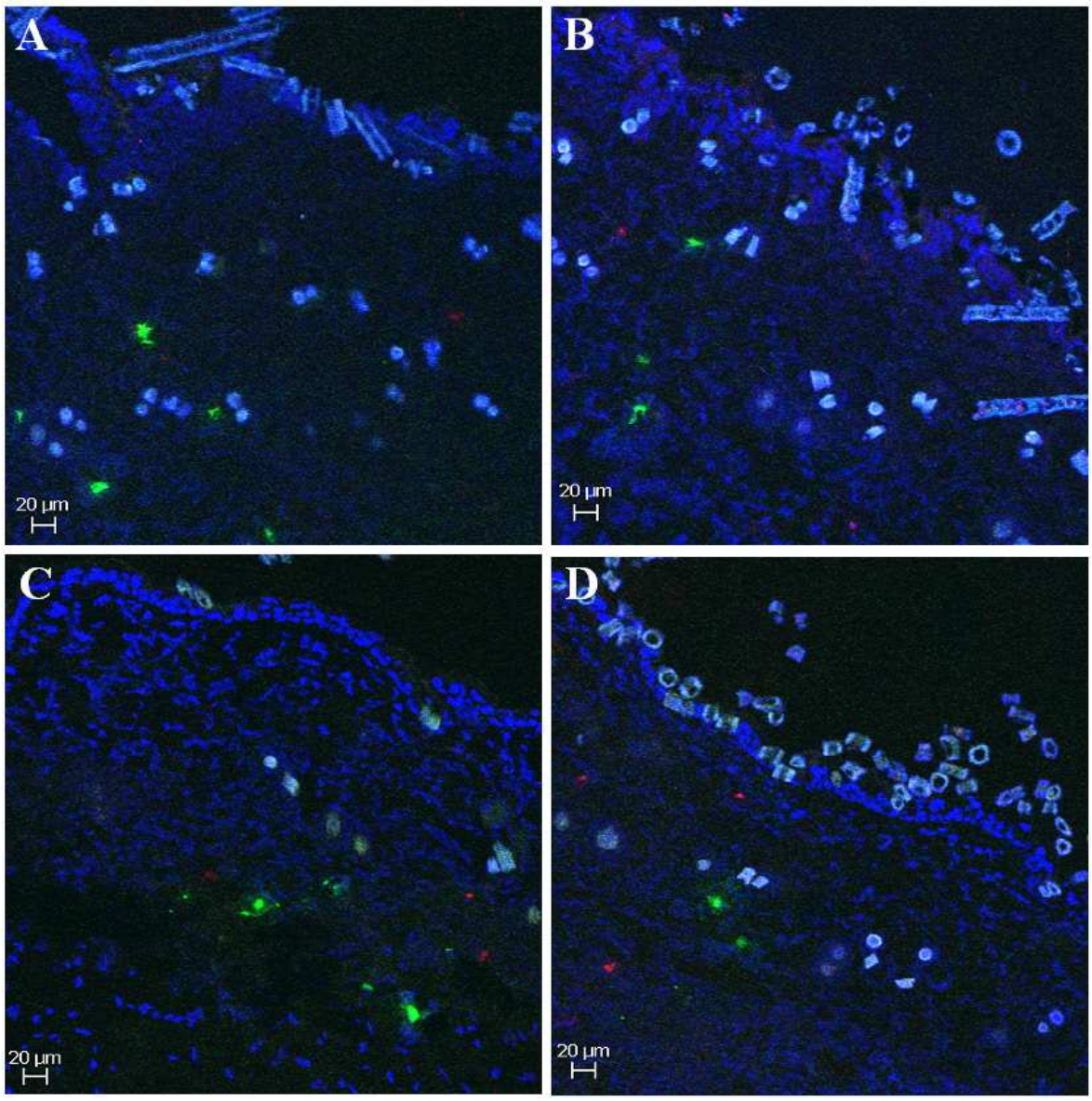

Figure 3-11: Skin sections showing labelled neutrophils from neutrophil adoptive transfer protocol 26/07/07

Skin sections from 129/Bl6 D6KO mice that received TPA painting followed by tail vein injection of labelled WT and D6KO neutrophils (protocol 26/07/07, more details in tables 3.1 and 3.2). Skin sections were mounted with Vectashield plus DAPI and analysed using the LSM 510 Meta confocal microscope. A & B – skin sections from D6KO mouse that received TAMRA labelled D6KO neutrophils and CFSE labelled WT neutrophils, following induction of inflammation with TPA. C & D – Skin sections from D6KO mice that received CFSE labelled D6KO neutrophils and TAMRA WT neutrophils following TPA painting. Images taken at 200x magnification, n = 2 per group.

Analysis of labelled neutrophils could now be carried out, using the skin sections from the adoptive transfer performed on 26/07/07. Control skin sections, from mice that received inflammation but no fluorescent neutrophils consistently showed no fluorescent cells, suggesting that the cells we were seeing in the skin of these mice were labelled neutrophils. The lungs of treated mice were taken throughout these experiments, to check for the presence of labelled cells. This was carried out as the lungs are the first capillary bed that cells will encounter after being injected into the tail vein, so it is

possible they may become trapped here. No fluorescent cells could be detected in the lungs, see figure 3.12.

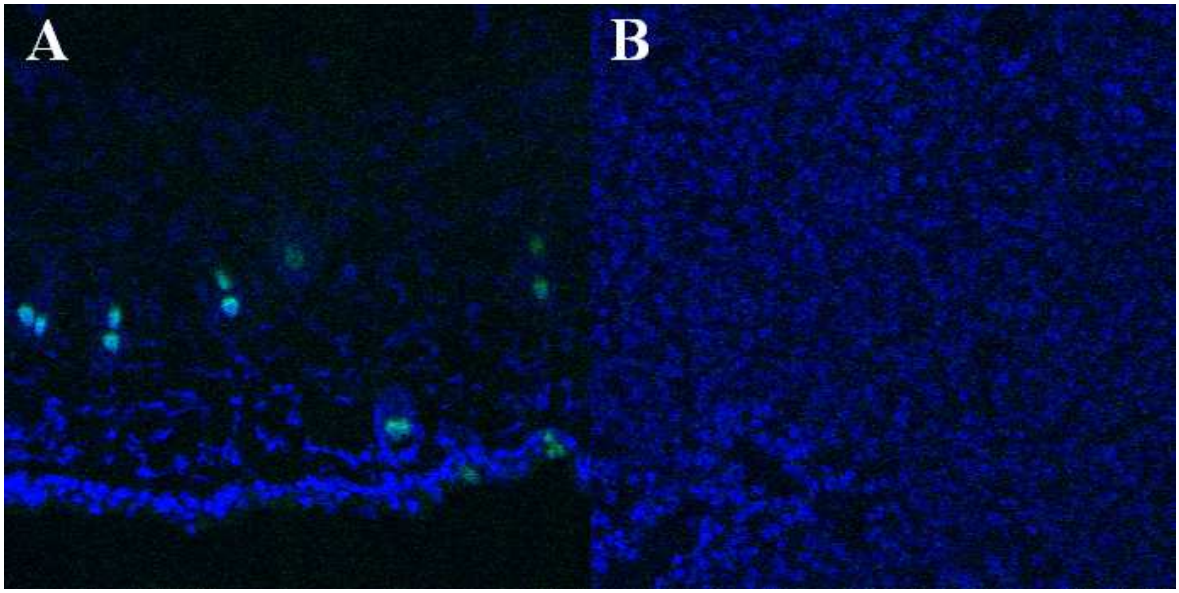

Figure 3-12: Control skin and lung sections from neutrophil adoptive transfer experiments.

Picture A: All neutrophil adoptive transfer experiments included control mice that received no fluorescent neutrophils, but underwent TPA treatment. These skin sections were analysed for the presence of fluorescent cells and were consistently negative. Picture B: Lung sections from treated mice were analysed for the presence of fluorescent neutrophils, as the cells may become trapped here after injection. Again, these sections were consistently negative. 200x magnification, LSM 510 Meta confocal microscope.

The entire skin section for each mouse was analysed (see figure 3.13) and the total number of labelled neutrophils was counted using the Axiovision software. At 11 hours after TPA painting, an average of 24.75 (+/- 29.6) WT neutrophils could be found in skin sections, compared to 15.5 (+/- 9.94) D6KO neutrophils. At the 24 hour timepoint, 16 (+/- 16.43) WT neutrophils could be detected in skin sections, compared to 10.25 (+/-15.1) D6KO neutrophils. Figure 3.14 shows that, at both time-points after TPA treatment (11 hours and 24 hours), more WT neutrophils can be detected in the skin than D6 KO neutrophils, but this difference was not significant. Both neutrophil genotypes showed a drop in number at the 24-hour time-point, but again this difference was not significant.

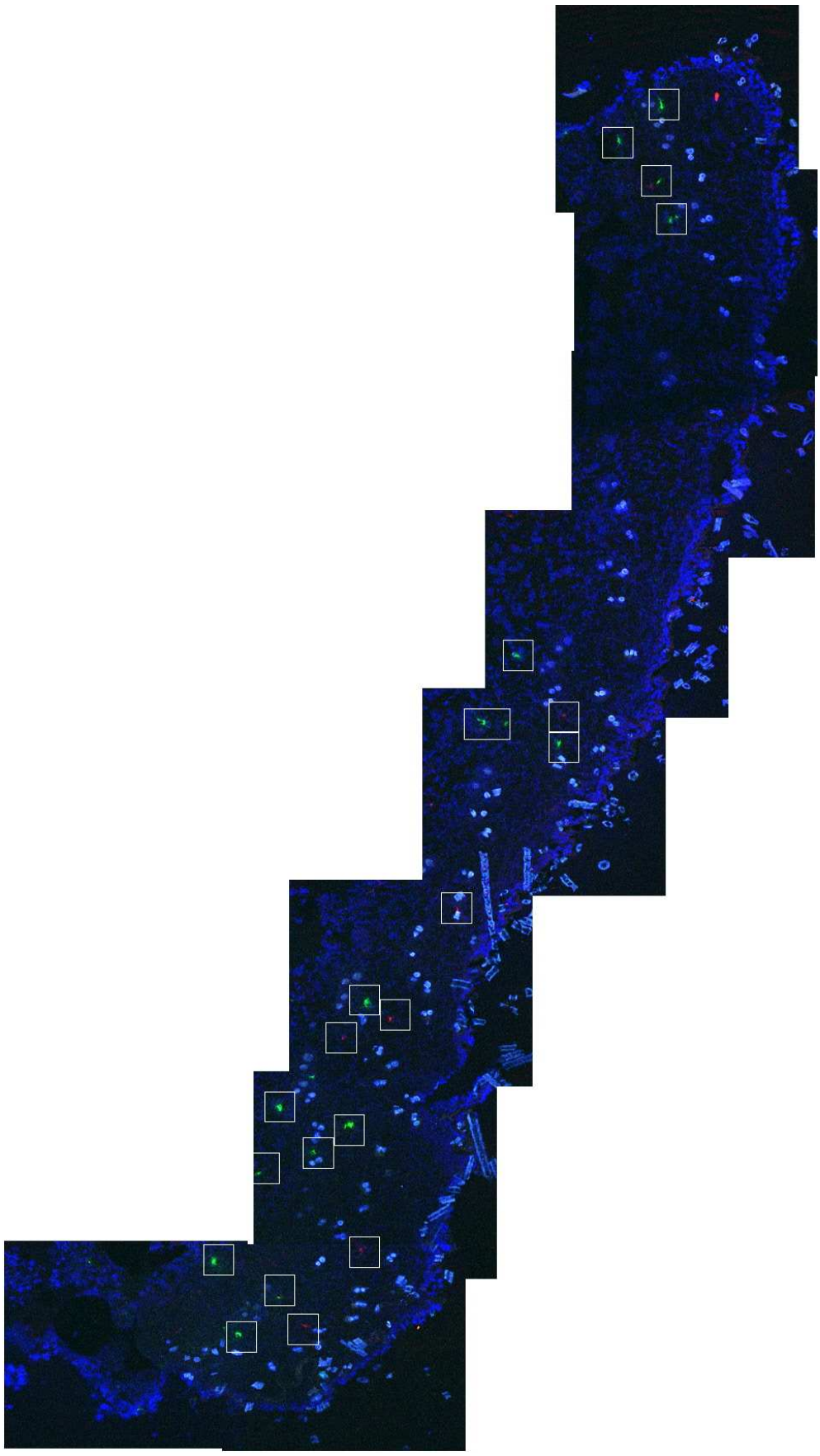

Figure 3-13: Entire skin section from a D6KO mouse showing labelled neutrophils

Representative image of the skin from a 129/Bl6 D6KO mouse that was treated with neutrophil adoptive transfer protocol 26/07/07. Skin sections were mounted with Vectashield plus DAPI. Images taken at 200x magnification using the LSM 510 Meta confocal could be 'overlaid' to create an image of the entire skin section. TAMRA labelled D6KO neutrophils and CFSE labelled WT neutrophils have been highlighted.

In order to determine if D6KO neutrophils had any differences in migration into inflamed skin (suggested by results from TPA skin painting shown in figure 3.2), the distance from labelled neutrophils to the epidermis was measured using the Axiovision software for all mice. 11 hours after TPA treatment, WT neutrophils were significantly closer to the epidermis, with an average distance of 168.37µm (+/-58.6), than D6KO neutrophils that had an average distance of 191.81 µm (+/- 63.51) from the epidermis. This difference was statistically significant, p=0.0179 (Students unpaired t test). At 24 hours after TPA painting, there was no significant difference in the location of neutrophils, with respect to the distance from the epidermis. WT neutrophils had an average distance of 202.49µm (+/-21.8) from the epidermis, compared to 185.5µm (+/- 68.98) shown by D6KO neutrophils. At the 24 hour timepoint, WT neutrophils were significantly further away from the epidermis, compared to their location at 11 hours, ($p<0.0001$, Students unpaired t test) suggesting that these cells may be moving away from the site of inflammation, or simply dying off, as graph A shows reduced neutrophil numbers at the 24 hour timepoint.

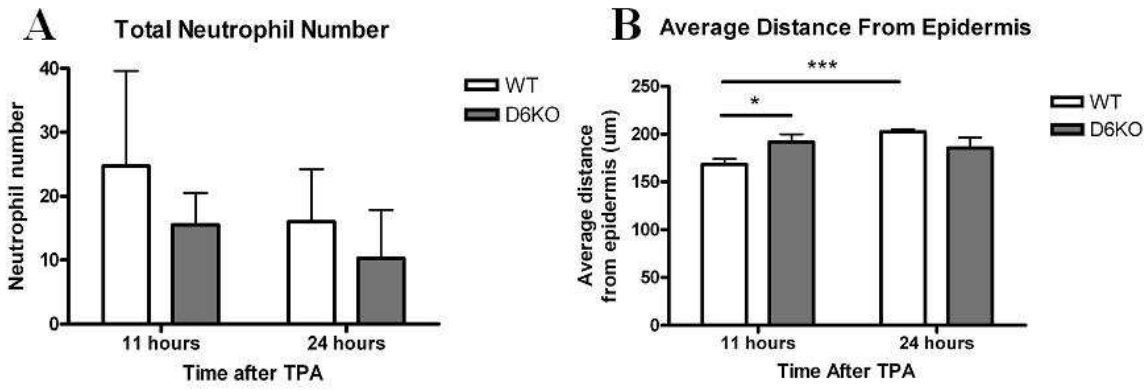

Figure 3-14: Analysis of labelled neutrophil number and location in inflamed D6KO skin.

Skin sections from neutrophil adoptive transfer protocol 26/07/07, showed both WT and D6KO fluorescently labelled neutrophils could be detected in the inflamed skin of 129/Bl6 D6KO mice. A – the total number of labelled neutrophils was determined using the Axiovision software on full length skin sections from each treated mouse. These results are expressed as the total neutrophil number in a full skin section from an 8mm punch biopsy, n = 4, NS – Students unpaired t test. B – the distance between labelled neutrophils and the epidermis could be measured using Axiovision software and is expressed as the average distance of neutrophils from the epidermis, n = 4, WT vs D6KO at 11 hours p= 0.0179, Students unpaired t test, WT 11 hours vs 24 hours, p <0.0001, Students unpaired t test.

These results show that fluorescently labelled neutrophils can be detected in TPA treated skin of D6KO 129/Bl6 mice. At 11 hours after TPA painting, WT neutrophils are significantly closer to the epidermis than D6KO neutrophils, suggesting that a lack of D6 on neutrophils does affect their position in inflamed skin. A lack of D6 on neutrophils means that neutrophils are further from the epidermis, suggesting that in the results shown in figure 3.2, the differential positioning of neutrophils is not due to a lack of D6 on

these cells. These results suggest that it may be the location of chemokine production that affects the placement of neutrophils in TPA inflamed D6KO skin.

3.3 Summary

Initially this chapter set out to analyse the role that D6 may play in cell chemotaxis, this was going to be analysed using both in vitro and in vivo techniques. Unfortunately the in vitro experiments were unsuccessful. These experiments used two different types of chemotaxis assay, the Transwell assay and the Neuroprobe assay. The Transwell assay is a 24 well disposable plate that has 12 wells for the analysis of chemotaxis. The Neuroprobe assay is a modified version of the chamber assay initially described by Boyden in 1962 (344), which contains 48 wells for the analysis of chemotaxis. In comparison to the Transwell assay, the Neuroprobe chamber would allow the use of smaller volumes of chemokines and reduced cell numbers. Attempts were made to create cell lines that would stably express D6, along with their own endogenous chemokine receptors – cells were chosen carefully to include those that had inflammatory CC chemokine receptors and homeostatic CC chemokine receptors. The plan was to use these cells in chemotaxis assays towards a range of inflammatory and homeostatic CC chemokines to determine the effect, if any, D6 would have on chemotaxis towards these ligands. These assays failed due to repeated technical problems.

An alternative approach was taken, involving isolating various cell populations from WT and D6KO mice, and analysing their chemotactic responses in vitro. This approach had the benefit that no cell manipulation, other than the isolation protocol, would be required, and would allow examination of the influence of D6 on these responses. Unfortunately, the use of chemotaxis assays, both the Transwell assay and the modified Boyden chamber (Neuroprobe) gave extremely variable results. The inconsistencies in these results can be attributed to problems with the technical aspects of these assays, and as a result, these data have been omitted as they failed to meet the aims of this thesis. After abandoning this approach, subsequent data has emerged suggesting that D6 may influence neutrophil migration in the chemotaxis assay system. These results show that in a Boyden chamber system, the migration of D6KO and WT neutrophils remains the same towards CXCL8 and CCL4, but migration towards CCL3 is enhanced in D6KO neutrophils. These data suggest that on neutrophils, D6 may limit chemotactic responses towards CCL3, and is supported

by an in vivo model of intraperitoneal injection of CCL3, which shows increased neutrophil accumulation in D6KO mice, compared to WT (140).

Rather than continue with the in vitro analysis of the affect of D6 on chemotaxis, an in vivo approach was taken. This used the well characterised model of TPA skin inflammation, and was based on observations that neutrophils in D6KO skin are aberrantly located at the dermal/epidermal junction, compared to the position of neutrophils in WT skin. Experiments were designed which aimed to determine if D6 on neutrophils affects their position in inflamed skin. Optimisation of these experiments took some time, but a successful neutrophil adoptive transfer protocol was designed, and allowed the detection of labelled neutrophils in the inflamed skin of D6KO mice. These results show that both WT and D6KO neutrophils can be detected in the skin, at both 11 hours and 24 hours after TPA painting. At the 11 hour timepoint, there is a significant difference in the location of labelled neutrophils, with WT neutrophils being significantly closer to the epidermis than D6KO neutrophils. These results suggest that D6 on neutrophils does not affect their location in the skin, the differences in location exhibited in D6KO skin (shown here (137)) is likely to be due to altered chemokine localisation, affecting neutrophil positioning, which requires further investigation.

In order to improve this experimental protocol, it would have been desirable to test the labelling of neutrophils prior to transfer, using a flow cytometer. Unfortunately due to the short time course, and lengthy neutrophil isolation procedure, there was not enough time, or enough cells to perform this control. Any spare labelled neutrophils were spun down onto a slide and labelling was checked using the confocal microscope (data not shown). Another control that would be desirable for these experiments would be to stain the skin sections with an antibody specific for neutrophils, to be entirely sure that the labelled cells are indeed neutrophils. Skin sections from mice that did not receive fluorescently labelled neutrophils showed no features that resemble those shown in figures 3.11 and 3.13, suggesting that the cells shown in these skin sections are indeed labelled neutrophils.

4 Tumour Development

4.1 B16 Melanoma

Tumour growth and development is a complex process, which involves interactions with stromal cells, angiogenesis, lymphangiogenesis and interactions with immune cells. Chemokines and inflammatory cells are known to play a role in melanoma development (220, 275), more details of which can be found in the introduction (section 1.12 and 1.13). Previous work in our group has shown that D6 can be protective in the inflammatory driven model of skin carcinoma (142). Since D6 is expressed in the skin, and has been shown to have an effect on squamous cell carcinoma, it seems feasible that D6 may play a role in other models of skin carcinogenesis, e.g. melanoma. In order to investigate the broader role of D6 in other models of skin cancer, it was necessary to find a model that was easy to manipulate and differed in action to the model of inflammatory driven skin cancer.

The B16 model has been well characterised and can be used as a model of melanoma in the mouse. The murine B16 cell line was originally discovered in the 1950s from a spontaneously arising melanoma in a C57Bl/6 mouse (284). Cells from this tumour were cultured in vitro and in vivo to create variations on the original F0 cell line, with different organ colonising capabilities. B16 F0 cells retain the ability to form melanomas when injected subcutaneously into syngeneic mice (284, 311). It was decided to use this model of melanoma in WT and D6KO mice to determine if D6 has a role in regulating tumour growth. This model is easy to manipulate and will allow extensive analysis into the roles that D6 may play in tumour growth.

4.1.1 Tumour Growth

B16 F0 cells grow rapidly in culture and are easily maintained. The tumour model involves subcutaneously injecting cells into syngeneic mice and monitoring the growth of the resultant tumour. WT and D6KO C57Bl/6mice received a subcutaneous injection of 5×10^5 B16 F0 cells (as described in materials and methods, section 2.3.1) and were monitored daily for tumour growth. Once the tumour became palpable, as shown in figure 4.1 the mean diameter was measured using callipers (two diameters measured each time). The

tumours were allowed to grow until they reached a mean diameter of 1.2cm, at which point the mice were sacrificed, in accordance with Home Office regulations.

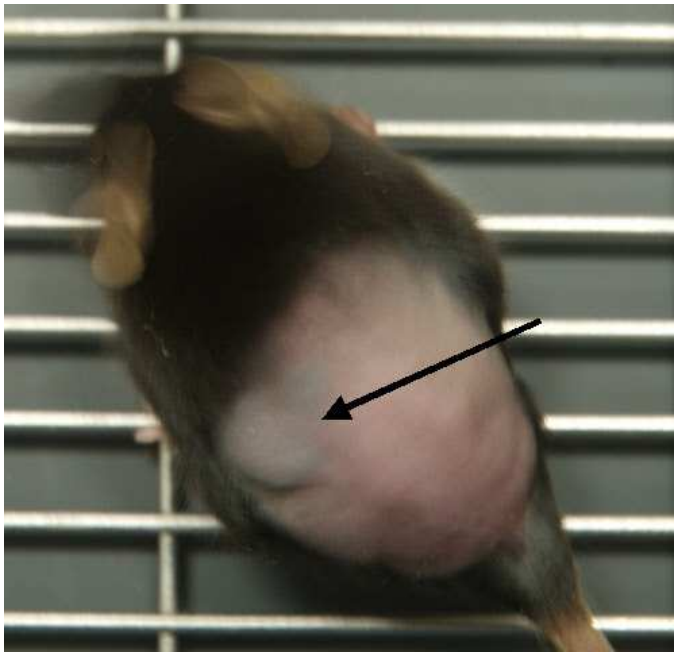

Figure 4-1: WT C57Bl/6 mouse that received a subcutaneous injection of B16 F0 cells 12 days previously.

WT and D6KO mice on a C57Bl/6 background received B16 F0 cells subcutaneously, in the dorsal skin. Mice were monitored daily for the development of tumours, the skin was shaved to aid identification. Once tumours began to appear, two diameters were measured using callipers, and the mean tumour growth was calculated. The dorsal skin has been shaved for ease of identifying and measuring the tumours.

The average tumour growth rate was plotted for WT and D6KO mice against time, and the results are shown in figure 4.2. Graph A shows the average tumour growth plotted against time. Tumours began to appear in D6KO mice (day 8) before they appeared in WT mice (day 10). The tumours in D6KO mice grew at a faster rate, which resulted in a delay in tumour growth in WT mice, but this difference was not significant (two way ANOVA) At day 13, WT tumours had an average diameter of 0.63cm, compared to D6KO tumours which had an average diameter of 1.03cm. At day 16 the average diameter of tumours in WT mice reached their peak at 1.05 cm, compared to 1.32 cm in tumours that developed in D6KO mice. At day 17, WT tumours remained with an average diameter of 1.05cm whilst D6KO tumours had an average diameter of 1.33 cm.

This increased growth rate meant that tumours developing in D6KO mice reached the point where mice had to be sacrificed before WT mice, resulting in a decreased survival rate, as shown in graph B (figure 4.2). Tumours reached the size that resulted in sacrifice at the same time in WT and D6KO mice at day 11, but the increased growth rate in D6KO mice resulted in all D6KO mice being sacrificed by day 19. The final mouse in the WT

group was sacrificed at day 28. Although the survival curve data was not statistically significant (p=0.1786, Logrank test), the results were reproducible. In summary, B16 F0 tumours developing in D6KO mice display a faster growth rate than tumours developing in WT mice, although this difference was not significant.

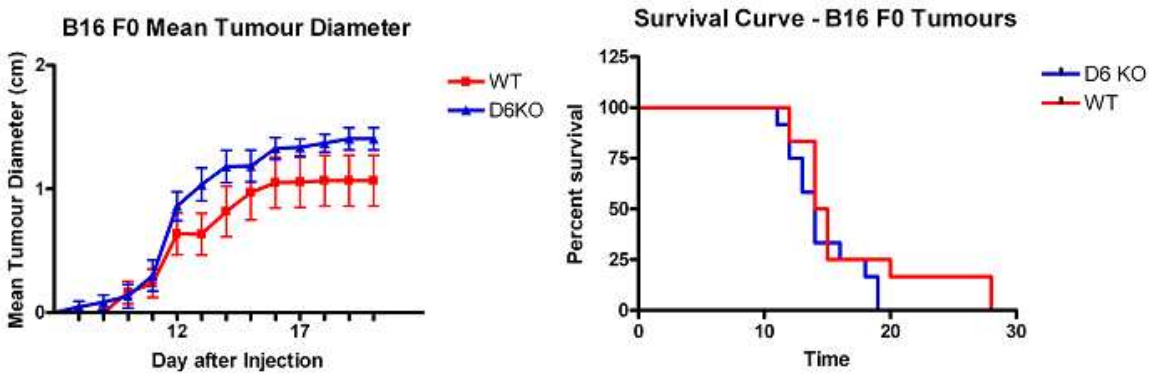

Figure 4-2: B16 F0 tumour growth in WT and D6KO C57Bl/6 mice

Following injection of B16 F0 tumour cells, mice were monitored daily for the development of tumours. Tumours appeared in D6KO mice before WT mice, which meant that D6KO mice had an increased tumour growth rate (graph A), although this is not significant (Two way ANOVA). When tumours reached 1.2cm mean diameter, mice were sacrificed. As tumours in D6KO mice grew faster than in WT, this resulted in a reduced survival rate (graph B) but again this is not significant (Logrank test). Results are pooled from 3 separate experiments, n = 12 per group. Results shown are mean tumour diameter +/- SEM.

4.1.2 B16 F0 Tumour Histology

In order to try to determine what could be causing this difference in growth rate, tumours from both WT and D6KO mice were analysed by histology to determine if there were any differences in the tumour structure or histological characteristics. When tumours reached a mean diameter of 1.2cm, they were excised from WT and D6KO mice and placed in 10% NBF for at least 24 hours before processing as described in the materials and methods (section 2.3.5). Tumour sections were cut (4µm) and were stained with H&E to analyse the histological characteristics of the tumours. In both genotypes, tumours developed close to the site of injection at the dorsal skin. When the tumours were removed, the surrounding skin was also removed, which allowed orientation of tumour sections. Figure 4.3 shows representative H&E stained tumour sections from WT and D6KO mice. Tumours were well defined, with obvious blood vessels and distinct areas of tumour cells and 'necrotic looking' areas.

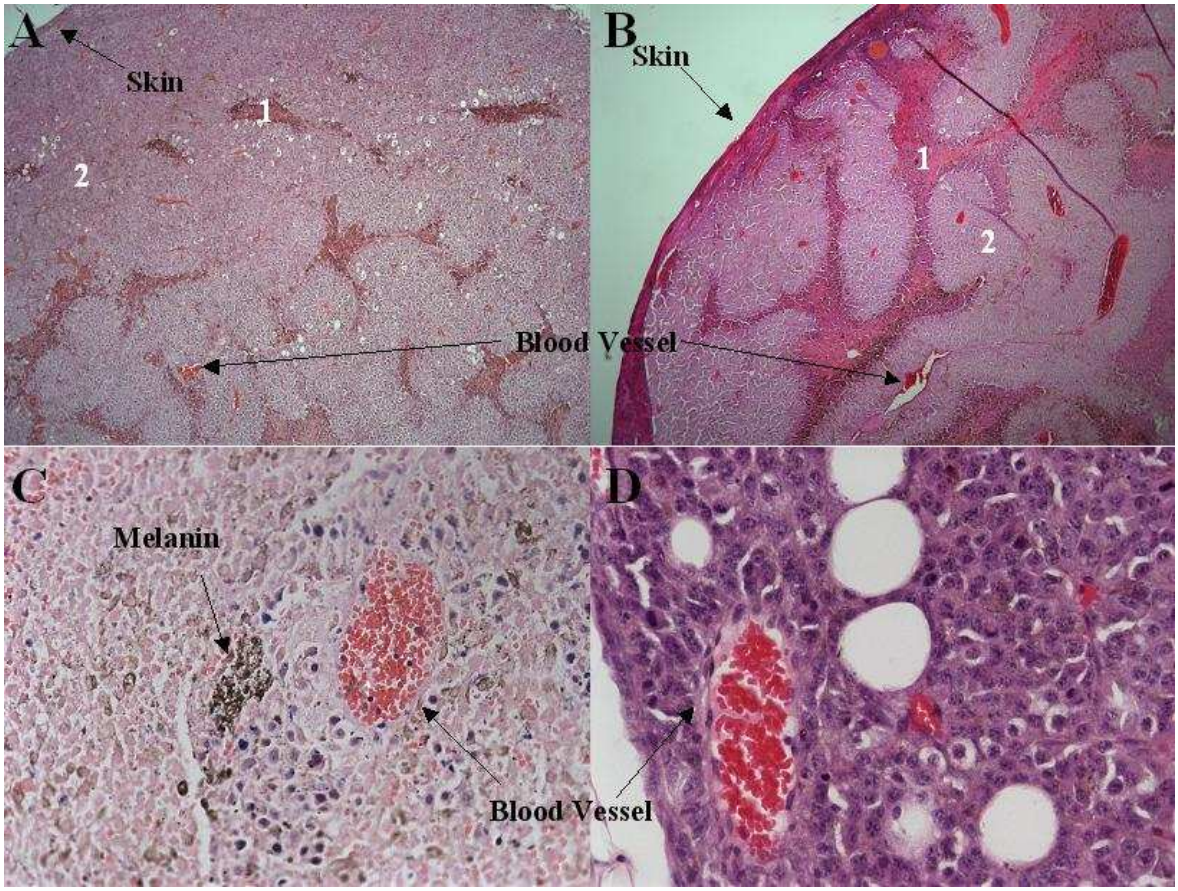

Figure 4-3: H&E stained B16 F0 tumour sections.

Tumours were excised from mice when they reached 1.2 cm mean diameter, and were processed for histology. Numerous features could be identified in H&E stained sections, including blood vessels, skin and melanin. The tumours could be divided into two distinct areas which appeared to contain 'necrotic looking' cells (1) and areas of densely packed tumour cells (2). A & B – tumours from WT and D6KO mice respectively, taken at 100x magnification. C – image from D6KO tumour taken at 400x magnification illustrating the presence of melanin. D – D6 KO tumour showing densely packed tumour cells, 400x magnification.

Tumours from both WT and D6KO mice have areas that appeared necrotic, along with areas of densely packed tumour cells. These areas are indicated in figure 4.3, pictures A and B, with 1 representing areas of cell death and 2 representing areas of densely packed tumour cells Picture D in figure 4.3, shows a higher magnification image of densely packed tumour cells. Melanin could be detected throughout the tumours, often concentrated in specific areas (see figure 4.3 C). Overall the histological features for both WT and D6KO tumours were similar. Although at first it appeared that D6KO tumours had increased areas of cell death, this was not consistently seen throughout tumour sections.

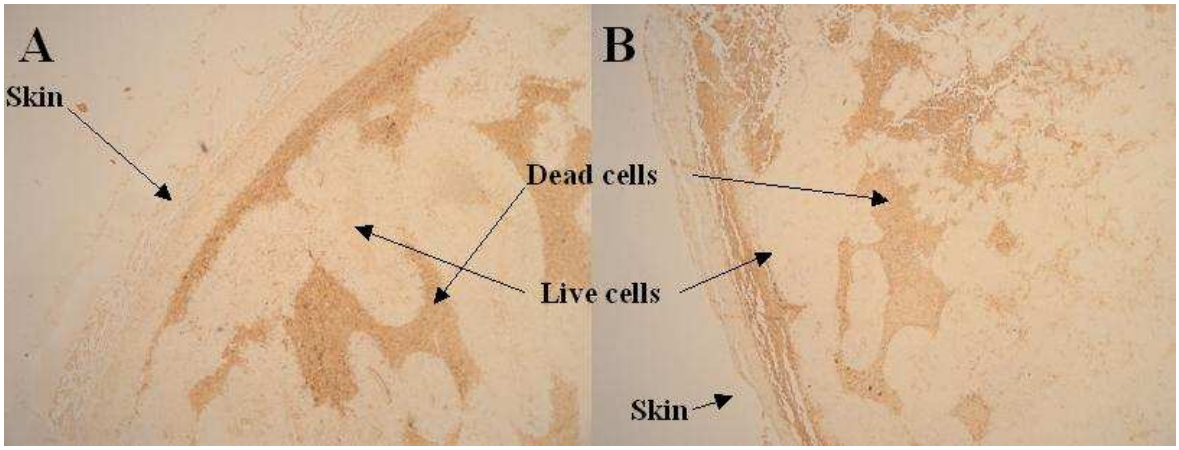

Figure 4-4: TUNEL stained B16 F0 tumours

B16 F0 tumours from WT and D6KO mice were stained using TUNEL to identify areas of dying cells within the tumour sections. A- D6KO tumour section, B- WT tumour section, images taken at 200x magnification

In order to try and confirm that the areas that looked like areas of cell death did contain dead cells, TUNEL staining was performed (see materials and methods section 2.3.5.4). This staining technique identifies DNA strand breakages, which defines apoptotic cells. Figure 4.4 shows that the dark stained TUNEL positive areas correlated with the 'necrotic looking' areas in the H&E stained tumour sections. Although TUNEL staining is routinely used for identification of apoptotic cells, it may also stain necrotic cells, as they undergo DNA fragmentation (345). As a result, areas of positive TUNEL staining in these tumours are referred to as areas of cell death. When the areas of cell death were measured, using the Axiovision software, no differences were found comparing D6KO tumours to WT, and there were no differences in the location of dying cells (data not shown).

4.1.3 B16 F0 Tumour Immunohistochemistry

The tumour growth results showed that D6KO mice developed tumours faster than WT mice, although this difference is not significant. As mentioned previously, tumour development is a complex process. The tumour cells must interact with stromal cells in order to create an environment conducive to their growth. Inflammatory cell infiltration is known to play a role in tumour growth and tumour associated macrophages (TAMs) in particular can influence tumour growth (see section 1.10.2.1). Angiogenesis must occur, once the tumour reaches a certain size, to allow cells within the tumour to survive (more detail can be found in section 1.10.4). The complexity of tumour growth means that there could be a wide range of factors causing the difference in tumour growth exhibited in D6KO mice. To try to characterise the cell populations present in B16 F0 tumours that developed in WT and D6KO mice, immunohistochemical analysis was used.

4.1.3.1 Blood Vessel Staining

Von Willebrand factor (vWF) is a glycoprotein that is produced by endothelial cells and megakaryocytes which is commonly used as a marker for blood vessels (346). An antibody against vWF was purchased from Dako and was used to stain blood vessels in tumours from WT and D6KO mice (as described in section 2.3.5.1 of materials and methods). The staining protocol required extensive optimisation. Various different steps were altered throughout optimisation; antigen retrieval methods, antibody incubation time, peroxidase blocking, and antibody concentration. Initially DAB was used as the peroxidase substrate, but even with the addition of nickel to make the DAB darker, melanin positive cells made identification of positively stained blood vessels difficult. An alternative HRP substrate, Novared, was purchased which gives a red product rather than brown. The Novared gave a lot of non-specific background on the tissue sections. The antibody was tested on human tonsil tissue (which should give positive staining with the vWF antibody). Positive staining was evident but the non-specific background was still high. Despite this, positive vessels can still readily be identified, in the tonsil section shown in figure 4.5.

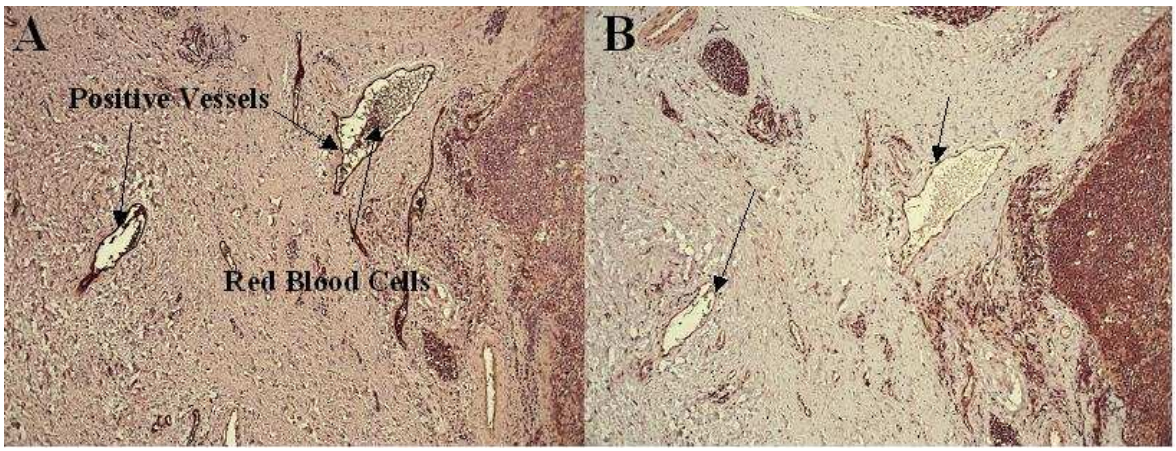

Figure 4-5: Optimisation of vWF staining

Initial optimisation of the vWF antibody, which was used to identify blood vessels within tumour sections, was performed using human tonsil sections, as this antibody cross-reacts with human vWF. A – vWF stained blood vessels within human tonsil. B – isotype control for vWF antibody showing unstained blood vessels. Images taken at 200x magnification

An optimised vWF protocol was therefore developed and used to stain all tumour sections from WT and D6KO mice. Novared was used as the HRP substrate to stain positive vessels red. Despite the high background, mentioned above, it was still possible to identify vWF positive vessels within tumour sections. Representative images from D6KO and WT tumours are shown in figure 4.6. Positive vessels can be easily recognised

in both D6KO and WT tumour sections. The morphology of the blood vessels varies, as can be seen in figure 4.6, depending on the plane at which the sections were cut. Blood vessels could also be confirmed by the presence of red blood cells within vWF stained vessels (not shown). The extent of blood vessel development in tumours was quantified by counting the number of positive vessels in eight random fields within the tumour at 200x magnification.

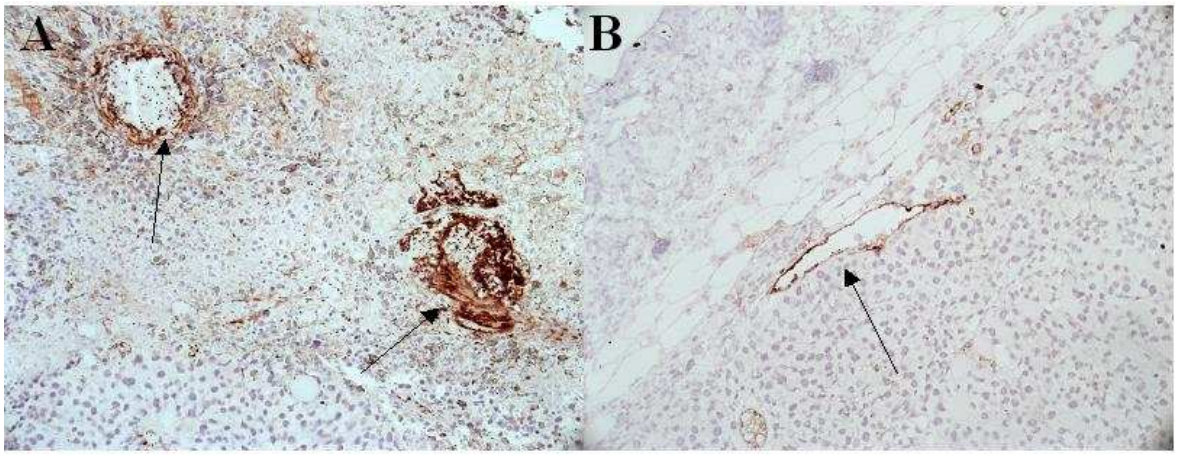

Figure 4-6: vWF stained B16 F0 tumour sections

Blood vessels were identified in B16 F0 tumours from WT and D6KO mice using an antibody against vWF. A – D6KO tumour section, B – WT tumour section. Images were taken at 400x magnification and are representative of 3 separate experiments

A quantitative analysis of vWF staining is shown in graph A, figure 4.7, and shows that B16 F0 melanomas developing in WT or D6KO mice have the same number of blood vessels within the tumour, with a mean of 2.44 positive vessels per 200x field (+/- 1.80) for WT tumours, and a mean of 3.28 positive vessels (+/- 1.19) for D6KO tumours. These data are pooled from three separate experiments and the p value is 0.1951 (students unpaired t test).

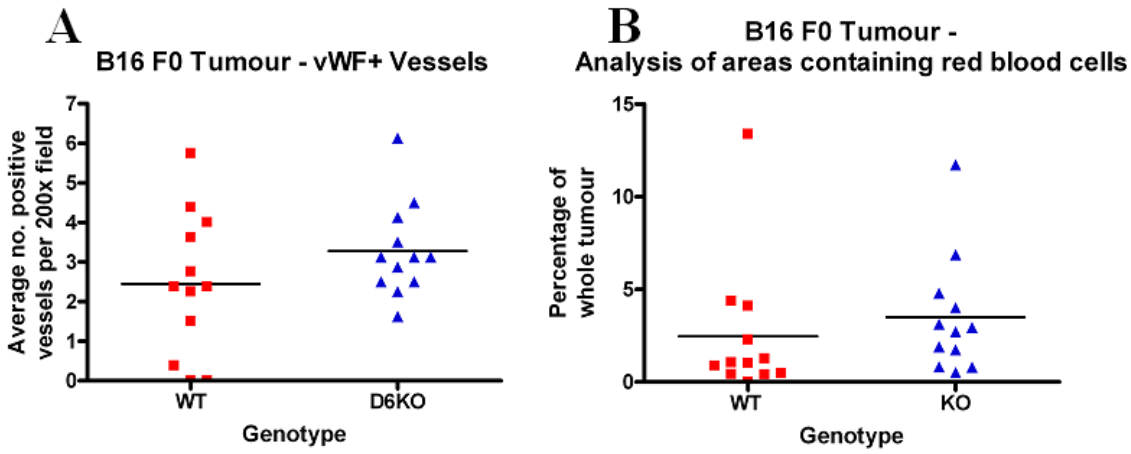

Figure 4-7: Analysis of blood vessels in B16 F0 tumours

A- B16 F0 tumour sections from both WT and D6KO C57Bl/6 mice were stained for vWF to identify blood vessels. The number of positive vessels were counted per random 200x magnification field and are expressed as the average number of vessels per field. B- optimisation of vWF staining was taking some time, so H&E stained tumour sections were used to analyse areas containing red blood cells, which could be used as a surrogate for vWF staining. Areas containing red blood cells were measured using Axiovision software, results are expressed as a percentage of the entire tumour section. Results are pooled from 3 experiments, n = 12 per group. NS – Students unpaired t test

As optimisation of vWF was ongoing for quite some time, an alternative method of measuring the extent of haemorrhage was also used in parallel. Areas within the tumours that contained red blood cells (as identified with H&E staining) were measured using Axiovision software. The total area of each tumour was measured and the percentage of 'red areas' (i.e. areas which contained blood) was calculated. Although this was not a specific measurement of blood vessels, it gave an indication of the distribution of blood throughout the tumours. This technique had the advantage that it would pick up areas of haemorrhage within the tumour, which may not be identified by vWF staining. These can also be called 'blood lakes', and can be found within tumours (347). The results from this analysis are shown in graph B, figure 4.7 and these show no significant difference in the percentage red areas in WT and D6KO tumours, which correlates well with the vWF data. In WT tumours the mean percentage red areas was 2.46% (+/- 3.71) and in D6KO tumours the mean percentage was 3.5% (+/- 3.17). The results from blood vessel analysis of WT and D6KO tumour have shown that the difference in tumour growth in D6KO mice is not due to, or associated with, a difference in blood vessel number, or areas of blood within the tumours.

4.1.3.2 Macrophage Staining

Macrophages are known to play a crucial role in tumour development, especially in the B16 model (269, 281, 289). The balance of macrophages is essential; too few macrophages can help promote tumour growth, but too many may promote tumour killing (289). The level of macrophage infiltration was analysed to determine if a difference in macrophage number could account for the altered tumour growth seen in D6KO mice. Tumour sections were stained with a Mac-2 antibody, which recognises a galactose specific lectin, expressed on mature macrophages (348). The staining protocol is described in materials and methods (section 2.3.5.3). DAB could be used as the HRP substrate for this protocol as it was easy to tell the difference between melanin and DAB staining, as their distribution was different. Mac-2 positive cells appeared rounded, whilst melanin, distributed throughout the tumour, appeared thread-like.

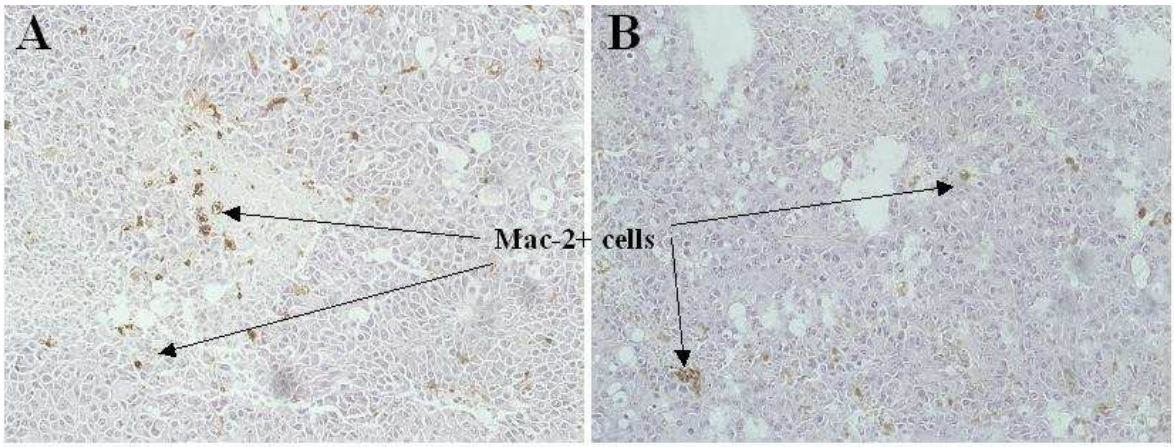

Figure 4-8: Identification of macrophages in B16 F0 tumours

B16 F0 tumour sections from WT and D6KO mice were stained for the presence of macrophages using an antibody against Mac-2. Macrophages are shown in brown (DAB) and counterstained with haematoxylin. Images are representative of 3 separate experiments, taken at 200x magnification. A – D6KO tumour section, B – WT tumour section.

Representative sections from D6KO and WT mice are shown in figure 4.8, showing Mac-2 positive cells within D6KO (picture A) and WT tumours (picture B). Similar to vWF staining analysis, the extent of Mac-2 staining was quantified by counting the number of positive cells in at least eight random fields throughout the entire tumour section at 200x magnification.

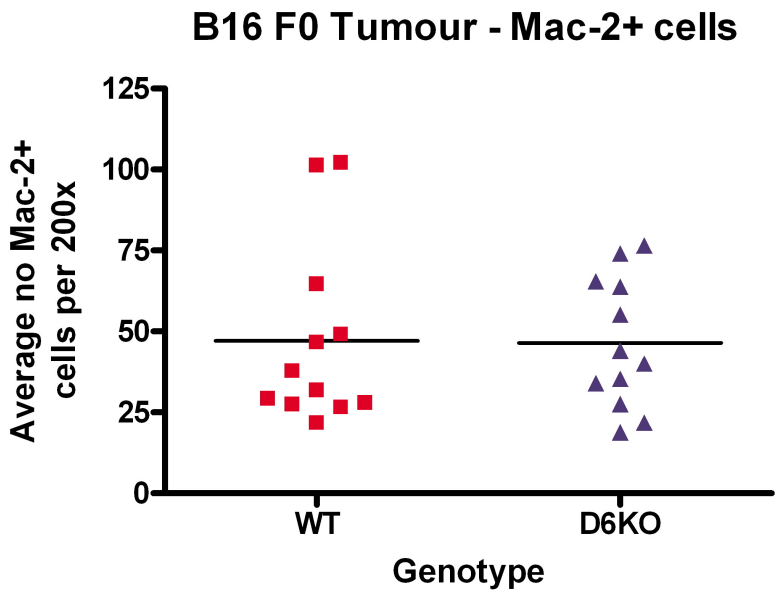

Figure 4-9: Analysis of macrophage staining of B16 F0 tumours.

WT and D6KO B16 F0 tumours were stained for macrophages using an antibody against Mac-2. Positive cells were counted in at least 8 random 200x magnification fields, results are expressed as the average cell number per field. Results are pooled from 3 separate experiments, n= 12 per group. NS – students unpaired t test.

The results from Mac-2 analysis of tumour sections are shown in figure 4.9. WT tumour sections had on average 47 macrophages per 200x field (+/- 28.16) and D6KO tumour sections had on average 46 macrophages per 200x field (+/- 20.13). Statistical analysis (students unpaired t test) shows that there is no difference between the number of macrophages in tumours developing in D6KO mice, compared to tumours in WT mice ($p = 0.9441$). These results show that the level of macrophage infiltration is not altered in D6KO tumours, compared to WT tumours.

4.1.3.3 T Cell Staining

Another cell type known to play a role in tumour development are T cells, more details of this can be found in section 1.10. It was decided to stain for all T cell populations to determine if there were any differences in T cell numbers in WT and D6KO tumours. T cells were stained using an anti-CD3 antibody, which identified both CD4+ and CD8+ T cells which may have been infiltrating the tumour. The staining was carried out as described in materials and methods (section 2.3.5.5). Figure 4.10 shows an example of CD3 staining in WT (picture A) and D6KO (picture B) tumours. Positive cells were stained with Novared. Analysis of T cell numbers within the main tumour mass was performed by counting positive cells in at least eight random fields, at 400x magnification using the

Axiovision software. In separate sections it appeared as if there were T cells infiltrating at the very edge of the tumours, so positive cells around the edge of the tumours were counted separately, and were expressed as the number of positive cells per µm of tumour edge.

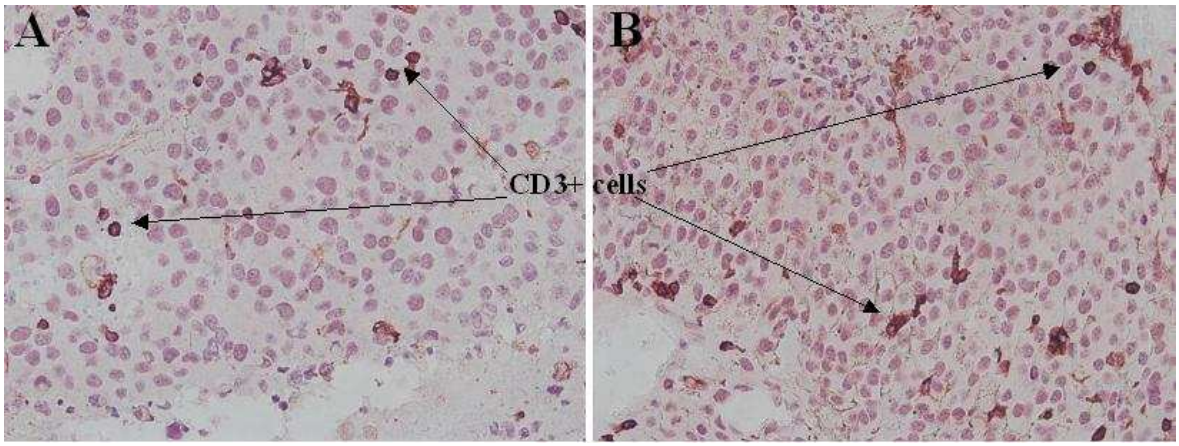

Figure 4-10: CD3 stained B16 F0 tumour sections

CD3 staining was used to identify T cells in WT and D6KO B16 F0 tumours. A – WT tumour section, B – D6KO tumour section. Images taken at 400x magnification

Figure 4.11 shows the results from the quantitation of the CD3 staining analysis. The numbers of CD3+ cells within the tumour (graph A) are similar in WT (mean 17.63 +/- 8.04) and D6KO mice (mean 14.72 +/- 6.06), but the numbers of CD3 cells at the edge of the tumours (graph B) were slightly reduced in D6KO tumours. The mean number of CD3 + cells per µm tumour was 0.01536 (+/- 0.009026) in WT tumours and 0.010906 (+/- 0.006758) in D6KO tumours, however this difference is not significant (p= 0.1850 students unpaired t test).

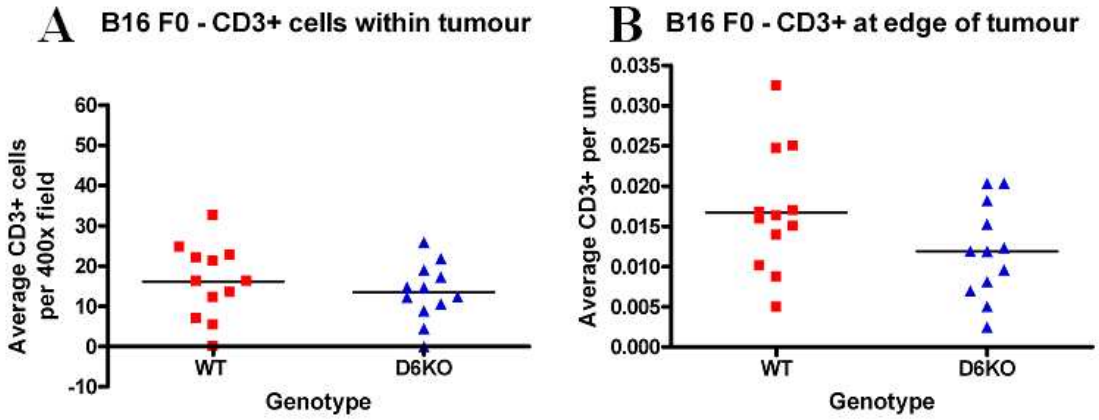

Figure 4-11: Analysis of T cells within B16 F0 tumours

A – CD3 positive cells were counted in at least 8 random 400x magnification field per section and are expressed as the average positive cells per 400x field. NS – Students unpaired t test. B – the distance around the tumours edge was measured using Axiovision software, then the number of CD3+ cells along the tumours edge were counted. Results are expressed as the average number of cells per µm. NS – Students unpaired t test. Results are pooled from 3 experiments, n = 12 per group.

4.1.3.4 Other Staining

Numerous attempts were made to stain tumour sections for the presence of neutrophils, using an antibody to myeloperoxidase and using Naphthol AS-D Chloroacetate (which turns a pink colour when neutrophils are present in tissue sections). Unfortunately both methods were repeatedly unsuccessful. LYVE-1 staining for lymphatic vessels was also performed (using both protocols described in materials and methods, section 2.3.5.2) but again this consistently failed to work on tumour sections, despite extensive optimisation. It is possible that the tumours do not express any lymphatic vessels, but each tumour was removed with the overlying skin still attached, this skin sample would contain lymphatics which would act as a positive control for lymphatic vessel staining. This staining protocol was later optimised for lung sections as shown in figure 5.15.

4.1.4 Summary

To summarise these results, B16 F0 tumours that develop in D6KO mice grow at a faster rate than in WT mice, although this difference is not significant. Immunohistochemical analysis of B16 F0 tumours from WT and D6KO mice, show that there are no differences in the number of blood vessels, the level of macrophage or CD3+ T cell infiltration. Analysis of the contribution of lymphatic vessels to the development of these tumours could not be performed, so this could not be ruled out.

4.2 D6 Expressing Tumours

4.2.1 B16 F0 Chemokine Receptor Expression

The results shown above, demonstrate that B16 F0 tumours appear to grow slightly faster in D6KO compared to WT mice, which suggests that D6 may play a role in tumour development. As a lack of D6 displayed a mild effect on delaying tumour development, it seemed plausible that D6 over-expression may have the reverse effect on tumour growth. In order to examine this, B16 F0 cells were stably transfected with D6. Prior to transfection, the chemokine receptor profile of B16 F0 cells was analysed by RT-PCR. This was performed to try and identify chemokine receptors that may be influenced by over-expression of D6, for example inflammatory CC chemokine receptors, as previous evidence has suggested that D6 over-expression may affect chemotactic responses to CCL4 (141). This was carried out as described in materials and methods, section 2.4. Briefly, RNA was extracted from B16 F0 cells, cDNA was generated and the expression of chemokine receptors was analysed by routine PCR.

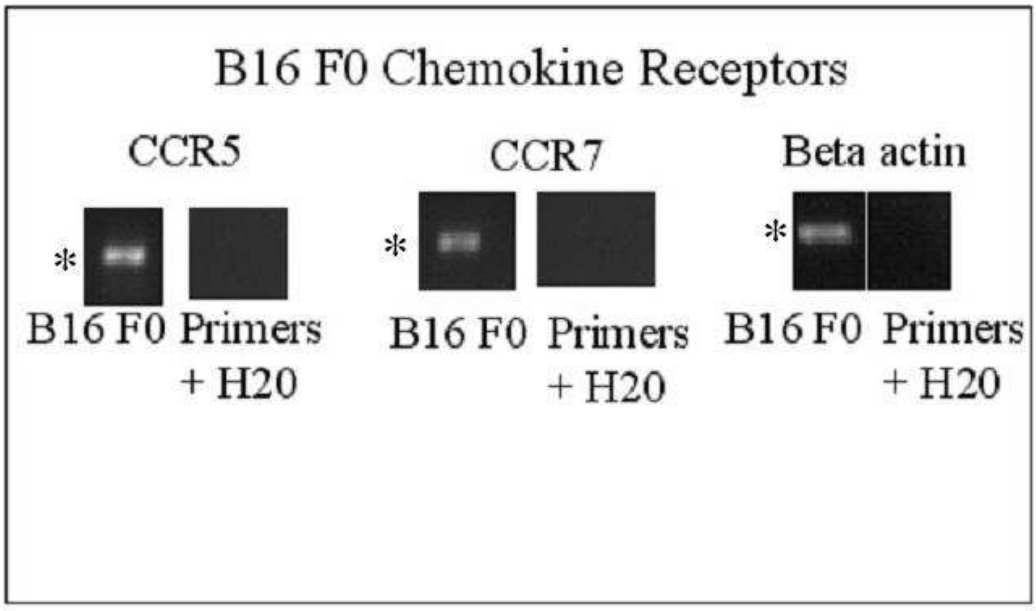

Figure 4-12: Chemokine receptor expression by B16 F0 cells.

The chemokine receptor profile of B16 F0 cells, was analysed by extracting RNA and performing RT-PCR. Primer sequences are detailed in table 2.6. RT-PCR reactions for CCR1, 2, 3, 4, CXCR4 and D6 were all negative (not shown).

RT-PCR results showed that B16 F0 cells did not express CCR1, 2, 3 and 4 (data not shown). They were also negative for D6. The only two chemokine receptors that were found to be expressed by B16 F0 cells were CCR5 and CCR7 as shown in figure 4.12, which

were present at the expected size (189bp for CCR5 and 154bp for CCR7). β-actin was used as a control to confirm the presence of cDNA. At the same time the chemokine receptor profile of the metastatic B16 F10 cells was analysed by PCR and these results are shown in section 5.1.7.1. These results, taken together with evidence from the literature (141), suggest that there is no potential for D6 to interact with any chemokine receptors expressed by B16 F0 cells.

B16 F0 cells were transfected with a plasmid containing murine D6, under the control of the CMV promoter (with a G418 resistance gene), using Fugene HD reagent, as described in materials and methods (section 2.1.3.1). The concentration of G418 used for selection of stable transfectants was determined by performing a 'kill curve', as described in materials and methods. Figure 4.13 shows the percentage of live B16 F0 cells remaining after culture with increasing G418 concentrations, for up to 2 weeks. 2mg/ml G418 was decided upon, as some cells were still alive after culture with 1.5 mg/ml G418.

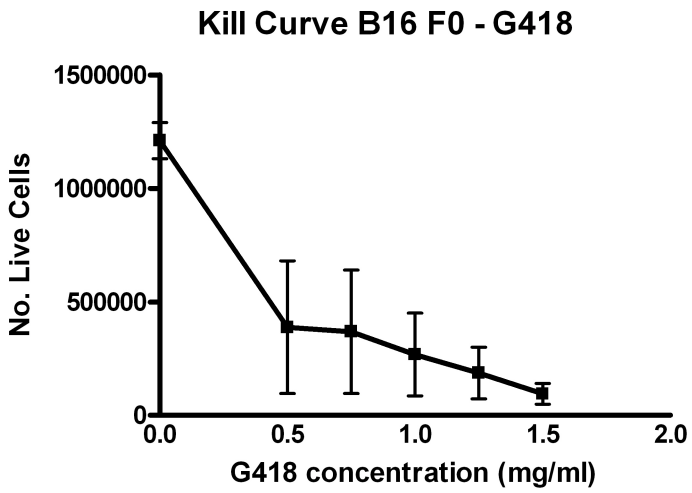

Figure 4-13: G418 kill curve for B16 F0 cells.

B16 F0 cells were cultured in increasing concentrations of G418 for up to 2 weeks. The number of live cells were counted using Trypan blue staining. Results are expressed as the number of live cells remaining in culture +/- SEM.

After selecting for stable transfectants (for at least 2 weeks) using 2mg/ml G418, pools of stable transfectants were tested for their ability to express D6. Analysis of D6 expression showed that un-transfected B16 F0 cells did not express D6. B16 F0 cells stably transfected with D6, were shown to be positive for D6 as shown by RT-PCR, see figure 4.14.

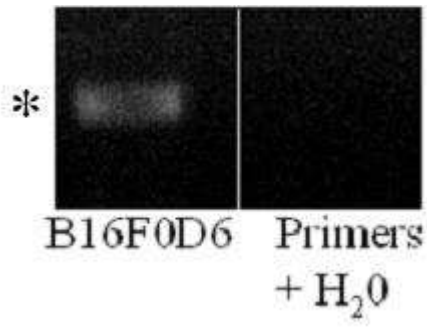

Figure 4-14: B16 F0 transfectant expression of D6

B16 F0 cells were transfected with a murine D6 plasmid and stable transfectants were selected by culturing in G418 containing media. RNA was extracted and D6 expression was confirmed by RT-PCR (un-transfected B16 F0 cells were D6 negative)

RT-PCR analysis shows that B16 F0 D6 cells express the mRNA for D6 (band size 98bp, figure 4.14), but expression at the mRNA level may not correspond to expression at the protein level. In order to be confident that D6 expressed in B16 F0 cells may have an effect on tumour growth, the D6 expressed by B16 F0 cells had to be functional. As there is no antibody available against murine D6, other methods had to be developed in order to assess D6 protein expression. A flow cytometry based assay was developed in our lab, which could be used to assess D6 function. This assay uses the principle that D6 is the only known chemokine receptor that can uptake both CCL2 and CCL3. CCL2 can bind CCR2 and D6; CCL3 can bind CCR1, CCR5 and D6. If the uptake of fluorescently labelled CCL2 could be out-competed by adding an excess of CCL3 (in this case PM2, a non-aggregating mutant of CCL3 was used (12)), then this suggested that the CCL2 was being uptaken by D6 meaning that it was functional. B16 F0 cells and B16 F0D6 cells were tested for D6 specific uptake, as described in materials and methods, section 2.1.5.1, the results are shown in figure 4.15.

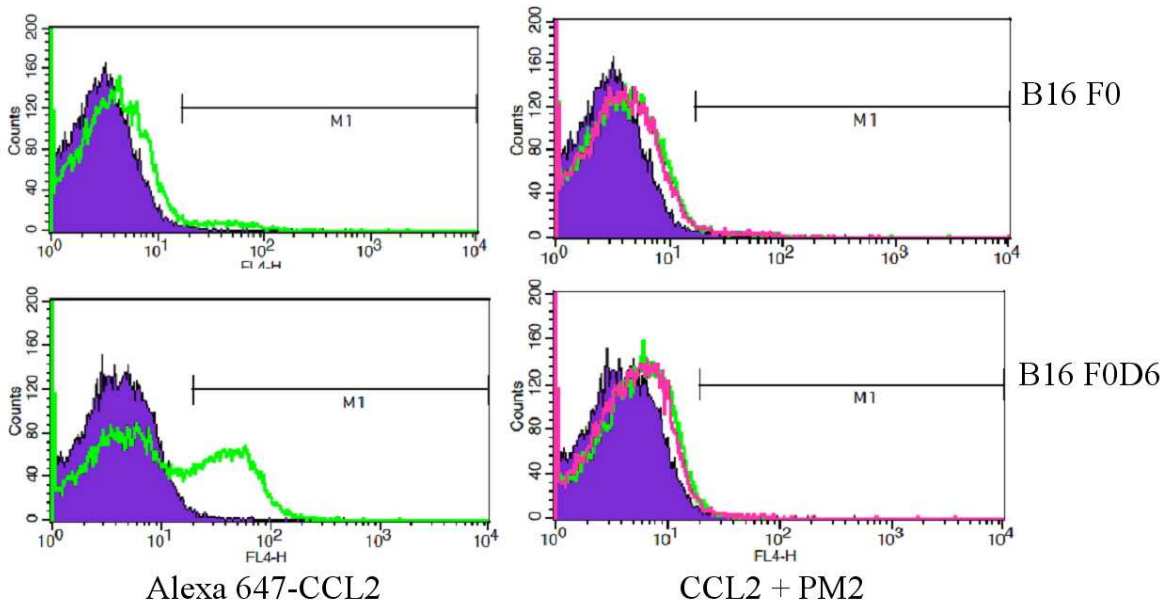

Figure 4-15: D6 expressed by B16 F0 transfectants is functional

B16 F0 D6 transfectants were tested for D6 functionality using a flow cytometry based chemokine binding assay. Cells were incubated in the presence of fluorescently labelled CCL2 with or without the presence of excess PM2 (CCL3). As D6 is the only chemokine receptor which can bind both CCL2 and CCL3, if CCL3 blocks CCL2 uptake then this indicates D6 is functional at binding chemokines. Untransfected cells are shown in the top two plots, showing no uptake of Alexa-647-CCL2. In contrast, D6 expressing B16 F0 cells shown uptake of Alexa-647-CCL2, which can be competed out with excess PM2, suggesting D6 expressed by these cells is able to bind chemokines.

The results shown in figure 4.15 (top graphs) show that un-transfected B16F0 cells did not bind CCL2, which correlates with the RT-PCR data showing these cells were CCR2 and D6 negative. When fluorescent-labelled CCL2 was added to B16 F0D6 cells, an increase in fluorescence intensity was evident (bottom graphs figure 4.15), showing that these cells were binding CCL2. There appears to be two populations of B16 F0D6 cells, one with a mean fluorescence intensity of 4.74 and the other population, which is binding fluorescent CCL2, has a mean fluorescence intensity of 35.14. When an excess of PM2 was added to the cells along with CCL2, the fluorescence intensity decreased which meant that PM2 was blocking the binding of fluorescent CCL2. Since D6 is the only chemokine receptor that can bind to both of these chemokines, this shows that B16 F0D6 cells were expressing functional D6. These results correlated with the RT-PCR results shown in figure 4.14, and confirmed the usefulness of these transfectants.

4.2.2 B16 F0D6 Tumour Growth

The results above show that the transfection of B16 F0 cells with D6 was successful and the D6 expressed by these cells is functional. B16 F0D6 cells were used to induce subcutaneous tumours, as described in materials and methods (section 2.3.1). Initially

B16 F0 and B16 F0D6 cells were injected subcutaneously into WT mice. The growth rate of the tumours were plotted against time and the data are shown in figure 4.16, graph A. Tumours in both groups appeared at day 9 after subcutaneous injection and by day 22, the majority of mice in both groups were sacrificed. One mouse that received B16 F0 cells had a slow growing tumour, which meant it survived until day 27. These data show that over-expression of D6 did not alter the growth rate of B16 F0 cells in WT mice – they grew at the same rate as B16 F0 cells, which resulted in similar survival in both groups as shown in graph B figure 4.16. In both groups, tumours reached the point of sacrifice at day 12 for B16 F0 cells, and day 14 for B16 F0D6 cells. The final mouse in the B16 F0D6 group was sacrificed at day 23, whilst the mouse with the slow growing B16 F0 tumour was sacrificed at day 27. The results from this experiment show that over-expression of D6 has no significant effect on B16 F0 tumour growth in WT mice.

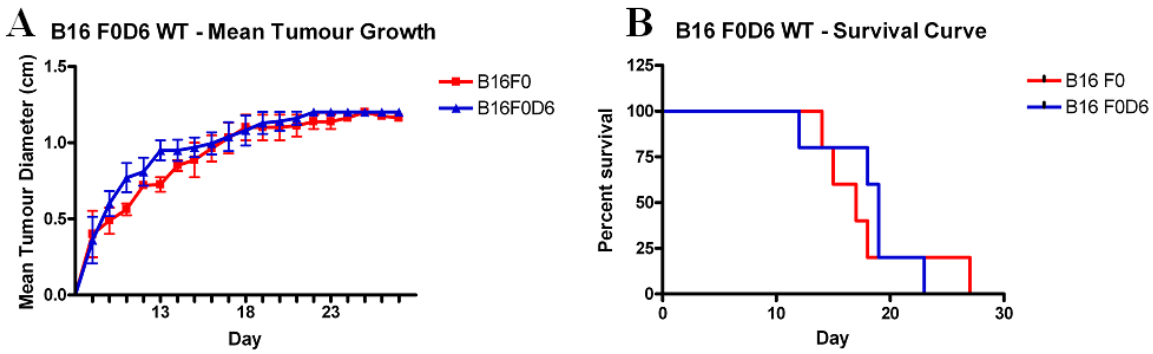

Figure 4-16: Growth and survival of B16 F0 tumours compared to B16 F0 D6 tumours in WT C57Bl/6 mice.

A – in WT C57Bl/6 mice the growth of tumours developing from B16 F0 cells was compared to B16 F0 D6 cells. The mean tumour diameter was measured after appearance of tumours and plotted against time. Results are expressed as mean tumour growth +/- SEM. NS – Two way ANOVA. B – mice were sacrificed when tumours reached 1.2cm mean diameter. Tumour growth was calculated by measuring the mean tumour diameter in cm each day from the first appearance of the tumours. NS – Logrank test. N = 5 per group

The above results show that there was no significant difference in growth rate when B16 F0 tumour cells over-express D6 in WT mice. B16 F0 D6 cells showed no difference in tumour growth rate in WT mice, compared to B16 F0 tumours in a WT background. These results suggest that D6 does not affect the growth of B16 F0 tumours. B16 F0 D6 tumour cells were injected into WT and D6KO mice, and the resultant tumour growth was compared. The growth rate of B16 F0D6 cells in WT and D6KO mice is shown in graph A of figure 4.17, and the relevant survival curve is shown in graph B of figure 4.17. These results show that in a D6KO background, tumours that developed from B16 F0D6 cells grow at a slower rate. This meant that tumours in D6KO mice were significantly smaller than D6 expressing tumours in a WT background. Tumours began to appear in D6KO mice

at day 6, and in WT mice at day 7. At day 7, B16 F0D6 tumours in WT mice had a mean diameter of 0.475cm (+/- 0.06455) whilst tumours in D6KO mice, which had a mean diameter of 0.4875 cm (+/- 0.326). By day 14, D6 expressing tumours in WT mice had a mean diameter of 1.056 cm (+/- 0.101), D6KO tumours had a mean diameter of 0.815 cm (+/- 0.114673). B16 F0D6 tumours developed at a significantly faster rate in WT mice, compared to B16 F0D6 tumours developing in D6KO mice ($p<0.0001$, Two way ANOVA test, with Bonferroni's correction)

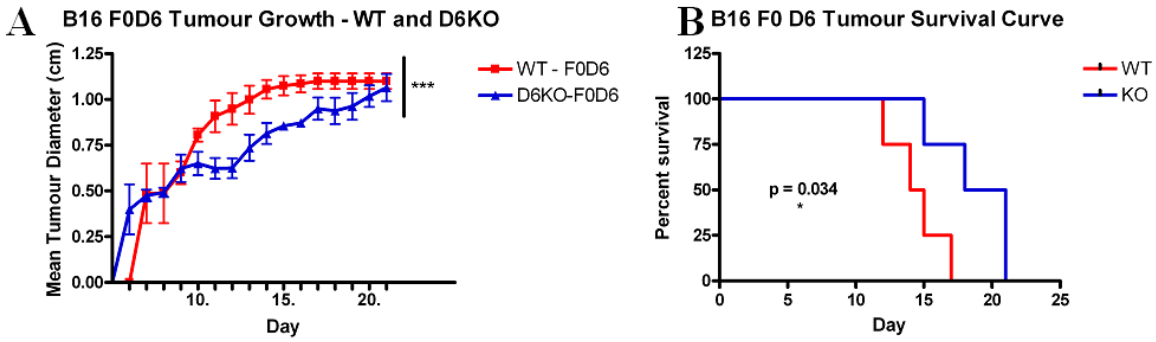

Figure 4-17: Growth and survival of B16 F0 D6 tumours in WT and D6KO mice.

A – tumour growth is shown as the mean tumour diameter +/- SEM. D6 expressing tumours appeared in WT mice before D6KO mice, resulting in a reduced tumour growth rate. P <0.0001 2 way ANOVA. B – survival of mice that received D6 expressing B16 F0 cells. Mice were sacrificed when tumours reached 1.2cm mean diameter. The delay in tumour growth shown in D6KO mice resulted in a significant difference in the survival of WT and D6KO mice that received D6 expressing tumour cells. p = 0.034, Logrank test. n= 5 per group.

This delay in tumour growth meant that D6KO mice survived for longer, as it took longer for their tumours to reach 1.2cm mean diameter, as shown in graph B (figure 4.17). The last WT mouse was sacrificed at day 17, whilst the last D6KO mouse to be sacrificed was at day 21, which resulted in a significant difference in survival ($p=0.034$, Logrank test).

The growth rate of B16 F0D6 tumours has been shown to be unchanged in WT mice, compared to B16 F0 tumours. In D6KO mice, B16 F0D6 tumours grow at a significantly slower rate compared to B16 F0D6 tumours in WT mice. B16 F0 and B16 F0D6 cells were injected subcutaneously into D6KO mice, to determine if B16 F0D6 cells grew at a slower rate in D6KO mice, compared to B16 F0 cells. The results from this experiment are shown in graph A, figure 4.18. These data show that in a D6KO background, D6 expressing tumours grow at a slower rate than un-transfected tumour cells. B16 F0 tumours began to appear in D6KO mice at day 8, whilst B16 F0D6 tumours did not appear in D6KO mice until day 11. The sample size in this experiment was small (3 mice for each cell group), so these results are not significant. One of the mice in the D6 transfected tumour group did

not develop a tumour until day 20, the inclusion of these results explains the large error bars in graph A. This was probably due to problems with the subcutaneous injections; this mouse may have received fewer cells than the others.

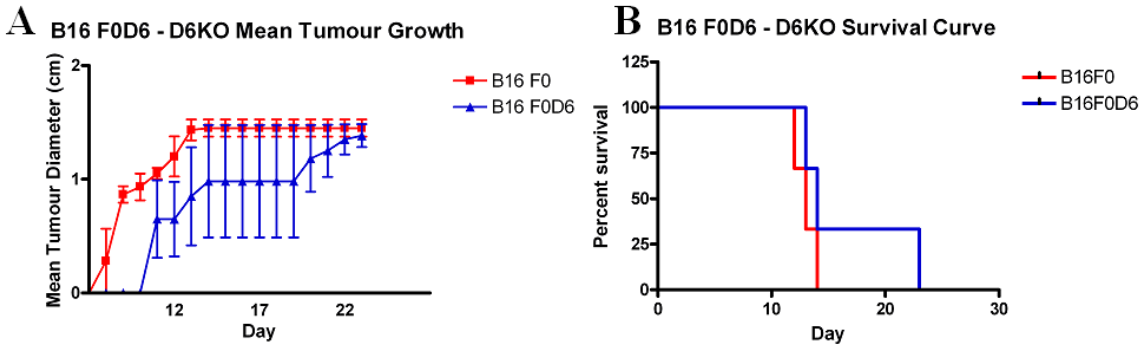

Figure 4-18: Tumour growth and survival of B16 F0 and B16 F0 D6 tumours in D6KO mice

A – Tumour growth is expressed as the mean tumour diameter +/- SEM. Each group had only 3 mice, one mouse in the B16 F0 D6 group did not develop a tumour until day 20, which accounts for the large error bars. NS – two way ANOVA. B – Survival of D6KO mice that developed B16 F0 and B16 F0D6 tumours. NS – Logrank test. n = 3 per group.

The survival curve comparing B16 F0 cells to B16 F0D6 cells in D6KO mice is shown in graph B of figure 4.18. Mice in the B16 F0 cell group were sacrificed between 12 and 14 days, whilst mice in the B16 F0D6 cell group were sacrificed between 13 and 23 days. The mouse that did not develop a tumour until day 20 has been included in the survival curve graph. It appears from these data that in D6KO mice, B16 F0D6 tumours develop later than B16 F0 tumours, and may grow at a faster rate, but the sample size is too small here for this difference to be significant.

To summarise these results; D6 expression on B16 F0 cells has no effect on the tumour growth in WT mice. However, in D6KO mice, D6 over-expression causes a reduction in tumour growth, when compared to B16 F0 tumour growth. B16 F0D6 tumours develop at a significantly slower rate in D6KO mice compared to D6 expressing B16 F0 cells in WT mice. These results suggest that in a D6KO background, D6 expressing cells are causing changes to the tumour microenvironment or cells within the tumour, to alter tumour growth. This experiment would need to be repeated to confirm the reproducibility of these results.

4.2.3 B16 F0D6 Tumour Histology

The histology of tumours which developed from B16 F0D6 cells were analysed to determine if there were any differences in tumours which over-expressed D6 compared to un-transfected tumours, which could be contributing to the differential growth rate, seen in D6KO mice. As with previous tumour experiments, tumours were excised, processed for histology and stained with H&E. Representative tumour sections are shown in figure 4.19. There appeared to be no obvious differences in the histology of D6 expressing tumours compared to un-transfected tumours. D6 expressing tumours had the same features as B16 F0 tumours; densely packed tumour cells, necrotic areas, blood vessels and melanin.

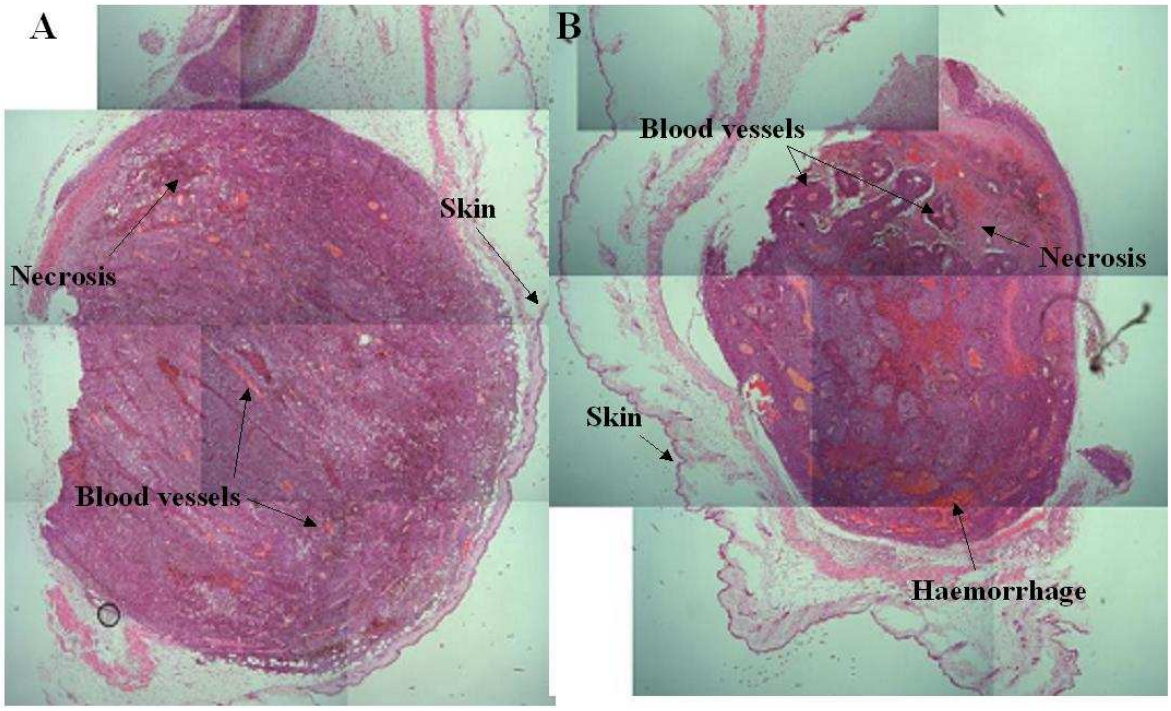

Figure 4-19: Histological analysis of B16 F0 D6 tumours in WT and D6KO mice

B16 F0 and B16 F0 D6 tumours were processed for histological analysis following sacrifice. D6 expressing tumours showed similar features to B16 F0 tumours, namely blood vessels, densely packed tumour cells and areas of necrosis. A – B16 F0 D6 tumour from WT mouse, B – B16 F0 D6 tumour from D6KO mouse. Images are taken at 50x magnification and 'overlaid' to show the entire tumour section

4.2.4 B16 F0D6 Tumour Immunohistochemistry

As mentioned above, tumour development is a complex process that involves growth of new blood vessels, macrophage and T cell infiltration (see section 1.10). Staining for vWF, Mac-2 and CD3 was performed on tumour sections from B16 F0D6 tumours, as described previously (materials and methods, section 2.3.5). vWF expression was quantified by

counting the number of positive vessels in at least eight random 200x fields throughout the tumour sections. Mac-2 analysis was carried out by counting the number of positive cells in at least eight random 200x fields. CD3 staining analysis was performed by counting the number of positive cells in at least eight random 400x fields within the tumour, as well as counting the total numbers of CD3+ cells at the edge of the tumour, which was expressed as the average cell number per µm. Representative staining is shown in figure 4.20. Picture A shows a vWF stained D6 positive tumour section; a positive vessel is shown in red. Picture B shows a CD3 stained D6 positive tumour section, with red stained CD3+ cells throughout. Picture C shows Mac-2+ cells within a D6 positive tumour.

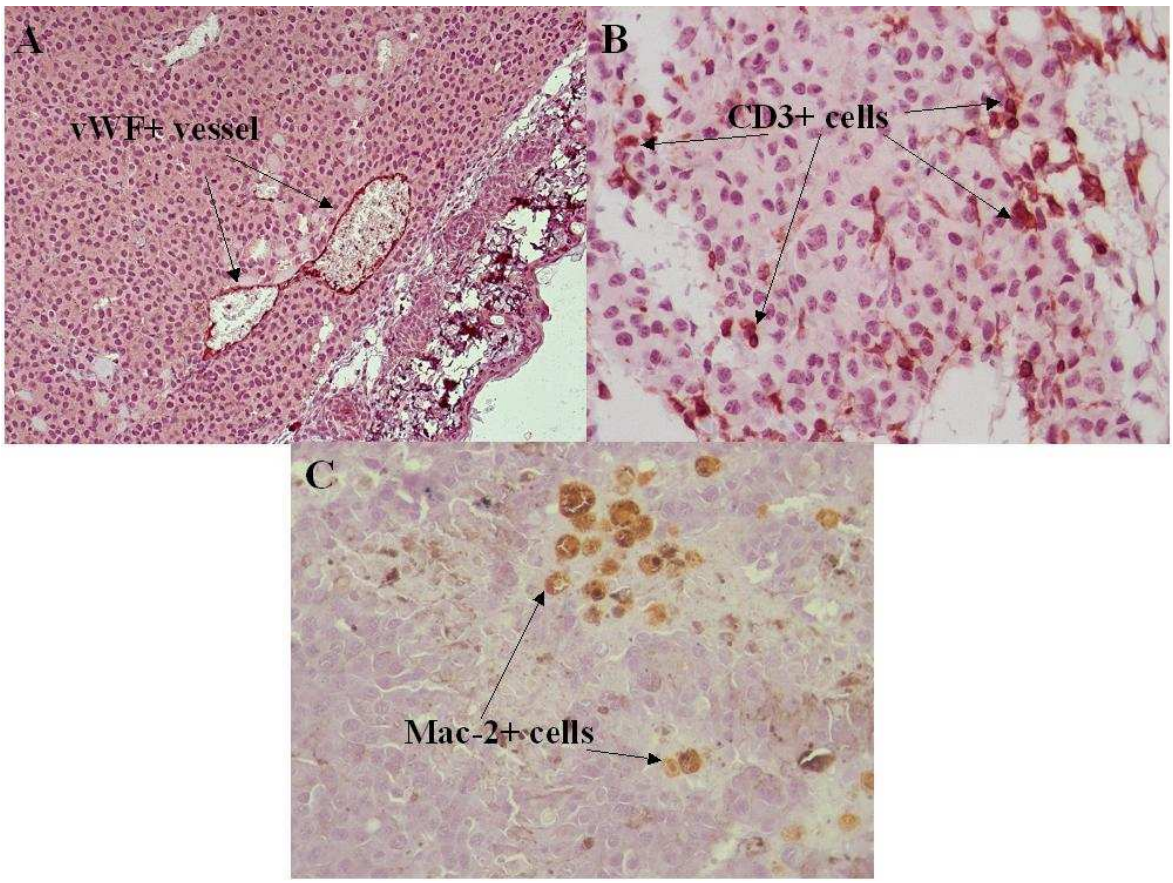

Figure 4-20: Immunohistochemical staining of B16 F0 D6 tumours

B16 F0D6 tumours from WT and D6KO mice were stained for A - blood vessels (vWF), B - T cells (CD3) and C - macrophages (Mac-2). Pictures shown are representative of three separate experiments. Taken at 200x magnification (A) and 400x magnification (B and C).

Analysis of vWF staining (graph A figure 4.21) suggested that there may be a trend towards a decrease in blood vessel number in D6 expressing tumours, in both WT and D6KO mice, but these differences were not significant. B16 F0 tumours in WT mice had an average number of 2.2 (+/- 1.59) vWF positive vessels per 200x field, in D6KO mice B16 F0 tumours had an average of 4 (+/- 0.353) vWF positive vessels. Comparing B16 F0D6

tumours, in WT mice these tumours had on average 1.69 (+/- 1.08) positive vessels compared to 2.38 (+/- 1.96) positive vessels in D6 expressing tumours in D6KO mice.

Results for Mac-2 staining, shown in graph B in figure 4.21, showed a significant difference in the number of macrophages in B16 F0 tumours. D6KO mice had a significantly higher number of macrophages than WT mice, with D6KO tumours having on average 40.33 (+/-10.01) positive cells per field, and WT tumours having 25.4 (+/- 5.23) positive cells per field. This difference was significant, p = 0.0158 (students unpaired t test). Looking at B16 F0D6 tumours in D6KO mice, they appear to have a slight increase in Mac-2 positive cells (43.19 cells +/- 11.47), compared to B16 F0D6 tumours in WT mice (31.63 cells +/- 10.28), but this difference is not significant (p = 0.0797 students unpaired t test). These data did not correlate with the previous results for Mac-2 staining in B16 F0 tumours (see figure 4.9), where there was no difference in the number of macrophages in WT and D6KO mice. The difference may be significant here due to the small sample size (3-5 mice per group).

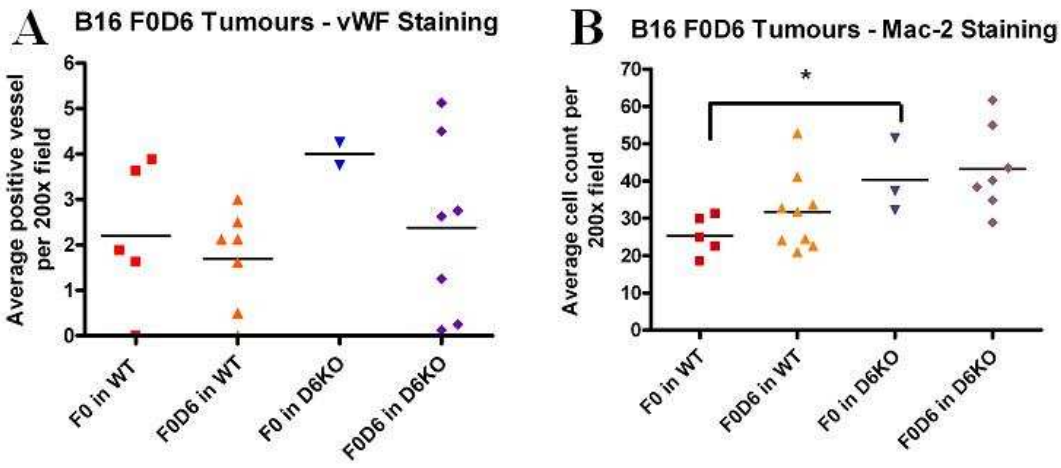

Figure 4-21: Immunohistochemical analysis of B16 F0 D6 tumours

B16 F0 D6 tumours that developed in WT and D6KO C57Bl/6 mice were stained with antibodies against vWF and Mac-2. Positive vessels and cells were counted in 8 random fields at 200x magnification, results are expressed as the average positive vessels (graph A) and average positive cells (graph B) per random field. Results are from 3 separate experiments , n = 5 (B16 F0 tumours in WT mice); n = 9 (F0D6 in WT mice); n = 3 (B16 F0 in D6KO mice); n = 7 (B16F0D6 tumours in D6KO mice). A – NS, students unpaired t test. B – p = 0.0291, students unpaired t test

The results from CD3 staining analysis are shown in figure 4.22. Graph A shows the results from quantifying the number of CD3+ cells within the tumour, and graph B shows the number of CD3+ cells present at the edge of the tumours, expressed as the average number of cells per µm of tumour edge. Graph A shows that there are no differences in the number of CD3 + cells within the tumours, irrespective of the expression of D6 by B16

F0 cells. B16 F0 tumours in WT mice had an average number of 17.25 (+/- 14.99) CD3 positive cells, whilst B16 F0 tumours in D6KO mice had on average 19.25 (+/- 13.099) CD3 positive cells. In B16 F0D6 tumours, those that developed in WT mice had on average 18.33 (+/- 10.97) CD3 positive cells, whilst those that developed in D6KO mice had on average 18.85 (+/-13.12) CD3 positive cells within the tumour.

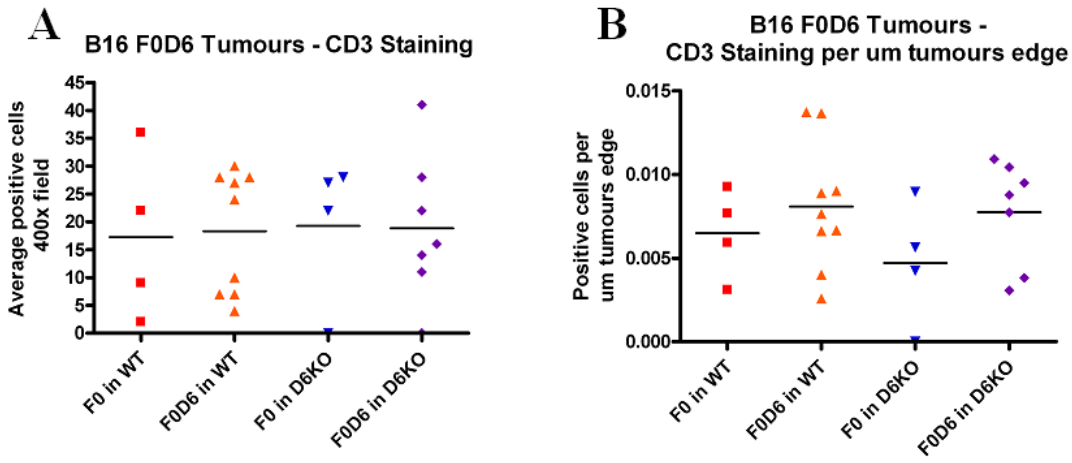

Figure 4-22: Immunohistochemical analysis of T cell infiltration of B16 F0 tumours

B16 F0 and B16 F0 D6 tumours, in WT and D6KO C57Bl/6 mice were stained for T cells using an antibody against CD3. A – positive cells were counted in at least 8 random 400x fields, and are expressed as the average cell number per 400x field. B- Positive cells were counted at the edge of the tumour and are expressed as the average cell number per µm of tumours edge. Results are pooled from 3 experiments, n= 4 (F0 in WT), 9 (F0D6 in WT), 4 (F0 in D6KO), 7 (F0D6 in D6KO). NS – Students unpaired t test

Graph B shows the average number of CD3+ cells per µm of the tumours edge. B16 F0 tumours developing in WT mice had on average 0.00649 (+/- 0.00263) cells per µm, compared to 0.00471 (+/-0.003711) cells per µm in D6KO mice. B16 F0D6 tumours had on average 0.008087 (+/- 0.003802) cells per µm in WT mice, and 0.007745 (+/- 0.00313) cells per µm in D6KO mice. These data show that there are no significant differences in the number of CD3+ cells infiltrating the tumour, or at the tumours edge, in D6 expressing tumours compared to un-transfected tumours.

As with previous tumour experiments, staining for neutrophils and lymphatic vessels was carried out, but this was unsuccessful.

In conclusion, these results show that D6 expressing tumours develop at a significantly slower rate in D6KO mice, compared to D6 expressing tumours in a WT background. In a D6KO background, D6 expressing tumours develop at a slower rate than B16 F0 tumours, but this difference was not significant. The results from immunohistochemistry show that there are no differences in the number of blood vessels within the tumour. The number

of macrophages and CD3+ T cells infiltrating the tumour showed no significant differences comparing B16 F0 tumours to B16 F0D6 tumours in WT or D6KO mice. This suggests that some other mechanism is likely to be responsible for the reduced growth rate.

4.3 Summary

The results presented in this chapter show that B16 F0 tumours developing in D6KO mice grow at a faster rate, although not significant, than B16 F0 tumours developing in WT mice. No differences could be found with respect to blood vessels, CD3+ T cell infiltration or macrophage number of location, when comparing tumours in WT and D6KO mice.

The data presented here show that B16 F0 cells that have been transfected with D6 express it in a stable and functional manner. B16 F0D6 tumours have no obvious differences in growth compared to their un-transfected counterparts, when injected in to WT or D6KO mice. When comparing B16 F0D6 growth in WT and D6KO mice, these tumours develop at a significantly slower rate in D6KO mice, compared to WT. Analysis of the tumours by histology shows that this difference in growth is not due to any gross morphological differences in D6 expressing tumours, nor any differences in T cell or macrophage infiltration. Initially it was hypothesised that D6KO mice were mounting an immune response against previously unseen D6, but this is unlikely to be the case, as tumour sizes are largely similar and no increase in T cell or macrophage infiltration has been shown. Ideally these experiments would be repeated with a more comprehensive study of the leukocyte populations infiltrating the tumours, by flow cytometry, to study the relative populations of B cells, T cells, NK cells and macrophages in more detail.

The only other chemokine receptors that are expressed by B16 F0 cells are CCR5 and CCR7. D6 expression on B16 F0 cells is unlikely to affect CCR7 function, as CCR7 binds CCL19 and CCL21, which D6 cannot bind to. It is more likely that D6 may have an effect on CCR5, as the CCR5 ligands CCL3, CCL4 and CCL5 can also bind to D6. In B16 F0 tumours, which lack D6 expression, CCR5 may be influencing tumour cell survival, as CCR5 has been shown to be anti-apoptotic in macrophages and has been shown to promote the survival of lymphoma cells (349, 350). In D6KO mice, there may be a general increase in inflammatory chemokine levels, including the CCR5 ligands, CCL3-5. It is possible that in D6KO mice this increased level of inflammatory chemokines induces signalling via CCR5, which enhances survival and proliferation of B16 F0 cells, resulting in increased tumour

growth. In B16 F0D6 cells, the presence of D6 may reduce the levels of inflammatory chemokines in the local tumour environment of D6KO mice, which would result in reduced CCR5 signalling, as its ligands are being degraded by D6. This would cause a reduction in tumour cell proliferation, resulting in a reduced growth rate. Another possibility is that degradation of inflammatory chemokines by D6 causes some interference in CCR5 induced signalling, which results in reduced tumour cell growth. The importance of CCR5 expression could be tested by performing knock-down of CCR5 expression in B16 F0 cells with siRNA, this would allow analysis of cell survival in vitro and these cells could be tested for their ability to induce tumour growth.

The role of D6 has been investigated in the DMBA/TPA model of skin tumourigenesis, which acts by inducing mutations in the skin, followed by repeated rounds of inflammation, to drive tumourigenesis. In this model, tumour development is dependent on TNFα and T cells. A lack of D6 expression renders B6/129 mice (that are normally resistant to tumours in this model) susceptible, and in FvB/N mice (which are already susceptible) D6KO mice develop a higher tumour burden compared to WT. Tumours that develop in D6KO mice contain more mast cells and T cells (142). The data presented here shows that B16 F0 (whether D6 positive or negative) tumours developing in D6KO mice have no increase in CD3+ T cells. Mast cell populations were not examined in this model. The role of mast cells in tumourigenesis has conflicting reports, evidence exists to support both a pro-tumourigenic role, and evidence also suggests that mast cells may have anti-tumour effects. In related B16 tumour models, mast cells have been shown to have anti-tumour effects after activation via TLR2 (351), and mast cell deficient mice have been shown to have delayed tumour growth in the B16 BL6 model of tumour growth, suggesting they may be pro-tumourigenic (352). As mast cells are increased in D6KO mice, in both the model of skin tumourigenesis and the TPA skin inflammation model (142, 152), in the B16 F0 model, mast cells may be increased in the skin of D6 KO mice, which may negatively influencing tumour growth when these cells express D6. This could be tested by looking at mast cell infiltration and localisation in B16 F0 tumours, by immunohistochemistry and flow cytometry.

The results with over-expression of D6 in B16 F0 cells show similarities to the work with the DMBA/TPA skin tumour model. In the DMBA/TPA model of tumourigenesis, over-expression of D6 in the epidermis was able to suppress tumour formation, in comparison, in the B16 F0 model, it appears that D6 expression on the melanoma cells is able to

suppress tumour growth, although not completely. If the K14 transgenic D6 mice used in this model were on a C57Bl/6 background then the contribution of epidermal expressed D6 to tumour growth could be compared to B16 F0 D6 expressing cells (142). In the DMBA/TPA model of skin tumourigenesis, the ability of D6 to suppress tumours was dependent on chemokine burden, D6 could be overwhelmed and tumours could still develop (142). No data exists as to the relative contribution of chemokines to the growth of “wild type” B16 F0 tumours; most of the data relating to chemokines and B16 F0 cells uses transfected cells that have been modified to express chemokines or receptors.

The B16 F0 model of tumourigenesis relies on injection of cells into syngeneic mice. The number of cells injected has been shown to influence the amount of time from injection to first appearance, fewer cells results in a longer lag period, but once tumours appear, they grow at the same rate. In these experiment, all tumours grew uncontrollably until they killed the mouse, with no evidence of gross metastases (284). It would be interesting to see if reducing or increasing the dose of B16 F0D6 cells is able to alter tumour growth. The results presented here suggest that D6 is able to limit the development of tumours in D6KO mice, but this inhibition of tumour growth appears to be incomplete as tumours are still able to grow.

5 Metastasis

5.1 B16 F10 Experimental Metastasis

5.1.1 Metastasis

The results presented above, together with evidence from the literature (142), suggest that D6 is involved in tumour growth. As mentioned in the introduction (section 1.11), when a tumour develops a vasculature and lymphatic supply, the tumour can become metastatic and tumour cells can spread throughout the body. The role of chemokines and their receptors in metastasis has been well described, for example expression of CCR9 by human melanoma is associated with metastasis to the small intestine, and CCR10 expression by melanoma cells is associated with metastasis to the skin (274, 282). Since D6 is expressed on lymphatic endothelial cells, which line afferent lymphatics (143), and lymphatics can play a role in metastasis, it was decided to investigate the role of D6 in metastasis

A model of metastasis was chosen which was directly related to the B16 F0 model of tumour growth. As mentioned above (section 1.13.2), B16 F10 cells have been selectively cultured in vitro and in vivo to generate variants on the original parental cell line. This process of selective culture has created a cell line which is able to colonise the lungs after intravenous injection (286, 311) an ability that is retained after repeated passages in vitro (303). This makes B16 F10 cells ideal to be used in a model of experimental metastasis. Experimental metastasis models differ from models of spontaneous metastasis in that the metastatic colonies do not come from a primary tumour within the mouse (283). As B16 F10 cells were easy to culture in vitro, and are similar to the B16 F0 cells used in the tumour model, it was decided use these cells to investigate the role of D6 in melanoma metastasis.

5.1.2 B16 F10 Metastasis Model

In the model of melanoma growth described in chapter 4, D6KO mice have an increased rate of tumour growth (although this is not significant), compared to WT mice, which is not caused by differences in cell populations (T cells and macrophages) or the development of blood vessels in the tumours. As D6 seems to play a role in tumour growth, it is possible that D6 may affect metastasis. In order to determine if D6KO mice have any differences in melanoma metastasis, the B16 F10 experimental metastasis model was performed on WT and D6KO mice. The model involved injecting B16 F10 cells into the tail vein of WT and D6KO C57Bl/6 mice, as described in materials and methods (section 2.3.2). Fourteen days after injection, mice were sacrificed and the lungs perfused with formalin before removal, followed by further fixation in formalin.

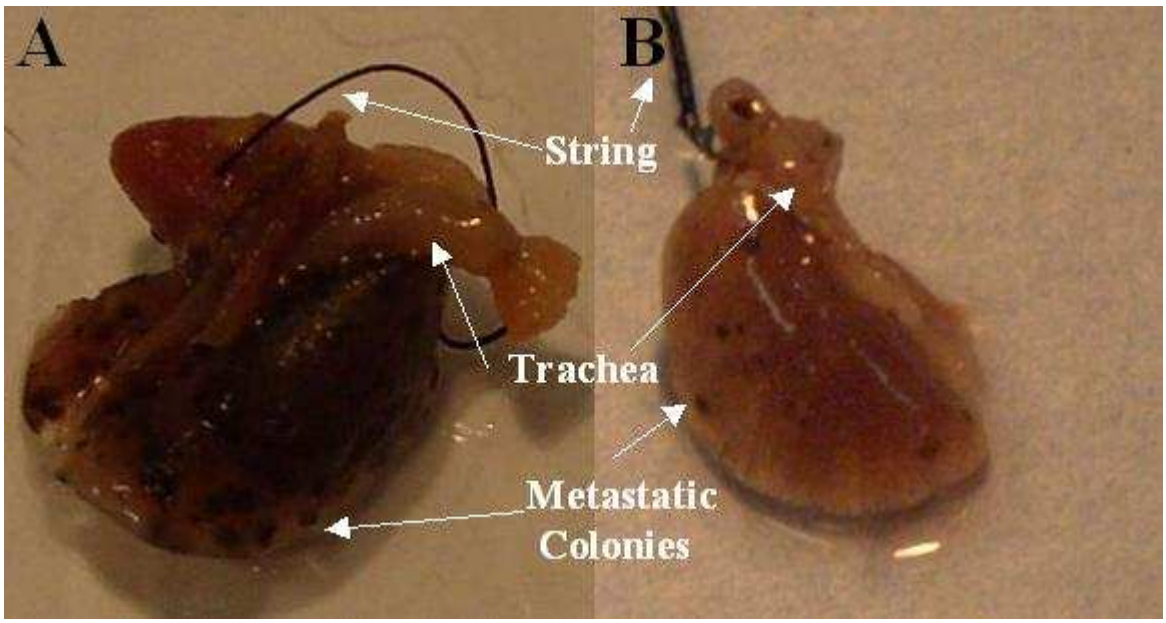

Figure 5-1: Metastatic colonies on lungs from B16 F10 treated C57Bl/6 mice.

14 days following B16 F10 cell intravenous injection, WT and D6KO C57Bl6 mice were sacrificed and their lungs were perfused with formalin to facilitate removal for histological analysis. Colonies were identified by the presence of melanin. A – WT mouse lungs, B – D6KO mouse lungs. String was tied around the trachea following formalin perfusion to prevent formalin from leaking out.

Figure 5.1 shows lungs taken from WT and D6KO mice following intravenous injection of B16 F10 cells. Metastatic colonies are visible on the external surface of the lungs, as they produce melanin. When the lungs are perfused with formalin, the trachea is ligated with string, to prevent the formalin from leaving the lungs, which is shown in figure 5.1. Picture A shows lungs from a WT mouse, with visible metastatic colonies covering the entire surface of the lungs. Picture B shows lungs taken from a D6KO mouse, which shows very few surface metastatic colonies, compared to the WT lungs. The metastatic colonies

were only present on the lung surface, not on the trachea. Lungs from WT mice had metastatic colonies all over the lungs surface, on all lobes of both the right and left lung. In D6KO mice, external colonies could be found on all surfaces of the lungs, but at a much lower number, with some mice having no evidence of metastatic colonies on the lungs surface.

There was an obvious visual difference in the number of external metastatic colonies, comparing WT to D6KO mice, so the external colonies were counted per lung and the results are shown in figure 5.2. Metastatic colonies were counted using a dissecting microscope, which allowed the entire surface of the lungs to be viewed. The sizes of colonies was not measured, a colony was defined as an area of melanin containing cells, which could be easily identified on the dissecting microscope. The colony sizes appeared similar in D6KO and WT lungs, the only observable difference being the number of colonies. These data show that D6KO mice have a significant reduction in the number of metastatic colonies developing on the surface of their lungs, compared to WT mice. WT mice had an average of 35.9 (+/- 28.46) metastatic colonies on the surface of the lungs, whilst D6KO mice had an average of 5.7 (+/- 8.5) colonies on the lungs surface. This difference was statistically significant ($p < 0.0001$ Students unpaired t test).

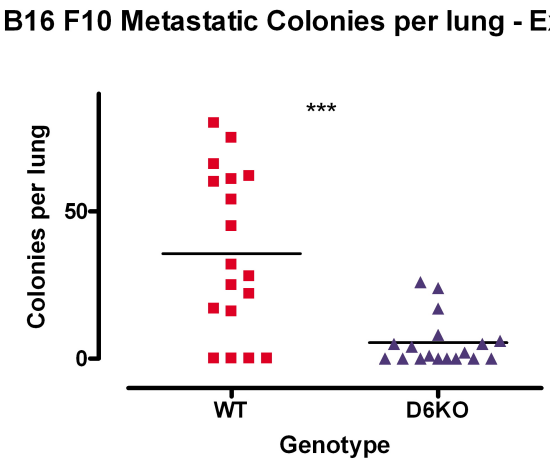

Figure 5-2: B16 F10 external lung colony counts

Colonies that could be identified on the external surface of B16 F10 treated WT and D6KO C57Bl/6 mice were counted using a dissecting microscope. Metastatic colonies could be identified by the presence of melanin. Results are expressed as the number of colonies per lung. Results are from 3 separate experiments, n = 9 per group. P <0.0001, Students unpaired t test.

Once the external colonies had been counted, the lungs from both D6KO and WT mice were processed for histological analysis in order to evaluate the internal structures of the lungs, and to identify any internal metastatic colonies. Lung sections were cut and stained

with H&E, as described in section 2.3.7. Figure 5.3 shows representative lung sections from D6KO and WT mice. Picture A shows a section from a D6KO mouse lung with blood vessels, bronchioles and alveoli identified. These features could easily be identified in sections from both WT and D6KO lungs. Metastatic colonies within the lung tissue were also easy to identify, as they appeared more densely packed than the surrounding lung tissue. Identification was aided by the presence of melanin, which was often detected within these colonies. Internal metastatic colonies could be identified in both WT and D6KO lung sections. The location of these colonies was throughout the lung tissue, with some next to blood vessels and bronchioles, whilst some colonies were distant from these features. Picture B in figure 5.3, shows a section from a WT mouse lung, and shows a section through a metastatic colony that is present at the lungs surface. This would have been one of the external metastatic colonies that would have been counted using the dissecting microscope.

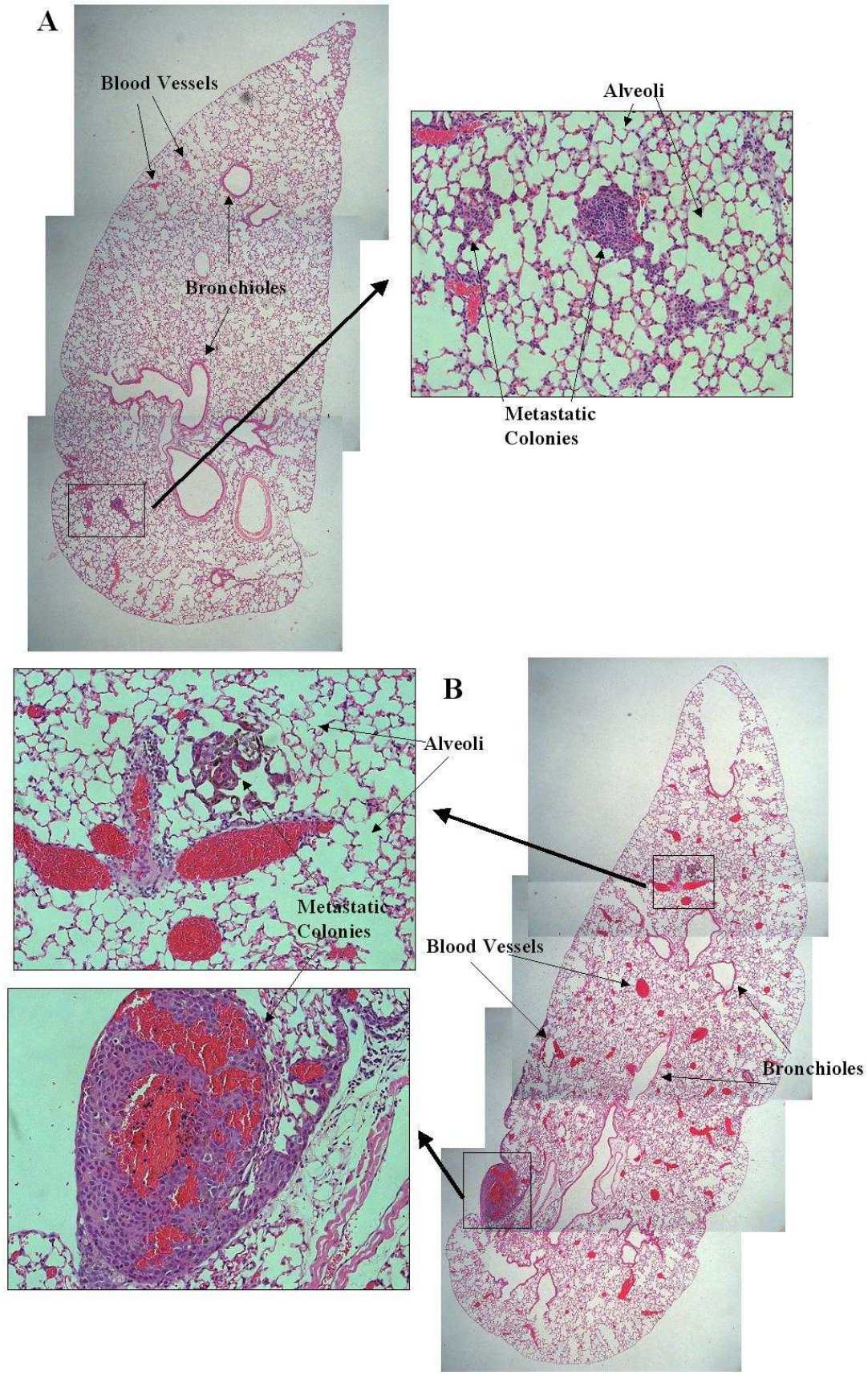

Figure 5-3: H&E stained lung sections from B16 F10 treated mice

WT and D6KO C57Bl/6 mice that received B16 F10 cells were sacrificed 2 weeks after injection and lungs were processed for histological analysis. Serial lung sections were taken from processed lungs and stained for H&E. Metastatic colonies could be identified by the presence of melanin and the different morphology from the surrounding lung tissue, as shown above. Images shown were taken at 50x magnification, to create the 'overlay pictures', close up images taken at 400x magnification. A – D6KO lung section, B- WT lung section.

The numbers of internal colonies were counted per tissue section and an average number of colonies per lung section were calculated. WT mice had, on average, 2.08 (+/- 2.03) internal metastatic colonies, whilst D6KO mice had, on average, 0.6 (+/-0.633) internal metastatic colonies. These data are presented in figure 5.4 and show that D6KO mice have a trend towards a reduced number of internal colonies, although this difference is not quite statistically significant (p=0.0759 Students unpaired t test). Examination of the sizes of the metastatic colonies, revealed no apparent differences in the size of internal metastatic colonies, in WT or D6KO mice.

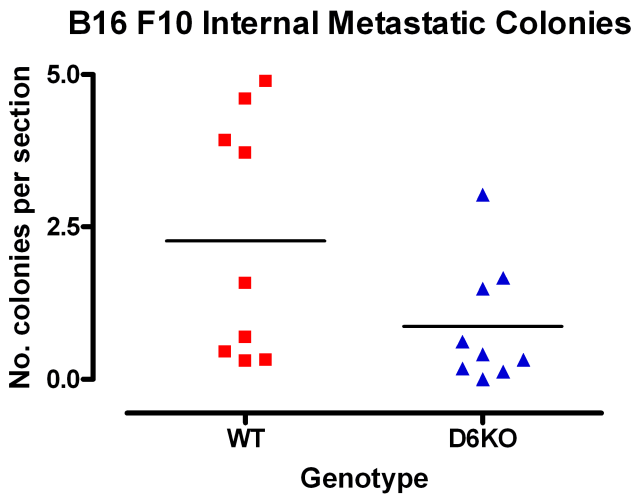

Figure 5-4: Internal metastatic colony counts from B16 F10 treated mice

Metastatic colonies inside the lungs were analysed by counting the number of colonies in serial sections from WT and D6KO C57Bl/6 mice that received B16 F10 cells. The number of internal colonies were counted on H&E stained sections and are expressed as the number of metastatic colonies per section. N = 9, from 3 separate experiments. NS, Students unpaired t test.

To summarise these results, using a model of experimental metastasis, D6KO mice develop significantly fewer metastatic colonies on the surface of the lungs than WT mice. As well as having a significant reduction in external metastatic colonies, D6KO mice also have a reduction in the number of internal metastatic colonies within the lungs, compared to WT mice, although this difference is not significant.

5.1.3 Lung Cell Analysis

The data above show that there is a significant reduction in the number of external metastatic colonies developing in D6KO mice, as well as a potential reduction in the number of internal colonies. D6 expression has been shown on various different leukocyte populations (143, 144). Analysis of the populations of leukocytes within the

lungs of D6KO mice has never been performed, so it was decided to look at the leukocyte populations within the lungs, to try to identify if a lack of D6 has altered cell populations, which might have relevance for the development of metastatic colonies. In order to do this, lungs from resting WT and D6KO mice, as well as WT and D6KO mice which had received B16 F10 cells, were digested (as described in materials and methods section 2.3.6) and stained with a panel of lineage markers, to identify different leukocyte populations by flow cytometry. Cells were analysed using the MACSQuant, selecting for live cells based on their FSC and SSC, these results are shown in figure 5.5.

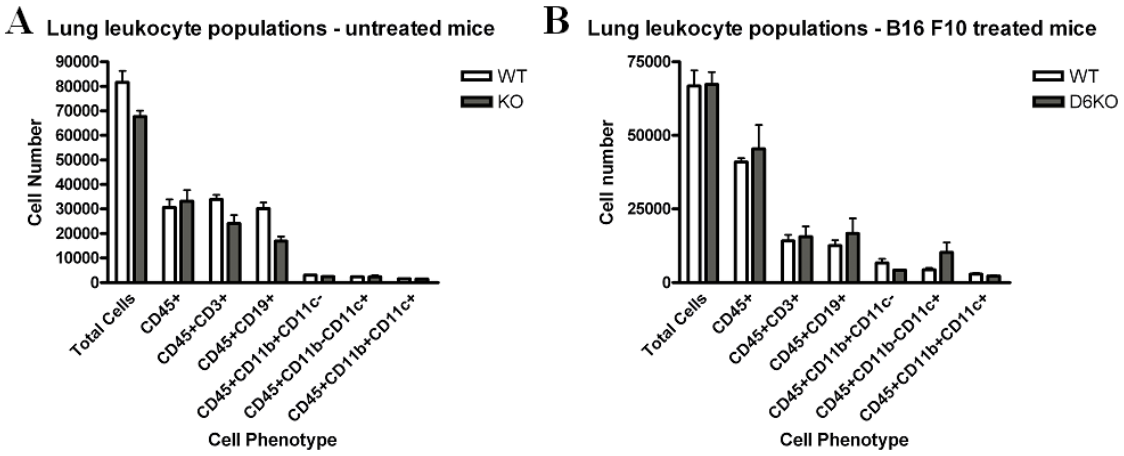

Figure 5-5: FACS analysis of cell populations in the lung from WT and D6KO mice.

Lungs from untreated mice (A) and B16 F10 treated mice (B) were digested with collagenase and a single cell suspension was stained with a panel of lineage markers to define the cell populations within the lungs by flow cytometry. A – Lungs from WT and untreated mice were stained with the markers described above, results are expressed as the number of live cells, which were gated on using FSC and SSC. N = 2 per group, NS, students unpaired t test. B- Lungs from WT and D6KO mice that received B16 F10 cells. Cell numbers are a proportion of the total cells, which were gated to exclude dead cells using FSC and SSC. N = 3 per group, NS, Students unpaired t test.

The results above show the number of cells identified for each population. The markers used were CD45 to identify leukocytes, CD3 to identify T cells, CD19 to identify B cells, CD11b and CD11c were used together to identify dendritic cells. Only CD45+ cells were analysed for their expression of the relevant lineage markers. Graph A shows the comparison between lung populations from resting lungs from WT and D6KO mice. There were no significant differences comparing the number of gated live cells in resting WT and D6KO lungs, untreated WT lungs had 86250 gated live cells (+/- 6554) gated live cells, compared to 67696 (+/- 3337) gated live cells in D6KO lungs. In the resting lungs, there were no significant differences in any cell population in D6KO mice compared to WT.

In B16 F10 treated lungs, again there was no difference in the average number of gated live cells, with WT B16 F10 treated mice having an average of 67429 (+/-9193) gated live cells, and D6KO B16 F10 treated mice had an average of 67251 (+/- 7378) gated live cells. Looking at the other leukocyte populations, there were no significant differences comparing any of the cell populations, between WT and D6KO lungs. Results shown in graph B, suggests that in D6KO mice there is an increase in CD45+ CD11b-CD11c+ cells, but this difference is not significant. This cell population could be a population of antigen presenting cells resident in the lungs (353), but this experiment would have to be repeated to confirm this difference and to fully characterise these cells. As these results showed no significant differences in the leukocyte populations in the lungs of D6KO mice, it is not possible to account for the differences seen in metastatic colony numbers. The results from resting lungs were from two mice per group, so it is possible that there may be an increase in certain populations of CD45+ leukocytes in the lungs of D6KO mice, but more mice would be required to detect this difference. Three mice were used for both genotypes in the B16 F10 treated graph, and these results suggest that there are no significant differences in the number of total leukocytes, or specific populations, in the lungs of D6KO mice compared to WT. Although they do suggest that there may be differences in a CD45+ CD11b+CD11c- cells, but this difference is not significant.

5.1.4 Pleura

The data above show a striking difference in the number of colonies developing in D6KO mice, which is more pronounced in the development of external colonies. This difference appears not to be caused by a difference in leukocyte populations within the lung. The major difference in colony development is seen at the surface of the lungs, so it seems there could be two options as to the fate of B16 F10 cells. The cells may enter the lungs and move out to the lung surface, where they can develop into colonies. On the other hand B16 F10 cells could be entering the lungs via the alternative vasculature of the pleura, and forming colonies at the lung surface. This led to the theory that the anatomy of the lungs may be somehow altered in D6KO mice, which causes the difference in colony formation.

The external surface of the lung is covered by a thin serous membrane known as the pleura (see figure 5.6), which is present to help provide lubrication as the lungs expand and contract during inhalation and exhalation (354, 355). There is evidence to suggest

that the pleura may play a role in cancer. In human melanoma, metastasis can occur to the pleura, as well as to the lungs but the two do not always go hand in hand (356). Mesothelioma is a cancer of the pleura, which is often fatal (357). The pleura also has a different blood vasculature and lymphatic supply from the lungs (354). This evidence led to the decision to look at the pleura in WT and D6KO mice, since it is in contact with the external surface of the lungs, which is where the major differences in colony formation are evident. As D6 is known to play a role in the clearance of inflammatory chemokines (see section 1.8.1) it was thought to be possible that the levels of chemokines in the pleura may be altered in D6KO mice, which may be affecting the development of metastatic colonies.

Therefore what could be happening in the lungs is that in WT mice B16 F10 cells enter the lungs via the blood stream, where they can form colonies inside the lungs. Some of these tumour cells can then migrate to the external surface of the lungs, possibly in response to chemokines produced by the pleura, and here they form metastatic colonies. Alternatively, the cells may be entering the lungs via the pleural vasculature, as the vasculature of the pleura is reported to be different to that of the lungs (354), and forming colonies at their point of entry, at the pleural surface. In D6KO mice, the chemokine microenvironment at the pleural surface may be altered, due to the lack of D6 in the lungs. This altered environment may either be undesirable for the growth of B16 F10 cells, and cause cell death, or the B16 F10 cells may migrate out of the lungs via the lymphatic or vasculature drainage of the pleura.

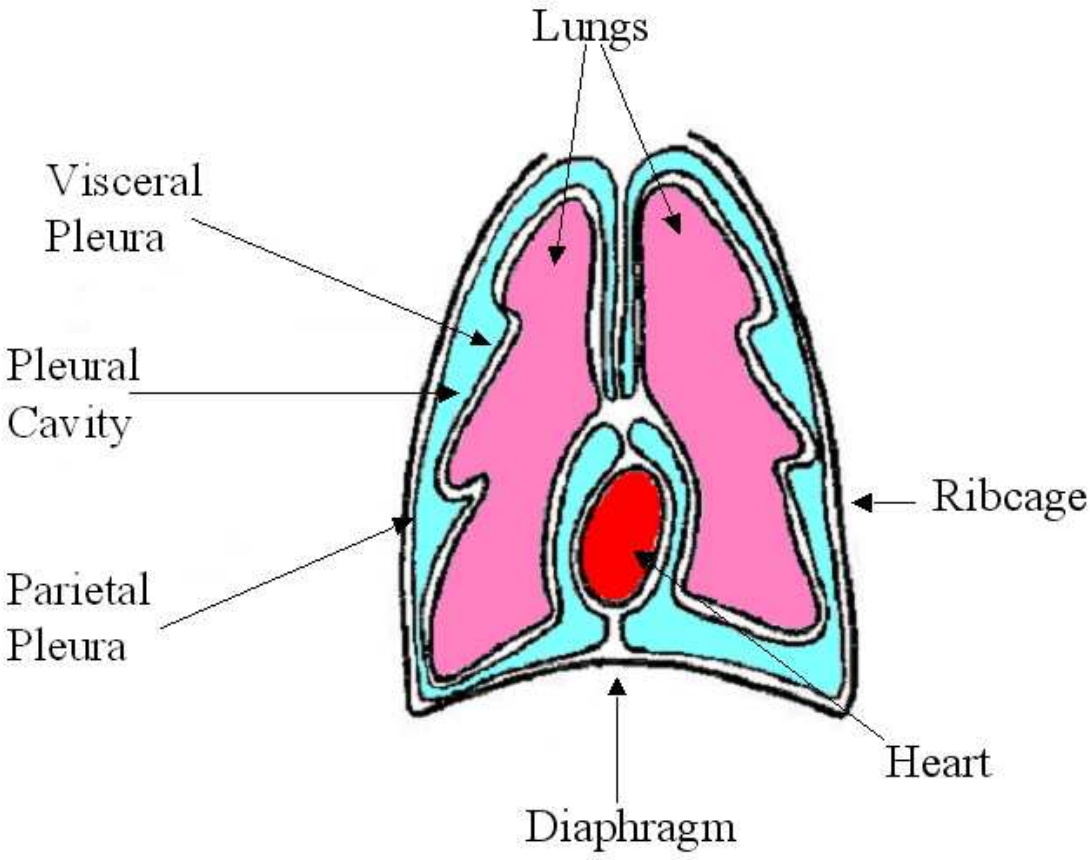

Figure 5-6: The thoracic cavity

The lungs and the heart are surrounded by the pleura, a thin serous membrane which provides lubrication for the lungs during respiration. The pleura is one continuous membrane, but it is referred to as the parietal pleura when covering the ribcage, and the visceral pleura when covering the lungs. The pleural cavity forms between the visceral and the parietal pleura, and contains a small amount of fluid. (Diagram adapted from (354))

When the lungs were removed from mice that had received B16 F10 cells intravenously, the pleura was easy to identify within the thoracic cavity. Unfortunately it tended to shrivel up when the ribcage was opened, which made it very difficult to remove. Numerous attempts were made to isolate the pleura from WT and D6KO mice – both untreated mice and those that received B16 F10 cells - but these repeatedly failed. Metastatic colonies had been noted on the pleura in both WT and D6KO mice, but their number could not be analysed properly, due to problems with trying to remove the pleura, which was very fragile and easily torn.

It was therefore assumed that when the lungs were removed, the visceral pleura (see figure 5.6 and 5.7) remained on the surface of the lungs. Lungs from WT and D6KO mice were removed as before, and snap frozen in liquid nitrogen. The surface of the lungs, where it was assumed the visceral pleura remained, was then scraped off, in the hope that enough tissue could be collected to analyse the expression of chemokines, by RT-PCR. This approach failed due to the small amount of tissue isolated.

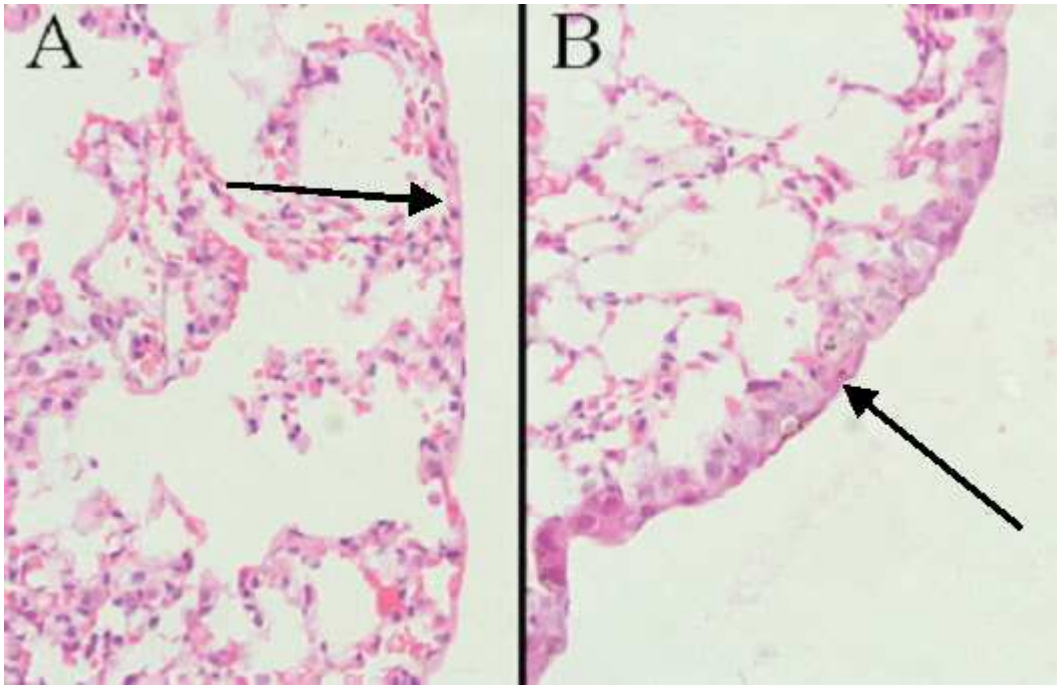

Figure 5-7: H&E stained lung sections showing the location of the pleura

Lung sections from B16 F10 treated mice stained with H&E. The pleura is a thin serous membrane which covers the lungs, which is indicated in these sections. A metastatic colony has developed at the pleural edge of the lungs (B). Pictures were taken at 200x magnification.

As mentioned above, the pleura could be causing differences in the lung microenvironment due to the production of chemokines, which may account for the differences in colony numbers at the external surface of the lungs. As the isolation of the pleura was repeatedly unsuccessful, an alternative approach was taken, to try to analyse the chemokine levels in the space between the lungs and the pleura. This technique involved injecting ~5mls sterile PBS into the pleural cavity (between the ribs, without piercing the lungs) and removing the fluid, which could be analysed for the presence of chemokines and other proteins. Pleural washes were collected successfully and protein concentrations were analysed. These ranged from 0.01mg/ml – 0.36 mg/ml. Since the protein concentrations were low, pleural washes were concentrated (as described in materials and methods, section 2.3.2.1) and the final concentrations ranged from 0.06mg/ml – 1.57 mg/ml. Analysis of chemokine levels was performed using a custom made Luminex kit (11-plex) from Millipore, as described in materials and methods (section 2.3.2.2). Table 5.1 describes the chemokines and cytokines that were analysed using this kit.

Chemokine/Cytokine	Systematic Name	Luminex results
Eotaxin	CCL11	See figure 5.9
TNF-α		See figure 5.9
MCP-1	CCL2	WT F10 sample alone
RANTES	CCL5	WT F10 sample alone
MIG	CXCL9	WT F10 sample alone
MIP-1α	CCL3	Out of range (too low)
MIP-1β	CCL4	Out of range (too low)
KC	CXCL1	Out of range (too low)
MIP-2	CXCL2	Out of range (too low)
IP-10	CXCL10	Out of range (too low)
IL-17		Out of range (too low)

Table 5-1: Chemokines and cytokines analysed in pleural washes.

A summary of the chemokines and cytokines which were analysed by Luminex, in pleural washes from untreated and B16 F10 treated WT and D6KO mice. Chemokines and cytokines could not be analysed in all samples, those that could be detected are indicated.

For the majority of chemokines tested, the levels in pleural wash samples were too low to be detected. The only analytes that were detectable in all samples were CCL11 and TNF-α. The results for these two analytes are shown in figure 5.9. The results for CCL11 (graph A) show that there appears to be a trend towards a reduction in CCL11 in D6KO mice – untreated WT had a mean CCL11 concentration of 9.9 (+/- 17.15) pg/ml compared to untreated D6KO which had a mean CCL11 concentration of 21.67 pg/ml (+/- 5.5). This difference is not significant, p = 0.04358, Students unpaired t test. Examination of mice that received B16 F10 cells showed WT mice to have a mean CCL11 concentration of 33.46 pg/ml (+/-23.4) compared to 17.8 pg/ml (+/- 16.1) in D6KO mice that received B16 F10 cells. Again, these values were not statistically significant (p = 0.3939 students unpaired t test).

Untreated WT mice had a mean TNFα concentration of 0.633 pg/ml (+/- 0.756) compared to D6KO mice, which had a mean TNFα concentration of 0.58 pg/ml (+/-0.39). The results (shown in graph B of figure 5.8) from mice that received B16 F10 cells are again at the low end of detection – WT plus B16 F10 cells had a mean TNFα concentration of 0.44 pg/ml (+/-0.43), whilst D6KO mice that received B16 F10 cells had a mean TNFα concentration of 0.07 pg/ml (+/- 0.075). These results for TNFα suggest that D6KO mice that received B16 F10 melanoma cells have a reduction in TNFα in the pleural cavity, however these values are not statistically significant (p=0.2102 students unpaired t test). As so few samples gave a positive result, a difference in pleural chemokine levels in D6KO mice, and

their effects on metastatic colony formation, is difficult to rule out. Increased sample numbers are required to provide statistical significance.

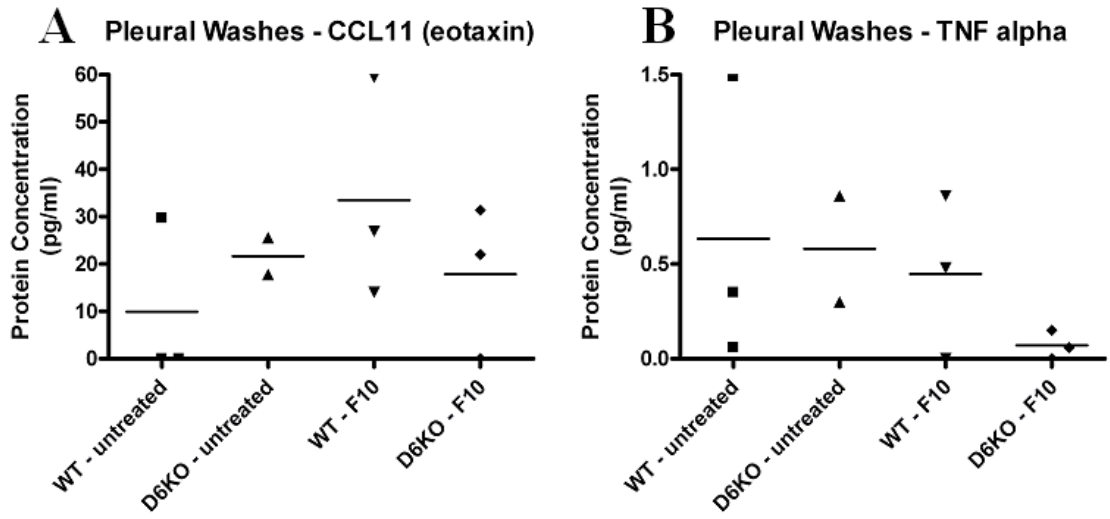

Figure 5-8: Chemokines and cytokines detected in pleural washes from untreated and B16 F10 treated D6KO and WT mice

The only two analytes which could be detected in pleural wash samples were CCL11 and TNFα, but not in all pleural wash samples. A – CCL11 levels detected in pleural washes from untreated WT and D6KO mice, and B16 F10 treated WT and D6KO mice. n = 3 per group, 2 per group in D6KO untreated. NS – Students unpaired t test. B – TNFα levels detected in pleural wash samples. NS Students unpaired t test. Both CCL11 and TNFα levels were at the lower limits of the detection system.

Looking at other chemokines analysed by Luminex, the only samples that gave a positive result for the majority of analytes were from two WT mice that had received B16 F10 cells. These samples were positive for CCL2, CCL5, CXCL9 (data not shown), CCL11 and TNFα. These results suggest that in WT mice that receive B16 F10 cells there may be an increased inflammatory microenvironment in the pleural cavity, which is missing in D6KO mice. This increased inflammatory microenvironment may be beneficial for B16 F10 cell growth, and may account for the increased colony number on the surface of the lungs. This result is unexpected, as a lack of D6 has been shown to increase the inflammatory microenvironment in a variety of in vivo models (152, 157). These results are from two separate mice, and may suggest that after injection of B16 F10 cells, WT mice have increased levels of inflammatory chemokines in the pleural cavity, which may contribute to the differences seen in metastatic colony numbers.

To summarise, the role of the pleura in the development of metastatic colonies cannot be ruled out. Isolation of the pleura proved difficult for both WT and D6KO mice. Analysis of the chemokine levels in the pleural cavity could not be performed fully, as the levels of majority of chemokines were too low to detect. The only analytes that could be detected

were TNFα and CCL11, with no significant differences between genotypes and no differences with the addition of B16 F10 cells. Samples from WT mice that received B16 F10 cells were found to have CCL2, CCL5, CXCL9, CCL11 and TNFα, which may suggest that WT mice receiving B16 F10 cells have higher levels of inflammatory chemokines than D6KO mice, but this was only on two samples. The experiment would need to be repeated in order to confirm this hypothesis.

5.1.5 Immunohistochemistry

The data shown previously demonstrated that D6KO mice have a significant reduction in external metastatic colony number on the lungs compared to WT mice. This difference is not caused by any alterations in leukocyte abundance, and the evidence shown in section 5.1.4 suggests that differences in pleural chemokine concentration may not be responsible for this difference. When B16 F10 cells are administered, they are injected into the tail vein, and so they must use the vasculature to get to the lungs. Once in the lungs, what could be happening is B16 F10 cells move to the external surface of the lungs, where the majority of colonies form. Alternatively B16 F10 cells may be using the vasculature of the pleura to reach the lungs surface where they can form colonies. Within the lungs, B16 F10 cells may be interacting with leukocytes in the lung tissue, which may alter the lung microenvironment to encourage or discourage colony growth, or even promote B16 F10 cell survival or death.

Analysis of the leukocyte populations of the lungs showed that there were no significant differences in total leukocyte populations within the lungs. As the metastatic colonies differ in their location within the lungs, the location of leukocyte populations within the lungs was analysed using immunohistochemistry. T cells and macrophages were analysed, as both cell populations are known to play roles in tumour development and metastasis (see section 1.10 and 1.11). To determine if differences in the vasculature or lymphatic vessels of the lungs may be responsible for the differences seen in colony number, immunohistochemistry and immunofluorescence was performed to stain blood vessels and lymphatic vessels. These results are presented below.

5.1.5.1 Macrophage Staining

Macrophages can have a role in metastasis by secreting growth factors that can help to create the pre-metastatic niche, as described in section 1.11.1.3. It was decided to stain lung sections for macrophages to determine if a difference in macrophage number or location could be responsible for the differences in metastatic colony numbers. Mac-2 immunohistochemistry was carried out as described in materials and methods (section 2.4.5.3), on lung sections from WT and D6KO mice that had received B16 F10 melanoma cells.

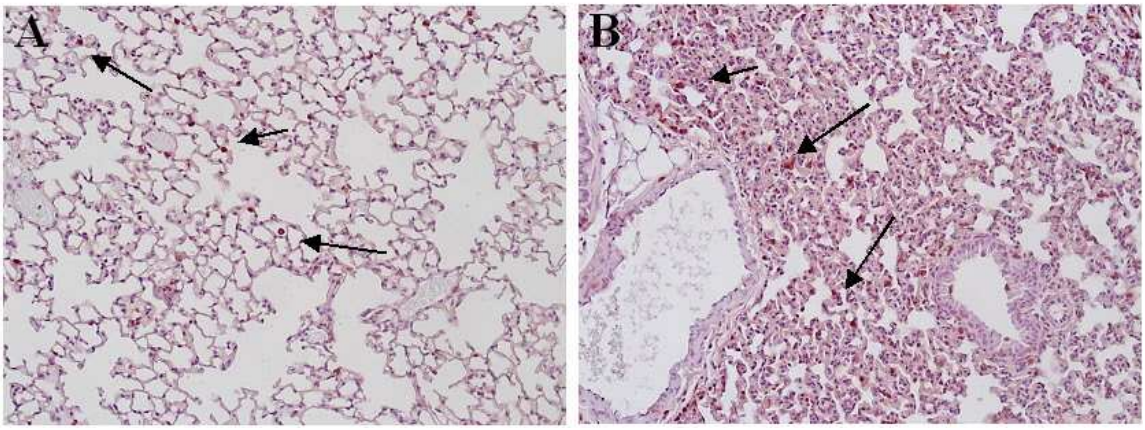

Figure 5-9: Identification of macrophages in lungs of B16 F10 treated mice

Lung sections from B16 F10 treated WT and D6KO C57Bl/6 mice were processed for histological analysis and stained with an antibody against Mac-2 to identify macrophages. A – positive cells in a lung section from a WT mouse. B – Positive cells highlighted in a lung section from a D6KO mouse. Images are taken at 400x magnification

Figure 5.9 shows representative staining from both WT and D6KO mice. These sections show red stained macrophages present within the lung tissue in WT and D6KO mice and this positive staining was distributed throughout the lungs in both genotypes. Mac-2 positive cells could be found surrounding and within metastatic colonies, as well as being present along the pleural edge of the lungs. Quantitative analysis of staining was performed by counting the total number of macrophages within the lung tissue, in a minimum of eight random fields, at 200x magnification. Counting the number of positive cells at the pleural edge, and measuring the distance around the lungs was separately carried out to measure the number of macrophages present at the pleura. Macrophages were counted at the pleural edge in order to try and determine if any differences in cell populations at the pleural surface could be accounting for the differences in metastatic colony development. These results were expressed as the average cell number per μm.

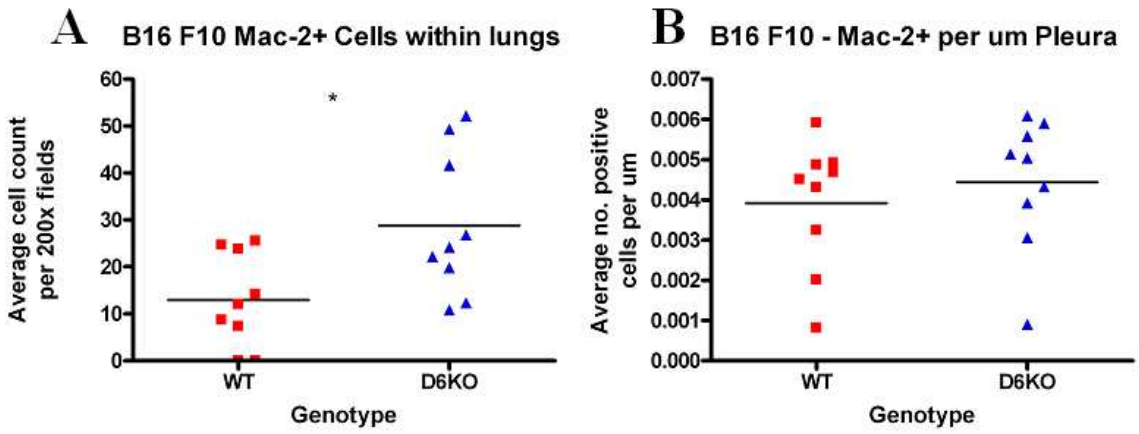

Figure 5-10: Analysis of macrophage staining of B16 F10 treated lungs

A- Mac-2 positive cells were counted in lung sections from B16 F10 treated mice, in at least 8 random fields at 200x magnification. Results are expressed as the average number of cells per 200x field, n = 9 per group, p = 0.0190, students unpaired t test. B – Positive cells were counted at the pleural edge, and are expressed as the number of positive cells per µm of pleura (measured using Axiovision software). NS, Students unpaired t test, n = 9 per group. Results are from 3 separate experiments.

The results in graph A of figure 5.10 show that there was an increase in macrophage numbers in the lungs of D6KO mice, that received B16 F10 cells, compared to WT mice. WT mice had an average of 12.9 (+/- 10.005) Mac-2 positive cells within the lungs, compared to 28.81 (+/- 15.31) Mac-2 positive cells in D6KO lungs. This difference is statistically significant (p=0190, Students unpaired t test). The number of macrophages at the pleural edge (shown in graph B of figure 5.10) in B16 F10 treated mice remained at similar numbers in WT and D6KO mice (WT mice had an average of 0.0039 (+/-0.0016) positive cells compared to 0.0044 (+/-0.0016) positive cells in D6KO lungs, p = 0.5070 Students unpaired t test). From these results, it can be concluded that the difference in the number of metastatic colonies in WT and D6KO mice may be due to an increased number of macrophages in D6KO lungs.

5.1.5.2 T cell Staining

Many leukocyte populations are known to play a role in metastasis (see section 1.11). With respect to the B16 F10 metastasis model, T cells have been shown to influence the development of metastatic colonies. They may do this by interacting with B16 F10 cells in the blood or within the lungs during colonisation (286, 315). Lung sections from both WT and D6KO mice were stained for CD3 to identify T cells. This was carried out to determine if alterations in the numbers of T cells, or their location may correlate with the development of metastatic colonies. The staining was performed as described in materials and methods (section 2.4.5.5). Representative images are shown in figure 5.11,

picture A and B from WT lungs, picture C and D from D6KO lungs. CD3+ cells were distributed throughout the lung tissue, and at the pleural edge of the lungs. When metastatic colonies were visualised, CD3+ cells could be found bordering the edges of the colonies as well as being inside the metastatic colonies. Quantitative analysis of this staining was performed by counting the number of T cells within metastatic colonies, counting positive cells bordering metastatic colonies as well as positive cells per µm of pleura.

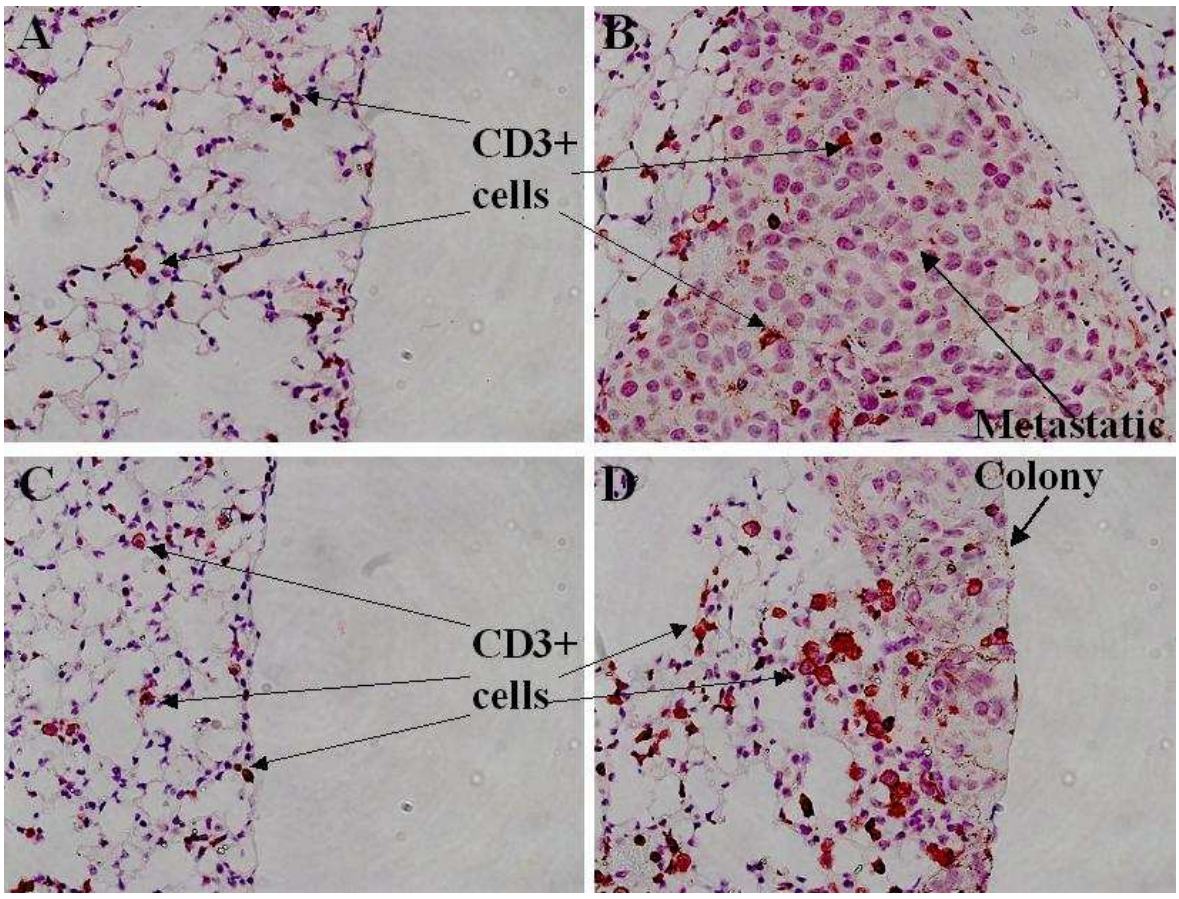

Figure 5-11: Identification of T cells in the lungs from B16 F10 treated mice

T cells were identified in lung sections from B16 F10 treated WT and D6KO mice using an antibody specific for CD3. Positive cells could be identified throughout the lungs, at the pleural edge (picture A – WT mouse, picture C – D6KO mouse) and within metastatic colonies (picture B – WT mouse, picture D – D6KO mouse). Images are representative of 3 experiments, taken at 400x magnification.

The results of CD3+ cell analysis are shown in figure 5.12. The number of CD3+ cells bordering metastatic colonies was similar in WT and D6KO mice, this data is shown in graph A (mean CD3+ cell number – WT = 8.6 (+/-3.57), D6KO = 7 (+/- 7)). Graph B in figure 5.12 shows the average number of CD3+ cells per µm of pleura, which was 0.006 cells (+/- 0.0026) for WT mice, and 0.0056 cells (+/- 0.0033) for D6KO mice. This difference was not significant ($p = 0.7444$ Students unpaired t test). The number of CD3+

cells within metastatic colonies was quantified; WT mice had an average of 10.89 (+/- 10.11) positive cells, whilst D6KO mice had on average 7.17 (+/- 9.57) positive cells. These data are shown in graph C and show that there is no significant difference between the numbers of CD3+ cells within metastatic colonies when comparing WT to D6KO mice (p = 0.4343 Students unpaired t test). These results show that the distribution and number of T cells is unlikely to be responsible for the difference seen in the number of metastatic colonies, comparing D6KO mice to WT mice.

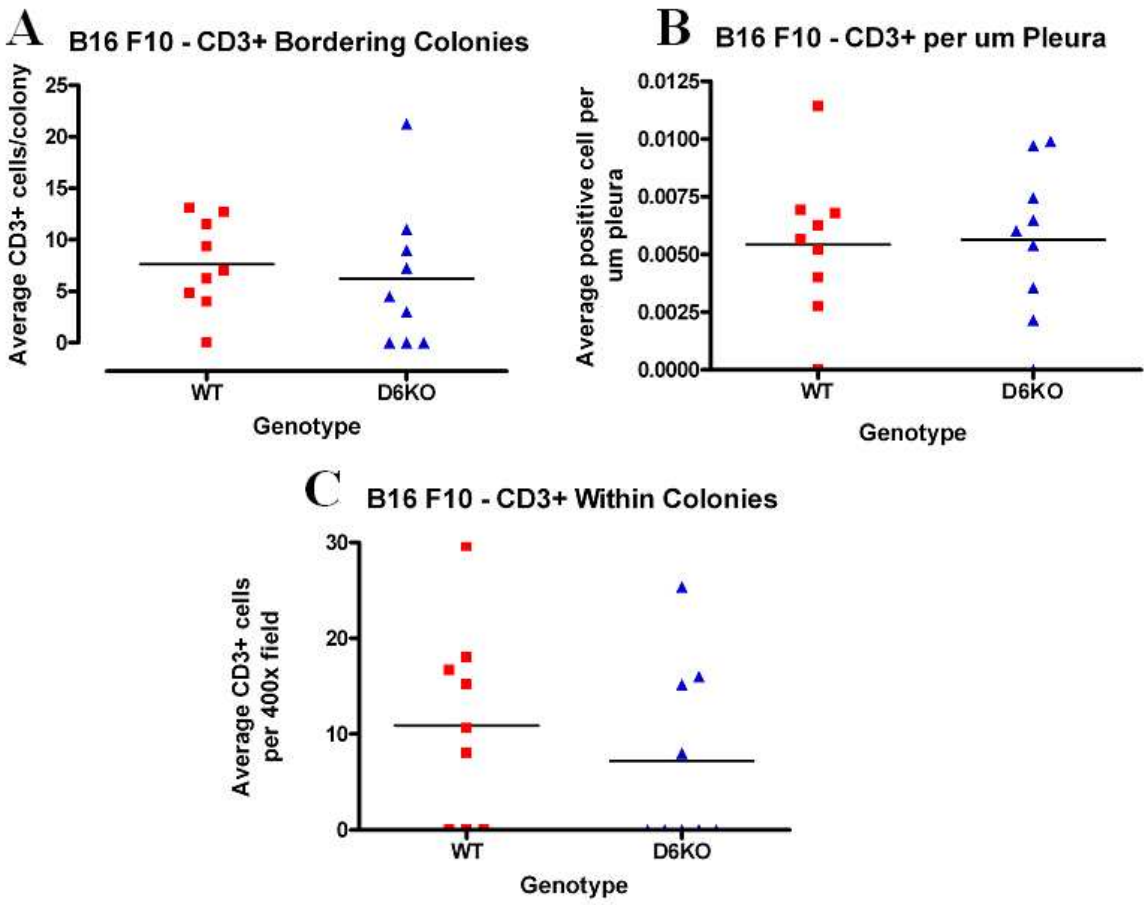

Figure 5-12: Analysis of T cell staining of B16 F10 lung sections

T cells were identified using an antibody against CD3; these were present at the edges of metastatic colonies, at the pleural edge and bordering metastatic colonies. A – CD3+ cells were identified at the edge of metastatic colonies, in both WT and D6KO B16 F10 treated mice. These cells were counted at 400x magnification and are expressed as the number of positive cells per metastatic colony. B –CD3+ cells were counted at the pleural edge of lung sections and are expressed as the number of positive cells per µm pleura, 400x magnification. C – CD3+ cells were counted within metastatic colonies, in at least 8 random 400x fields. These results are expressed as the average number of cells per 400x field. Results are pooled from 3 separate experiments, n = 9 per genotype, NS – Students unpaired t test.

To summarise, analysis of macrophage and T cell staining in the lungs of WT and D6KO mice that received B16 F10 cells shows that there are no significant differences in either absolute cell numbers or in their location with respect to metastatic colonies. These data suggest that it is unlikely that T cells are contributing to the differences seen in metastatic

colony number, but it is possible that the increased macrophage number within the lungs of D6KO mice may be responsible for the reduction in metastatic colonies.

5.1.5.3 Blood Vessel Staining

B16 F10 cells are injected intravenously, so the circulation plays a vital role in allowing these cells to reach the lungs. Since the blood vessel supply to the lungs is required in order for metastatic colonies to develop in the lungs, it may be possible that differences in blood vessel number and/or location may differ comparing WT to D6KO lungs, and these differences may account for the differences in metastatic colony formation. In order to try to examine this, vWF staining, which identifies blood vessels, was performed on lung sections (materials and methods section 2.4.5.1). Figure 5.13 shows representative vWF stained lung sections. Blood vessels were present throughout lung sections, as shown by vWF positive staining, as well as the presence of red blood cells and leukocytes within the vessels. Blood vessels could be found close to metastatic colonies and within metastatic colonies, in both WT and D6KO lungs. The size of blood vessels within the lungs did not appear to differ between WT and D6KO lungs (data not shown).

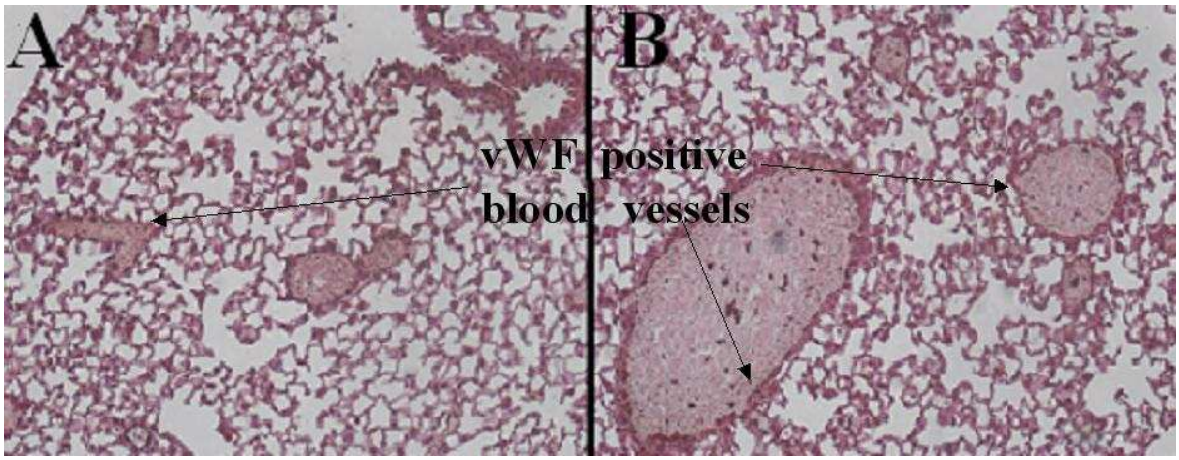

Figure 5-13: Identification of blood vessels in lungs from WT and D6KO B16 F10 treated mice

Blood vessels were stained using an antibody against vWF in lung sections from B16 F10 treated mice. Images shown are at 200x magnification and are representative of both WT (picture A) and D6KO (picture B) lungs.

This staining was analysed by counting the total number of positive vessels per lung section for each experiment, these results are shown in graph A of figure 5.14. WT mice that had received B16 F10 cells had an average of 59.28 (+/-22.89) vWF positive vessels throughout lung sections, compared to 58 (+/- 28.06) vWF positive vessels present in D6KO lungs that had received B16 F10 cells. These data show that there is no significant

difference between the numbers of vWF positive vessels in B16 F10 treated WT and D6KO lungs ($p = 0.9170$ Students unpaired t test).

The distance between positive vessels and metastatic colonies was measured, to determine if there was a correlation between blood vessel proximity and number of metastatic colonies. These results are shown in graph B, figure 5.14. WT mice had an average distance of 146.13 µm (+/-72.44) between vWF positive blood vessels and metastatic colonies. D6KO mice had an average distance of 94.78 µm (+/- 111.99) between vWF positive vessels and metastatic colonies. This difference is not statistically significant ($p = 0.2651$ Students unpaired t test). The proximity of blood vessels to the pleura was also analysed to determine if blood vessels were closer to the pleura in WT mice, which may contribute to the increased colony numbers on the surface of the lungs. These results are shown in graph C, figure 5.14. The average distance between vWF vessels and the pleura was 209.27 µm (+/-56.3) in WT lungs and 211.39 µm (+/-26.84) in D6KO lungs. These data show that there is no significant difference in the distance between blood vessels and the pleura in D6KO lungs, compared to WT ($p = 0.92$ Students unpaired t test).

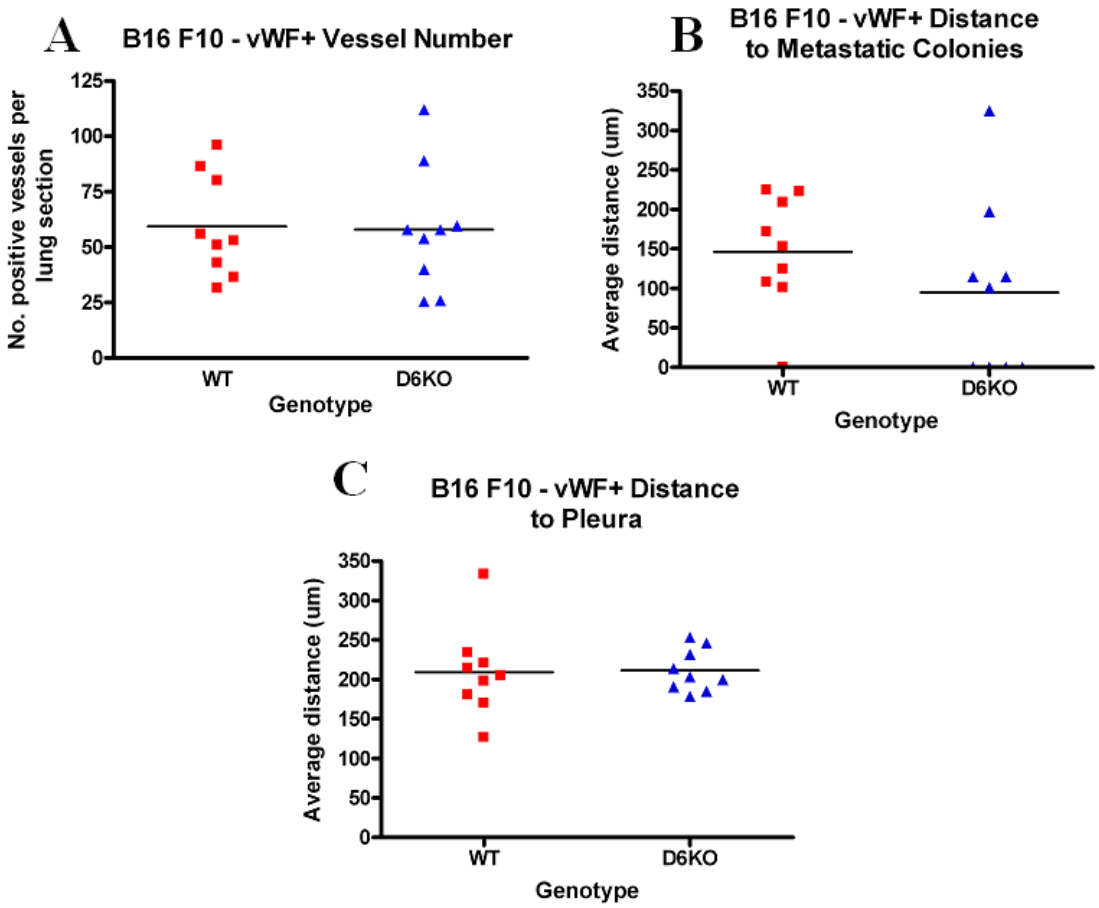

Figure 5-14: Analysis of vWF staining of B16 F10 treated lungs

Blood vessels were identified using an antibody against vWF. A – the total number of positive vessels were counted throughout lung sections from WT and D6KO B16 F10 treated mice, at 200x magnification, and are expressed as the total number of positive vessels per section. B – the distance between vWF positive vessels and metastatic colonies was measured at 200x magnification using Axiovision software, results are expressed in µm. C- the distance between positive vessels and the pleura was measured using Axiovision software. Results are pooled from 3 experiments, n = 9 per group, NS – Students unpaired t test.

Taken together, these results show that in WT and D6KO mice, there is no difference in the location of blood vessels with respect to metastatic colonies or the pleura. Although it appears that in D6KO mice there is a slight reduction in the number of vWF vessels, this difference is not significant. These data suggest that differences in blood vessel number or location are unlikely to be responsible for the differences seen in colony numbers.

5.1.5.4 Lymphatic Vessel Staining

Lymphatics are also known to play a role in metastasis. D6 expression has been demonstrated in the lung in mice, and shown to be expressed by lymphatic endothelial cells in humans (143). Whilst D6 expression has not been demonstrated on murine cells, two recent studies looking at D6 in models of colitis, have attributed differences in colitis

susceptibility to non-haematopoeitic cells in the gut, and suggested these may be lymphatic cells (158, 159). Whilst B16 F10 cells use blood vessels to get into the lungs, lymphatics may be responsible for the clearance of these cells. Once B16 F10 cells enter the lungs, they may migrate through the lung tissue and leave via lymphatic drainage of either the lungs or the pleura. It is at this point that differences between WT and D6KO mice may account for the differences in metastatic colony number. In order to try and address this theory, lung sections from WT and D6KO mice that received B16 F10 cells were stained for LYVE-1 to identify lymphatic vessels.

Lymphatic vessels within the lungs were stained using an antibody against LYVE-1, as described previously (materials and methods section 2.4.5.2). Staining was initially performed using streptavidin coupled HRP, followed by DAB as the HRP substrate on paraffin embedded lungs, (see figure 5.15, picture A and B) but this protocol could not be easily reproduced on sections from all experiments. The protocol was altered (see materials and methods section 2.4.5.2), to use a fluorescent secondary and counter stain (streptavidin coupled to Cy5, with DAPI). This fluorescent protocol could be used to analyse lymphatics on paraffin embedded lung sections that could not be stained with the DAB protocol. Pictures A and B show lung sections from WT and D6KO mice, which have been stained using LYVE-1 with DAB as the HRP substrate. Brown coloured vessels can clearly be seen throughout the lung tissue. Pictures C and D (figure 5.15) show lung sections from WT and D6KO mice that have been stained with LYVE-1 using streptavidin coupled Cy-5 as the HRP substrate. Positive vessels are shown with a pink outline, and again were present throughout the lung tissue. Lymphatics could be identified close to metastatic colonies, but no lymphatic vessels could be identified within metastatic colonies.

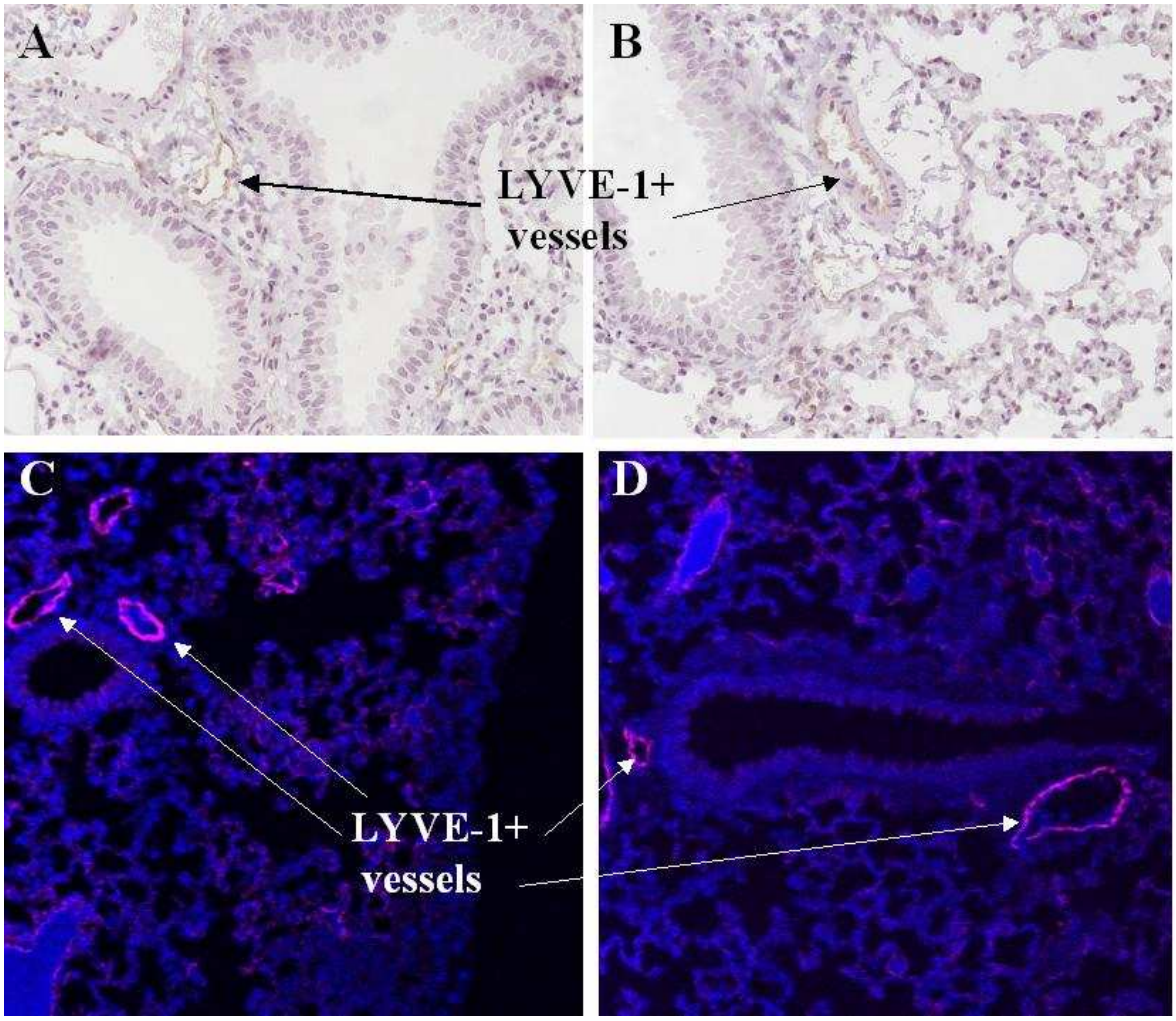

Figure 5-15: Identification of lymphatic vessels in lungs from B16 F10 treated mice

Initially an immunohistochemical protocol was used to stain lung sections from WT and D6KO B16 F10 treated mice, picture A – LYVE-1 positive vessel in WT lung section, picture B – LYVE-1 positive vessel in D6KO lung section (200x magnification). The protocol was altered as subsequent staining attempts were unsuccessful. Immunofluorescent staining of lymphatic vessels in lungs from D6KO B16 F10 treated lungs (picture C) and WT B16 F10 treated lungs (picture D). 200x magnification. Images are representative of 3 separate experiments.

The analysis of LYVE-1 staining was performed by counting the number of positive vessels in stained tissue sections. Lungs from WT mice had on average 75.17 (+/-13.32) LYVE-1 positive vessels whilst D6KO lungs had on average 77 (+/-21.62) LYVE-1 positive vessels. The results shown in figure 5.16 (graph A) show there was no significant difference in the total number of LYVE-1+ vessels comparing D6KO mice to WT mice. The size of LYVE-1 vessels was measured using the Axiovision software, as it appeared there was a visual difference in the cross-sectional area of lymphatic vessels, comparing WT to D6KO lungs. LYVE-1 positive vessels in WT lungs had an average diameter of 108.4 µm (+/- 28.98), and LYVE-1 positive vessels in D6KO lungs had an average diameter of 119.37 µm (+/- 38.12). These results are shown in figure 5.16 (graph B) and illustrate that there was no

significant difference in the size of the lymphatics comparing D6KO and WT lungs (p = 0.5017 Students unpaired t test).

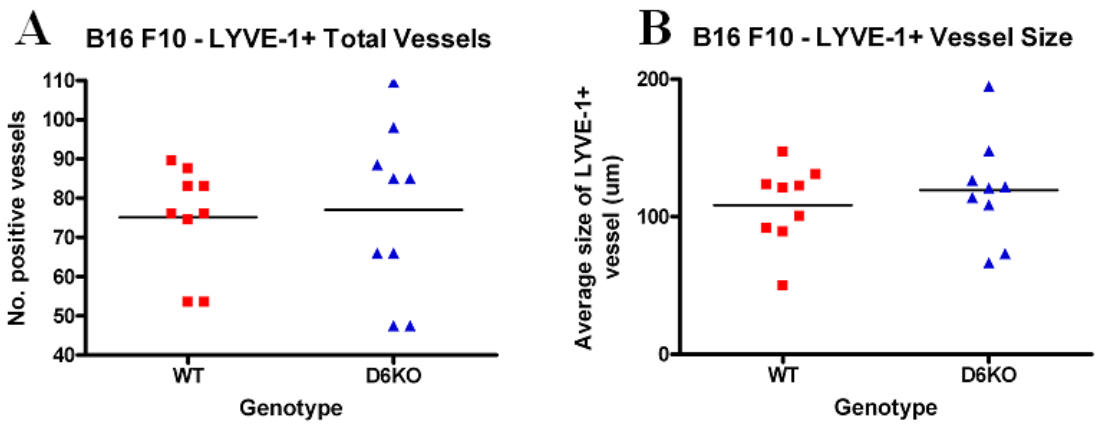

Figure 5-16: Analysis of lymphatic vessel staining in B16 F10 treated lung sections

The number of positive vessels were counted in entire lung sections from WT and D6KO B16 F10 treated mice, at 200x magnification. A – total numbers of positive vessels throughout lung sections. B – the size of LYVE-1 positive vessels were measured using Axiovision software and these results are expressed as the average diameter per lung section. Results are pooled from 3 experiments, n = 9 per group, NS – students unpaired t test.

As with vWF staining, the distance of LYVE-1+ vessels from metastatic colonies and the pleura was measured using the Axiovision software. Looking at the distance from LYVE-1 positive vessels to metastatic colonies, WT mice had an average distance of 102.8 µm (+/- 68.37) and D6KO mice had an average distance of 17.16 µm (+/- 35.74). These results are shown in graph A of figure 5.17, and show that there is a significant difference in the distance between LYVE-1 positive vessels and metastatic colonies, with WT mice having a greater distance between the two (p = 0.0042 Students unpaired t test). The distance between LYVE-1 positive vessels and the pleura was also measured; WT mice had a mean distance of 169.38 µm (+/- 24.09) and D6KO mice had a mean distance of 150.62 µm (+/- 28.22). This difference was not significant (p = 0.1488 Students unpaired t test). These results are shown in graph B of figure 5.17. It may be possible that the difference in the location of the lymphatics, with respect to metastatic colonies, may contribute to the difference in the number of metastatic colonies.

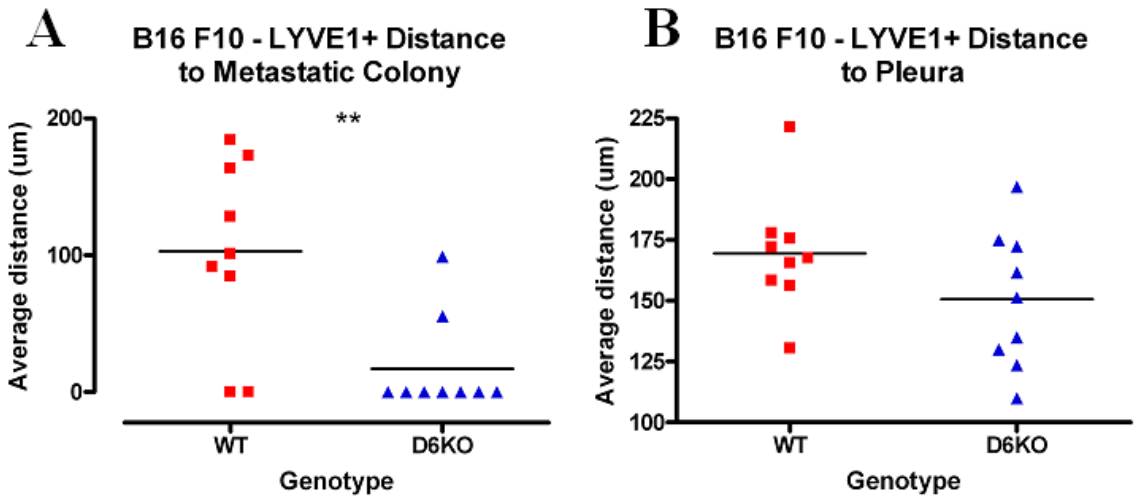

Figure 5-17: Distances of LYVE-1 positive vessels to metastatic colonies and the pleura

A- The distance between LYVE-1 positive vessels and metastatic colonies was measured using Axiovision software, throughout lung sections of WT and D6KO B16 F10 treated mice. Results are expressed as the average distance in µm. P= 0.0042, Students unpaired t test. B- the distance between LYVE-1 positive vessels and the pleura was measured using the Axiovision software throughout lung sections of WT and D6KO B16 F10 treated mice. NS (Students unpaired t test) Results are pooled from 3 separate experiments, n = 9 per group.

5.1.5.5 Summary

To summarise, there are no significant differences between the number and location of T cells within the lungs of WT and D6KO mice that received B16 F10 cells. Looking at macrophages, there is a significant increase in the number of macrophages within the lungs of D6KO mice, compared to WT mice, suggesting that the number of macrophages may be contributing to the development of metastatic colonies. These data suggest that differences in T cell number or location are unlikely to be responsible for the differences seen in metastatic colony numbers. Analysis of blood vessel number and location show that there are no significant differences between WT and D6KO lungs. Looking at lymphatic vessels, again there are no significant differences between the number and the size of lymphatic vessels comparing D6KO to WT lungs. However, when the distances between lymphatic vessels and metastatic colonies were measured, D6KO lungs were found to have lymphatic vessels significantly closer to metastatic colonies than WT lungs. There were no significant differences in the distance between lymphatic vessels and the pleura, comparing D6KO lungs to WT lungs. In conclusion, it is unlikely that the number or location of blood vessels is responsible for the difference in metastatic colonies. The number and size of lymphatics is also unlikely to be responsible for this effect. It is possible that the distance between lymphatics and metastatic colonies may play a role in the differences in colony number. In D6KO mice, lymphatics are significantly closer, which

may mean that when B16 F10 cells are in the lungs of D6KO mice, rather than forming colonies, they are leaving the lungs via lymphatics, which leads to the reduction seen in colony numbers in D6KO mice.

5.1.6 B16 F10 Chemokine Receptors

Results shown above demonstrate that there is a clear difference in the number of surface colonies on the lungs of WT and D6KO mice, which is unlikely to be attributed to differences in T cell, macrophage, and blood vessel number or location. As mentioned above, it is possible that the location of lymphatics plays a role in the differences in metastatic colony number. As there were no major differences in the structure of the lungs, it was decided to investigate this further by examining how B16 F10 cells get to the lungs. B16 F10 cells have been selected to specifically colonise the lungs, possibly due to the lungs being the first capillary bed they encounter (308), but this lung colonisation may be specific, and may be related to chemokine receptor expression. In order to try to address this, the chemokine receptor profile of B16 F10 cells was analysed.

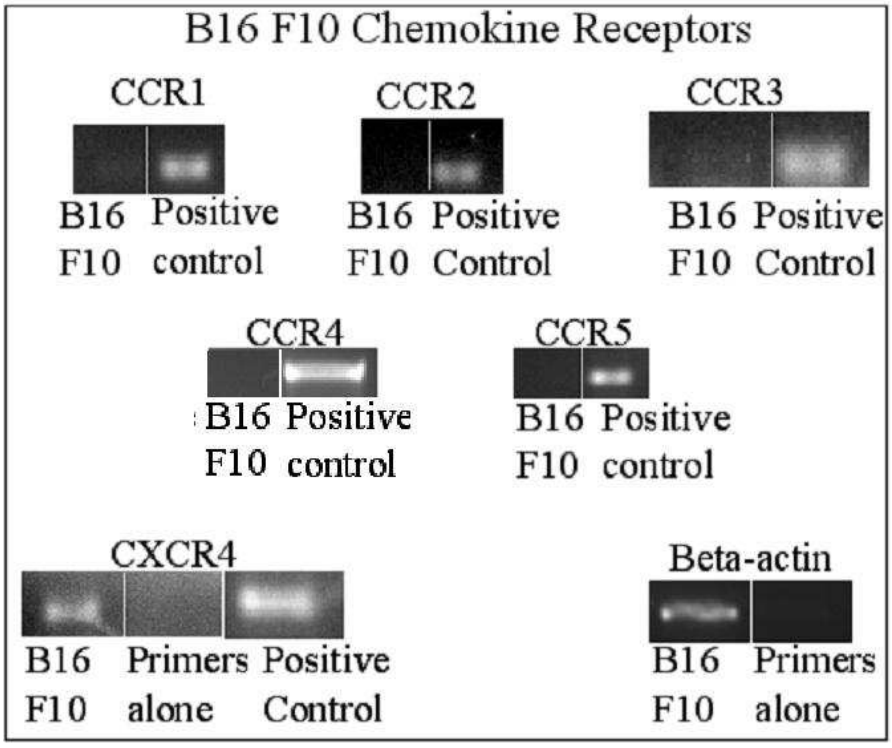

Figure 5-18: Chemokine receptor expression by B16 F10 cells

Chemokine receptor expression of B16 F10 cells was analysed by isolating RNA from cultured cells and performing RT-PCR, as described in materials and methods.

Chemokine receptor expression analysis was performed using RT-PCR as described previously (materials and methods section 2.5). The results in figure 5.18 show the RT-

PCR analysis of chemokine receptors expressed by B16 F10 cells. These data show that B16 F10 cells do not express CCR 1-5, but they are CXCR4 positive. The positive control here was a mixture of murine lung, spleen, liver and skin cDNA. The only chemokine receptor that was detected on B16 F10 cells was CXCR4, so these cells may potentially use CXCR4 to get to the lungs.

5.1.6.1 AMD3100

As shown above, CXCR4 is the only chemokine receptor shown to be expressed by B16 F10 cells. As CXCR4 is known to play a role in metastasis to the lungs when over-expressed by B16 F10 cells and in human melanoma, (292, 332, 337) it is possible that CXCR4 expressed on these cells could be responsible for their specific colonisation of the lungs. If this is the case then CXCR4 may be involved in the initial colonisation of the lungs, and D6 may act at a later stage of metastatic colony development.

AMD 3100 was originally discovered as an impurity in cyclam samples and was named as the bicyclam JM3100. It was found to block the entry of HIV into cells. AMD3100 (AnorMed) specifically interacts with CXCR4, and inhibits the signal transduction downstream of CXCL12 binding CXCR4. Trials with HIV patients led to the discovery that AMD3100 can mobilise CD34+ stem cells, and has a potential role in cancer (335). AMD3100 is a specific reversible antagonist of CXCR4 and is licensed for use in stem cell mobilisation in humans (Plerixafor).

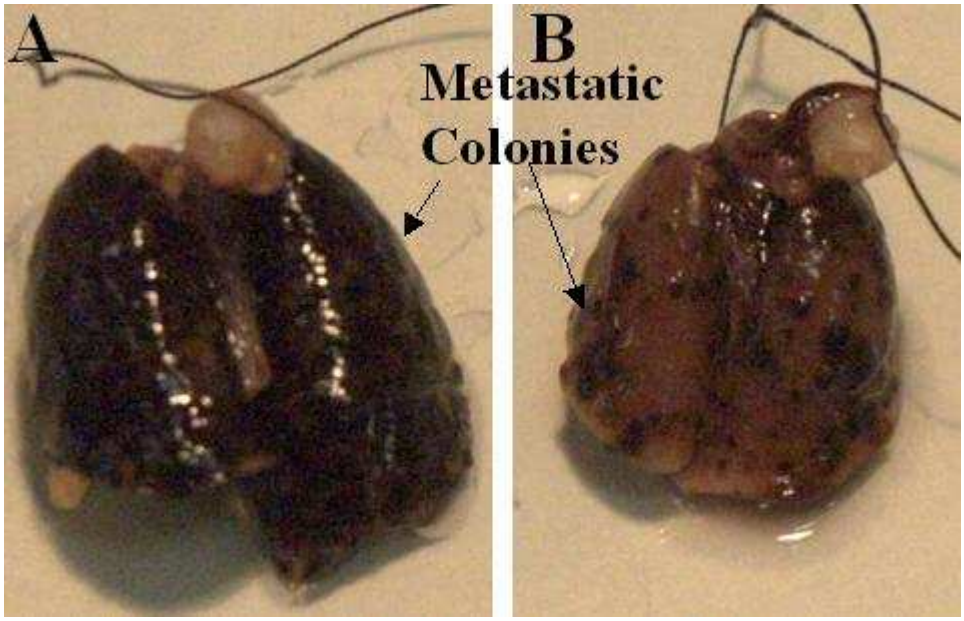

Figure 5-19: Metastatic colonies on lungs from WT C57Bl/6 mice that received B16 F10 cells followed by treatment with AMD3100

Picture A shows lungs from control mice that received B16 F10 cells followed by daily PBS injections for 14 days. Picture B shows lungs from mice that received B16 F10 cells followed by daily injections of AMD3100 for 14 days.

An experiment was designed in which mice received B16 F10 cells intravenously, as previously described (materials and methods section 2.3.2.3), but were treated with twice daily doses of AMD3100, in order to try and block B16 F10 cell movement to the lungs. If CXCR4 was essential in this colonisation, then AMD3100 should prevent metastasis formation in the lungs. Figure 5.19 shows the lungs taken from control and AMD3100 treated mice. There are visibly more colonies present on the surface of control lungs than lungs taken from AMD3100 treated mice. Lungs were processed for histology as described previously (materials and methods section 2.3.2) – internal metastatic colonies were counted on H&E stained serial lung sections. Representative sections are shown in figure 5.20. These images show whole lung sections taken from control and AMD3100 treated mice. Picture A shows lungs from a control mouse, with metastatic colonies identified, these are present throughout the lung tissue and external colonies can be seen at the edges of the section. Picture B shows a lung section from an AMD3100 treated mouse, with fewer internal and external metastatic colonies visible.

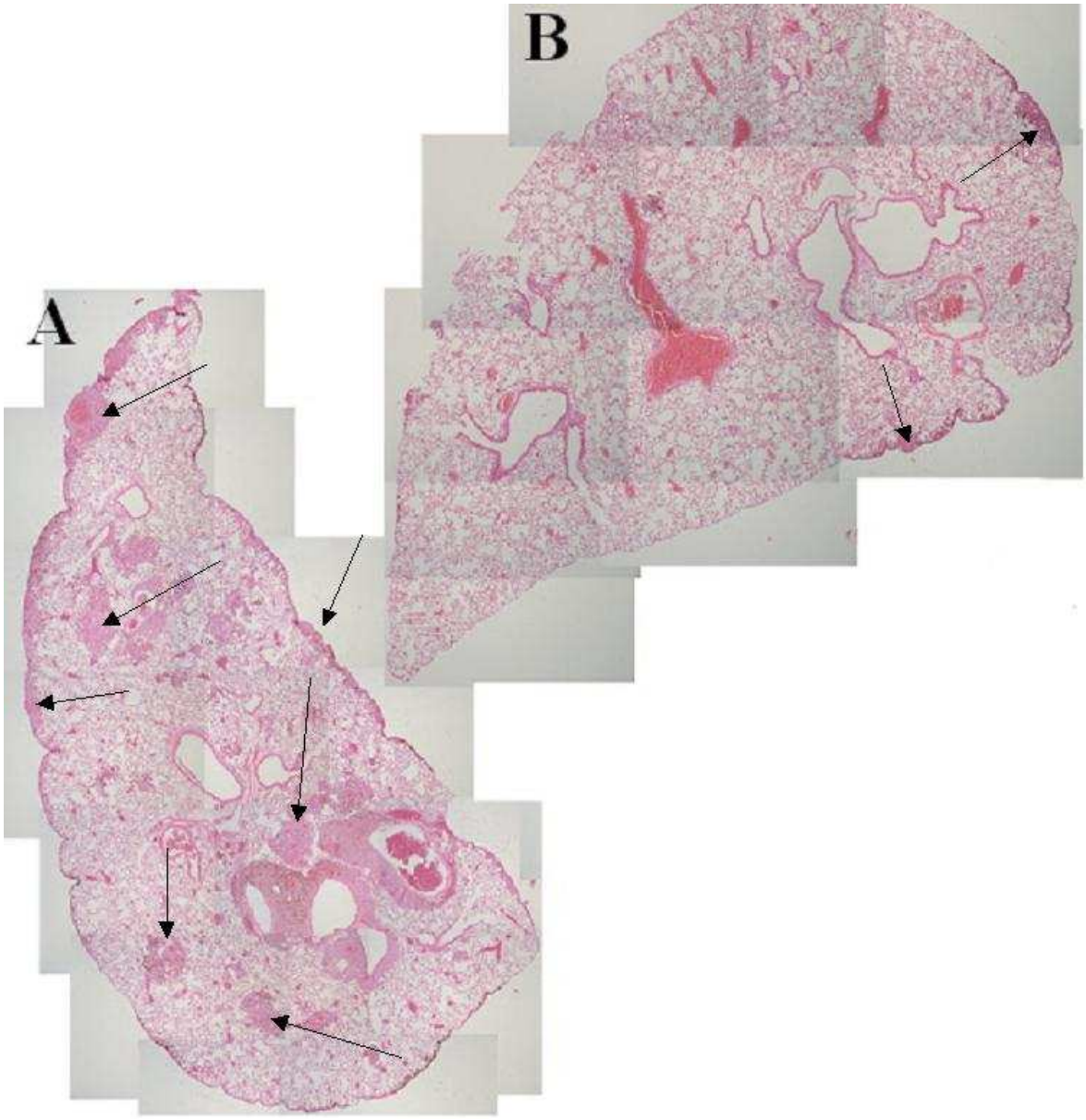

Figure 5-20: H&E stained lung sections from WT mice treated with B16 F10 cells and AMD3100.

Lungs from both control (picture A) and AMD3100 treated (picture B) WT mice that received B16 F10 cells were processed for histology and stained with H&E. Images were taken at 50x magnification and 'overlaid' to show the entire lung section. Metastatic colonies are identified with arrows.

External colonies were counted as described previously (section 5.1.2). Graph A in figure 5.21 shows the average number of external metastatic colonies for control and AMD3100 treated mice. In the control group, the average number of external metastatic colonies was 260.33 (+/- 102.34) compared to 52.33 (+/- 42.77) external colonies in the AMD3100 treated group. This difference is statistically significant ($p = 0.0314$ Students unpaired t test). Graph B shows the number of internal metastatic colonies from control and AMD3100 treated mice. The control group had on average 8.53 (+/- 3.6) internal metastatic colonies, compared to 2.93 (+/- 1.09) internal metastatic colonies in the AMD3100 treated group. This difference was not statistically significant ($p = 0.0614$ Students unpaired t test). These data show that AMD3100 treatment significantly reduces

the number of external colonies on the lungs of WT mice that received B16 F10 cells. As well as reducing external colonies, AMD3100 treatment reduced the number of internal colonies in B16 F10 treated lungs, but this difference was not significant.

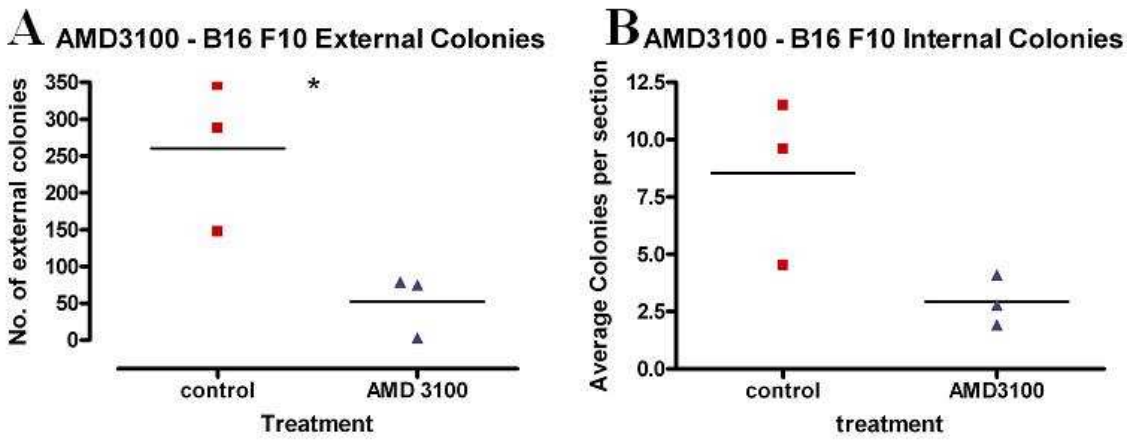

Figure 5-21: Enumeration of metastatic colonies of untreated and AMD3100 treated WT mice that received B16 F10 cells

WT C57Bl/6 mice received B16 F10 cells followed by daily injections of PBS control or AMD3100 for 14 days. External metastatic colonies were counted using the dissecting microscope (graph A), internal colonies were counted on H&E stained serial sections and are expressed as the average number of colonies per section (graph B). A – p=0.0314, students unpaired t test, B – NS, students unpaired t test. n= 3 per group

These results show, for the first time, that AMD3100 treatment significantly reduced the number of external metastatic colonies and caused a reduction in the number of internal metastatic colonies in the B16 F10 model of metastasis. These data show that CXCR4 is involved in B16 F10 colonisation of the lungs, and is required for the development of both internal and external colonies. As AMD3100 treatment did not fully prevent the development of metastatic colonies, it is likely that other mechanisms are involved in lung colonisation. What may be happening in the lungs is that CXCR4 is involved in getting B16 F10 cells to the lungs, and once there, the cells may grow or they may leave via pleural lymphatics. It may be here that D6 plays an important role. D6 may alter the chemokine levels within the lungs, which may affect the lung tissue, making the environment suitable for metastatic colony growth. Similar experiments have been performed, using B16 F10 cells transfected with CXCR4, these show that when CXCR4 is over-expressed in B16 F10 cells, the number of metastatic colonies increases, and CXCR4 can also promote cell survival in vitro (292, 330). The enhanced metastasis to the lungs caused by CXCR4 can be blocked using T22, an inhibitor of CXCR4 (330)

5.1.7 B16 F10 Overload

The results above (figure 5.2) show that D6KO mice had a significant reduction in the number of metastatic colonies that developed in the lungs. B16 F10 cells are well known for their lung colonisation capabilities (see section 1.13.2), but it may be possible that in D6KO mice, due to altered chemokine levels, they are colonising other organs rather than the lungs. This may reduce the number of cells that reach the lungs, explaining the reduction in colony numbers. If this was the case, giving mice double the number of cells, so 'overloading' the system, may show where these metastases are present in other organs. This 'overload' experiment (same protocol as described in section 2.3.2. with double the cell number) was performed on both WT and D6KO backgrounds. Table 5.2 shows the organs in which metastatic colonies were present in WT and D6KO mice.

Organ	WT	D6KO
Lung	+++	+
Liver	-	+
Heart	-	+
LN	+	+
Spleen	-	+
Testicles	-	+
Seminal Vesicles	-	+
Kidney	+	+
Membranes (omentum/peritoneum)	-	+

Table 5-2: Organs that contained metastatic colonies from WT and D6KO mice after receiving B16 F10 cells

WT and D6KO C57Bl/6 mice received double the dose of B16 F10 cells; 14 days later mice were sacrificed and organs which displayed metastatic colonies were noted. Results are representative of 2 separate experiments. Plus signs indicate the presence of metastatic colonies on that organ; multiple symbols indicate increased colony numbers. A minus sign indicates no colonies were present on that organ.

In both backgrounds lung colonies were present, consistent with previous experiments. Graph A of figure 5.22 shows that, as with previous results (figure 5.2), D6KO mice had a significant reduction ($p < 0.0001$ Students unpaired t test) in the number of external metastatic colonies. WT mice had on average 83.5 (+/- 10.85) metastatic colonies whilst D6KO mice had on average 30 (+/- 12.26) external metastatic colonies. Graph B shows that D6KO mice also have a significant ($p < 0.0001$ Students unpaired t test) reduction in the number of internal metastatic colonies (WT mice had an average of 20.37 (+/- 4.07) internal colonies whilst D6KO had on average 4.5 (+/- 1.97) internal colonies).

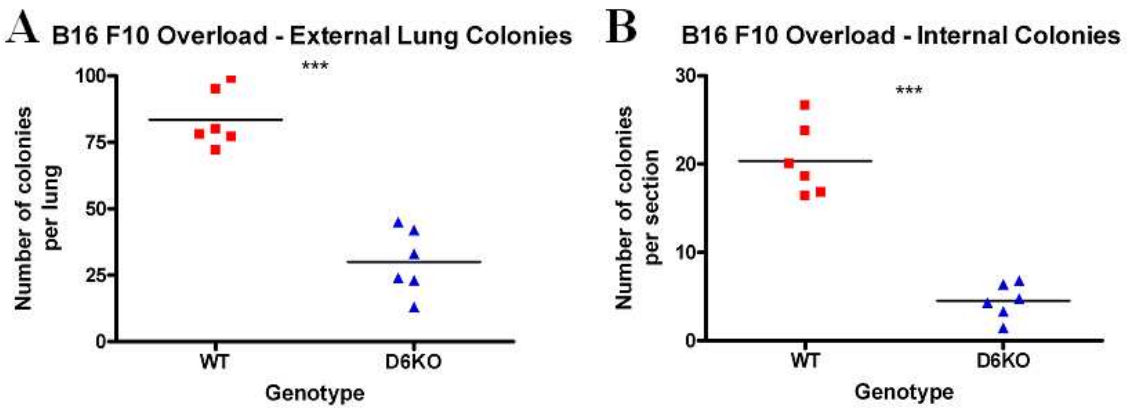

Figure 5-22: Metastatic colony counts on lungs from B16 F10 overload experiments

WT and D6KO mice received double the dose of B16 F10 cells and metastatic colonies were counted on the external surface of the lungs, and within the lung tissue. A – external colony counts, analysed using a dissecting microscope, and expressed as the number of colonies per lung. P<0.001 (Students unpaired t test). B – Internal colonies were counted on H&E stained lung sections, at 50x magnification. Results are expressed as the average number of colonies per section, p<0.001 (Students unpaired t test), n= 3 per group.

Other organs, which had obvious metastatic colonies on their surface, were removed, fixed and processed for histology, usually only one metastatic colony was evident upon dissection in each of the above organs. External colonies that could be identified by eye were confirmed by H&E staining of tissue sections. Representative sections from the mediastinal lymph node and testicle from a D6KO mouse are shown in figure 5.23; these organs contain metastatic colonies. Picture A shows a section from the testicle of a D6KO mouse that had been 'overloaded' with B16 F10 cells. Metastatic colonies could be identified on the external surface of the organ, and an internal metastatic colony can also be identified. The mediastinal lymph node from an 'overloaded' mouse is shown in picture B. This was isolated using a dissecting microscope and could be easily identified due to the large metastatic colony which is shown in the picture.

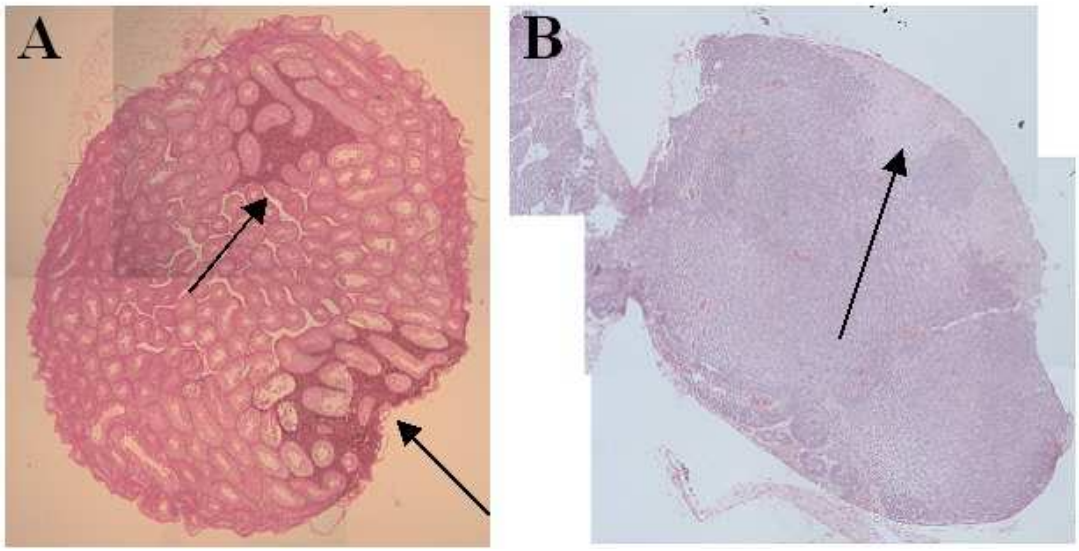

Figure 5-23: Organs containing metastatic colonies from mice that received double the dose of B16 F10 cells

WT and D6KO C57Bl/6 mice that received double the dose of B16 F10 cells had any organs with obvious metastatic colonies excised and processed for histological analysis. Picture A shows a testicle from a D6KO mouse with metastatic colonies identified. Picture B shows a lymph node from a D6KO mouse that contains a metastatic colony. Pictures were taken at 50x and 'overlaid' to show the entire tissue section.

Looking at the results presented in table 5.2, D6KO mice appeared to have metastatic colonies in many more organs than WT mice, e.g. liver, heart, spleen, testicles and seminal vesicles. These results suggest that in D6KO mice, B16 F10 cells have the ability to colonise many more organs than in WT mice. This may be due to an altered chemokine environment within these mice, caused by a lack of D6. The colonisation of other organs may explain the reduction in lung colonies in D6KO mice. In D6KO mice B16 F10 cells may initially enter the lungs, but encountering an environment that is unsuitable for metastatic growth may results in the cells leaving the lungs, possibly via pleural lymphatics or vasculature. This may then allow B16 F10 cells to go on and colonise other organs. The cell number used in the original metastasis experiments may not have been enough to allow the development of visible metastatic colonies on other organs, which explains why these organs were not selected for analysis. Evidence in the literature has shown that B16 F10 cells preferentially grow in the lungs. Grafts of pulmonary and renal tissue show the same degree of B16 F10 cell arrest, but only metastatic colonies developed in the lungs (309). Taken together, these results that a lack of D6 in the lungs is causing alterations to the pulmonary microenvironment, which makes them unsuitable for B16 F10 metastatic colony growth.

5.2 Summary

The data presented above show that D6KO mice have a significant reduction in external metastatic colonies, compared to WT mice. D6KO mice also have a reduction in internal colony number, although this difference is not significant. There is a significant reduction in internal colony number in D6KO lungs compared to WT lungs in the overload experiment, so this suggests that this difference in internal colony number, although not significant in the initial experiments, is a true observation. Immunohistochemical analysis has shown that these differences are unlikely to be due to differences in T cell location or number. There is a significant increase in the number of macrophages in the lungs of D6KO mice, suggesting that differences in macrophage number may be contributing to differences in metastatic colonies. These results suggest D6 inhibits macrophages within the lungs, which are crucial to the development of metastases in this model. Analysis of blood vessel number and location shows that there are no significant differences when comparing D6KO to WT lungs, which suggests that differences in blood vessels are not responsible for differences in metastatic colonies. Analysis of lymphatic vessel number and size, again, shows no differences comparing D6KO to WT lungs. There is a significant difference between locations of lymphatics with respect to metastatic colonies; D6KO mice have lymphatic vessels significantly closer to metastatic colonies than WT mice, which suggest the location of lymphatics may affect metastatic colony number.

The chemokine receptor profile of B16 F10 cells was analysed in order to try to determine how these cells were getting to the lungs. The only chemokine receptor that was found to be expressed was CXCR4. To try and determine if CXCR4 is responsible for B16 F10 colonisation of the lungs, WT mice were treated with a specific CXCR4 antagonist, AMD3100, which significantly reduced the number of internal and external metastatic colonies compared to control mice. These data suggest that CXCR4 is involved in B16 F10 cell colonisation of the lungs. The microenvironment of the lungs is essential to the growth of B16 F10 cells (309), as D6 has been shown to be expressed by the lungs, it seems possible that a lack of D6 may alter the chemokine microenvironment of the lungs. This different microenvironment may no longer allow growth of B16 F10 cells within the lungs in D6KO mice. In D6KO mice, the B16 F10 cells may simply not be able to survive within the lungs, or they may be able to leave and colonise other organs.

An ‘overload’ experiment was performed to try to determine if B16 F10 cells are able to colonise more organs in D6KO mice, possibly due to altered chemokine levels. These results show that in D6KO mice, whilst B16 F10 cells form fewer colonies in the lungs, they are able to form metastatic colonies in the liver, heart, spleen, testicles, seminal vesicles and the peritoneum, which are not seen in WT mice. This suggests that whilst the lungs may be suitable for B16 F10 growth, in D6KO mice these cells are able to colonise many more organs.

Taken together, these results suggest that CXCR4 may be involved in colonisation of the lungs. A hypothesis for the situation in D6KO mice could be that CXCR4 directs B16 F10 cells to the lungs. Once B16 F10 cells have entered the lungs, in WT mice they are able to grow and form metastatic colonies, but this does not happen in D6KO lungs. This could be due to an altered environment in the lungs which may not be suitable for B16 F10 cell growth, so these cells either die, or are able to re-enter the circulation and form metastatic colonies in other organs.

6 Discussion

The chemokine decoy receptor D6 was initially reported in 1997 during a search for novel CCL3 receptors (130, 131). Since then, D6 has been shown to have the ability to bind to 12 different CC chemokines, all of which fall into the category of inflammatory chemokines (128). D6 is referred to as a decoy receptor, as it is able to bind to inflammatory CC chemokines, internalise and target them for degradation, without appearing to induce any classical chemokine related signalling pathways. As a result, it is known as a member of the atypical chemokine receptor family, along with DARC, CCX-CKR and CXCR7. Expression of D6 has been shown in the skin, gut, lungs and placenta, as well as cellular expression on lymphatic endothelial cells and D6 is expressed by a wide variety of leukocytes (130, 143, 144). Leukocyte expression of D6 has been shown to be at the highest levels in B cells and DCs, and its expression can be modulated by pro and inflammatory stimuli (144, 145). On leukocytes and lymphatic endothelial cells, D6 may be present in order to scavenge and help to clear inflammatory CC chemokines from the environment. On leukocytes D6 may scavenge chemokines, but evidence suggests that D6 expressing cells may have reduced chemotaxis towards ligands that can bind both D6 and signalling chemokine receptors. This work showed no effect on chemotaxis towards non-D6 ligands when D6 was over-expressed with a CXCR; this work was carried out using transfected cells, so this observation may be a result of the artificial system (141).

The function of D6 in vivo has been studied extensively using animal models. Using the TPA model of skin inflammation, D6 has been shown to be required for the resolution phase of the inflammatory response (152). In the EAE model, D6KO mice have a reduced disease severity, which is thought to be a result of DCs being unable to leave site of inoculation (153). Transgenic D6 expression in the epidermis has been shown to be protective in a model of inflammation driven tumour formation, and D6 may be involved in colon cancer (142, 158, 159). In the placenta, D6 has a role in protecting the foetus from inflammation induced foetal loss (149).

As mentioned above, there is evidence to suggest that, despite its apparent inability to signal, D6 may be able to affect chemotaxis and may affect leukocyte chemotaxis in vivo. The work presented in this thesis set out to further elucidate the role that D6 may play in chemotaxis, using both in vitro and in vivo models.

Evidence in the literature has suggested that D6 may be involved in blunting chemotactic responses to the CC chemokines that D6 is able to bind. This has been shown in cell lines which co-express D6 and CCR4; the expression of D6 prevents migration towards CCL4. This phenomenon seems to be restricted to D6 ligands, as D6 co-expression with CXCR4 has no effect on migration towards CXCL12 (141). This effect of D6 on this chemotactic response may be artificial, as these cells were transfected with both D6 and the appropriate signalling chemokine receptor, in other words, this phenomenon may only be observed in transfected cells. Initially we set out to try to investigate the effect that co-expression of D6 would have in chemotaxis of cell lines. The approach taken involved using cells which expressed either inflammatory CC chemokine receptors (THP1 cells) or homeostatic chemokine receptors (Hut78). Attempts were made to stably transfect these cells with D6, with the aim of measuring their chemotactic capabilities in vitro, unfortunately the generation of stable transfectants proved unsuccessful. The baseline migration capabilities of these cells could be determined, but the chemotaxis assays gave highly variable results, which made analysis difficult.

An alternative approach involved looking at primary murine cells from WT and D6KO mice. Splenocytes and neutrophils were isolated from the spleen and bone marrow respectively, dendritic cells were generated by culturing bone marrow cells in GM-CSF. Using both the Transwell assay system and the modified Boyden chamber (Neuroprobe), chemotaxis results for all these cell types were highly variable, despite repeated attempts to optimise these assays. As a result, these data have been omitted from this thesis.

Although, in my hands, these assays were highly variable and did not yield reproducible results, these assays have been used successfully in other studies. In particular, a recent report shows that neutrophils isolated from D6KO mice have an increased chemotactic response to CCL3, compared to WT neutrophils, suggesting D6 may be limiting the responses of neutrophils to CCL3 (140). These data also show that migration towards CCL4 and CXCL8 is unaffected in primary neutrophils from D6KO mice (140). Previous evidence showing D6 has an effect on CCR4 mediated migration in response to CCL4 was performed in transfected cell lines, so D6 expression is likely to be higher than normal, and it may only be in this ‘artificial’ situation that D6 can affect other signalling chemokine receptors (108).

The next approach aimed to investigate a phenomenon observed in the skin of TPA treated D6KO mice. This model of TPA skin inflammation has been well described in D6KO mice, and results in an exaggerated inflammatory response, characterised by increased levels of inflammatory chemokines, T cell and mast cell infiltration, and a delayed resolution of inflammation (152). The skin of 129/Bl6 D6KO mice develops a psoriasis like pathology, which does not occur in WT mice of the same genetic background (152). Other features of this model include the altered positioning of neutrophils in the skin of D6KO mice. In WT mice, after TPA inflammation, neutrophils are found in the dermal compartment of the skin, shown by myeloperoxidase staining (see figure 3.2, (140)). However in D6KO skin, neutrophils are found closer to the dermal/epidermal junction. In order to explain this altered neutrophil positioning, two hypotheses were proposed – D6 has been shown to be expressed by neutrophils, so a lack of D6 on neutrophils may affect their chemotaxis on a cell autonomous basis, meaning they are unable to halt their migration in the dermal compartment, and continue to the dermal/epidermal junction. This theory has been supported by the in vitro chemotaxis work mentioned in (140). Alternatively, after TPA inflammation, D6KO skin has been shown to have an increased accumulation of chemokines, and it could simply be the increased chemokine levels, which are attracting neutrophils to the dermal/epidermal junction, irrespective of D6 expression on the neutrophils.

In order to try to test these hypotheses, a model of neutrophil adoptive transfer was designed. This model involved inducing inflammation in the skin of 129/Bl6 D6KO mice with TPA, injecting fluorescently labelled WT and D6KO neutrophils into the tail vein, and looking at samples of the inflamed skin at certain timepoints following induction of inflammation. Extensive optimisation of this protocol had to be undertaken, but eventually a successful protocol was developed. This allowed the identification of labelled neutrophils in the skin of D6KO mice, and allowed enumeration and measurement of their distance from the epidermis. Control skin sections were consistently negative for fluorescent cells, so it was assumed that any fluorescent cells within the skin of treated mice were neutrophils. An additional control to confirm that these cells were in fact neutrophils, would be to co-stain skin sections with a neutrophil marker, myeloperoxidase for example. If D6 on neutrophils was influencing their positioning in the skin, it was expected that D6KO neutrophils would be situated closer to the dermal/epidermal junction. These results showed that WT neutrophils were significantly

closer to the epidermis 11 hours after TPA treatment, compared to D6KO neutrophils. 24 hours after TPA treatment, WT neutrophils were significantly further away from the epidermis, compared to their position at 11 hours. These results suggest that D6 expressed on neutrophils may affect their position relative to the dermal/epidermal junction, early on in the inflammatory response, but as the inflammatory response progresses, D6 on neutrophils does not affect their positioning within the skin.

Results from the neutrophil adoptive transfer experiments are included in a study investigating the regulation of neutrophil migration by D6 (140). In this study, it is suggested that these results show that D6 does not affect the point of entry of neutrophils into the inflamed skin. However, this experiment cannot be used to determine the point of entry of neutrophils into the skin, as both neutrophil genotypes are injected into the tail vein together. As the neutrophils re-circulate, they will enter the skin at the same point, in vessels situated below the epidermis. In order to get to the dermal/epidermal junction, neutrophils will have to migrate through the dermis to the epidermis (358). These results show that D6 may influence the positioning of neutrophils in inflamed skin, but a lack of D6 does not explain their positioning at the dermal/epidermal junction, observed in D6KO skin (140). This report also states that D6KO neutrophils are not restricted in their migration in the inflamed skin, which allows them to accumulate at the dermal/epidermal junction (140). The results presented here suggest the opposite, WT neutrophils, that express D6, are found closer to the dermal/epidermal junction, compared to D6KO neutrophils, suggesting that a lack of D6 is restricting their location in the skin.

Neutrophil migration into inflamed skin can be regulated by CXCL1 and CXCL2, under the influence of CXCR2 (359). These chemokines are not able to bind to D6, but when CXCL2 blocking is carried out on D6KO mice, this reduces the development of the psoriasis-like pathology (140). Whilst D6 and CC chemokines are important in this model, CXCL2 is also important and may be influencing the positioning of neutrophils in inflamed skin. Neutrophils are known to express CXCR2, and they have been shown to express CCR1, which is able to bind to the D6 ligands CCL3 and CCL5. Administration of a CCR1 antagonist to D6KO mice reverses the aberrant neutrophil accumulation at the dermal/epidermal junction, so CCR1 is crucial to these neutrophils getting to the dermal/epidermal junction in D6KO skin. Looking at CCL3 expression, the major site of CCL3 expression seems to be the epidermal compartment, CCL5 expression was not

analysed. These results suggest that CCR1 is required for neutrophil positioning in inflamed D6KO skin (140).

It is possible that the results presented here are not a true reflection of the differential positioning seen in D6KO skin, as this is an artificial system, where neutrophils are removed from the bone marrow, stained and re-infused. This process may affect the neutrophils and could potentially alter chemokine receptor expression. An alternative method of testing these hypotheses would be to use bone marrow chimeras, putting WT bone marrow into D6KO mice, and vice versa, to determine conclusively if D6 is affecting the positioning of neutrophils in inflamed skin, or if the work in (140) suggests, other chemokine receptors or secondary effects of the increased inflammation is responsible. Further work to identify the location of chemokine expression in inflamed D6KO skin is required to clarify why neutrophils are found at the dermal/epidermal junction. These results contribute to the body of work investigating the TPA inflammation model in D6KO mice, but further work is required to fully elucidate the mechanisms of alternative neutrophil placement in the skin of these mice.

Much of the knowledge regarding D6 has come from a variety of different in vivo models, including skin inflammation, tuberculosis infection, EAE, skin and colon cancer (142, 152, 153, 157-159). In a model of inflammation driven skin tumour formation, transgenic over expression of D6 in the epidermis has been shown to be protective. In the same model, a lack of D6 is able to render resistant mice susceptible to tumour formation (B6/129) and increase the tumour burden in susceptible mice (Fvb/N) (142). In models of colitis driven colon cancer, D6KO mice are more susceptible to the development of cancer (158). D6 expression has also been demonstrated on lymphatic endothelial cells in squamous cell carcinomas, endometrial carcinoma, Kaposis sarcoma and cases of IBD that developed into colon cancer. Both of these models of tumourigenesis are similar in the fact that they rely on repeated rounds of inflammation to promote the tumour formation (142, 158). We decided to investigate the role of D6 in a different model of skin cancer, melanoma, which has a different mechanism of tumourigenesis, injecting melanoma cells into syngeneic mice. Using WT and D6KO mice, it would be possible to identify any potential role that D6 may play in affecting this model of tumour growth.

The B16 F0 model of melanoma was chosen as it differed in action to the model of skin tumourigenesis used previously, and was easy to manipulate. Tumour cells were injected

into WT and D6KO mice and the resultant tumour growth was measured against time. Initial experiments showed that D6KO mice developed tumours before WT mice, and tumours in D6KO mice subsequently grew at a faster rate, although this difference was not significant. This enhanced growth rate resulted in a reduced survival for the D6KO mouse group, as tumours reached the point of sacrifice sooner, again this difference was not significant Tumours were excised for histological and immunohistochemical analysis. There were no visible differences in tumours that developed in D6KO mice, compared to WT; tumours from both WT and D6KO mice had the same general histological features (see section 4.1.2). Immunohistochemical analysis showed that there were no differences in T cell or macrophage numbers in WT and D6KO tumours, and there were no differences in the number of blood vessels that developed within the tumours. Together, these results show that there are no significant differences in the cell composition, blood vessel development and growth rate of B16 F0 tumours in D6KO mice compare to WT.

Tumour growth appeared to be slightly enhanced in D6KO mice, although not significantly increased, so B16 F0 cells were stably transfected with D6 (as they were previously shown to be D6 negative), to investigate the effect of D6 expression in tumour growth. The growth of tumours derived from B16 F0 D6 cells was compared to that of B16 F0 cells in both WT and D6KO mice. These results showed that in D6KO mice, D6 expressing tumours developed at a significantly slower rate than D6 expressing tumours in WT mice. As with B16 F0 tumours before, all B16 F0D6 tumours were analysed by histology and immunohistochemistry. To summarise these results, there were no differences in blood vessels, T cells or macrophages that could explain this difference in observed growth rate.

Initially, it was hypothesised that D6KO mice were developing an immune response against the previously unseen D6 expressed by the tumour cells, which was causing the reduced growth rate. However this is unlikely to be the case, as a higher number of T cells and macrophages would be expected in the tumours if these mice were mounting an immune response against the tumour cells. Another explanation for what could be happening in these D6 expressing tumour cells may lie in their chemokine receptor expression. B16 F0 cells were shown to be CCR5 and CCR7 positive by RT-PCR. D6 can bind to the same ligands as CCR5 (CCL3, 4, 5) but not to CCL19 and 21, which bind CCR7. This suggests that D6 expressed on these tumour cells may be able to somehow interfere with CCR5 function. Without D6 on B16 F0 cells, CCR5 may be influencing the cell survival and the subsequent tumour development. Evidence in the literature suggests that CCR5

can be anti-apoptotic in macrophages, and can promote the survival of lymphoma cells (349, 350).

In D6KO mice, there may be a general increase in levels of inflammatory CC chemokines, such as CCL3, 4, and 5, all of which can bind to CCR5. In D6KO mice, these chemokines may induce signalling via CCR5 that promotes the survival of B16 F0 cells and results in a faster tumour growth rate, compared to WT mice. In B16 F0 cells that express D6, D6 may be acting to reduce the local levels of inflammatory chemokines, which may result in reduced CCR5 signalling therefore decreased tumour cell survival. Alternatively, D6 degradation of inflammatory chemokines may somehow interfere with CCR5 induced signalling, with the same end results of reducing the tumour cell growth rate, or a reduction in the levels of inflammatory chemokines may simply create an unfavourable environment for melanoma growth.

Chemokines are known to contribute to the survival of melanoma cells (274, 276, 277), it would be useful to look at the effects of D6 ligands on B16 F0 cells, to try to explain the possible differences in tumour growth. Although this study showed no differences in T cell or macrophage numbers, the subsets of these cells may be altered in D6 expressing tumours. The balance of macrophages, in particular, is known to be crucial to tumour growth; too many M1 macrophages can cause tumour suppression, too many M2 macrophages can promote tumour growth (238, 241, 242). The cell subsets within B16 F0 and B16 F0D6 tumours would need to be analysed in more detail, by flow cytometry for example, to determine the leukocyte subsets that may be contributing or inhibiting tumour growth. An altered chemokine microenvironment in D6KO mice, which normally promotes tumour growth, perhaps by recruiting M2 macrophages, may be altered by the expression of D6 within the tumour. Evidence in the literature suggests that chemokines are able to inhibit growth in this type of tumour model (289, 291), but these studies have the drawback of only looking at one chemokine at a time, using transfected tumour cells. In the case of D6, multiple CC chemokines (and possibly CXC chemokines (152)) may be affected, and are likely to have multiple and cumulative effects on different cell populations. In conclusion, these results show that B16 F0 tumours grow at a faster rate in D6KO mice, which can be reversed by expression of D6 in the tumour cells. These results suggest that D6 is having some effect on the local chemokine environment, or other chemokine receptors expressed by B16 F0 cells to influence tumour growth. These

results highlight a potential therapeutic role for D6 expression in solid tumours and contributes to the existing data showing a role for D6 in tumourigenesis (142, 158).

The role of chemokines and their receptors in metastasis has been well defined in many types of cancer. In melanoma, chemokine receptor expression has been shown to influence the site of metastasis (see introduction section 1.12.1.2). As D6 has been shown have an effect tumour growth using the B16 F0 model, it was decided to determine if D6 has a role in melanoma metastasis. This was carried out using model related to the B16 F0 melanoma model. The B16 F10 model uses cells which have been derived from the original B16 F0 cell line, that have been selected to be highly selective for the lungs (286, 311). As a result, when these cells are injected intravenously into syngeneic mice, metastatic colonies form in the lungs. This model was administered to WT and D6KO mice to determine if D6 plays a role in melanoma metastasis.

The B16 F10 model of melanoma metastasis results in the formation of metastatic colonies on the external surfaces of the lungs and inside the lungs. A striking difference was observed, with D6KO mice having a significant reduction in the number of external metastatic colonies, with a reduction in internal metastatic colonies, although this difference was not significant. To investigate what could be contributing to the differences in metastatic colony formation, lungs were digested to create a single cell suspension, which was then stained for a panel of lineage markers and analysed by flow cytometry. No significant differences were found in relation to leukocyte populations of untreated WT and D6KO lungs, and those that received B16 F10 cells. There seemed to be an increase in a population of CD45+ CD11b+ CD11c- cells in the lungs of D6KO mice that received B16 F10 cells, but this increase was not significant. Previous studies looking at the role of D6 in colitis development, have showed that CD45- cells, or non-haematopoeitic cells, express D6, and these cells may be responsible for the D6 expression in the gut (158, 159). It would be useful to sort out the various cell populations and characterise the expression of D6 within the lungs, as this has not been characterised fully, it is possible that CD45- cells may be influencing metastatic colony formation, perhaps by influencing the development of the premetastatic niche (261, 263).

The major difference in metastatic colony formation was shown at the external surface of the lungs, which, in vivo, is covered by the pleura, a thin serous membrane. Metastatic colonies were observed on the pleura, but technically it was challenging to enumerate

these, or to analyse the pleura to compare differences between WT and D6KO. Pleural washes yielded low protein concentrations that made analysis of chemokine and cytokine levels difficult. The only samples which could be detected were those from B16 F10 treated WT mice, which although these were at the limits of detection, may suggest that in WT mice that receive B16 F10 cells, there may be a low level of inflammation within the lungs. It may be that lungs of mice that received B16 F10 cells may have an increased baseline inflammatory microenvironment, compared to D6KO and untreated WT mice. In order to confirm this, the experiment would have to be repeated with many more mice.

Lungs from B16 F10 treated mice were processed for immunohistochemical analysis, to analyse the cell populations within the lungs, and to define their location with respect to metastatic colonies. T cells have been shown to influence the development of metastatic colony formation by forming clusters with B16 cells, the more clusters form with T cells, the more metastatic colonies (286, 306). Lung sections were stained for CD3, and show that there are no differences in the number or location of T cells in B16 F10 treated WT and D6KO lungs. Macrophages are well known for their role in tumour formation and can also influence the development of metastatic colonies (255). Macrophage staining within the lungs was carried out and showed that there was a significant increase in the number of macrophages within the lungs of D6KO mice. This increased number did not alter their location with respect to the pleura or metastatic colonies. It is possible that this increase in macrophages correlates with the increased number of CD45+CD11b+CD11c- found in the lungs of B16 F10 treated D6KO mice, by flow cytometry. These cells may be responsible for causing the reduction in colony formation in the lungs. Evidence in the literature suggests that after OVA induced inflammation, a population of CD11b+ $CD11c^{int}$ cells increase in the lungs, and these cells stain positive for macrophage markers (360). Within the lungs, populations of CD11b+CD11c- cells have been identified as antigen presenting cells (353). The lungs are full of alveolar macrophages, which typically express CD11c+CD11b-, whilst macrophages that are CD11c-CD11b+ are typically found in the tissues (361). The results presented here, although preliminary, suggest that there may be differences in macrophage populations in the lungs of D6KO mice. If an altered macrophage population is present in the lungs of D6KO mice, these cells may be destroying the injected B16 F10 cells before they are able to develop into metastatic colonies. Alternatively, different populations of macrophages may influence the microenvironment of the lungs, and may alter the development of the pre-metastatic

niche, which has been shown to be contribute to the growth of B16 F0 metastatic colonies (328, 329).

Blood vessels and lymphatic vessels were analysed by immunohistochemistry; no differences were observed with respect to blood vessels within the lungs. However lymphatic vessels in D6KO lungs were significantly close to metastatic colonies than in T mice. This may have implications for B16 F10 cell exit from the lungs. It may be possible that when the colonies are developing, if a lymphatic vessel is close, some of the cells may be able to leave, which may reduce the number of metastatic colonies which can form in that area. Whilst D6 expression has not been shown on murine lymphatic endothelial cells, two recent studies looking at D6 in colitis have suggested that D6 on non-haematopoietic cells or CD45- cells may be affecting colitis development (158, 159). It is possible that these same cells may express D6 in the lungs, and may influence the development of metastatic colonies, through the development of the pre-metastatic niche (329).

Other variables which could influence the development of metastatic colonies, include the initial stages of lung colonisation. Chemokines, receptors in particular, are known to influence metastasis (274, 282), so the chemokine receptor expression of B16 F10 cells was analysed to determine if they express specific receptors that may direct them to the lungs. RT-PCR analysis of chemokine receptor expression showed expression of CXCR4 alone, this receptor has been linked to metastasis in murine and human cancer (213, 267, 274). The use of the specific reversible antagonist of CXCR4, AMD3100, showed that B16 F10 cells rely on CXCR4 to colonise the lungs, this was the first time that AMD3100 has been used in this model. A similar technique was used with CXCR4 transfected B16 cells; using T22, an inhibitor of CXCR4, showed that the colonisation of the lungs could be prevented in these transfected cells (330). It is possible that CXCR4 may be involved in the initial colonisation stages of the lungs, but once B16 F10 cells reach the lungs, the lung microenvironment may be crucial for metastatic colony growth.

It seems plausible that D6KO mice may have a general increase in inflammatory chemokines in the numerous organs where D6 is expressed, and this increase in chemokines may alter the normal colonisation patterns of B16 F10 cells. Once injected, B16 F10 cells may alter their chemokine receptor expression, meaning that CXCR4 may not be the only receptor directing their colonisation. In order to try to address this, an

experiment was designed which used double the number of B16 F10 cells, in order to try to 'overload' the system. This would provide enough cells in the system to identify any other organs where metastatic colonisation was taking place. These results showed that in WT mice, the only organs which had metastatic colonies were the lungs, kidney and mediastinal lymph node, whilst in D6KO mice, multiple organs, including the heart, liver, spleen, peritoneum and testes, developed metastatic colonies. These results suggest that despite being unable to detect inflammatory CC chemokine receptor expression by RT-PCR, B16 F10 cells may express receptors that are able to bind to D6 ligands. Knowing the function of D6, it is likely that increased levels of pro-inflammatory CC chemokines in these organs may be causing this difference. Isolating organs and performing Luminex or ELISA analysis to determine the chemokines and their relative levels in each organ could test this relatively easily. There is no evidence in the literature looking at the effects of inflammatory chemokines on chemokine receptor expression of B16 F10 cells.

Based on the functions of D6, it seems plausible to assume that a reduction in D6 would increase the levels of pro-inflammatory chemokines in the lungs, which may explain the reduction in metastatic colonies. However, evidence suggests that a pro-inflammatory environment may actually promote lung colonisation. S100A8 and S100A9 are proteins which are chemotactic for neutrophils and are useful markers in diseases associated with inflammation (362) and are known to be pro-inflammatory. In the B16 model, S100A8 and S100A9 are upregulated in the lungs prior to melanoma cell colonisation, neutralisation of these reduces the number of lung colonies (261, 262). Mice that have been treated with a model of OVA induced lung inflammation show increased lung colonies, and this can be reduced by treatment with corticosteroids, showing that the inflammatory milieu is permitting enhanced colony growth (363). A wound healing environment, whilst not thought of as pro-inflammatory, also increases the development of lung colonies (310). It appears that simply thinking of the environment as pro or anti inflammatory is too simplistic, as IFNγ administration decreases the number of lung colonies, due to increasing MHC I expression on B16 F10 cells surface (313, 314). The chemokine microenvironment of the lungs in D6KO mice needs to be fully characterised, which may determine a potential mechanism for the reduction in metastatic colony growth.

The pre-metastatic niche has been mentioned above, this describes the phenomenon by which tumour cells can increase fibronectin expression in the lungs, and cause recruitment of VLA4+VEGFR1+ haematopoietic cells, which interact with stromal cells to

produce chemokines, growth factors and MMPs (261, 262, 364). B16 F10 cells can recruit CCR5+ pulmonary fibrocytes to the lungs, which produce MMP9, which creates the ideal environment for metastatic colony growth. If CCR5 is knocked out, these mice display a phenotype similar to that of D6KO mice, with significant reductions in metastatic colony formation. These studies used bone marrow chimeras to demonstrate that CCR5 expression on non-haematopoietic cells was essential for the development of metastatic colonies (328, 329). In D6KO mice, it is possible that there may be a cell population similar to pulmonary fibrocytes that are missing, which would explain the reduction in metastatic colony formation. Bone marrow chimera experiments would help to determine if D6 expressed on haematopoietic cells, or non-haematopoietic cells are involved in B16 F10 lung colonisation.

The B16 F10 model has been shown to be influenced by cell interactions, in particular B1 cells, T cells and platelets (306, 318, 326). B1 cells are an interesting subset of B cells, known as innate B cells. B1 cells are found in the peritoneal and pleural cavity, express IgM and CD5. They have a limited antibody diversity and are capable of self-renewal (316, 317). When B1 cells are co-cultured with low metastatic B16 cells, they increase their metastatic potential in a cell contact dependent mechanism, associated with an upregulation of CXCR4 and MMP9 (318). When B1 cells are depleted, the number of metastatic colonies in the lungs is reduced (318). Recent unpublished work has shown that B1 cells in the peritoneal cavity express D6 (personal communication, Chris Hansell). At this moment, it is unknown if B1 cells in the pleural cavity express D6, but since these cells derive from a common precursor (317), it seems feasible that they may express D6. As B1 cells are linked to metastatic colony formation in this model, the numbers of B1 cells in the pleura may be reduced in D6KO mice, which may be causing the reduction in metastatic colonies. B16 F10 cells preferentially grow at blood vessels and the pleura, their pleural growth may be linked to the B1 cells found in the pleura (308). It would be interesting to look at models of mesothelioma, a malignancy of the pleura, and metastasis to the peritoneal cavity to examine the roles that D6 may play in the pleural and peritoneal cavities. Platelets have been shown to aggregate with B16 F10 cells, and this aggregation can increase the size of metastatic colonies, conversely thrombocytopenia is associated with a reduction in colony development (252, 253, 324). D6 expression has been shown on T cells and platelets ((144) and Catherine Wilson,

personal communication), so it is possible that these cells may be altered in D6KO mice and this could be causing the phenotype exhibited.

In conclusion, the work presented in this thesis contributes to the body of work describing a role for D6 in neutrophil migration in the well-characterised TPA skin inflammation model. These data show that D6 on neutrophils does not affect their positioning in inflamed skin, further work is needed to investigate the hypothesis that altered chemokine clearance within the skin is responsible for the altered neutrophisl positioning. With respect to melanoma growth this work shows that D6 over-expression may be a potential therapeutic target for melanoma growth, although further work is required to elucidate the precise role D6 plays in melanoma growth. Finally, this data shows for the first time, the significant role that D6 plays in melanoma metastasis to the lungs. Further work is required to define the involvement of D6 in metastasis, but this work suggests that D6 may be involved in the development of metastasis to the lungs and the pleura, by affecting both macrophages and lymphangiogenesis, and may represent a novel therapeutic target for the treatment of metastasis and possibly mesothelioma.

7 References

1. Zlotnik, A., and O. Yoshie. 2000. Chemokines: A New Classification System and Their Role in Immunity. *Immunity* 12:121-127.
2. Rot, A., and U. von Andrian, H. . 2004. Chemokines in Innate and Adaptive Host Defense: Basic Chemokinese Grammer for Immune Cells. *Annual Reviews Immunology* 22:891-928.
3. Mellado, M., J. M. Rodriguez-Frade, S. Manes, and C. Martinez-A. 2001. Chemokine Signalling and Functional Responses: The Role of Receptor Dimerisation and TK Pathway Activation. *Annual Review of Immunology* 19:397-421.
4. Luster, A. D. 1998. Chemokines -- Chemotactic Cytokines That Mediate Inflammation. *The New England Journal of Medicine* 338:436-445.
5. Rollins, B. J. 1997. Chemokines. *Blood* 90:909-928.
6. Pease, J. E., and T. J. Williams. 2006. The attraction of chemokines as a target for specific anti-inflammatory therapy. *British Journal of Pharmacology* 147:S212-S221.
7. Allen, S. J., S. E. Crown, and T. M. Handel. 2007. Chemokine: Receptor Structure, Interactions, and Antagonism. *Annual Reviews Immunology* 25:787-820.
8. Mantovani, A., R. Bonecchi, and M. Locati. 2006. Tuning inflammation and immunity by chemokine sequestration:decoys and more. *Nature Reviews Immunology* 6:907-918.
9. Proudfoot, A. E. 2002. Chemokine receptors: multifaceted therapeutic targets. *Nature Reviews Immunology* 2:106-115.
10. Comerford, I., W. Litchfield, Y. Harata-Lee, R. J. B. Nibbs, and S. R. McColl. 2007. Regulation of chemotactic networks by 'atypical' receptors. *Bioessays* 29:237-247.
11. Clore, G. M., and A. M. Gronenborn. 1995. Three-dimensional structures of alpha and beta chemokines. *FASEB J.* 9:57-62.
12. Graham, G. J., J. MacKenzie, S. Lowe, M. L.-S. Tsang, J. A. Weatherbee, A. Issacson, J. Medicherla, F. Fang, P. C. Wilkinson, and I. B. Pragnell. 1994. Aggregation of the chemokine MIP-1alpha is a dynamic and reversible phenomenon. Biochemical and biological analyses. *The Journal of Biological Chemistry* 269:4974-4978.
13. Witt, D. P., and A. D. Lander. 1994. Differential binding of chemokines to glycosaminoglycan subpopulations. *Current Biology* 4:394-400.
14. Crown, S. E., Y. Yu, M. D. Sweeney, J. A. Leary, and T. M. Handel. 2006. Heterodimerization of CCR2 chemokines and regulation by glycosaminoglycan binding. *Journal of Biological Chemistry* 281:25438-25446.
15. Guan, E., J. Wang, and M. A. Norcross. 2001. Identification of human macrophage inflammatory proteins 1alpha and 1beta as a native secreted heterodimer. *Journal of Biological Chemistry* 276:12404-12409.
16. Turnbull, J., A. Powell, and S. Guimond. 2001. Heparan sulfate: decoding a dynamic multifunctional cell regulator. *Trends in Cell Biology* 11:75-82.
17. Proudfoot, A. E. 2006. The biological relevance of chemokine-proteoglycan interactions. *Biochemical Society Transactions* 34:422-426.
18. Proudfoot, A. E., T. M. Handel, Z. Johnson, E. K. Lau, P. LiWang, I. Clark-Lewis, F. Borlat, T. N. Wells, and M. H. Kosco-Vilbois. 2003. Glycosaminoglycan binding and oligomerization are essential for the in vivo activity of certain chemokines. *Proceedings of the National Academy of Sciences* 100:1885-1890.
19. Rot, A. 1992. Endothelial cell binding of NAP-1/IL-8 : role in neutrophil emigration. *Immunology Today* 13:291-294.

20. Kuschert, G. S., F. Coulin, C. A. Power, A. E. Proudfoot, R. E. Hubbard, A. J. Hoogewerf, and T. N. Wells. 1999. Glycosaminoglycans interact selectively with chemokines and modulate receptor binding and cellular responses. *Biochemistry* 38:12959-12968.
21. Webb, L. M., M. U. Ehrengruber, I. Clark-Lewis, M. Baggiolini, and A. Rot. 1993. Binding to heparan sulfate or heparin enhances neutrophil responses to interleukin 8. *Proceedings of the National Academy of Sciences* 90:7158-7162.
22. Hoogewerf, A. J., G. S. Kuschert, A. E. Proudfoot, F. Borlat, I. Clark-Lewis, C. A. Power, and T. N. C. Wells. 1997. Glycosaminoglycans mediate cell surface oligomerization of chemokines. *Biochemistry* 36:13570-13578.
23. Van Damme, J., S. Struyf, A. Wuyts, E. Van Coillie, P. Menten, D. Schols, S. Sozzani, I. De Meester, and P. Proost. 1999. The role of CD26/DPP IV in chemokine processing. *Chemical Immunology* 72:42-56.
24. Overall, C. M., G. A. McQuibban, and I. Clark-Lewis. 2002. Discovery of chemokine substrates for matrix metalloproteinases by exosite scanning: a new tool for degradomics. *Biological Chemistry* 383:1059-1066.
25. McQuibban, G. A., G. S. Butler, J.-H. Gong, L. Bendall, C. Power, I. Clark-Lewis, and C. M. Overall. 2001. Matrix metalloproteinase activity inactivates the CXC chemokine stromal cell-derived factor-1. *Journal of Biological Chemistry* 276:43503-43508.
26. McQuibban, G. A., J.-H. Gong, J. P. Wong, J. L. Wallace, I. Clark-Lewis, and C. M. Overall. 2002. Matrix metalloproteinase processing of monocyte chemoattractant proteins generates CC chemokine receptor antagonists with anti-inflammatory properties in vivo. *Blood* 100:1160-1167.
27. Van Lint, P., and C. Libert. 2007. Chemokine and cytokine processing by matrix metalloproteinases and its effect on leukocyte migration and inflammation. *Journal of Leukocyte Biology* 82:1375-1381.
28. Murphy, P. M., M. Baggiolini, I. F. Charo, C. A. Hebert, R. Horuk, K. Matsushima, L. H. Miller, J. J. Oppenheim, and C. A. Power. 2000. International Union of Pharmacology. XXII. Nomenclature for Chemokine Receptors. *Pharmacological Reviews* 52:145-176.
29. Balkwill, F. 2004. Cancer and the chemokine network. *Nature Reviews Cancer* 4:540-550.
30. Mayer, K. L., and M. J. Stone. 2000. NMR solution structure and receptor peptide binding of the CC chemokine eotaxin-2. *Biochemistry* 39:8382-8395.
31. Booth, V., D. W. Keizer, M. B. Kamphuis, I. Clark-Lewis, and B. D. Sykes. 2002. The CXCR3 binding chemokine IP-10/CXCL10: structure and receptor Interactions. *Biochemistry* 41:10418-10425.
32. Mellado, M., C. Martinez-A, and J. M. Rodriguez-Frade. 2002. Analysis of G-protein-coupled receptor dimerization following chemokine signalling. *Methods* 27.
33. Trettel, F., S. Di Bartolomeo, C. Lauro, M. Catalano, M. T. Ciotti, and C. Limatola. 2003. Ligand-independent CXCR2 dimerization. *Journal of Biological Chemistry* 278:40980-40988.
34. Babcock, G. J., M. Farzan, and J. Sodroski. 2003. Ligand-independent dimerization of CXCR4, a principal HIV-1 coreceptor. *Journal of Biological Chemistry* 278:3378-3385.
35. Issafras, H., S. Angers, S. Bulenger, C. Blanpain, M. Parmentier, C. Labbe-Jullie, M. Bouvier, and S. Marullo. 2002. Constitutive agonist-independent CCR5 oligomerization and antibody-mediated clustering occurring at physiological levels of receptors. *Journal of Biological Chemistry* 277:34666-34673.

36. El-Asmar, L., J.-Y. Springael, S. Ballet, E. U. Andrieu, G. Vassart, and M. Parmentier. 2005. Evidence for negative binding cooperativity within CCR5-CCR2b heterodimers. *Molecular Pharmacology* 67:460-469.
37. Mackay, C. R. 2001. Chemokines: Immunology's high impact factors. *Nature Immunology* 2:95-101.
38. Viola, A., and A. D. Luster. 2008. Chemokines and Their Receptors: Drug Targets in Immunity and Inflammation. *Annual Review of Pharmacology and Toxicology* 48:171-197.
39. Kaul, M., and S. A. Lipton. 1999. Chemokines and activated macrophages in HIV gp120-induced neuronal apoptosis. *Proceedings of the National Academy of Sciences* 96:8212-8216.
40. Vlahakis, S. R., A. Villasis-Keever, T. Gomez, M. Vanegas, N. Vlahakis, and C. V. Paya. 2002. G protein-coupled chemokine receptors induce both survival and apoptotic signaling pathways. *Journal of Immunology* 169:5546-5554.
41. Ali, H., R. M. Richardson, B. Haribabu, and R. Snyderman. 1999. Chemoattractant receptor cross-desensitization. *Journal of Biological Chemistry* 274:6027-6030.
42. Mellado, M., J. M. Rodriguez-Frade, A. J. Vila-Coro, S. Fernandez, A. Martin de Ana, D. R. Jones, J. L. Toran, and C. Martinez-A. 2001. Chemokine receptor homo- or heterodimerization activates distinct signaling pathways. *EMBO J* 20:2497-2507.
43. Samanta, A. K., J. J. Oppenheim, and K. Matsushima. 1990. Interleukin 8 (monocyte-derived neutrophil chemotactic factor) dynamically regulates its own receptor expression on human neutrophils. *Journal of Biological Chemistry* 265:183-189.
44. Aragay, A. M., M. Mellado, J. M. Frade, A. M. Martin, M. C. Jimenez-Sainz, C. MartInez-A, and F. Mayor Jr. 1998. Monocyte chemoattractant protein-1-induced CCR2B receptor desensitization mediated by the G protein-coupled receptor kinase 2. *Proceedings of the National Academy of Sciences* 95:2985-2990.
45. Keller, H. U., P. C. Wilkinson, M. Abercrombie, E. L. Becker, J. Hirsch, G., M. E. Miller, W. S. Ramsey, and S. H. Zigmond. 1977. A Proposal for the Definition of Terms Related to Locomotion of Leukocytes and Other Cells. *The Journal of Immunology* 118:1912-1914.
46. Wilkinson, P. C. 1996. Cell Locomotion and Chemotaxis: Basic Concepts and Methodological Approaches. *Methods* 10:74-81.
47. Miller, M. J., S. H. Wei, I. Parker, and M. D. Cahalan. 2002. Two-Photon Imaging of Lymphocyte Motility and Antigen Response in Intact Lymph Node. *Science* 296:1869-1873.
48. Luster, A. D., R. Alon, and U. H. Von Andrian. 2005. Immune cell migration in inflammation: present and future therapeutic targets. *Nature Immunology* 6:1182-1190.
49. Nieto, M., J. M. Frade, D. Sancho, M. Mellado, C. Martinez-A, and F. Sanchez-Madrid. 1997. Polarization of chemokine receptors to the leading edge during lymphocyte chemotaxis. *Journal of Experimental Medicine* 186:153-158.
50. Xu, J., F. Wang, A. van Keymeulen, P. Herzmark, A. Straight, K. Kelly, Y. Takuwa, N. Sugimoto, T. Mitchison, and H. R. Bourne. 2003. Divergent signals and cytoskeletal assemblies regulate self-organizing polarity in neutrophils. *Cell* 114:201-214.
51. Ley, K., C. Laudanna, M. I. Cybulsky, and S. Nourshargh. 2007. Getting to the site of inflammation: the leukocyte adhesion cascade updated. *Nature Reviews Immunology* 7:678-689.
52. Alon, R., H. Rossiter, X. Wang, T. A. Springer, and T. S. Kupper. 1994. Distinct cell surface ligands mediate T lymphocyte attachment and rolling on P and E selectin under physiological flow. *Journal of Cell Biology* 127:1485-1495.

53. Mackay, C. R. 2008. Moving targets: cell migration inhibitors as new anti-inflammatory therapies. *Nature Immunology* 9:988-998.
54. Wang, S., M.-B. Voisin, K. Y. Larbi, J. Dangerfield, C. Scheiermann, M. Tran, P. H. Maxwell, L. Sorokin, and S. Nourshargh. 2006. Venular basement membranes contain specific matrix protein low expression regions that act as exit points for emigrating neutrophils. *Journal of Experimental Medicine* 203:1519-1532.
55. Sixt, M., B. Engelhardt, F. Pausch, R. Hallmann, O. Wendler, and L. M. Sorokin. 2001. Endothelial cell laminin isoforms, laminins 8 and 10, play decisive roles in T cell recruitment across the blood-brain barrier in experimental autoimmune encephalomyelitis. *Journal of Cell Biology* 153:933-946.
56. Stüve, O., R. Gold, A. Chan, E. Mix, U. Zettl, and B. Kieseier. 2008. alph4-integrin antagonism with natalizumab: effects and adverse effects. *Journal of Neurology* 255:58-65.
57. Wehner, N. G., C. Gasper, G. Shopp, J. Nelson, K. Draper, S. Parker, and J. Clarke. 2009. Immunotoxicity profile of natalizumab. *Journal of Immunotoxicology* 6:115-129.
58. Ma, Q., D. Jones, P. R. Borghesani, R. A. Segal, T. Nagasawa, T. Kishimoto, R. T. Bronson, and T. A. Springer. 1998. Impaired B-lymphopoiesis, myelopoiesis, and derailed cerebellar neuron migration in CXCR4- and SDF-1- deficient mice. *Proceedings of the National Academy of Sciences* 95:9448-9453.
59. Ma, Q., D. Jones, and T. A. Springer. 1999. The chemokine receptor CXCR4 is required for the retention of B lineage and granulocytic precursors within the bone marrow microenvironment. *Immunity* 10:463-471.
60. Zou, Y.-R., A. H. Kottmann, M. Kuroda, I. Taniuchi, and D. R. Littman. 1998. Function of the chemokine receptor CXCR4 in haematopoiesis and in cerebellar development. *Nature* 393:595-599.
61. Nagasawa, T., S. Hirota, K. Tachibana, N. Takakura, S.-i. Nishikawa, Y. Kitamura, N. Yoshida, H. Kikutani, and T. Kishimoto. 1996. Defects of B-cell lymphopoiesis and bone-marrow myelopoiesis in mice lacking the CXC chemokine PBSF/SDF-1. *Nature* 382:635-638.
62. Nagasawa, T., K. Tachibana, and T. Kishimoto. 1998. A novel CXC chemokine PBSF/SDF-1 and its receptor CXCR4: their functions in develpoment, hematopoiesis and HIV infection. *Seminars in Immunology* 10:179-185.
63. Campbell, J. J., J. Pan, and E. C. Butcher. 1999. Cutting Edge: developmental switches in chemokine responses during T cell maturation. *Journal of Immunology* 163:2353-2357.
64. Kim, C. H., L. M. Pelus, J. R. White, and H. E. Broxmeyer. 1998. Differential chemotactic behavior of developing T cells in response to thymic chemokines. *Blood* 91:4434-4443.
65. Ueno, T., F. Saito, D. H. D. Gray, S. Kuse, K. Hieshima, H. Nakano, T. Kakiuchi, M. Lipp, R. L. Boyd, and Y. Takahama. 2004. CCR7 Signals Are Essential for Cortex-Medulla Migration of Developing Thymocytes. *The Journal of Experimental Medicine* 200:493-505.
66. Misslitz, A., O. Pabst, G. Hintzen, L. Ohl, E. Kremmer, H. T. Petrie, and R. Forster. 2004. Thymic T Cell Development and Progenitor Localization Depend on CCR7. *The Journal of Experimental Medicine* 200:481-491.
67. Luther, S. A., H. L. Tang, P. L. Hyman, A. G. Farr, and J. G. Cyster. 2000. Coexpression of the chemokines ELC and SLC by T zone stromal cells and deletion of the ELC gene in the plt/plt mouse. *Proceedings of the National Academy of Sciences of the United States of America* 97:12694-12699.

68. Vassileva, G., H. Soto, A. Zlotnik, H. Nakano, T. Kakiuchi, J. A. Hedrick, and S. A. Lira. 1999. The Reduced Expression of 6ckine in the plt Mouse Results from the Deletion of One of Two 6ckine Genes. *The Journal of Experimental Medicine* 190:1183-1188.
69. Davalos-Misslitz, A. C. M., T. Worbs, S. Willenzon, G. Bernhardt, and R. Forster. 2007. Impaired responsiveness to T-cell receptor stimulation and defective negative selection of thymocytes in CCR7-deficient mice. *Blood* 110:4351-4359.
70. Kurobe, H., C. Liu, T. Ueno, F. Saito, I. Ohigashi, N. Seach, R. Arakaki, Y. Hayashi, T. Kitagawa, M. Lipp, R. L. Boyd, and Y. Takahama. 2006. CCR7-Dependent Cortex-to-Medulla Migration of Positively Selected Thymocytes Is Essential for Establishing Central Tolerance. *Immunity* 24:165-177.
71. Forster, R., A. C. Davalos-Misslitz, and A. Rot. 2008. CCR7 and its ligands: balancing immunity and tolerance. *Nature Reviews Immunology* 8:362-371.
72. Ansel, K. M., and J. G. Cyster. 2001. Chemokines in lymphopoiesis and lymphoid organ development. *Current Opinion in Immunology* 13:172-179.
73. Mebius, R. E. 2003. Organogenesis of lymphoid tissues. *Nat Rev Immunol* 3:292-303.
74. Cupedo, T., and R. E. Mebius. 2003. Role of chemokines in the development of secondary and tertiary lymphoid tissues. *Seminars in Immunology* 15:243-248.
75. Muller, G., U. E. Hopken, H. Stein, and M. Lipp. 2002. Systemic immunoregulatory and pathogenic functions of homeostatic chemokine receptors. *Journal of Leukocyte Biology* 72:1-8.
76. Cyster, J. G. 2005. Chemokines, Sphingosine-1-Phosphate, and Cell Migration in Secondary Lymphoid Organs. *Annual Review of Immunology* 23:127-159.
77. Forster, R., A. Schubel, D. Breitfeld, E. Kremmer, I. Renner-Muller, E. Wolf, and M. Lipp. 1999. CCR7 coordinates the primary immune response by establishing functional microenvironments in secondary lymphoid organs. *Cell* 99:23-33.
78. Nakano, H., and M. D. Gunn. 2001. Gene Duplications at the Chemokine Locus on Mouse Chromosome 4: Multiple Strain-Specific Haplotypes and the Deletion of Secondary Lymphoid-Organ Chemokine and EBI-1 Ligand Chemokine Genes in the plt Mutation. *J Immunol* 166:361-369.
79. Gunn, M. D., S. Kyuwa, C. Tam, T. Kakiuchi, A. Matsuzawa, L. T. Williams, and H. Nakano. 1999. Mice lacking expression of secondary lymphoid organ chemokine have defects in lymphocyte homing and dendritic cell localization. *Journal of Experimental Medicine* 189:451-460.
80. Förster, R., A. E. Mattis, E. Kremmer, E. Wolf, G. Brem, and M. Lipp. 1996. A Putative Chemokine Receptor, BLR1, Directs B Cell Migration to Defined Lymphoid Organs and Specific Anatomic Compartments of the Spleen. *Cell* 87:1037-1047.
81. Ansel, K. M., V. N. Ngo, P. L. Hyman, S. A. Luther, R. Forster, J. D. Sedgwick, J. L. Browning, M. Lipp, and J. G. Cyster. 2000. A chemokine-driven positive feedback loop organizes lymphoid follicles. *Nature* 406:309-314.
82. Shi, K., K. Hayashida, M. Kaneko, J. Hashimoto, T. Tomita, P. E. Lipsky, H. Yoshikawa, and T. Ochi. 2001. Lymphoid chemokine B cell-attracting chemokine-1 (CXCL13) is expressed in germinal center of ectopic lymphoid follicles within the synovium of chronic arthritis patients. *Journal of Immunology* 166:650-655.
83. Hjelmstrom, P., J. Fjell, T. Nakagawa, R. Sacca, C. A. Cuff, and N. H. Ruddle. 2000. Lymphoid tissue homing chemokines are expressed in chronic inflammation. *American Journal of Pathology* 156:1133-1138.
84. Smiley, S. T., J. A. King, and W. W. Hancock. 2001. Fibrinogen stimulates macrophage chemokine secretion through Toll-Like Receptor 4. *Journal of Immunology* 167:2887-2894.

85. Devaney, J. M., C. M. Greene, C. C. Taggart, T. P. Carroll, S. J. O'Neill, and N. G. McElvaney. 2003. Neutrophil elastase up-regulates interleukin-8 via toll-like receptor 4. *FEBS Letters* 544:129-132.
86. Biragyn, A., P. A. Ruffini, C. A. Leifer, E. Klyushnenkova, A. Shakhov, O. Chertov, A. K. Shirakawa, J. M. Farber, D. M. Segal, J. J. Oppenheim, and L. W. Kwak. 2002. Toll-like receptor 4-dependent activation of dendritic cells by beta -defensin 2. *Science* 298:1025-1029.
87. Janeway, C. A., and R. Medzhitov. 2002. Innate immune recognition. *Annual Review of Immunology* 20:197-216.
88. Charo, I. F., and R. M. Ransohoff. 2006. The many roles of chemokines and chemokine receptors in inflammation. *The New England Journal of Medicine* 354:610-621.
89. Cavanagh, L. L., and U. H. Von Andrian. 2002. Travellers in many guises: The origins and destinations of dendritic cells. *Immunology and Cell Biology* 80:448-462.
90. McKimmie, C. S., M. Moore, A. R. Fraser, T. Jamieson, D. Xu, C. Burt, N. I. Pitman, R. J. Nibbs, I. B. McInnes, F. Y. Liew, and G. J. Graham. 2009. A TLR2 ligand suppresses inflammation by modulation of chemokine receptors and redirection of leukocyte migration. *Blood* 113:4224-4231.
91. Martin-Fontecha, A., S. Sebastiani, U. E. Hopken, M. Uguccioni, M. Lipp, A. Lanzavecchia, and F. Sallusto. 2003. Regulation of dendritic cell migration to the draining lymph node: impact on T lymphocyte traffic and priming. *Journal of Experimental Medicine* 198:615-621.
92. Ngo, V. N., H. Korner, M. D. Gunn, K. N. Schmidt, D. Sean Riminton, M. D. Cooper, J. L. Browning, J. D. Sedgwick, and J. G. Cyster. 1999. Lymphotoxin {alpha}/{beta} and Tumor Necrosis Factor Are Required for Stromal Cell Expression of Homing Chemokines in B and T Cell Areas of the Spleen. *J. Exp. Med.* 189:403-412.
93. Debes, G. F., C. N. Arnold, A. J. Young, S. Krautwald, M. Lipp, J. B. Hay, and E. C. Butcher. 2005. CC chemokine receptor 7 required for T lymphocyte exit from peripheral tissues. *Nature Immunology* 6:889-894.
94. Bromley, S. K., T. R. Mempel, and A. D. Luster. 2008. Orchestrating the orchestrators: chemokines in control of T cell traffic. *Nature Immunology* 9:970-980.
95. Moser, B., and P. Loetscher. 2001. Lymphocyte traffic control by chemokines. *Nature Immunology* 2:123-128.
96. Bromley, S. K., D. A. Peterson, M. D. Gunn, and M. L. Dustin. 2000. Cutting Edge: hierarchy of chemokine receptor and TCR signals regulating T cell migration and proliferation. *Journal of immunology* 165:15-19.
97. Weaver, C. T., and R. D. Hatton. 2009. Interplay between the TH17 and TReg cell lineages: a (co-)evolutionary perspective. *Nat Rev Immunol* 9:883-889.
98. Korn, T., E. Bettelli, M. Oukka, and V. K. Kuchroo. 2009. IL-17 and Th17 Cells. *Annual Review of Immunology* 27:485-517.
99. Weaver, C. T., L. E. Harrington, P. R. Mangan, M. Gavrieli, and K. M. Murphy. 2006. Th17: An Effector CD4 T Cell Lineage with Regulatory T Cell Ties. *Immunity* 24:677-688.
100. Littman, D. R., and A. Y. Rudensky. 2010. Th17 and Regulatory T Cells in Mediating and Restraining Inflammation. *Cell* 140:845-858.
101. Samy, E. T., K. M. Wheeler, R. J. Roper, C. Teuscher, and K. S. K. Tung. 2008. Cutting Edge: Autoimmune Disease in Day 3 Thymectomized Mice Is Actively Controlled by Endogenous Disease-Specific Regulatory T Cells. *The Journal of Immunology* 180:4366-4370.

102. Fontenot, J. D., M. A. Gavin, and A. Y. Rudensky. 2003. Foxp3 programs the development and function of CD4+CD25+ regulatory T cells. *Nat Immunol* 4:330-336.
103. Hori, S., T. Nomura, and S. Sakaguchi. 2003. Control of Regulatory T Cell Development by the Transcription Factor Foxp3. *Science* 299:1057-1061.
104. Khattri, R., T. Cox, S.-A. Yasayko, and F. Ramsdell. 2003. An essential role for Scurfin in CD4+CD25+ T regulatory cells. *Nat Immunol* 4:337-342.
105. Groux, H., A. O'Garra, M. Bigler, M. Rouleau, S. Antonenko, J. E. De Vries, and M. G. Roncarolo. 1997. A CD4+ T cell subset inhibits antigen specific T cell responses and prevents colitis. *Nature* 389:737-742.
106. Chen, W., W. Jin, N. Hardegen, K.-j. Lei, L. Li, N. Marinos, G. McGrady, and S. M. Wahl. 2003. Conversion of Peripheral CD4+CD25- Naive T Cells to CD4+CD25+ Regulatory T Cells by TGF-beta Induction of Transcription Factor Foxp3. *The Journal of Experimental Medicine* 198:1875-1886.
107. Mantel, P.Y., H. Kuipers, O. Boyman, C. Rhyner, N. Ouaked, B. Ruckert, C. Karagiannidis, B. N. Lambrecht, R. W. Hendriks, R. Crameri, C. A. Akdis, K. Blaser, and C. B. Schmidt-Weber. 2007. GATA3-Driven Th2 Responses Inhibit TGF-beta Induced FOXP3 Expression and the Formation of Regulatory T Cells. *PLoS Biol* 5:2847-2861.
108. Dardalhon, V., A. Awasthi, H. Kwon, G. Galileos, W. Gao, R. A. Sobel, M. Mitsdoerffer, T. B. Strom, W. Elyaman, I. C. Ho, S. Khoury, M. Oukka, and V. K. Kuchroo. 2008. IL-4 inhibits TGF-beta induced Foxp3+ T cells and, together with TGF-beta, generates IL-9+ IL-10+ Foxp3- effector T cells. *Nature Immunology* 9:1347-1355.
109. Veldhoen, M., C. Uyttenhove, J. van Snick, H. Helmby, A. Westendorf, J. Buer, B. Martin, C. Wilhelm, and B. Stockinger. 2008. Transforming growth factor-beta 'reprograms' the differentiation of T helper 2 cells and promotes an interleukin 9-producing subset. *Nature Immunology* 9:1341-1346.
110. Kim, C. H., L. S. Rott, I. Clark-Lewis, D. J. Campbell, L. Wu, and E. C. Butcher. 2001. Subspecialization of Cxcr5+ T Cells. *The Journal of Experimental Medicine* 193:1373-1382.
111 Kim, C. H., H. W. Lim, J. R. Kim, L. Rott, P. Hillsamer, and E. C. Butcher. 2004. Unique gene expression program of human germinal center T helper cells. *Blood* 104:1952-1960.
112. Ebert, L. M., M. P. Horn, A. B. Lang, and B. Moser. 2004. B cells alter the phenotype and function of follicular-homing CXCR5+ T cells. *European Journal of Immunology* 34:3562-3571.
113. Sallusto, F., D. Lenig, R. Forster, M. Lipp, and A. Lanzavecchia. 1999. Two subsets of memory T lymphocytes with distinct homing potentials and effector functions. *Nature* 401:708-712.
114. Legler, D. F., M. Loetscher, R. S. Roos, I. Clark-Lewis, M. Baggiolini, and B. Moser. 1998. B cell-attracting chemokine 1, a human CXC chemokine expressed in lymphoid tissues, selectively attracts B lymphocytes via BLR1/CXCR5. *Journal of Experimental Medicine* 187:655-660.
115. ``Gunn, M. D., V. N. Ngo, K. M. Ansel, E. H. Ekland, J. G. Cyster, and L. T. Williams. 1998. A B-cell-homing chemokine made in lymphoid follicles activates Burkitt's lymphoma receptor-1. *Nature* 391:799-803.
116. Forster, R., A. E. Mattis, E. Kremmer, E. Wolf, G. Brem, and M. Lipp. 2002. A putative chemokine receptor, BRL1, directs B cell migration to defined lymphoid organs and specific anatomic compartments of the spleen. *Cell* 87:1037-1047.

117. Dudda, J. C., J. C. Simon, and S. Martin. 2004. Dendritic cell immunization route determines CD8+ T cell trafficking to inflamed skin: role for tissue microenvironment and dendritic cells in establishment of T cell-homing subsets. *Journal of Immunology* 172:857-863.
118. Campbell, D. J., and E. C. Butcher. 2002. Rapid acquisition of tissue-specific homing phenotypes by CD4+ T cells activated in cutaneous or mucosal lymphoid tissues. *Journal of Experimental Medicine* 195:135-141.
119. Sigmundsdottir, H., J. Pan, G. F. Debes, C. Alt, A. Habtezion, D. Soler, and E. C. Butcher. 2007. DCs metabolize sunlight-induced vitamin D3 to 'program' T cell attraction to the epidermal chemokine CCL27. *Nat Immunol* 8:285-293.
120. Campbell, J. J., G. Haraldsen, J. Pan, J. Rottman, S. Qin, P. Ponath, D. P. Andrew, R. Warnke, N. Ruffing, N. Kassam, L. Wu, and E. C. Butcher. 1999. The chemokine receptor CCR4 in vascular recognition by cutaneous but not intestinal memory T cells. *Nature* 400:776-780.
121. Homey, B., W. Wang, H. Soto, M. E. Buchanan, A. Wiesenborn, D. Catron, A. Muller, T. K. McClanahan, M.-C. Dieu-Nosjean, R. Orozco, T. Ruzicka, P. Lehmann, E. Oldham, and A. Zlotnik. 2000. Cutting Edge: the orphan chemokine receptor G protein-coupled receptor-2 (GPR-2, CCR10) binds the skin-associated chemokine CCL27 (CTACK/ALP/ILC). *Journal of Immunology* 164:3465-3470.
122. Iwata, M., A. Hirakiyama, Y. Eshima, M. Kagechika, C. Kato, and S.-Y. Song. 2004. Retinoic Acid Imprints Gut-Homing Specificity on T Cells. *Immunity* 21:527-538.
123. Zabel, B. A., W. W. Agace, J. J. Campbell, H. M. Heath, D. Parent, A. I. Roberts, E. C. Ebert, N. Kassam, S. Qin, M. Zovko, G. J. LaRosa, L.-L. Yang, D. Soler, E. C. Butcher, P. D. Ponath, C. M. Parker, and D. P. Andrew. 1999. Human G protein-coupled receptor Gpr-9-6/CC chemokine receptor 9 is selectively expressed on intestinal homing T lymphocytes, mucosal lymphocytes, and thymocytes and is required for thymus-expressed chemokine-mediated chemotaxis. *Journal of Experimental Medicine* 190:1241-1256.
124. Cook, D. N., D. Prosser, M., R. Forster, J. Zhang, N. A. Kuklin, S. J. Abbondanzo, X.-D. Niu, S.-C. Chen, D. J. Manfra, M. T. Wiekowski, L. M. Sullivan, S. R. Smith, H. B. Greenberg, S. Narula, M. Lipp, and S. A. Lira. 2000. CCR6 mediates dendritic cell localisation, lymphocyte homeostasis and immune responses in mucosal tissue. *Immunity* 12:495-503.
125. Damaj, B. B., S. R. McColl, K. Neote, N. Songqing, K. T. Ogborn, C. A. Hebert, and P. H. Naccache. 1996. Identification of G-protein binding sites of the human interleukin-8 receptors by functional mapping of the intracellular loops. *FASEB J.* 10:1426-1434.
126. Kraft, K., H. Olbrich, I. Majoul, M. Mack, A. Proudfoot, and M. Oppermann. 2001. Characterization of Sequence Determinants within the Carboxyl-terminal Domain of Chemokine Receptor CCR5 That Regulate Signaling and Receptor Internalization. *Journal of Biological Chemistry* 276:34408-34418.
127. Alexander, S. P. H., A. Mathie, and J. A. Peters. 2008. Guide to Receptors and Channels (GRAC), 3rd edition. *British Journal of Pharmacology* 153:S1-S1.
128. Graham, G. J. 2009. D6 and the atypical chemokine receptor family:novel regulators of immune and inflammatory processes. *European Journal of Immunology* 39:342-351.
129. Hansell, C., and R. Nibbs. 2007. Professional and Part-Time Chemokine Decoys in the Resolution of Inflammation. *Science* 384.
130. Nibbs, R. J., S. M. Wylie, J. Yang, N. R. Landau, and G. J. Graham. 1997. Cloning and characterization of a novel promiscuous human beta-chemokine receptor D6. *The Journal of Biological Chemistry* 272:32078-32083.

131. Nibbs, R. J., S. M. Wylie, I. B. Pragnell, and G. J. Graham. 1997. Cloning and characterization of a novel murine beta-chemokine receptor, D6. *The Journal of Biological Chemistry* 272:12495-12504.
132. Struyf, S., P. Proost, and J. Van Damme. 2003. Regulation of the imune response by the interaction of chemokines and proteases. *Advances in Immunology* 81:1-44.
133. Nibbs, R. J., J. Yang, N. R. Landau, J.-H. Mao, and G. J. Graham. 1999. LD78beta, A non-allelic variant of human MIP-1alpha (LD78alpha), has enhanced receptor interactions and potent HIV suppressive activity. *The Journal of Biological Chemistry* 274:17478-17483.
134. Blackburn, P. E., C. V. Simpson, R. J. Nibbs, M. O'Hara, R. Booth, J. Poulos, N. W. Isaacs, and G. J. Graham. 2004. Purification and biochemical characterisation of the D6 chemokine receptor. *Biochemical Journal* 379:263-272.
135. Fra, A. M., M. Locati, K. Otero, M. Sirino, P. Signorelli, M. L. Massardi, M. Gobbi, A. Vecchi, S. Sozzani, and A. Mantovani. 2003. Cutting Edge: Scavenging of Inflammatory CC Chemokines by the Promiscuous Putatively Silent Chemokine Receptor D6. *The Jounal of Immunology* 170:2279-2282.
136. Weber, M., E. Blair, C. V. Simpson, M. O'Hara, P. E. Blackburn, A. Rot, G. J. Graham, and R. J. Nibbs. 2004. The chemokine receptor D6 constitutively traffics to and from the cell surface to internalize and degrade chemokines. *Molecular Biology of the Cell* 15:2492-2508.
137. Bonecchi, R., E. M. Borroni, A. Anselmo, A. Doni, B. Savino, M. Mirolo, M. Fabbri, V. R. Jala, B. Haribabu, A. Mantovani, and M. Locati. 2008. Regulation of D6 chemokine scavenging activity by ligand and Rab11-dependent surface upregulation. *Blood* 112:493-503.
138. McCulloch, C. V., V. Morrow, S. Milasta, I. Comerford, G. Milligan, G. J. Graham, N. W. Isaacs, and R. J. B. Nibbs. 2008. Multiple roles for the C-terminal tail of the chemokine scavenger D6. *The Journal of Biological Chemistry* 283:7972-7982.
139. Galliera, E., V. R. Jala, J. O. Trent, R. Bonecchi, P. Signorelli, R. J. Lefkowitz, A. Mantovani, M. Locati, and B. Haribabu. 2004. beta-arrestin- dependent constitutive internalization of the human chemokine decoy receptor D6. *The Journal of Biological Chemistry* 279:25590-25597.
140. Rot, A., J.-Y. Springael, C. Burt, M. Parmentier, T. Jamieson, L. Thorpe, C. McKimmie, M. Pruenster, R. Horuk, and G. J. Graham. 2009. Cell autonomous regulation of neutrophil migration by the D6 chemokine decoy receptor. *submitted*.
141. Bonecchi, R., M. Locati, E. Galliera, M. Vulcano, M. Sironi, A. M. Fra, M. Gobbi, A. Vecchi, S. Sozzani, B. Haribabu, J. Van Damme, and A. Mantovani. 2004. Differential recognition and scavenging of native and truncated macrophage-derived chemokine (macrophage-derived chemokine/CC chemokine ligand 22) by the D6 decoy receptor. *The Journal of Immunology* 172:4972-4976.
142. Nibbs, R. J., D. S. Gilchrist, V. King, A. Ferra, S. Forrow, K. D. Hunter, and G. J. Graham. 2007. The atypical chemokine receptor D6 suppresses the development of chemically induced skin tumours. *The Journal of Clinical Investigation* 117:1884-1892.
143. Nibbs, R. J., E. Kriehuber, P. D. Ponath, D. Parent, S. Qin, J. D. Campbell, A. Henderson, D. Kerjaschki, D. Maurer, G. J. Graham, and A. Rot. 2001. The beta-chemokine receptor D6 is expressed by lymphatic endothelium and a subset of vascular tumors. *American Journal of Pathology* 158:867-877.
144. McKimmie, C. S., A. R. Fraser, C. Hansell, L. Gutierrez, S. Philipsen, L. Connell, A. Rot, M. Kurowska-Stolarska, P. Carreno, M. Pruenster, C.-C. Chu, G. Lombardi, C. Halsey, I. B. McInnes, F. Y. Liew, R. J. Nibbs, and G. J. Graham. 2008.

Hematopoietic cell expression of the chemokine decoy receptor D6 is dynamic and regulated by GATA1. *The Journal of Immunology* 181:8171-8181.

145. McKimmie, C. S., and G. J. Graham. 2006. Leukocyte expression of the chemokine scavenger D6. *Biochemical Society Transactions* 34:1002-1004.
146. Wu, F.-Y., Z.-L. Ou, L.-Y. Feng, J.-M. Luo, L.-P. Wang, Z.-Z. Shen, and Z.-M. Shao. 2008. Chemokine decoy receptor D6 plays a negative role in human breast cancer. *Molecular Cancer Research* 6:1276-1288.
147. Kin, N. W., D. M. Crawford, J. Liu, T. W. Behrens, and J. F. Kearney. 2008. DNA Microarray Gene Expression Profile of Marginal Zone versus Follicular B Cells and Idiotype Positive Marginal Zone B Cells before and after Immunization with Streptococcus pneumoniae. *J Immunol* 180:6663-6674.
148. Graham, G. J., and C. S. McKimmie. 2006. Chemokine scavenging by D6: a moveable feast? *Trends in Immunology* 27:381-386.
149. Martinez de la Torre, Y., M. Locati, C. Buracchi, J. Dupor, D. N. Cook, R. Bonecchi, M. Nebuloni, D. Rukavina, L. Vago, A. Vecchi, S. A. Lira, and A. Mantovani. 2005. Increased inflammation in mice deficient for the chemokine decoy receptor D6. *European Journal of Immunology Highlights* 35:1342-1346.
150. Borroni, E. M., C. Buracchi, Y. Martinez de la Torre, E. Galliera, A. Vecchi, R. Bonecchi, A. Mantovani, and M. Locati. 2006. The chemoattractant decoy receptor D6 as a negative regulator of inflammatory responses. *Biochemical Society Transactions* 34:1014-1017.
151. Martinez de la Torre, Y., C. Buracchi, E. M. Borroni, J. Dupor, R. Bonecchi, M. Nebuloni, F. Pasqualini, A. Doni, E. Lauri, C. Agostinis, R. Bulla, D. N. Cook, B. Haribabu, P. Meroni, D. Rukavina, L. Vago, F. Tedesco, A. Vecchi, S. A. Lira, M. Locati, and A. Mantovani. 2007. Protection against inflammation- and autoantibody- caused fetal loss by the chemokine decoy receptor D6. *Proceedings of the National Academy of Sciences* 104:2319-2324.
152. Jamieson, T., D. N. Cook, R. J. Nibbs, A. Rot, C. Nixon, P. McLean, A. Alcami, S. A. Lira, M. Wiekowski, and G. J. Graham. 2005. The chemokine receptor D6 limits the inflammatory response in vivo. *Nature Immunology* 6:403-411.
153. Liu, L., G. J. Graham, A. Damodaran, T. Hu, S. A. Lira, M. Sasse, C. Canasto-Chibuque, D. N. Cook, and R. M. Ransohoff. 2006. Cutting Edge: the silent chemokine receptor D6 is required for generating T cell responses that mediate experimental autoimmune encephalomyelitis. *The Journal of Immunology* 177:17-21.
154. Ransohoff, R. M. 2009. Chemokines and Chemokine Receptors: Standing at the Crossroads of Immunobiology and Neurobiology. *Immunity* 31:711-721.
155. Whitehead, G. S., T. Wang, L. M. DeGraff, J. W. Card, S. A. Lira, G. J. Graham, and D. N. Cook. 2007. The chemokine receptor D6 has opposing effects on allergic inflammation and airway reactivity. *American Journal of Respiratory and Critical Care Medicine* 175:243-249.
156. Colotta, F., P. Allavena, A. Sica, C. Garlanda, and A. Mantovani. 2009. Cancer-related inflammation, the seventh hallmark of cancer: links to genetic instability. *Carcinogenesis* 30:1073-1081.
157. Di Liberto, D., M. Locati, N. Caccamo, A. Vecchi, S. Meraviglia, A. Salerno, G. Sireci, M. Nebuloni, N. Cacere, P.-J. Cardona, F. Dieli, and A. Mantovani. 2008. Role of the chemokine decoy receptor D6 in balancing inflammation, immune activation, and antimicrobial resistance in Mycobacterium tuberculosis infection. *Journal of Experimental Medicine* 205:2075-2084.
158. Vetrano, S., E. M. Borroni, A. Sarukhan, B. Savino, R. Bonecchi, C. Correale, V. Arena, M. Fantini, M. Roncalli, A. Malesci, A. Mantovani, M. Locati, and S. Danese.

2009. The lymphatic system controls intestinal inflammation and inflammation-associated colon cancer through the chemokine decoy receptor D6. *Gut* 59:197-206.

159. Bordon, Y., C. A. H. Hansell, D. P. Sester, M. Clarke, A. M. Mowat, and R. J. B. Nibbs. 2009. The Atypical Chemokine Receptor D6 Contributes to the Development of Experimental Colitis. *The Journal of Immunology* 182:5032-5040.
160. Berres, M.-L., C. Trautwein, M. M. Zaldivar, P. Schmitz, K. Pauels, S. A. Lira, F. Tacke, and H. E. Wasmuth. 2009. The chemokine scavenging receptor D6 limits acute toxic liver injury in vivo. *Biological Chemistry* 390:1039-1045.
161. Wiederholt, T., M. von Westernhagen, M. M. Zaldivar, M.-L. Berres, P. Schmitz, C. Hellerbrand, T. Muller, T. Berg, C. Trautwein, and H. E. Wasmuth. 2008. Genetic variations of the chemokine scavenger receptor D6 are associated with liver inflammation in chronic hepatitis C. *Human Immunology* 69:861-866.
162. Miller, L. H., S. J. Mason, J. A. Dvorak, M. H. McGinniss, and I. K. Rothman. 1975. Erythrocyte receptors for (Plasmodium knowlesi) malaria: Duffy blood group determinants. *Science* 189:561-563.
163. Neote, K., J. Y. Mak, L. F. Kolakowski, Jr., and T. J. Schall. 1994. Functional and biochemical analysis of the cloned Duffy antigen: identity with the red blood cell chemokine receptor. *Blood* 84:44-52.
164. Tournamille, C., Y. Colin, J. P. Cartron, and C. Le Van Kim. 1995. Disruption of a GATA motif in the Duffy gene promoter abolishes erythroid gene expression in Duffy-negative individuals. *Nature Genetics* 10:224-228.
165. Darbonne, W. C., G. C. Rice, M. A. Mohler, T. Apple, C. A. Hebert, A. J. Valente, and J. B. Baker. 1991. Red blood cells are a sink for interleukin 8, a leukocyte chemotaxin. *Journal of Clinical Investigation* 88:1362-1369.
166. Dawson, T. C., A. B. Lentsch, Z. Wang, J. E. Cowhig, A. Rot, N. Maeda, and S. C. Peiper. 2000. Exaggerated response to endotoxin in mice lacking the Duffy antigen/receptor for chemokines (DARC). *Blood* 96:1681-1684.
167. Fukuma, N., N. Akimutsu, H. Hamamoto, H. Kusuhara, Y. Sugiyama, and K. Sekimizu. 2003. A role of the Duffy antigen for the maintenance of plasma chemokine concentrations. *Biochemical and Biophysical Research Communications* 303:137-139.
168. Pruenster, M., L. Mudde, P. Bombosi, S. Dimitrova, M. Zsak, J. Middleton, A. Richmond, G. J. Graham, S. Segerer, R. J. B. Nibbs, and A. Rot. 2009. The Duffy antigen receptor for chemokines transports chemokines and supports their promigratory activity. *Nature Immunology* 10:101-108.
169. Shen, H., R. Schuster, K. F. Stringer, S. E. Waltz, and A. B. Lentsch. 2006. The Duffy antigen/receptor for chemokines (DARC) regulates prostate tumour growth. *FASEB J.* 20:59-64.
170. Pruenster, M., and A. Rot. 2006. Throwing light on DARC. *Biochemical Society Transactions* 34:1005-1008.
171. Middleton, J., S. Neil, J. Wintle, I. Clark-Lewis, H. Moore, C. Lam, M. Auer, E. Hub, and A. Rot. 1997. Transcytosis and surface presentation of IL-8 by venular endothelial cells. *Cell* 91:385-395.
172. Lee, J. S., C. W. Frevert, M. M. Wurfel, S. C. Peiper, V. A. Wong, K. K. Ballman, J. T. Ruzinski, J. S. Rhim, T. R. Martin, and R. B. Goodman. 2003. Duffy antigen facilitates movement of chemokine across the endothelium in vitro and promotes neutrophil transmigration in vitro and in vivo. *Journal of Immunology* 170:5244-5251.
173. Gosling, J., D. J. Dairaghi, Y. Wang, M. Hanley, D. Talbot, Z. Miao, and T. J. Schall. 2000. Cutting Edge: identification of a novel chemokine receptor that binds

dendritic cell- and T cell-active chemokines including ELC, SLC, and TECK. *Journal of Immunology* 164:2851-2856.

174. Townson, J. R., and R. J. B. Nibbs. 2002. Characterization of mouse CCX-CKR, a receptor for the lymphocyte-attracting chemokines TECK/mCCL25, SLC/mCCL21 and MIP-3{beta}/mCCL19: comparison to human CCX-CKR. *European Journal of Immunology* 32:1230-1241.
175. Heinzel, K., C. Benz, and C. C. Bleul. 2007. A silent chemokine receptor regulates steady-state leukocyte homing in vivo. *Proceedings of the National Academy of Sciences* 104:8421-8426.
176. Comerford, I., S. Milasta, V. Morrow, G. Milligan, and R. Nibbs. 2006. The chemokine receptor CCX-CKR mediates effective scavenging of CCL19 in vitro. *European Journal of Immunology* 36:1904-1916.
177. Burns, J. M., B. C. Summers, Y. Wang, A. Melikian, R. Berahovich, Z. Miao, M. E. Penfold, M. J. Sunshine, D. R. Littman, C. J. Kuo, K. Wei, B. E. McMaster, K. Wright, M. C. Howard, and T. J. Schall. 2006. A novel chemokine receptor for SDF-1 and I-TAC involved in cell survival, cell adhesion, and tumor development. *Journal of Experimental Medicine* 203:2201-2213.
178. Balabanian, K., B. Lagane, S. Infantino, K. Y. C. Chow, J. Harriague, B. Moepps, F. Arenzana-Seisdedos, M. Thelen, and F. Bachelerie. 2005. The Chemokine SDF-1/CXCL12 Binds to and Signals through the Orphan Receptor RDC1 in T Lymphocytes. *Journal of Biological Chemistry* 280:35760-35766.
179. Miao, Z., K. E. Luker, B. C. Summers, R. Berahovich, M. S. Bhojani, A. Rehemtulla, C. G. Kleer, J. J. Essner, A. Nasevicius, G. D. Luker, M. C. Howard, and T. J. Schall. 2007. CXCR7 (RDC1) promotes breast and lung tumor growth in vivo and is expressed on tumor-associated vasculature. *Proceedings of the National Academy of Sciences* 104:15735-15740.
180. Madden, S. L., B. P. Cook, M. Nacht, W. D. Weber, M. R. Callahan, Y. Jiang, M. R. Dufault, X. Zhang, W. Zhang, J. Walter-Yohrling, C. Rouleau, V. R. Akmaev, C. J. Wang, X. Cao, T. B. St Martin, B. L. Roberts, B. A. Teicher, K. W. Klinger, R. V. Stan, B. Lucey, C.-W. E. B, J. Laterra, and K. A. Walter. 2004. Vascular gene expression in nonneoplastic and malignant brain. *American Journal of Pathology* 165:601-608.
181. Schutyser, E., Y. Su, Y. Yu, M. Gouwy, S. Zaja-Milatovic, J. Van Damme, and A. Richmond. 2007. Hypoxia enhances CXCR4 expression in human microvascular endothelial cells and human melanoma cells. *European Cytokine Network* 18:59-70.
182. Maksym, R. B., M. Tarnowski, K. Grymula, J. Tarnowska, M. Wysoczynski, R. Liu, B. Czerny, J. Ratajczak, M. Kucia, and M. Z. Ratajczak. 2009. The role of stromal-derived factor-1 -- CXCR7 axis in development and cancer. *European Journal of Pharmacology* 625:31-40.
183. Wang, J., Y. Shiozawa, J. Wang, Y. Wang, Y. Jung, K. J. Pienta, R. Mehra, R. Loberg, and R. S. Taichman. 2008. The role of CXCR7/RDC1 as a chemokine receptor for CXCL12/SDF-1 in prostate cancer. *Journal of Biological Chemistry* 283:4283-4294.
184. Boldajipour, B., H. Mahabaleshwar, E. Kardash, M. Reichman-Fried, H. Blaser, S. Minina, D. Wilson, Q. Xu, and E. Raz. 2008. Control of chemokine-guided cell migration by ligand sequestration. *Cell* 132:463-473.
185. Sierro, F., C. Biben, L. Martinez-Munoz, M. Mellado, R. M. Ransohoff, M. Li, B. Woehl, H. Leung, J. Groom, M. Batten, R. P. Harvey, C. Martinez-A, C. R. Mackay, and F. Mackay. 2007. Disrupted cardiac development but normal hematopoiesis in mice deficient in the second CXCL12/SDF-1 receptor, CXCR7. *Proceedings of the National Academy of Sciences* 104:14759-14764.

186. D'Amico, G., G. Frascaroli, G. Bianchi, P. Transidico, A. Doni, A. Vecchi, S. Sozzani, P. Allavena, and A. Mantovani. 2000. Uncoupling of inflammatory chemokine receptors by IL-10: generation of functional decoys. *Nat Immunol* 1:387-391.
187. Cardona, A. E., M. E. Sasse, L. Liu, S. M. Cardona, M. Mizutani, C. Savarin, T. Hu, and R. M. Ransohoff. 2008. Scavenging roles of chemokine receptors: chemokine receptor deficiency is associated with increased levels of ligands in circulation and tissues. *Blood* 112:256-263.
188. Violla, A., and A. D. Luster. 2008. Chemokines and Their Receptors: Drug Targets in Immunity and Inflammation. *Annual Reviews of Pharmacology and Toxicology* 48:171-197.
189. Proudfoot, A. E., T. N. Wells, and P. R. Clapham. 1999. Chemokine receptors - future therapeutic targets for HIV? *Biochemical Pharmacology* 57:451 - 463.
190. Feng, Y., C. C. Broder, P. E. Kennedy, and E. A. Berger. 1996. HIV-1 Entry Cofactor: Functional cDNA Cloning of a Seven-Transmembrane, G Protein-Coupled Receptor. *Science* 272:872-877.
191. Samson, M., F. Libert, B. J. Doranz, J. Rucker, C. Liesnard, C.-M. Farber, S. Saragosti, C. Lapoumeroulie, J. Cognaux, C. Forceille, G. Muyldermans, C. Verhofstede, G. Burtonboy, M. Georges, T. Imai, S. Rana, Y. Yi, R. J. Smyth, R. G. Collman, R. W. Doms, G. Vassart, and M. Parmentier. 1996. Resistance to HIV-1 infection in Caucasian individuals bearing mutant alleles of the CCR-5 chemokine receptor gene. *Nature* 382:722-725.
192. Lim, J. K., W. G. Glass, D. H. McDermott, and P. M. Murphy. 2006. CCR5: no longer a 'good for nothing' gene - chemokine control of West Nile virus infection. *Trends in Immunology* 27:308-312.
193. Kieseier, B. C., M. Tani, D. Mahad, N. Oka, T. Ho, N. Woodroofe, J. W. Griffin, K. V. Toyka, R. M. Ransohoff, and H.-P. Hartung. 2002. Chemokines and chemokine receptors in inflammatory demyelinating neuropathies: a central role for IP-10. *Brain* 125:823-834.
194. Sorensen, T. L., M. Tani, J. Jensen, V. Pierce, C. Lucchinetti, V. A. Folcik, S. Qin, J. Rottman, F. Sellebjerg, R. M. Strieter, J. L. Frederiksen, and R. M. Ransohoff. 1999. Expression of specific chemokines and chemokine receptors in the central nervous system of multiple sclerosis patients. *The Journal of Clinical Investigation* 103:807-815.
195. Elhofy, A., R. W. DePaolo, S. A. Lira, N. W. Lukacs, and W. J. Karpus. 2009. Mice deficient for CCR6 fail to control chronic experimental autoimmune encephalomyelitis. *Journal of Neuroimmunology* 213:91-99.
196. Ricardo, V., C. Vanessa, L. María, A. Luis, Z. Angel, A. Carlos Martínez, and V. Rosa. 2009. CCR6 regulates EAE pathogenesis by controlling regulatory CD4+ T-cell recruitment to target tissues. *European Journal of Immunology* 39:1671-1681.
197. Izikson, L., R. S. Klein, I. F. Charo, H. L. Weiner, and A. D. Luster. 2000. Resistance to experimental autoimmune encephalomyelitis in mice lacking the CC chemokine receptor (CCR)2. *Journal of Experimental Medicine* 192:1075-1080.
198. Takuji, I., O. Hiroshi, T. Yoshiaki, and M. Shigeki. 2008. Molecular aspects of rheumatoid arthritis: chemokines in the joints of patients. *FEBS Journal* 275:4448-4455.
199. Koch, A. E., S. L. Kunkel, L. A. Harlow, B. Johnson, H. L. Evanoff, G. K. Haines, M. D. Burdick, R. M. Pope, and R. M. Strieter. 1992. Enhanced production of monocyte chemoattractant protein-1 in rheumatoid arthritis. *The Journal of Clinical Investigation* 90:772-779.
200. Robinson, E., E. C. Keystone, T. J. Schall, N. Gillett, and E. N. Fish. 1995. Chemokine expression in rheumatoid arthritis (RA): evidence of RANTES and macrophage

inflammatory protein (MIP)-1{beta} production by synovial T cells. *Clinical & Experimental Immunology* 101:398-407.

201. Koch, A. E., S. L. Kunkel, L. A. Harlow, D. D. Mazarakis, G. K. Haines, M. D. Burdick, R. M. Pope, and R. M. Strieter. 1994. Macrophage inflammatory protein-1 alpha. A novel chemotactic cytokine for macrophages in rheumatoid arthritis. *The Journal of Clinical Investigation* 93:921-928.
202. García-Vicuña, R., M. V. Gómez-Gaviro, M. J. Domínguez-Luis, M. K. Pec, I. González-Alvaro, J. M. Alvaro-Gracia, and F. Díaz-González. 2004. CC and CXC chemokine receptors mediate migration, proliferation, and matrix metalloproteinase production by fibroblast-like synoviocytes from rheumatoid arthritis patients. *Arthritis & Rheumatism* 50:3866-3877.
203. Hancock, W. W., B. Lu, W. Gao, V. Csizmadia, K. Faia, J. A. King, S. T. Smiley, M. Ling, N. P. Gerard, and C. Gerard. 2000. Requirement of the chemokine receptor CXCR3 for acute allograft rejection. *Journal of Experimental Medicine* 192:1515-1520.
204. Liang, M., C. Mallari, M. Rosser, H. P. Ng, K. May, S. Monahan, J. G. Bauman, I. Islam, A. Ghannam, B. Buckman, K. Shaw, G.-P. Wei, W. Xu, Z. Zhao, E. Ho, J. Shen, H. Oanh, B. Subramanyam, R. Vergona, D. Taub, L. Dunning, S. Harvey, R. M. Snider, J. Hesselgesser, M. M. Morrissey, H. D. Perez, and R. Horuk. 2000. Identification and characterization of a potent, selective, and orally active antagonist of the CC chemokine receptor-1. *Journal of Biological Chemistry* 275:19000-19008.
205. Gong, J.-H., L. G. Ratkay, J. D. Waterfield, and I. Clark-Lewis. 1997. An antagonist of monocyte chemoattractant protein 1 (MCP-1) inhibits arthritis in the MRL-lpr mouse model. *Journal of Experimental Medicine* 186:131-137.
206. Proudfoot, A. E., R. Buser, F. Borlat, S. Alouani, D. Soler, R. E. Offord, J.-M. Schroder, C. A. Power, and T. N. Wells. 1999. Amino-terminally Modified RANTES Analogues Demonstrate Differential Effects on RANTES Receptors. *Journal of Biological Chemistry* 274:32478-32485.
207. Dragic, T., A. Trkola, D. A. D. Thompson, E. G. Cormier, F. A. Kajumo, E. Maxwell, S. W. Lin, W. Ying, S. O. Smith, T. P. Sakmar, and J. P. Moore. 2000. A binding pocket for a small molecule inhibitor of HIV-1 entry within the transmembrane helices of CCR5. *Proceedings of the National Academy of Sciences of the United States of America* 97:5639-5644.
208. Vandekerckhove, L., C. Verhofstede, and D. Vogelaers. 2008. Maraviroc: integration of a new antiretroviral drug class into clinical practice. *J. Antimicrob. Chemother.* 61:1187-1190.
209. DiPersio, J. F., G. L. Uy, U. Yasothan, and P. Kirkpatrick. 2009. Plerixafor. *Nat Rev Drug Discov* 8:105-107.
210. Inoue, K.-i., H. Takano, R. Yanagisawa, and T. Yoshikawa. 2005. Interleukin-8 Neutralization for COPD. *Chest* 128:464-465.
211. Mahler, D. A., S. Huang, M. Tabrizi, and G. M. Bell. 2004. Efficacy and Safety of a Monoclonal Antibody Recognizing Interleukin-8 in COPD*. *Chest* 126:926-934.
212. Vergunst, C. E., D. M. Gerlag, L. Lopatinskaya, L. Klareskog, M. D. Smith, F. van den Bosch, H. J. Dinant, Y. Lee, T. Wyant, E. W. Jacobson, D. Baeten, and P. P. Tak. 2008. Modulation of CCR2 in rheumatoid arthritis: A double-blind, randomized, placebo-controlled clinical trial. *Arthritis & Rheumatism* 58:1931-1939.
213. Nguyen, D. X., P. D. Bos, and J. Massague. 2009. Metastasis: from dissemination to organ-specific colonization. *Nature Reviews Cancer* 9:274-284.

214. Hariss, R. E., J. Beebe-Donk, and K. K. Namboodiri. 2001. Inverse association of non-steroidal anti-inflammatory drugs and malignant melanoma among women. *Oncology Reports* 8:655-657.
215. Ramirez, C. C., F. Ma, D. G. Federman, and R. S. Kirsner. 2005. Use of Cyclooxygenase Inhibitors and Risk of Melanoma in High-Risk Patients. *Dermatologic Surgery* 31:748-753.
216. Joyce, J. A., and J. W. Pollard. 2009. Microenvironmental regulation of metastasis. *Nature Reviews Cancer* 9:239-252.
217. Balkwill, F. 2009. Tumour necrosis factor and cancer. *Nat Rev Cancer* 9:361-371.
218. Voronov, E., D. S. Shouval, Y. Krelin, E. Cagnano, D. Benharroch, Y. Iwakura, C. A. Dinarello, and R. N. Apte. 2003. IL-1 is required for tumour invasiveness and angiogenesis. *Proceedings of the National Academy of Sciences* 100:2645-2650.
219. Murdoch, C., M. Muthana, S. B. Coffelt, and C. E. Lewis. 2008. The role of myeloid cells in the promotion of tumour angiogenesis. *Nat Rev Cancer* 8:618-631.
220. Krieg, C., and O. Boyman. 2009. The role of chemokines in cancer immune surveillance by the adaptive immune system. *Seminars in Cancer Biology* 19:76-83.
221. Burnet, F. M. 1970. The concept of immunological surveillance. *Progress in Experimental Tumour Research* 13:1-27.
222. Raman, D., P. J. Baugher, Y. M. Thu, and A. Richmond. 2007. Role of chemokines in tumor growth. *Cancer Letters* 256:137-165.
223. Dunn, G. P., L. J. Old, and R. D. Schreiber. 2004. The Immunobiology of Cancer Immunosurveillance and Immunoediting. *Immunity* 21:137-148.
224. Shankaran, V., H. Ikeda, A. T. Bruce, J. M. White, P. E. Swanson, L. J. Old, and R. D. Schreiber. 2001. IFN[gamma] and lymphocytes prevent primary tumour development and shape tumour immunogenicity. *Nature* 410:1107-1111.
225. Girardi, M., D. E. Oppenheim, C. R. Steele, J. M. Lewis, E. Glusac, R. Filler, P. Hobby, B. Sutton, R. E. Tigelaar, and A. C. Hayday. 2001. Regulation of Cutaneous Malignancy by gamma delta T Cells. *Science* 294:605-609.
226. Smyth, M. J., N. Y. Crowe, D. G. Pellicci, K. Kyparissoudis, J. M. Kelly, K. Takeda, H. Yagita, and D. I. Godfrey. 2002. Sequential production of interferon-gamma by NK1.1+ T cells and natural killer cells is essential for the antimetastatic effect of alpha -galactosylceramide. *Blood* 99:1259-1266.
227. Boehm, U., T. Klamp, M. Groot, and J. C. Howard. 1997. Cellular responses to IFN-gamma. *Annual Review of Immunology* 15:749-795.
228. Coughlin, C. M., K. E. Salhany, M. S. Gee, D. C. LaTemple, S. Kotenko, X. Ma, G. Gri, M. Wysocka, J. E. Kim, L. Liu, F. Liao, J. M. Farber, S. Pestka, G. Trinchieri, and W. M. Lee. 1998. Tumour cell responses to IFNgamma affect tumorigenicity and response to IL-12 therapy and antiangiogenesis. *Immunity* 9:25-34.
229. Boon, T., and P. van der Bruggen. 1996. Human tumor antigens recognised by T lymphocytes. *Journal of Experimental Medicine* 183:725-729.
230. Rosenberg, S. A. 1999. A new era for cancer immunotherapy based on the genes that encode cancer antigens. *Immunity* 10:281-287.
231. Groh, V., J. Wu, C. Yee, and T. Spies. 2002. Tumour-derived soluble MIC ligands impair expression of NKG2D and T-cell activation. *Nature* 419:734-738.
232. MacKie, R. M., R. Reid, and B. Junor. 2003. Fatal Melanoma Transferred in a Donated Kidney 16 Years after Melanoma Surgery. *N Engl J Med* 348:567-568.
233. Yee, C., J. A. Thompson, D. Byrd, S. R. Riddell, P. Roche, E. Celis, and P. D. Greenberg. 2002. Adoptive T cell therapy using antigen-specific CD8+ T cell clones for the treatment of patients with metastatic melanoma: In vivo persistence, migration, and antitumor effect of transferred T cells. *Proceedings of the National Academy of Sciences of the United States of America* 99:16168-16173.

234. Khong, H. T., and N. P. Restifo. 2002. Natural selection of tumour variants in the generation of "tumour escape" phenotypes. *Nature Immunology* 3:999-1005.
235. Uyttenhove, C., L. Pilotte, I. Theate, V. Stroobant, D. Colau, N. Parmentier, T. Boon, and B. J. Van den Eynde. 2003. Evidence for a tumoural immune resistance mechanism based on tryptophan degradation by indoleamine 2,3-dioxygenase. *Nature Medicine* 9:1269-1274.
236. DeNardo, D., M. Johansson, and L. Coussens. 2008. Immune cells as mediators of solid tumor metastasis. *Cancer and Metastasis Reviews* 27:11-18.
237. Kakinuma, T., and S. T. Hwang. 2006. Chemokines, chemokine receptors, and cancer metastasis. *Journal of Leukocyte Biology* 79:639-651.
238. Allavena, P., C. Garlanda, M. G. Borello, A. Sica, and A. Mantovani. 2008. Pathways connecting inflammation and cancer. *Current opinion in Genetics & Development* 18:1-8.
239. Lewis, C. E., and J. W. Pollard. 2006. Distinct Role of Macrophages in Different Tumor Microenvironments. *Cancer Res* 66:605-612.
240. Lin, E. Y., J.-F. Li, L. Gnatovskiy, Y. Deng, L. Zhu, D. A. Grzesik, H. Qian, X.-n. Xue, and J. W. Pollard. 2006. Macrophages regulate the angiogenic switch in a mouse model of breast cancer. *Cancer Research* 66:11238-11246.
241. Richmond, A., J. Yang, and Y. Su. 2009. The good and the bad of chemokines/chemokine receptors in melanoma. *Pigment Cell Melanoma Research* 22:175-186.
242. Mantovani, A., S. Sozzani, M. Locati, P. Allavena, and A. Sica. 2002. Macrophage polarisation: tumour-associated macrophages as a paradigm for polarised M2 mononuclear phagocytes. *Trends in Immunology* 23:549-555.
243. Hagemann, T., T. Lawrence, I. McNeish, K. A. Charles, H. Kulbe, R. G. Thompson, S. C. Robinson, and F. Balkwill. 2008. "Re-educating" tumour-associated macrophages by targeting NF-kB. *Journal of Experimental Medicine* 205:1261-1268.
244. Schioppa, T., B. Uranchimeg, A. Saccani, S. K. Biswas, A. Doni, A. Rapisarda, S. Bernasconi, S. Saccani, M. Nebuloni, L. Vago, A. Mantovani, G. Melillo, and A. Sica. 2003. Regulation of the Chemokine Receptor CXCR4 by Hypoxia. *J. Exp. Med.* 198:1391-1402.
245. Klein, C. A. 2009. Parallel progression of primary tumours and metastasis. *Nature Reviews Cancer* 9:302-312.
246. Keeley, E. C., B. Mehrad, R. M. Strieter, and F. V. W. a. G. K. George. 2010. CXC Chemokines in Cancer Angiogenesis and Metastases. In *Advances in Cancer Research*. Academic Press. 91-111.
247. Richmond, A., and H. G. Thomas. 1988. Melanoma growth stimulatory activity: isolation from human melanoma tumours and characterisation of tissue distribution. *Journal of Cellular Biochemistry* 36:185-198.
248. Lasagni, L., M. Francalanci, F. Annunziato, E. Lazzeri, S. Giannini, L. Cosmi, C. Sagrinati, B. Mazzinghi, C. Orlando, E. Maggi, F. Marra, S. Romagnani, M. Serio, and P. Romagnani. 2003. An Alternatively Spliced Variant of CXCR3 Mediates the Inhibition of Endothelial Cell Growth Induced by IP-10, Mig, and I-TAC, and Acts as Functional Receptor for Platelet Factor 4. *The Journal of Experimental Medicine* 197:1537-1549.
249. Ehlert, J. E., C. A. Addison, M. D. Burdick, S. L. Kunkel, and R. M. Strieter. 2004. Identification and Partial Characterization of a Variant of Human CXCR3 Generated by Posttranscriptional Exon Skipping. *The Journal of Immunology* 173:6234-6240.
250. Rinderknecht, M., and M. Detmar. 2008. Tumor lymphangiogenesis and melanoma metastasis. *Journal of Cellular Physiology* 216:347-354.

251. Collins, V. P., R. K. Loeffler, and H. Tivey. 1956. Observations on growth rates of human tumours. *The American Journal of Roentgenology, Radium Therapy and Nuclear Medicine* 76:988-1000.
252. Im, J. H., W. Fu, H. Wang, S. K. Bhatia, D. A. Hammer, M. A. Kowalska, and R. J. Muschel. 2004. Coagulation facilitates tumor cell spreading in the pulmonary vasculature during early metastatic colony formation. *Cancer Research* 64:8613-8619.
253. Nieswandt, B., M. Hafner, B. Echtenacher, and D. N. Mannel. 1999. Lysis of Tumor Cells by Natural Killer Cells in Mice Is Impeded by Platelets. *Cancer Res* 59:1295-1300.
254. Nathanson, S. D. 2003. Insights into the mechanisms of lymph node metastasis. *Cancer* 98:413-423.
255. Hussein, M. R. 2006. Tumour-associated macrophages and melanoma tumourigenesis: integrating the complexity. *International Journal of Experimental Pathology* 87:163-176.
256. Okahara, H., H. Yagita, K. Miyake, and K. Okumura. 1994. Involvement of Very Late Activation Antigen 4 (VLA-4) and Vascular Cell Adhesion Molecule 1 (VCAM-1) in Tumor Necrosis Factor {alpha} Enhancement of Experimental Metastasis. *Cancer Res* 54:3233-3236.
257. Paget, S. 1989. The distribution of secondary growths in cancer of the breast. 1889. *Cancer Metastasis Reviews* 8:98-101.
258. Ewing, J. 1928. *Neoplastic Diseases. A Treatise on Tumous*. W.B. Saunders Co, Philadelphia & London.
259. Chambers, A. F., A. C. Groom, and I. C. MacDonald. 2002. Dissemination and growth of cancer cells in metastatic sites. *Nature Reviews Cancer* 2:563-572.
260. Hiratsuka, S., A. Watanabe, H. Aburatani, and Y. Maru. 2006. Tumour-mediated upregulation of chemoattractants and recruitment of myeloid cells predetermines lung metastasis. *Nat Cell Biol* 8:1369-1375.
261. Kaplan, R. N., R. D. Riba, S. Zacharoulis, A. H. Bramley, L. Vincent, C. Costa, D. D. MacDonald, D. K. Jin, K. Shido, S. A. Kerns, Z. Zhu, D. Hicklin, Y. Wu, J. L. Port, N. Altorki, E. R. Port, D. Ruggero, S. V. Shmelkov, K. K. Jensen, S. Rafii, and D. Lyden. 2005. VEGFR1-positive haematopoietic bone marrow progenitors initiate the pre-metastatic niche. *Nature* 438:820-827.
262. Rafii, S., and D. Lyden. 2006. S100 chemokines mediate bookmarking of premetastatic niches. *Nature Cell Biology* 8:1321-1323.
263. Psaila, B., and D. Lyden. 2009. The metastatic niche: adapting the foreign soil. *Nature Reviews Cancer* 9:285-293.
264. Zaidi, M. R., C.-P. Day, and G. Merlino. 2008. From UVs to Metastases: Modeling Melanoma Initiation and Progression in the Mouse. *Journal of Investigative Dermatology* 128:2381-2391.
265. Ascierto, P. A., S. Scala, A. Ottaiano, E. Simeone, I. de Michele, G. Palmieri, and G. Castello. 2006. Adjuvant treatment of malignant melanom: where are we? *Critical Reviews in Oncology/Hematology* 57:45-52.
266. Harlin, H., Y. Meng, A. C. Peterson, Y. Zha, M. Tretiakova, C. Slingluff, M. McKee, and T. F. Gajewski. 2009. Chemokine Expression in Melanoma Metastases Associated with CD8+ T-Cell Recruitment. *Cancer Research* 69:3077-3085.
267. Zbytek, B., J. Carlson, Andrew, J. Granese, J. Ross, M. C. Mihm, and A. Slominski. 2008. Current concepts of metastasis in melanoma. *Expert Reviews in Dermatology* 3:569-585.
268. Gauci, C. L., and P. Alexander. 1975. The macrophage content of some human tumours. *Cancer Letters* 1:29-32.

269. Payne, A. S., and L. A. Cornelius. 2002. The Role of Chemokines in Melanoma Tumor Growth and Metastasis. *Journal of Investigative Dermatology* 118:915-922.
270. Robinson, S. C., K. A. Scott, and F. Balkwill. 2002. Chemokine stimulation of monocyte matrix metalloproteinase-9 requires endogenous TNF-alpha. *European Journal of Immunology* 32:404-412.
271. Hartmann, E., B. Wollenberg, S. Rothenfusser, M. Wagner, D. Wellisch, B. Mack, T. Giese, O. Gires, S. Endres, and G. Hartmann. 2003. Identification and functional analysis of tumor-infiltrating plasmacytoid dendritic cells in head and neck cancer. *Cancer Research* 63:6478-6487.
272. Fuertes, M. B., M. V. Girart, L. L. Molinero, C. I. Domaica, L. E. Rossi, M. M. Barrio, J. Mordoh, G. A. Rabinovich, and N. W. Zwirner. 2008. Intracellular retention of the NKG2D ligand MHC class I chain-related gene A in human melanomas confers immune privilege and prevents NK cell-mediated cytotoxicity. *Journal of Immunology* 180:4606-4614.
273. Murakami, T., A. R. Cardones, S. E. Finkelstein, N. P. Restifo, B. A. Klaunberg, F. O. Nestle, S. S. Castillo, P. A. Dennis, and S. T. Hwang. 2003. Immune evasion by murine melanoma mediated through CC chemokine receptor- 10. *The Journal of Experimental Medicine* 198:1337-1347.
274. Murakami, T., A. R. Cardones, and S. T. Hwang. 2004. Chemokine receptors and melanoma metastasis. *Journal of Dermatological Science* 36:71-78.
275. Navarini-Meury, A. A., and C. Conrad. 2009. Melanoma and innate immunity-Active inflammation or just erroneous attraction? Melanoma as the source of leukocyte-attracting chemokines. *Seminars in Cancer Biology* 19:84-91.
276. Singh, S., K. C. Nannuru, A. Sadanandam, M. L. Varney, and R. K. Singh. 2009. CXCR1 and CXCR2 enhances human melanoma tumourigenesis, growth and invasion. *British Journal of Cancer* 100:1638-1646.
277. Varney, M. L., S. L. Johansson, and R. K. Singh. 2006. Distinct expression of CXCL8 and its receptors CXCR1 and CXCR2 and their association with vessel density and aggressiveness in malignant melanoma. *American Journal of Clinical Pathology* 125:209-216.
278. Monteagudo, C., J. M. Martin, E. Jorda, and A. Llombart-Bosch. 2007. CXCR3 chemokine receptor immunoreactivity in primary cutaneous malignant melanoma: correlation with clinicopathological prognostic factors. *Journal of Clinical Pathology* 60:596-599.
279. Seidl, H., E. Richtig, H. Tilz, M. Stefan, U. Schmidbauer, M. Asslaber, K. Zatloukal, M. Herlyn, and H. Schaider. 2007. Profiles of chemokine receptors in melanocytic lesions: de novo expression of CXCR6 in melanoma. *Human Pathology* 38:168-180.
280. Schadendorf, D., A. Moller, B. Algermissen, M. Worm, M. Sticherling, and B. M. Czarnetzki. 1993. IL-8 produced by human malignant melanoma cells in vitro is an essential autocrine growth factor [published erratum appears in J Immunol 1994 Oct 1;153(7):3360]. *J Immunol* 151:2667-2675.
281. Graves, D. T., R. Barnhill, T. Galanopoulos, and H. N. Antoniades. 1992. Expression of monocyte chemotactic protein-1 in human melanoma in vivo. *American Journal of Pathology* 140:9-14.
282. Letsch, A., U. Keilholz, D. Schadendorf, G. Assfalg, A. M. Asemissen, E. Thiel, and C. Scheibenbogen. 2004. Functional CCR9 Expression Is Associated with Small Intestinal Metastasis. *J Investig Dermatol* 122:685-690.
283. Welch, D. R. 1997. Technical considerations for studying cancer metastasis in vivo. *Clinical and Experimental Metastasis* 15:272-306.
284. Bystryn, J.-C., R. S. Bart, P. Livingston, and A. W. Kopf. 1974. Growth and Immunogenicity of Murine B16 Melanoma. *J Investig Dermatol* 63:369-373.

285. Fidler, I. J. 1973. Selection of successive tumour lines for metastasis. *Nature: New Biology* 242:148-149.
286. Nicolson, G. L., K. W. Brunson, and I. J. Fidler. 1978. Specificity of Arrest, Survival, and Growth of Selected Metastatic Variant Cell Lines. *Cancer Res* 38:4105-4111.
287. Avent, J., C. Vervaert, and H. F. Seigler. 1979. Non-specific and specific active immunotherapy in a B16 murine melanoma system. *Journal of Surgical Oncology* 12:87-96.
288. Bohm, W., S. Thoma, F. Leithauser, P. Moller, R. Schirmbeck, and J. Reimann. 1998. T Cell-Mediated, IFN-{gamma}-Facilitated Rejection of Murine B16 Melanomas. *J Immunol* 161:897-908.
289. Bottazzi, B., S. Walter, D. Govoni, F. Colotta, and A. Mantovani. 1992. Monocyte chemotactic cytokine gene transfer modulates macrophage infiltration, growth and susceptibility to IL-2 therapy of a murine melanoma. *The Jounal of Immunology* 148:1280-1285.
290. Koga, M., H. Kai, K. Egami, T. Murohara, A. Ikeda, S. Yasuoka, K. Egashira, T. Matsuishi, M. Kai, Y. Kataoka, M. Kuwano, and T. Imaizumi. 2008. Mutant MCP-1 therapy inhibits tumour angiogenesis and growth of malignant melanoma in mice. *Biochemical and biophysical Research Communications* 365:279-284.
291. Vianello, F., N. Papeta, T. Chen, P. Kraft, N. White, W. K. Hart, M. F. Kircher, E. Swart, S. Rhee, G. Palu, D. Irimia, M. Toner, R. Weissleder, and M. C. Poznansky. 2006. Murine B16 Melanomas Expressing High Levels of the Chemokine Stromal-Derived Factor-1/CXCL12 Induce Tumour-Specific T Cell Chemorepulsion and Escape from Immune Control. *Journal of Immunology* 176:2902-2914.
292. Murakami, T., W. Maki, A. R. Cardones, H. Fang, A. T. Kyi, F. O. Nestle, and S. T. Hwang. 2002. Expression of CXC Chemokine Receptor-4 Enhances the Pulmonary Metastatic Potential of Murine B16 Melanoma Cells. *Cancer Research* 62:7328-7334.
293. Ren, T., Q. Chen, Z. Tian, and H. Wei. 2007. Down-regulation of surface fractalkine by RNA interference in B16 melanoma reduced tumour growth in mice. *Biochemical and biophysical Research Communications* 364:978-984.
294. Kirk, C. J., D. Hartigan-O'Connor, B. J. Nickoloff, J. S. Chamberlain, M. Giedlin, L. Aukerman, and J. J. Mule. 2001. T Cell-dependent Antitumor Immunity Mediated by Secondary Lymphoid Tissue Chemokine: Augmentation of Dendritic Cell-based Immunotherapy. *Cancer Res* 61:2062-2070.
295. Fushimi, T., A. Kojima, M. A. S. Moore, and R. G. Crystal. 2000. Macrophage inflammatory protein 3{alpha} transgene attracts dendritic cells to established murine tumours and suppressed growth. *Journal of Clinical Investigation* 105.
296. Fang, L., V. C. Lee, E. Cha, H. Zhang, and S. T. Hwang. 2008. CCR7 regulates B16 murine melanoma cell tumorigenesis in skin. *Journal of Leukocyte Biology* 84:965-972.
297. Singh, S., M. Varney, and R. K. Singh. 2009. Host CXCR2-Dependent Regulation of Melanoma Growth, Angiogenesis, and Experimental Lung Metastasis. *Cancer Research* 69:411-415.
298. Horton, L. W., Y. Yu, S. Zaja-Milatovic, R. M. Streiter, and A. Richmond. 2007. Opposing Roles of Murine Duffy Antigen Receptor for Chemokine and Murine CXC Chemokine Receptor-2 Receptors in Murine Melanoma tumour Growth. *Cancer Research* 67:9791-9799.
299. Conesa, C. M., N. Á. Sánchez, V. V. Ortega, J. G. Reverte, F. P. Carpe, and M. C. Aranda. 2009. In vitro and in vivo effect of IFN[alpha] on B16F10 melanoma in two models: Subcutaneous (C57BL6J mice) and lung metastasis (Swiss mice). *Biomedicine & Pharmacotherapy* 63:305-312.

300. Duguay, D., F. Mercier, J. Stagg, D. Martineau, J. Bramson, M. Servant, R. Lin, J. Galipeau, and J. Hiscott. 2002. In vivo interferon regulatory factor 3 tumour suppressor activity in B16 melanoma tumours. *Cancer Research* 62:5148-5152.
301. Smyth, M. J., M. Taniguchi, and S. E. A. Street. 2000. The Anti-Tumor Activity of IL-12: Mechanisms of Innate Immunity That Are Model and Dose Dependent. *J Immunol* 165:2665-2670.
302. Zigrino, P., I. Kuhn, T. Bauerle, J. Zamek, J. W. Fox, S. Neumann, A. Licht, M. Schorpp-Kistner, P. Angel, and C. Mauch. 2009. Stromal Expression of MMP-13 Is Required for Melanoma Invasion and Metastasis. *J Invest Dermatol* 129:2686-2693.
303. Poste, G., J. Doll, and I. J. Fidler. 1981. Interactions among clonal subpopulations affect stability of the metastatic phenotype in polyclonal populations of B16 melanoma cells. *Proceedings of the National Academy of Sciences* 78:6226-6230.
304. Price, J. E., S. Naito, and I. J. Fidler. 1988. Growth in an organ microenvironment as a selective process in metastasis. *Clinical and Experimental Metastasis* 6:91-102.
305. Fidler, I. J., and M. L. Kripke. 1977. Metastasis results from preexisting variant cells within a malignant tumor. *Science* 197:893-895.
306. Fidler, I. J., and C. Bucana. 1977. Mechanism of Tumor Cell Resistance to Lysis by Syngeneic Lymphocytes. *Cancer Res* 37:3945-3956.
307. Raz, A., W. L. McLellan, I. R. Hart, C. D. Bucana, L. C. Hoyer, B. A. Sela, P. Dragsten, and I. J. Fidler. 1980. Cell Surface Properties of B16 Melanoma Variants with Differing Metastatic Potential. *Cancer Res* 40:1645-1651.
308. Cameron, M. D., E. E. Schmidt, N. Kerkvliet, K. V. Nadkarni, V. L. Morris, A. C. Groom, A. F. Chambers, and I. C. MacDonald. 2000. Temporal Progression of Metastasis in Lung: Cell Survival, Dormancy, and Location Dependence of Metastatic Inefficiency. *Cancer Research* 60:2541-2546.
309. Hart, I. R., and I. J. Fidler. 1980. Role of Organ Selectivity in the Determination of Metastatic Patterns of B16 Melanoma. *Cancer Res* 40:2281-2287.
310. Brown, L. M., D. R. Welch, and S. R. Rannels. 2002. B16F10 melanoma cell colonization of mouse lung is enhanced by partial pneumonectomy. *Clinical and Experimental Metastasis* 19:369-376.
311. Fidler, I. J., D. M. Gersten, and M. B. Budmen. 1976. Characterization in Vivo and in Vitro of Tumor Cells Selected for Resistance to Syngeneic Lymphocyte-mediated Cytotoxicity. *Cancer Res* 36:3160-3165.
312. Yang, H.-Z., B. Cui, H.-Z. Liu, S. Mi, J. Yan, H.-M. Yan, F. Hua, H. Lin, W.-F. Cai, W.-J. Xie, X.-X. Lv, X.-X. Wang, B.-M. Xin, Q.-M. Zhan, and Z.-W. Hu. 2009. Blocking TLR2 activity attenuates pulmonary metastases of tumor. *PLoS One* 4:e6520.
313. Kakuta, S., Y.-I. Tagawa, S. Shibata, M. Nanno, and Y. Iwakura. 2002. Inhibition of B16 melanoma experimental metastasis by interferon-gamma through direct inhibition of cell proliferation and activation of antitumour host mechanisms. *Immunology* 105:92-100.
314. Black, P. L., H. Phillips, H. R. Tribble, R. Pennington, M. schneider, and J. E. Talmadge. 1993. Antitumor response to recombinant murine interferon γ correlates with enhanced immune function of organ-associated, but not recirculating cytolytic T lymphocytes and macrophages. *Cancer Immunology, Immunotherapy* 37:299-306.
315. Taranova, A. G., D. Maldonado III, C. M. Vachon, E. A. Jacobsen, H. Abdala-Valencia, M. P. McGarry, S. I. Ochkur, C. A. Protheroe, A. Doyle, C. S. Grant, J. Cook-Mills, L. Birnbaumer, N. A. Lee, and J. J. Lee. 2008. Allergic Pulmonary Inflammation Promotes the Recruitment of Circulating Tumor Cells to the Lung. *Cancer Research* 68:8582-8589.

316. Kantor, A. B., and L. A. Herzenberg. 1993. Origin of Murine B Cell Lineages. *Annual Review of Immunology* 11:501-538.
317. Fagarasan, S., N. Watanabe, and T. Honjo. 2000. Generation, expansion, migration and activation of mouse B1 cells. *Immunological Reviews* 176:205-215.
318. Pérez, E. C., J. J. Machado, F. Aliperti, E. Freymüller, M. Mariano, and J. D. Lopes. 2008. B-1 lymphocytes increase metastatic behavior of melanoma cells through the extracellular signal-regulated kinase pathway. *Cancer Science* 99:920-928.
319. Staquicini, F. I., A. Tandle, S. K. Libutti, J. Sun, M. Zigler, M. Bar-Eli, F. Aliperti, E. C. Perez, J. E. Gershenwald, M. Mariano, R. Pasqualini, W. Arap, and J. D. Lopes. 2008. A Subset of Host B Lymphocytes Controls Melanoma Metastasis through a Melanoma Cell Adhesion Molecule/MUC18-Dependent Interaction: Evidence from Mice and Humans. *Cancer Res* 68:8419-8428.
320. Melnikova, V. O., and M. Bar-Eli. 2007. Inflammation and melanoma growth and metastasis: The role of platelet-activating factor (PAF) and its receptor. *Cancer Metastasis Reviews* 26:359-371.
321. Biancone, L., V. Cantaluppi, L. Del Sorbo, S. Russo, L. W. Tjoelker, and G. Camussi. 2003. Platelet-activating Factor Inactivation by Local Expression of Platelet-activating Factor Acetyl-Hydrolase Modifies Tumor Vascularization and Growth. *Clinical Cancer Research* 9:4214-4220.
322. Fallani, A., L. Calorini, A. Mannini, S. Gabellieri, G. Mugnai, and S. Ruggieri. 2006. Platelet-activating factor (PAF) is the effector of IFN{gamma} stimulated invasiveness and motility in a B16 melanoma line. *Prostaglandins and Other Lipid Mediators* 81:171-177.
323. Ko, H.-M., J.-H. Kang, B. Jung, H. A. Kim, S. J. Park, K.-J. Kim, Y.-R. Kang, H.-K. Lee, and S.-Y. Im. 2007. Critical role for matrix metalloproteinase-9 in platelet-activating factor-induced experimental tumor metastasis. *International Journal of Cancer* 120:1277-1283.
324. Gasic, G. J. 1984. Role of plasma, platelets, and endothelial cells in tumor metastasis. *Cancer and Metastasis Reviews* 3:99-114.
325. Ho-Tin-Noe, B., T. Goerge, S. M. Cifuni, D. Duerschmied, and D. D. Wagner. 2008. Platelet Granule Secretion Continuously Prevents Intratumor Hemorrhage. *Cancer Research* 68:6851-6858.
326. Jain, S., M. Zuka, J. Liu, S. Russell, J. Dent, J. A. Guerrero, J. Forsyth, B. Maruszak, T. K. Gartner, B. Felding-Habermann, and J. Ware. 2007. Platelet glycoprotein Ib {alpha} supports experimental lung metastasis. *Proceedings of the National Academy of Sciences* 104:9024-9028.
327. Fitzpatrick, F. A., and D. A. Stringfellow. 1979. Prostaglandin D2 formation by malignant melanoma cells correlates inversely with cellular metastatic potential. *Proceedings of the National Academy of Sciences* 76:1765-1769.
328. van Deventer, H. W., W. O'Connor Jr, W. J. Brickey, R. M. Aris, J. P. Y. Ting, and J. S. Serody. 2005. C-C Chemokine Receptor 5 on Stromal Cells Promotes Pulmonary Metastasis. *Cancer Research* 65:3374-3379.
329. Deventer, H. W. v., Q. P. Wu, D. T. Bergstralh, B. K. Davis, B. P. O'Connor, J. P.-Y. Ting, and J. S. Serody. 2008. C-C Chemokine Receptor 5 on Pulmonary Fibrocytes Facilitates Migration and Promotes Metastasis via Matrix Metalloproteinase 9. *The American Journal of Pathology* 173:253-264.
330. Cardones, A. R., T. Murakami, and S. T. Hwang. 2003. CXCR4 enhances adhesion of B16 tumour cells to endothelial cells in vitro and in vivo via beta1 integrin. *Cancer Research* 63:6751-6757.
331. Wei, M. Q., A. Mengesha, D. Good, and J. Anne. 2008. Bacterial targeted tumour therapy-dawn of a new era. *Cancer Letters* 259.

332. Scala, S., P. Giuliano, P. A. Ascierto, C. Ierano, R. Franco, M. Napolitano, A. Ottaiano, M. L. Lombardi, M. Luongo, E. Simeone, D. Castiglia, F. Mauro, I. De Michelle, R. Calemma, G. Botti, C. Caraco, G. Nicoletti, R. A. Satriano, and G. Castello. 2006. Human Melanoma Metastases Express Functional CXCR4. *Clinical Cancer Research* 12:2427-2433.
333. Caspi, R. R. 2008. Immunotherapy of autoimmunity and cancer: the penalty for success. *Nature Reviews Immunology* 8:970-976.
334. Homey, B., A. Muller, and A. Zlotnik. 2002. Chemokines: agents for the immunotherapy of cancer. *Nature Reviews Immunology* 2:175-184.
335. De Clercq, E. 2003. The bicyclam AMD3100 story. *Nature Reviews. Drug Discovery* 2:581-587.
336. Doitsidou, M., M. Reichman-Fried, J. Stebler, M. Köprunner, J. Dörries, D. Meyer, C. V. Esguerra, T. Leung, and E. Raz. 2002. Guidance of Primordial Germ Cell Migration by the Chemokine SDF-1. *Cell* 111:647-659.
337. Burger, J. A., and T. J. Kipps. 2006. CXCR4: a key receptor in the crosstalk between tumor cells and their microenvironment. *Blood* 107:1761-1767.
338. Notarangelo, L. D., and R. Badolato. 2009. Leukocyte trafficking in primary immunodeficiencies. *J Leukoc Biol* 85:335-343.
339. Sisskin, E. E., T. Gray, and J. C. Barrett. 1982. Correlation between sensitivity to tumour promotion and sustained epidermal hyperplasia of mice and rats treated with 12-O-tetra-decanoylphorbol-13-acetate. *Carcinogenesis* 3:403-407.
340. Lewis, J. G., and D. O. Adams. 1987. Early inflammatory changes in the skin of SENCAR and C57BL/6 mice following exposure to 12-O-tetradecanoylphorbol-13-acetate. *Carcinogenesis* 8:889-898.
341. McColl, S. R., and I. Clark-Lewis. 1999. Inhibition of Murine Neutrophil Recruitment In Vivo by CXC Chemokine Receptor Antagonists. *J Immunol* 163:2829-2835.
342. Mauer, A. M., J. W. Athens, H. Ashenbrucker, G. E. Cartwright, and M. M. Wintrobe. 1960. LEUKOKINETIC STUDIES. II. A METHOD FOR LABELING GRANULOCYTES IN VITRO WITH RADIOACTIVE DIISOPROPYLFLUOROPHOSPHATE (DFP32)*. *The Journal of Clinical Investigation* 39:1481-1486.
343. Worbs, T., T. R. Mempel, J. Bolter, U. H. von Andrian, and R. Forster. 2007. CCR7 ligands stimulate the intranodal motility of T lymphocytes in vivo. *Journal of Experimental Medicine* 204:489-495.
344. Boyden, S. 1962. The chemotactic effect of mixtures of antibody and antigen on polymorphonuclear leucocytes. *Journal of Experimental Medicine* 115:453-466.
345. Bettina Grasl, K., R.-N. Branislav, K. Helga, B. Krystyna, B. Wilfried, and S.-H. Rolf. 1995. In situ detection of fragmented dna (tunel assay) fails to discriminate among apoptosis, necrosis, and autolytic cell death: A cautionary note. *Hepatology* 21:1465-1468.
346. Jaffe, E. A., L. W. Hoyer, and R. L. Nachman. 1973. Synthesis of Antihemophilic Factor Antigen by Cultured Human Endothelial Cells. *Journal of Clinical Investigation* 52:2757-2764.
347. Hashizume, H., P. Baluk, S. Morikawa, J. W. McLean, G. Thurston, S. Roberge, R. K. Jain, and D. M. McDonald. 2000. Openings between Defective Endothelial Cells Explain Tumor Vessel Leakiness. *Am J Pathol* 156:1363-1380.
348. Leenen, P. J., M. F. de Bruijn, J. S. Voerman, P. A. Campbell, and W. van Ewijk. 1994. Markers of mouse macrophage development detected by monoclonal antibodies. *Journal of Immunological Methods* 174:5-19.
349. Tyner, J. W., O. Uchida, N. Kajiwara, E. Y. Kim, A. C. Patel, M. P. O'Sullivan, M. J. Walter, R. A. Schwendener, D. N. Cook, T. M. Danoff, and M. J. Holtzman. 2005.

CCL5-CCR5 interaction provides antiapoptotic signals for macrophage survival during viral infection. *Nature Medicine* 11:1180-1187.

350. Donatella, A., L. Debora, C. Lara, P. Antonio, G. Annunziata, C. Antonino, and C. Alfonso. 2008. Expression of CCR5 receptors on Reed-Sternberg cells and Hodgkin lymphoma cell lines: Involvement of CCL5/Rantes in tumor cell growth and microenvironmental interactions. *International Journal of Cancer* 122:769-776.
351. Oldford, S. A., I. D. Haidl, M. A. Howatt, C. A. Leiva, B. Johnston, and J. S. Marshall. 2010. A Critical Role for Mast Cells and Mast Cell-Derived IL-6 in TLR2-Mediated Inhibition of Tumor Growth. *The Journal of Immunology* 185:7067-7076.
352. Starkey, J. R., P. K. Crowle, and S. Taubenberger. 1988. Mast-Cell-Deficient W/Wv Mice Exhibit a Decreased Rate of Tumor Angiogenesis. *International Journal of Cancer* 42:48-52.
353. Matthews, K. E., A. Karabeg, J. M. Roberts, S. Saeland, G. Dekan, M. M. Epstein, and F. Ronchese. 2007. Long-Term Deposition of Inhaled Antigen in Lung Resident CD11b-CD11c+ Cells. *Am. J. Respir. Cell Mol. Biol.* 36:435-441.
354. Standring, S. 2009. *Gray's Anatomy, 40th Edition*. Churchill Livingstone.
355. Martini, F. H., and J. L. Nath. 2008. *Fundamentals of Anatomy and Physiology*. Benjamin Cummings.
356. Orr, F. W., L. Young, G. M. King, and I. Y. R. Adamson. 1988. Preferential growth of metastatic tumours at the pleural surface of the mouse lung. *Clinical and Experimental Metastasis* 6:221-232.
357. Brenner, J., P. P. Sordillo, G. B. Magill, and R. B. Golbey. 1982. Malignant mesothelioma of the pleura: Review of 123 patients. *Cancer* 49:2431-2435.
358. Roediger, B., L. Ng, A. Smith, B. de St Groth, and W. Weninger. 2008. Visualizing dendritic cell migration within the skin. *Histochemistry and Cell Biology* 130:1131-1146.
359. Cataisson, C., A. J. Pearson, M. Z. Tsien, F. Mascia, J.-L. Gao, S. Pastore, and S. H. Yuspa. 2006. CXCR2 ligands and G-CSF mediate PKCalpha-induced intraepidermal inflammation. *The Journal of Clinical Investigation* 116:2757-2766.
360. Moon, K. A., S. Y. Kim, T.-B. Kim, E. S. Yun, C.-S. Park, Y. S. Cho, H.-B. Moon, and K.-Y. Lee. 2007. Allergen-induced CD11b+ CD11cint CCR3+ macrophages in the lung promote eosinophilic airway inflammation in a mouse asthma model. *International Immunology* 19:1371-1381.
361. Guth, A. M., W. J. Janssen, C. M. Bosio, E. C. Crouch, P. M. Henson, and S. W. Dow. 2009. Lung environment determines unique phenotype of alveolar macrophages. *American Journal of Physiology - Lung Cellular and Molecular Physiology* 296:L936-L946.
362. Gebhardt, C., J. Németh, P. Angel, and J. Hess. 2006. S100A8 and S100A9 in inflammation and cancer. *Biochemical Pharmacology* 72:1622-1631.
363. Taranova, A. G., D. Maldonado, III, C. M. Vachon, E. A. Jacobsen, H. Abdala-Valencia, M. P. McGarry, S. I. Ochkur, C. A. Protheroe, A. Doyle, C. S. Grant, J. Cook-Mills, L. Birnbaumer, N. A. Lee, and J. J. Lee. 2008. Allergic Pulmonary Inflammation Promotes the Recruitment of Circulating Tumor Cells to the Lung. *Cancer Res* 68:8582-8589.
364. Hiratsuka, S., K. Nakamura, S. Iwai, M. Murakami, T. Itoh, H. Kijima, J. M. Shipley, R. M. Senior, and M. Shibuya. 2002. MMP9 induction by vascular endothelial growth factor receptor-1 is involved in lung-specific metastasis. *Cancer Cell* 2:289-300.